Part Two

TECHNIQUE OF ANALYZING PROPOSED SERVOMECHANISMS

By

William R. Ahrendt

The Ahrendt Instrument Co., College Park, Md.

The purpose of this paper, which deals with the elementary concepts of servo analysis, is to prepare for the more original and more significant papers which follow. In this paper we shall discuss some of the methods of analysis available to the designer of feedback control systems. Of course, the techniques described herein are recognized as guides to design, rather than means of determining the final answer. The final choice of design is the result of experiment - in the laboratory and in the field. The mathematical methods described herein are also a useful adjunct to laboratory experiments. If the equipment is physically available, a much more accurate evaluation of the system and its components can be made by a judicious choice of tests using extensions of the methods herein described to interpret the data. This paper presumes, however, that the apparatus is not yet constructed, and it is desired to analyze proposed systems to evaluate their merit.

The method used comprises four steps which consist of (1) obtaining a physical schematic of the system, (2) drawing a block diagram, (3) analyzing the elements and (4) analyzing the system. Later papers will apply aspects of the method to problems of more practical value. The methods described are restricted to linear systems, or those which are nearly so. Linear approximations can be used for many physical systems in order to simplify the mathematics. The methods of analysis are also restricted to continuous systems, although the transient and frequency techniques described herein can be applied to discontinuous, or on-off, systems as well.

The first step of analyzing a servomechanism is to obtain a physical schematic of the system, which shows the salient features of the device. The next step is to reduce this schematic to a block diagram which discards the information unessential to analysis, and is concerned with the functional aspects of the apparatus. The process of formulating the block diagram reduces the system to a number of interconnected elements, each of which can be analyzed separately. The third step consists of analyzing each part of the system, by writing differential equations and transforming them by operational means. The fourth step is to analyze the system, either in terms of its transient response to arbitrarily selected signals, or its steady state response to each of a number of sinusoidal signals of different frequencies.

In order to analyze a servomechanism without the confusion of a variety of electrical circuit components and wires, hydraulic components, and plumbing, and other miscellaneous servo components, it is desirable to represent a complex system by means of a much simplified diagram. One such simplification results from using a schematic diagram, rather than drawings of the equipment itself. The schematic diagram shows the principle of operation of the physical equipment, but such details as source of hydraulic fluid, the sump, the cables, the pulleys, and so on are omitted.

A physical schematic of a simple hydraulic servomechanism is shown in Figure 1. But even a clear schematic circuit diagram is difficult to analyze, because of the quantity of extraneous physical equipment represented. Block diagrams, which are concerned only with the *functions* performed by the equipment, permit visualization of

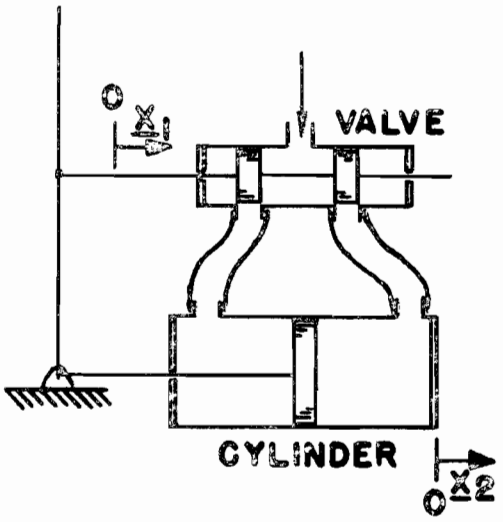

Fig. 1

the system operation much more simply. Problems of synthesis and design are also more conveniently attacked if the equipment can first be "designed" in the form of blocks having the desired performance characteristics.

A block diagram of a servomechanism is a graphical representation of the flow of information and the functions performed in the system. Blocks are used to denote functions performed by parts of the equipment, and lines represent the flow of information with arrowheads to indicate direction of flow. An amplifier, electrical or hydraulic, can be represented by a block; the signal input is a line entering the block, and the signal output is another line leaving the block. Functions which might be represented by block diagrams are those performed by amplifiers, (electrical, hydraulic, and mechanical), networks, motors, generators, mechanical assemblies, hydraulic valves, and many others. These aggregates of equipment, each of which performs a function, are known as elements. The information signals, which are represented by lines, might be electrical voltages, flow of hydraulic fluids, the angular positions of shafts, or any other quantitative means of denoting information.

No effort is made to convey the functions of an element by the shape of the block. Neither is there any differentiation made in the block diagram if the system is electrical, pneumatic, hydraulic, mechanical, or a combination of them all. By clearly showing the functional relationship of the various elements, the block diagram of a system aids in determining the influence that action of one part of a system has upon the others. Because the block diagram is not concerned with the particular manner in which a function is accomplished, the similarity of apparently unrelated systems is revealed.

The block diagram is concerned only with the flow of information and the functions performed by the equipment. In examining an entire system or its schematic diagram in order to draw its block diagram, it should be possible to recognize the function performed by an element or a group of elements. The entire system will be made up of these elements and groups, and each of them can be represented by a block in which are written words which describe the function, or which describe the equipment itself and imply the function. Later in the analysis, written descriptions may be supplanted by mathematical descriptions of the functions performed. The interrelation of the various blocks is likewise determined. The procedure, then, is to study the operation of an element in order to recognize its function, and to study the relationship of the various elements to learn the interconnection of the blocks. The results of this analysis are used to coordinate the blocks into one diagram, which

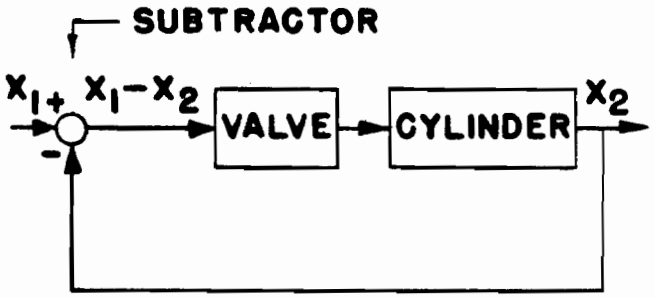

Fig. 2

shows the operation of the entire system. The block diagram of the system of Figure 1 is shown in Figure 2, assuming no load disturbances acting on the servo.

The third step of the analysis, after reducing the schematic diagram to the block diagram, consists of analyzing the individual elements. Each of the elements of the servo has an input, which may be a shaft displacement or rotation, a voltage, a current, a torque, a flow, a pressure or a variety of other ways of conveying information. Each of the elements also has an output, and the medium in which the information is expressed may differ from that of the input. That is, the element may have converted a voltage into a displacement or a force, or a position into a flow. A time plot of the input and output of a device may have the same appearance and may not, depending upon the dynamic characteristics of the device.

An example of a device which has an exact correspondence between output and input is a gear box, in which the output shaft duplicates any motion of the input, with a fixed reduction of angular displacement. A plot of input angle versus time and output angle versus time would look exactly alike, except for the angle scale factor of the plot equal to the gear reduction. On the other hand, consider an electric motor, to which is applied an electric potential which varies with time. A plot of the angular position of the shaft of the motor, while bearing a relationship to a plot of the voltage input, certainly does not duplicate it. In a similar manner, elements of hydraulic systems in which inertia, leakage, and compressibility are considered may have outputs which bear no resemblance to their inputs. Yet, servomechanisms are made up of many such elements whose inputs and outputs are all interrelated and combined in a variety of ways.

For systems (including any elements of a system) which are linear, there is a convenient method of expressing their properties. Although this technique is confined to linear systems, a device may very often be idealized by assuming linearity as a good engineering approximation. A linear element is completely defined by its transfer function, which is a mathematical expression relating the output of the element to its input. It is possible to determine the transfer functions of the various elements of a servomechanism, and then combine them to examine the transfer function of the entire system, thus permitting the analysis to take place in gradual steps. Before arriving at the transfer function of an element, however, it is usually necessary to write its differential equation of motion. After differential equations are written which relate the output of an element with its input, a simple step produces the transfer function, which completely defines the output response for any possible input stimulus.

The differential equations of the element are written, based on Newton's laws and various laws relating to pressure and flow. In order to write these equations

with any degree of accuracy, it may be necessary to revert to the original drawings or design of the equipment, and to call upon experience to furnish reasonable values of the parameters. Experience will also aid in taking all the significant characteristics of the element into account. Such factors as leakage, compressibility and the presence of disturbances may not be obvious from the schematic diagrams. Assuming the system of Figure 1 to be highly idealized, we have the following equation describing its elements:

$$q=K_1(x_1-x_2) \tag{1}$$

$$x_2=K_2\int q\ dt \tag{2}$$

where q is the volume flow rate from the valve to the cylinder.

The next step in obtaining a system's transfer function is to transform the equation to a function of a complex variable. This is done by means of the Laplace Transformation, and each term of the differential equation is transformed from a function of time into an algebraic expression, even though it was originally a constant, a time derivative, a time integral, or one of a variety of other functions. This transformation takes place using a table of Laplace Transforms, so that the transformation involves:

1. Finding the function of time t in the table
2. Substituting in the original expression the transformed function of s corresponding to the function of time

Instead of t appearing as a variable in the transformed expression, a new quantity s appears, which may be treated as a symbol following all the rules of algebra. The system is assumed to be at rest initially. The original differential equation, relating the output of an element to its input, has been transformed, by mechanically substituting for each time function in the equation, a new function of an algebraic quantity s. Most transfer functions can be obtained by use of the transform equivalence of s and d/dt. Equations (1) and (2) are transformed as follows:

$$Q = K_1 (X_1 - X_2) \tag{1a}$$

$$X_2 = K_2\frac{Q}{s} \tag{2a}$$

Capital letters are used to designate functions of s, the complex variable of the Laplace transform, to distinguish them from their lower case counterparts, the functions of time t.

The transfer function of a linear system may now be defined as the ratio of the transform of its output to the transform of its input under the condition that the initial values of both input and output quantitives and all their time derivatives and integrals are zero. Having a transformed differential equation which relates the two, one merely has to solve for their quotient, following rules of algebra. The transfer function G_1 of the valve is therefore

$$G_1 = K_1$$

and of the cylinder is

$$G_2 = K_2/s$$

The fourth step of the study is the system as a whole, either by transient or frequency analysis. What has been done so far is to determine the characteristics of the elements making up the servomechanism. By dealing with these small parts, the

analysis is much simplified. The block diagram describes how these individual characteristics are combined to describe the entire system. The equations implied by the block diagram can be used to determine both the transient response of the system to arbitrary signals and its frequency response.

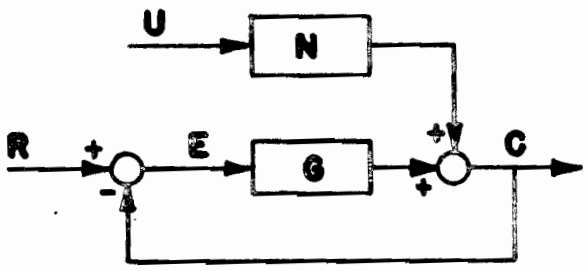

Fig. 3

The block diagram of Figure 3 describes a typical single loop servomechanism, in which C, the controlled variable, represents the actual position of the member being positioned, R is the reference input, the desired position of the member, and G is the transfer function of the mechanism which tends to make those two quantities equal. The disturbances or upsets U represent effects which tend to affect the controlled variable, other than by action of the servo itself. The nomenclature used is that recently adopted by the ASME and AIEE, and again capital letters indicate transforms.

From this block diagram, we obtain the following equation:

$$E = \frac{1}{1+G} R - \frac{1}{1+G} UN \qquad (3)$$

From the above equation, we may obtain the transient response to any reference input variation or disturbance that can be expressed analytically, or using more advanced methods, to any stimulus that can be expressed in the form of a curve as a function of time. We may also use it to obtain the steady state frequency response of the servo.

The transient response of a servomechanism is extremely important; the device is constantly responding to reference input variations and disturbances. Its entire operation is a succession of transients - the servo rarely achieves any steady state condition. In a sense, its input may be likened to that of a telephone circuit, which receives nothing but transients in the form of ever changing syllables of speech. The criterion of a servo's excellence of performance is its ability to deal with the reference input variations and disturbances it encounters.

Despite the importance of the transient response of servomechanisms to stimuli they actually encounter in service, we will discuss only the response of the servo to highly idealized signals, in order to simplify the discussion. By subjecting the servo to certain idealized signals, and comparing the response of the system to one known to be satisfactory for the application or similar application, one can see if the proposed system is satisfactory. The response may be determined by analytical means or analogue computers. The analytical means consists of determining the inverse Laplace transform of the system equation (equation 3). The use of an analogue computer, or model, consists usually of introducing the various system constants to the device, and letting it calculate the solution. This latter method will be discussed in one of the later papers.

Before obtaining the transient response of the servomechanism to some arbitrary stimulus, the stability of the system can be investigated. The stability of the system is a property of the system, in no way related to the disturbances or reference

inputs applied. It is determined solely by the total loop transfer function G of the servo. If the location of the roots of $1+G$ are known, it is known whether or not the system is stable. As a matter of fact, the denominator of equation (3) may be put in the form of an array, and stability determined using Routh's criterion without the effort necessary to locate the roots of the equation. If the system is unstable, the array sill show what changes can be made to the system parameters to make the system stable. After the stability of the system is assured, a test change of reference input or disturbance may be introduced in the equation, the inverse transform extracted, and plot of the variable of interest made as a function of time. If this variable is the error, the error response of a typical servo to a step change in reference input may appear as in Figure 4. Of course, the response to the step change could have been drawn before determining system stability, and that is what the computer would do. Instability would then be shown by oscillations of either constant or increasing magnitude or by ever increasing error with time. In a manner similar to the above, the response of the servo to the torque load disturbance can be calculated.

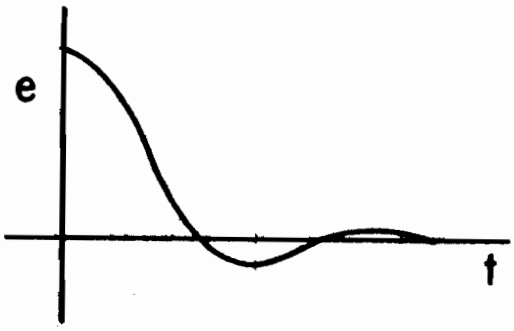

Fig. 4

The frequency response technique, on the other hand, does not involve the solution of differential equations. A study is made of the steady state response of the servomechanism to sinusoidal signals of each frequency from zero to infinity. Widely used in the closely allied field of electrical communications, the technique is employed to evaluate the performance of audio amplifiers, telephone filters, and related apparatus. If the system's response to sine wave signals over a range of frequencies has certain characteristics, it is known to be satisfactory in its actual application.

Although requiring some experience in order to interpret the results of tests and analytical studies, this method is found to be a convenient and effective design tool. The performance of a servo under actual operating conditions may also be predicted using frequency data. By means of sinusoidal responses, the margin of stability of a servo is determinable, along with data telling how much each component is affecting the stability of the system. Such information can be used to improve component design. Either empirical or analytical data are relatively easy to obtain, and the results of experimental and analytical investigations may be combined.

It is a characteristic of any stable linear system that if the input is excited with a sinusoidal function, the system will undergo transients, and the output will ultimately become sinusoidal at the same frequency. If the system under investigation is a servomechanism, and the reference input shaft is oscillated sinusoidally, the controlled shaft will oscillate at the same frequency, but not necessarily with the same magnitude or phase as the reference input.

If the reference input shaft of any practical servomechanism is oscillated at a very low frequency, the amplitude of oscillation of the controlled shaft will be very

nearly equal to that of the reference input, since the servo follows very accurately at low frequencies. At a very high frequency of oscillation of the reference input (above 5-50 cycles per second, depending upon the servo) the controlled shaft does not move at all. Its amplitude of oscillation is zero. The error, however, is equal to the reference input, since the controlled shaft is stationary. In general, at some intermediate frequency, the controlled variable and the error will be oscillating sinusoidally, with amplitudes depending upon system parameters.

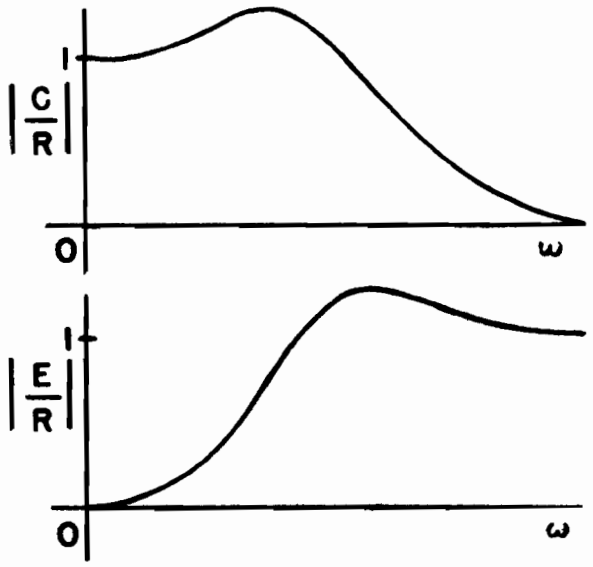

Fig. 5

Typical plots of the ratio of controlled variable to reference input amplitudes and error to reference input amplitudes are shown in Figure 5. These are designated as the magnitude of the control ratio and the error ratio respectively. For systems ordinarily encountered, either one of these curves gives the same information about the system that the transient response to a step change of reference input does. As a matter of fact, it is possible to obtain one from the other, although this is rarely done because of the effort involved. Again, if one knows the frequency response of a system known to be satisfactory for the same or a similar application, and if the proposed system duplicates the frequency response, the new system will be dynamically satisfactory.

Other facts can be generalized from the curves as well. For instance, the higher the peak value of either of the curves, the more oscillatory is the system. In most servo design, the peak value of either curve is held below 1.5. Another fact learned from examination of either curve is that the higher the frequency at which the peak value occurs, the faster the servo will respond to reference input variations. This may or may not be desirable, depending upon the application, and also the expense, weight, and complexity necessary to make this peak frequency high.

It is desirable to be able to calculate the steady state sinusoidal response of a servomechanism from a knowledge of the transfer function G of the servo loop. The well known method of accomplishing this is to substitute $jw = 2\pi f$ for s in the following expressions for error and control ratios.

$$\text{Error ratio} = \frac{1}{1+G(s)} = \frac{1}{1+G(jw)}$$

$$\text{Control ratio} = \frac{G(s)}{1+G(s)} = \frac{G(jw)}{1+G(jw)}$$

The expressions resulting will be complex, having magnitude and phase. The magnitudes of the expressions are the magnitude of the error ratio and the magnitude of the control ratio respectively. For the idealized system of Figure 1 these ratios become:

$$\text{Error ratio} = \frac{1}{1+\frac{K_1K_2}{s}} = \frac{1}{1+\frac{K_1K_2}{jw}} = \frac{jw}{K_1K_2+jw} \qquad (4a)$$

$$\text{Control ratio} = \frac{\frac{K_1K_2}{s}}{1+\frac{K_1K_2}{s}} = \frac{\frac{K_1K_2}{jw}}{1+\frac{K_1K_2}{jw}} = \frac{K_1K_2}{K_1K_2+jw} \qquad (5a)$$

In analyzing a servomechanism to study the effect of its component design on overall stability and performance, the transfer function yields more information than the effectiveness ratios described above. The most useful form in which to put this information is the transfer locus, which is a parametric plot of the vector ratio in magnitude and phase of the systems output to the input as a function of applied frequency. For each value of frequency w, the transfer function is evaluated as a specific complex number (by setting $s=jw$), which determines a point on the complex plane (a graph on which the horizontal coordinate represents the real part and the vertical coordinate represents the imaginary part of a complex number corresponding to the point). If the values of the transfer function are found for all frequencies in a certain range, a series of corresponding points may be found on the complex plane, and these jointed together to form the transfer locus. Although each point on this graph is plotted for a given frequency, the frequency itself does not appear as one of the coordinates of the graph. Rather, various points along the curve are labeled according to the frequencies with which they correspond. The transfer locus of output to input of a system is usually plotted on polar coordinates.

Stability of the servomechanism is revealed by the shape of the transfer locus of G. If the servo is unstable, the transfer locus will enclose the point $-1+j0$ of the graph. A precise determination of whether or not the point is enclosed involves the use of complex function theory, but the following simplified criterion will be correct in almost all cases encountered. Imagine a string fastened to the origin of the graph and lying along the G locus so that the string and the locus are coincident. Imagine further a spike of infinite height erected perpendicular to the complex plane at the minus one point. Grasp a point on the string corresponding to a very low frequency point on the locus. Pull the string taut and, if necessary, rotate the string counterclockwise about the origin until it lines up with the positive real axis. If the string does not loop the infinite spike (the minus one point) as a result of these operations, the system is stable, otherwise it is unstable.

By analyzing the effect of each of the servo elements on the shape of the transfer locus, it can be seen how much each is contributing toward stability of instability of the system. Furthermore, one can also determine what elements are contributing to the effectiveness of the servo, that is, what elements are causing the error ratio to be small over the range of frequencies of interest. To do so requires a method of obtaining the error and output ratios from the G transfer locus.

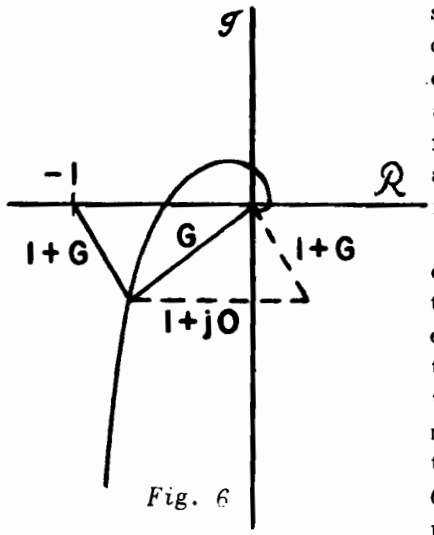

Fig. 6

If one has obtained the open loop transfer locus either experimentally, analytically, or a combination of them both, it is a simple matter to obtain the error ratio and the control ratio. On a representative transfer locus shown in Figure 6, a line from the origin to any point on the locus represents the magnitude and phase of G for one frequency. That is, the length of the line is the magnitude and phase of G for the frequency designated at point P, and the phase angle of G is the angle from the positive real axis to the line. The vector sum $1+G$ is obtained by adding 1 to G. Application of the parallelogram law shows that a line from the minus one point to P represents the quantity $1+G$, and phase is given by the angle measured clockwise from the real axis to the line. The error ratio is given in magnitude by the inverse of the length of this line. The magnitude of the control ratio is the ratio of the lengths of the two lines.

The above paper presents but one aspect of the technique of analyzing proposed servomechanisms. Actually, there are many variations in present usage. An excellent extension of the above described methods uses logarithmic presentation of the data, a technique often used in servo design. Mathematical methods, such as described above, have been successfully applied to many problems of analysis and evaluation. It is believed that their adoption, rather than resorting solely to trial and error, results in engineering economy even though the training and experience necessary on the part of the engineer may increase the initial cost. The ultimate result is an economical one.

It is not implied, however, that mathematics can take the place of field and laboratory tests. Rather, it is affirmed that many tests are rendered unnecessary by making mathematical analysis, that many tests are more expeditiously conducted and the results more accurately interpreted by using these methods, and that redesign of the servomechanism to improve its characteristics is more economically accomplished through the techniques mentioned in these paragraphs.

AN ANALYSIS OF NORTHROP AIRCRAFT POWERED FLIGHT CONTROLS

By

Duane T. McRuer

Northrop Aircraft, Inc., Hawthorne, Calif.

Introduction

This paper presents an analysis of a typical Northrop fully-powered hydraulic control-surface actuator. The purpose of the analysis is to develop the "transfer functions" and the most important "error coefficients" of the mechanism so that ordinary servomechanism techniques may be used in the design and further analysis of this type of system. While the analysis applies strictly to only one geometric configuration, the results may be (and have been) easily modified to apply to several other variations of this general type of mechanism.

The type of mechanism discussed is both inherently and purposely non-linear for almost all large input amplitudes; also, the system is complex enough to make a non-linear analysis difficult and lengthy. Therefore, the approach used considers small perturbations about steady-state operating points. This restriction is ordinarily unimportant, since normal mechanism inputs from the pilot or autopilot are small changes from a steady-state condition.

The development of this paper will proceed along the following lines: The system equations of motion are derived; from these equations of motion the transfer functions and a block diagram representation of the system are developed; a series for the steady-state error of the mechanism is derived; and approximations found valuable in practice are introduced. A table of symbols used is found on the next page.

I. Description of the Servomechanism

The servomechanism considered in this paper is a valve-cylinder hydraulic actuator of the type used in Northrop fully-powered control systems. The valve housing is integral with the cylinder and the valve is ported in such a manner that the cylinder moves in a direction tending to decrease any existing valve displacement from neutral. The double-ended piston is fixed to the aircraft structure; the load displacement is that of the cylinder relative to the piston. The load consists of an effective mass due to the inertia elements of the cylinder and control surface, an effective viscous friction due to the damping of the control surface and an effective spring force due to the control surface hinge moment. Also opposing the cylinder motion are the stiction and coulomb friction forces. Hydraulic leakage in the system is confined to the small neutral leakage purposely built into the system.

A schematic diagram of the system is shown in Figure 1.

SYMBOLS

A	Effective cross-sectional area of cylinder.
B	Viscous friction coefficient as seen by the cylinder.
B_h	Surface viscous damping coefficient.
$E = E_0 + \epsilon$	Servo error; valve displacement from its neutral position. E_0 has only one time derivative, ϵ is a perturbation.
J_h	Moment of inertia of the surface.
K	Spring constant as seen by the cylinder.
K'	A gain constant.
K_h	Spring constant of the surface (hinge moment gradient).
l	Effective moment arm from surface to cylinder.
M	Effective mass load of the cylinder.
m	Mass of the cylinder.
N	Bulk modulus of the hydraulic oil.
P_a	Pressure drop across the valve.
$P_c = P_{c_0} + p_c$	Pressure drop across the piston. P_{c_o} has only one time derivative, p_c is a perturbation.
$P_s = P_{s_0} + p_s$	System pressure.
$Q_a = Q_0 + q_a$	Flow from valve. Q_o is a constant, q_a a perturbation.
$Q_c = Q_{\Delta_\gamma} + Q_m$	Flow into the cylinder.
Q_{Δ_γ}	Compressibility flow.
Q_m	Flow tending to move cylinder.
s	Complex variable of LaPlace transform theory.
t	Time.
$V_i = V_{i_0} + v_i$	Input velocity (valve velocity relative to airplane).
$V_c = V_{c_0} + v_c$	Cylinder velocity relative to aircraft.
γ	Volume of oil under compression.
$\Delta\gamma$	Change in volume of oil under compression.
ω	Angular frequency.
ω_γ	Angular undamped natural frequency.
ζ	Damping ratio.

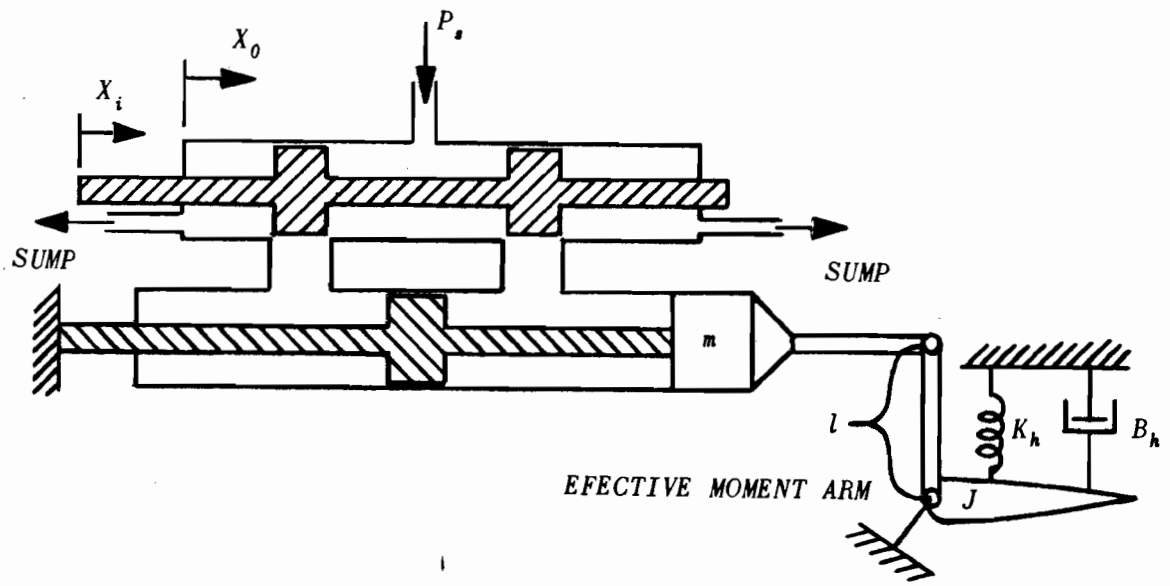

Fig. 1 - Schematic diagram of Northrop fully-powered control system

II. Development of Equations of Motion

A. Servo Error

The error E of this servomechanism is the difference between the valve displacement relative to the airplane $(\int V_i dt)$ and the cylinder displacement relative to the airplane $(\int V_c dt)$.

Therefore:

$$(1) \qquad \frac{d\,E}{d\,t} = \frac{d}{d\,t}\,(E_o + \epsilon) = V_i - V_c = (V_{i_o} - V_{c_o}) + (v_i - v_c)$$

where V_{i_o}, V_{c_o} and E_o are steady-state quantities and v_{i_o}, v_{c_o} and ϵ are small perturbations from the steady-state.

Hence:

$$(2) \qquad \frac{d\epsilon}{dt} = v_i - v_c \; ; \quad \frac{dE_o}{dt} = V_{i_o} - V_{c_o}$$

or in Laplace transform notation, with s as the complex variable of the transform theory.*

$$(2a) \qquad \epsilon(s) = \frac{v_i(s) - v_c(s)}{s} = X_i(s) - X_c(s)$$

B. Flow from the Valve

The flow from the valve may be expressed as:

$$(3) \qquad Q_a = f(E)\sqrt{P_a} = f(E)\sqrt{P_s - P_c}$$

To linearize equation (3) it is necessary to use a Taylor's series expansion, i.e.

$$(4) \qquad Q_a = f(E, P_s, P_c) = f(E_o + \epsilon, P_{s_o} + p_s, P_{c_o} + p_c)$$

$$= Q_o + \left[\frac{\partial Q_a}{\partial E}\right]_{P_s,P_c} \epsilon + \left[\frac{\partial Q_a}{\partial P_s}\right]_{P_c,E} p_s + \left[\frac{\partial Q_a}{\partial P_c}\right]_{P_s,E} p_c + \cdots$$

and,

$$(5) \qquad q_a = Q_a - Q_o$$

Combining equations (4) and (5), the perturbed flow from the valve is (dropping the notation of constants on the partial derivatives)

$$(6) \qquad q_a = \frac{\partial Q_a}{\partial E}\epsilon + \frac{\partial Q_a}{\partial P_s} p_s + \frac{\partial Q_a}{\partial P_c} p_c + \cdots$$

Typical variations of valve flow with pressure drop across the cylinder, with valve displacement held constant, are shown in Figure 2a. Typical variations of valve flow with valve displacement from neutral, with pressure drop across the cylinder held constant, are shown in Figure 2b.

* *Laplace transforms shall be used throughout this paper. However, any of the equations developed can be converted to Fourier transforms or frequency response relationships by replacing s with $j\omega$.*

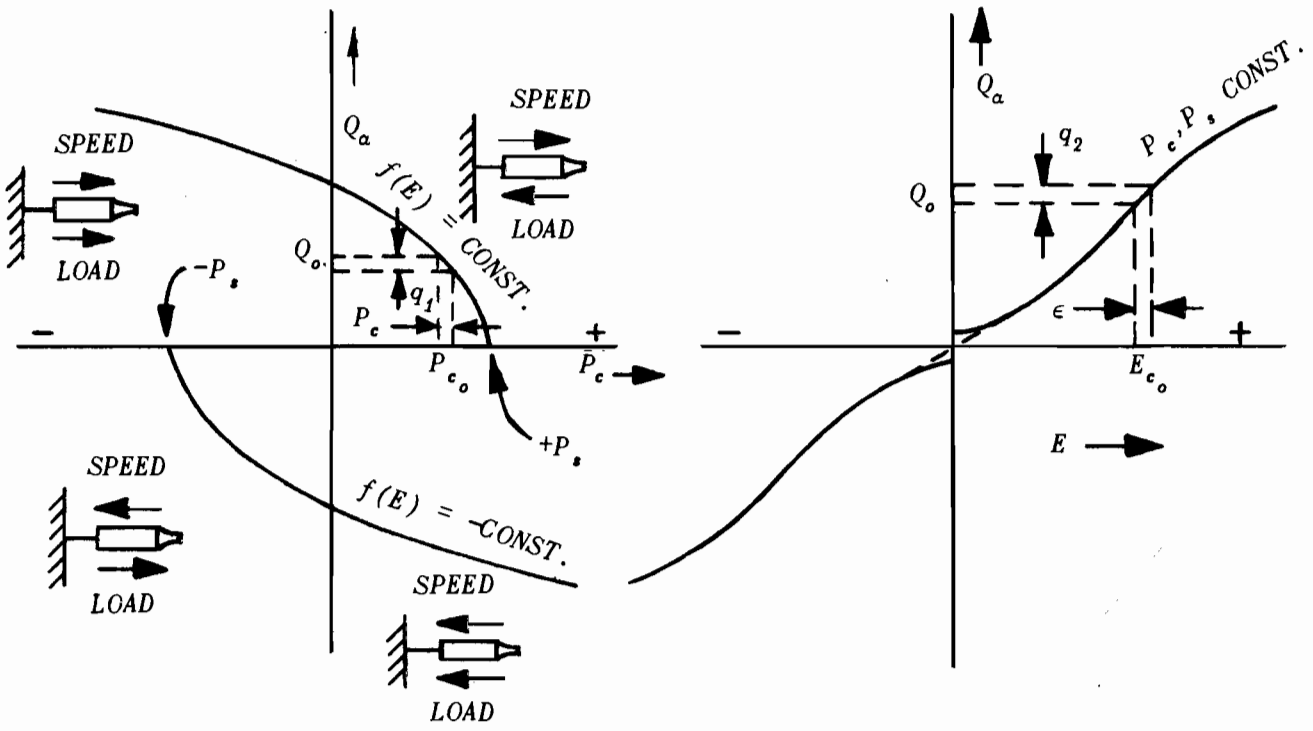

Variation of valve flow with pressure drop across the cylinder. (Valve displacement from neutral constant)

(a)

Varaition of valve flow with valve displacement from neutral. (Pressure drop across cylinder constant.)

(b)

Fig. 2

Figure 2 also shows a typical operating point, the steady-state quantities defining the operating point (Q_o, E_{c_o}, and P_{c_o}) and possible values of the perturbed quantities (p_c, ϵ, and $q_1 + q_2 = q_a$). The partial derivatives of equations (4) and (6) are the slopes of the curves evaluated at the operating point.

In the system discussed in this paper, and represented by the curves of Figure 2, the partial derivative $\frac{\partial Q_a}{\partial E}$ is always positive (or zero), and the partial derivative $\frac{\partial Q_a}{\partial P_c}$ is always negative (or zero). It will be advantageous in representing the system as a block diagram to make this situation apparant in the equations.

Therefore $\frac{\partial Q_a}{\partial E}$ and $\frac{\partial Q_a}{\partial P_c}$ shall be equal by definition to the following quantities:

$$(7)\quad \left[\begin{array}{ll} \dfrac{\partial Q_a}{\partial E} = k_E = f'(E)\sqrt{P_s - P_c}\Big|_{P_s,\,P_c} & k_E \text{ always positive} \\ \dfrac{\partial Q_a}{\partial P_c} = -k_p = \dfrac{-f(E)}{2\sqrt{P_s - P_c}}\Big|_{E,\,P_s} & k_p \text{ always positive} \\ \dfrac{\partial Q_a}{\partial P_s} = \dfrac{f(E)}{2\sqrt{P_s - P_c}}\Big|_{E,\,P_s} & \end{array}\right.$$

System pressure variations are functions of many other quantities and they will be considered in this paper only as a disturbance.

With the definitions of equations (7), the perturbed valve flow becomes:

$$(8)\qquad q_a(s) = k_E\,\epsilon(s) - k_p\,p_c(s) + \frac{\partial Q_a}{\partial P_s}\,p_s$$

C. Flow Into the Cylinder

Since the flow into the cylinder is equal to the flow from the valve, and neutral leakage may be considered negligible, the flow into the cylinder consists of two elements; the flow needed to overcome the effects of compressibility ($Q_{\Delta\gamma}$) and the flow tending to move the cylinder relative to the piston (Q_V). In equation form,

$$(9)\qquad Q_c = Q_a = Q_{\Delta\gamma} + Q_V$$

By the definition of compressibility, ($P_c = N\frac{\Delta\gamma}{\gamma}$, N is bulk modulus of oil),

$$(10)\qquad Q_{\Delta\gamma} = \frac{d}{dt}\Delta\gamma = \frac{d}{dt}\frac{\gamma}{N}P_c = \frac{\gamma}{N}\frac{dP_{c_o}}{dt} + \frac{\gamma}{N}\frac{dp_c}{dt}$$

The flow tending to move the cylinder will be,

$$(11)\qquad Q_V = AV_c = A(V_{c_o} + V_c)$$

Therefore the total flow into the cylinder is,

$$(12) \qquad Q_c = Q_a = q_a + Q_o = \frac{\gamma}{N}\frac{dp_c}{dt} + A_{v_c} + AV_{c_o} + \frac{\gamma}{N}\frac{dP_{c_o}}{dt}$$

Separating the perturbed quantities from the steady-state quantities,

$$(13) \qquad q_a(s) = s\frac{\gamma}{N} p_c(s) + Av_c(s),$$

$$(14) \qquad Q_o = AV_{c_o} + \frac{\gamma}{N}\frac{dP_{c_o}}{dt}$$

D. Forces on the Cylinder

Since the pressure drop across the cylinder is balanced by an effective mass, viscous friction and spring load the equation relating load forces and applied forces becomes,

$$(15) \qquad P_c A = M\frac{dV_c}{dt} + BV_c + K\int V_c\, dt$$

Separating equation (15) into its perturbation and steady-state components,

$$(16) \qquad P_{c_o} A = BV_{c_o} + K\int V_{c_o}\, dt,$$

$$(17) \qquad p_c A = M\frac{dv_c}{dt} + Bv_c + K\int v_c\, dt$$

Transforming equation equation (17),

$$(17a) \qquad Ap_c(s) = (Ms^2 + Bs + K)\frac{v_c(s)}{s}.$$

The system equations are summarized below:

TABLE I

STEADY-STATE RELATIONSHIPS	PERTURBED RELATIONSHIPS
$\frac{dE_o}{dt} = V_{i_o} - V_{c_o}$	$\epsilon(s) = \frac{v_i(s) - v_c(s)}{s}$
$Q_o = AV_{c_o} + \frac{\gamma}{N}\frac{dP_{c_o}}{dt}$	$q_a(s) = k_E\,\epsilon(s) - k_P\,p_c(s) + \frac{\partial Q_a}{\partial P_s} p_s$
$P_{c_o} = \frac{1}{A}\left(BV_{c_o} + K\int V_{c_o}\, dt\right)$	$q_a(s) = \frac{\gamma}{N} s\,p_c(s) + A\,v_c(s)$
	$p_c(s) = \frac{1}{A}(Ms^2 + Bs + K)\frac{v_c(s)}{s}$

III. Block Diagram and Transfer Functions

The equations developed in part II may be used to obtain an equivalent block diagram of the system. Developing transfer functions from Table I:

(19) $$Y_{px}(s) = \frac{X_c(s)}{p_c(s)} = \frac{A}{Ms^2 + Bs + K}, \text{ and}$$

(20) $$Y_{qp}(s) = \frac{p_c(s)}{q_a(s)} = \frac{N}{\gamma s}\left[\frac{Ms^2 + Bs + K}{Ms^2 + Bs + \frac{K + A^2N}{\gamma}}\right]$$

Combining the above transfer functions with

(2a) $$\epsilon(s) = X_i(s) - X_c(s)$$

and with

(8) $$q_a(s) = k_\epsilon \epsilon(s) - k_p p_c(s) + \frac{\partial Q_a}{\partial P_s} p_s$$

the block diagram of the system may be constructed; this block diagram is shown in Figure 3.

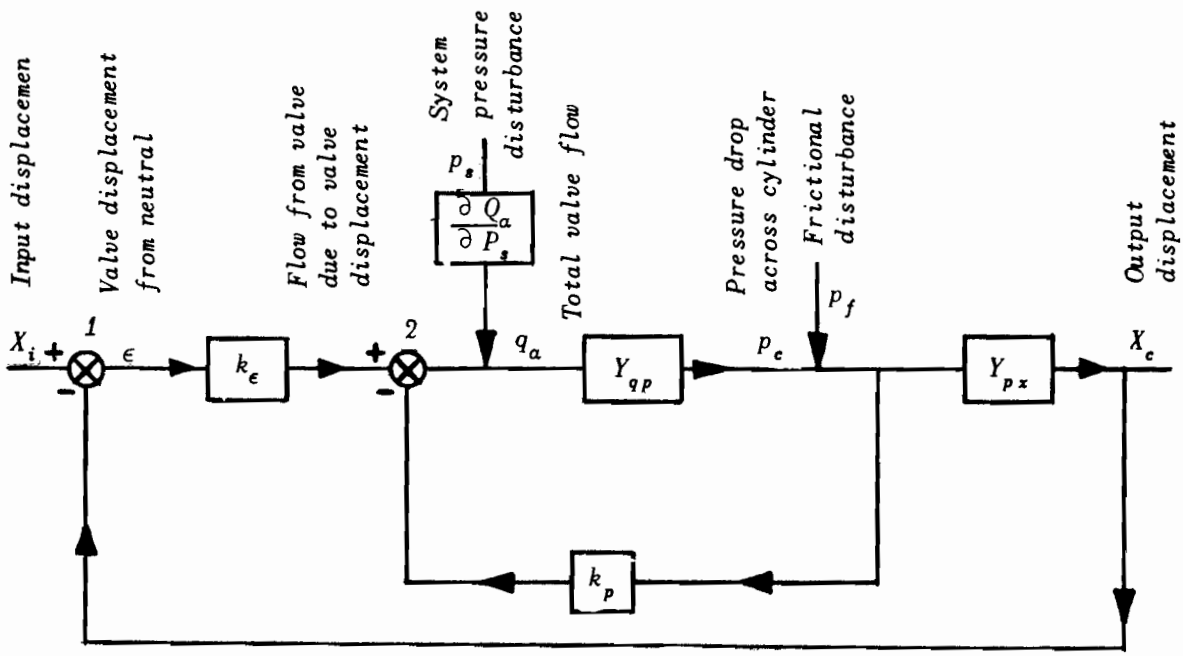

Fig. 3 - Block diagram of hydraulic control system.

The open-loop transfer function of the mechanism is,

$$(21) \qquad \frac{X_c(s)}{\epsilon(s)} = k_\epsilon Y_{pz}\left[\frac{Y_{qp}}{1 + k_p Y_{qp}}\right] = \frac{Y^o_{11}}{1 + Y_{22}}$$

where Y^o_{11} is the transfer function when k_p is zero and Y_{22} (equals $k_p Y_{qp}$) is the open-loop transfer function of the inner loop. The open-loop transfer function of the mechanism then becomes,

$$(22) \qquad \frac{X_c(s)}{\epsilon(s)} = \frac{k_\epsilon A}{\frac{\gamma M}{N} s^3 + \left(\frac{B\gamma}{N} + k_p M\right) s^2 + \left(\frac{K\gamma}{N} + A^2 + k_p B\right) s + k_p K}$$

The closed-loop transfer function of the system is then:

$$(23) \qquad \frac{X_c(s)}{X_i(s)} = \frac{k_\epsilon A}{\frac{\gamma M}{N} s^3 + \left(\frac{B\gamma}{N} + k_p M\right) s^2 + \left(\frac{K\gamma}{N} + A^2 + k_p B\right) s + k_p K + k_\epsilon A}$$

The Routh criteria may be applied to the denominator of this closed-loop transfer function to determine stability criteria. However, the frequency response methods of Bode and Nyquist and the root-locus method of Evans both yield more useful data regarding both stability and transient response and these methods are normally used by the Northrop Company to solve problems of this nature. Since the Evans root-locus method is as yet unpublished, only the frequency response method will be discussed at any length.

It has been the experience of the Northrop Company that the transfer function of equation (22) has one dominant real root and one conjugate pair; the latter produces a lightly damped oscillation with a high natural frequency. The determination of all the constants is straight-forward with the exception of B, the load damping, which causes the poor damping of the conjugate pair. However, on most systems this quantity may be obtained by use of Theodorsen's flutter equations for the moment of a surface.*

IV. Error Coefficients

The performance of the system in response to some given input is conveniently given by system parameters called "error coefficients". These coefficients provide a simple and useful way to consider the nature of the error response to nearly any arbitrary input. From equation (23) the closed loop transfer function is

$$(23a) \qquad \frac{X_c(s)}{X_i(s)} = \frac{k_\epsilon A}{\left(k_\epsilon A + k_p K\right)\left\{1 + \frac{s}{k_\epsilon A + k_p K}\left[\frac{K\gamma}{N} + A^2 + k_p B + \left(\frac{B\gamma}{N} + k_p M\right)s + \frac{\gamma M}{N} s^2\right]\right\}}$$

* *NACA TR 496 Theodore Theodorsen*
"General Theory of Aerodynamics Instability and the Mechanism of Flutter"

A portion of the denominator is of the form $[\,1 + Z\,(s)\,]^{-1}$;

by the binomial theorem,

$$(24) \qquad \frac{1}{1 + Z\,(s)} = 1 - Z\,(s) + [\,Z\,(s)\,]^2 - [\,Z\,(s)\,]^3 + \ldots$$

Expanding equation (23a),

$$(25) \qquad \frac{X_e\,(s)}{X_i\,(s)} = \left[\frac{k_\epsilon A}{k_\epsilon A + k_p K}\right] \left\{1 - \frac{s}{k_\epsilon A + k_p K}\left[\frac{K\gamma}{N} + A^2 + k_p B + \left(\frac{B\gamma}{N} + k_p M + \frac{\left(\frac{K\gamma}{N} + A^2 + k_p B\right)^2}{k_\epsilon A + k_p K}\right) s + \ldots\right]\right\}$$

The cylinder motion is then

$$(26) \qquad X_e\,(s) = \left[\frac{k_\epsilon A}{k_\epsilon A + k_p K}\right] X_i\,(s) - \left[\frac{k_\epsilon A \frac{K\gamma}{N} + A^2 + k_p B}{k_\epsilon A + k_p K^2}\right] s\, X_i\,(s)$$

$$- \left[\frac{k_\epsilon A}{k_\epsilon A + k_p K^2}\left(\frac{B\gamma}{N} + k_p M + \frac{\left[\frac{K\gamma}{N} + A^2 + k_p B\right]^2}{k_\epsilon A + k_p K}\right)\right] s^2 X_i\,(s) + \ldots$$

which becomes,

$$(27) \qquad X_e\,(s) = \left[\frac{k_\epsilon A}{k_\epsilon A + k_p K} - 1\right] X_i\,(s) + X_i\,(s) + \ldots$$

$$= \left[\frac{k_p K}{k_\epsilon A + k_p K}\right] X_i\,(s) + X_i\,(s) + \ldots$$

Noting that

$$\epsilon\,(s) = X_i\,(s) - X_e\,(s),$$

(28) $$\epsilon(s) = -\left[\frac{k_p K}{k_\epsilon A + k_p K}\right] X_i(s) + \left[\frac{k_\epsilon A\left(\frac{K\gamma}{N} + A^2 + k_p B\right)}{\left(k_\epsilon A + k_p K\right)^2}\right] s\, X_i(s)$$

$$+\left[\frac{k_\epsilon A}{\left(k_\epsilon A + k_p K\right)^2}\left(\frac{B\gamma}{N} + k_p M + \frac{\left(\frac{K\gamma}{N} + A^2 + k_p B\right)^2}{k_\epsilon A + k_p K}\right)\right] s^2 X_i(s) + \cdots$$

$$= [\Sigma C_n(s)]\, X_i(s)$$

The power series for $\epsilon(s)$ converges in the region of $s = 0$. Therefore, the series may be used to obtain an expression for $\epsilon(t)$ which is valid for the steady-state response after all the transients have died out (i.e. for large values of time). Hence,

(29) $$\underset{t \to \infty}{\epsilon(t)} = -\left[\frac{k_p K}{k_\epsilon A + k_p K}\right] X_i(t) + \left[\frac{k_\epsilon A\left(\frac{K\gamma}{N} + A^2 + k_p B\right)}{\left(k_\epsilon A + k_p\right)^2}\right] \frac{d}{dt} X_i(t)$$

$$+\left[\frac{k_\epsilon A}{\left(k_\epsilon A + k_p K\right)^2}\left(\frac{B\gamma}{N} + k_p M + \frac{\left[\frac{K\gamma}{N} + A^2 + k_p B\right]^2}{k_\epsilon A + k_p K}\right)\right] \frac{d^2 X_i(t)}{dt^2} + \cdots$$

$$= C_o X_i(t) + C_1 \frac{dX_i(t)}{dt} + C_2 \frac{d^2 X_i(t)}{dt^2} + \cdots\cdots$$

which is the desired expression for the error coefficients.*

It will be noted that the position-error coefficient is primarily dependent upon k_p, which in turn depends upon the magnitude of the load. Both the acceleration and velocity-error coefficients are largely dependent upon load and k_e, the amplifier effect of the valve.

V. Approximations and Experimental Verification

The above analysis assumes only linearity about a steady-state operating point together with the corollary assumption that the motions are small. At this point it will be advantageous to consider certain simplifications which are useful in practical Northrop systems.

A. Non-Compressible Fluid

The first assumption is that of non-compressible hydraulic fluid (i.e. $N \to \infty$).

* *C_o is the "position-error coefficient", C_1 the "velocity-error coefficient", and C_2 the "acceleration-error coefficient".*

The transfer functions changed by this assumption become

(20a) $$Y_{qp}(s) = \frac{Ms^2 + Bs + K}{sA^2}$$

(22a) $$\frac{X_c(s)}{\epsilon(s)} = \frac{k_\epsilon A}{k_p M s^2 + (A^2 + k_p B)s + k_p K},$$

(23a) $$\frac{X_c(s)}{X_i(s)} = \frac{k_\epsilon A}{k_p M s^2 + (A^2 + k_p B)s + (k_p K + k_\epsilon A)}.$$

The series for the steady-state error becomes

(29a) $$\underset{t \to \infty}{\epsilon(t)} = -\left[\frac{k_p K}{k_\epsilon A + k_p K}\right] X_i(t) + \left[\frac{k_\epsilon A (A^2 + k_p B)}{(k_\epsilon A + k_p K)^2}\right] \frac{d X_i(t)}{dt}$$

$$+ \left[\frac{k_\epsilon A}{(k_\epsilon A + k_p K)^2}\left(k_p M + \frac{[A^2 + k_p B]^2}{(k_\epsilon A + k_p K)^2}\right)\right] \frac{d^2 X_i(t)}{dt} + \cdots\cdots$$

These expressions are useful when load effects are to be considered.

B. Non-Compressible Fluid; Operating Point at Neutral

The second assumption greatly simplifies the equations when the problem of analyzing aircraft on autopilot is encountered. In this case, the emphasis is on small motions about the neutral point. At the neutral position $f(E)$ is very near to zero, making k_p zero. Physically this means that the load effects near the neutral position are negligible. When compressibility is also neglected the transfer functions become

(21a) $$Y_{22} = 0,$$

(22b) $$\frac{X_c(s)}{\epsilon(s)} = \frac{k_\epsilon}{A s},$$

and

(23b) $$\frac{X_c(s)}{X_i(s)} = \frac{k_\epsilon}{A s + k_\epsilon} = \frac{1}{\frac{A}{k_\epsilon} s + 1} = \frac{1}{T s + 1}$$

The open-loop transfer function under these assumptions is that of a perfect integrator and the closed-loop transfer function is that of a first order system. Frequency-response tests have been performed on mechanisms of this type (Figure 4) and the agreement of the theoretical and experimental results (even with these rather drastic assumptions) is excellent.

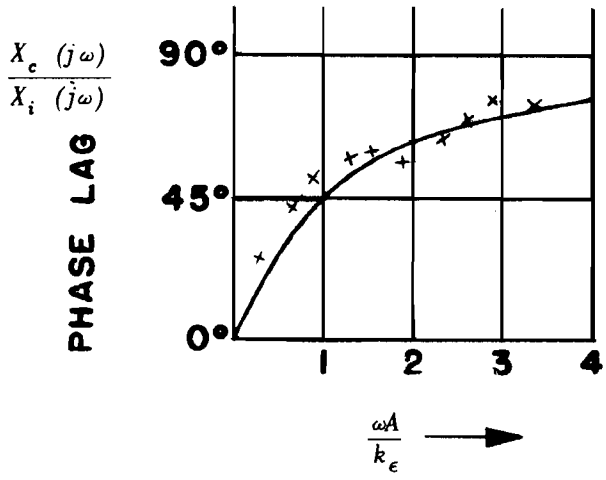

Phase response

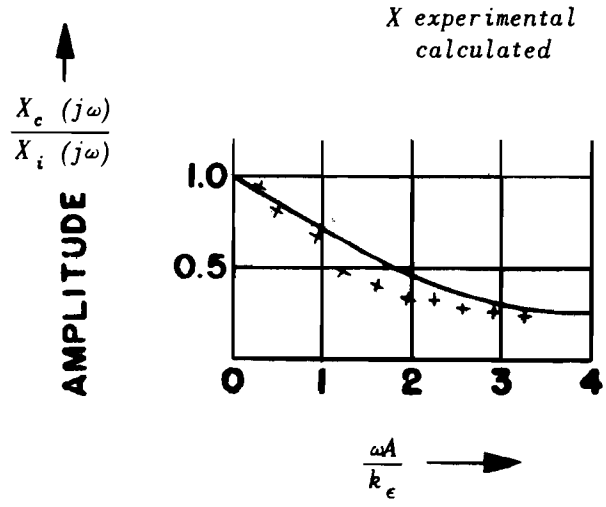

Amplitude response

Fig. 4

The series for the steady-state error also reduces to a very simple form:

$$(29b) \qquad \underset{t \to \infty}{\varepsilon\ (t)} = \frac{A}{k_\epsilon} \frac{d\ X_i\ (t)}{dt} + \frac{A^2}{k_\epsilon{}^2} \frac{d^2\ X_i\ (t)}{dt^2} + \cdots\cdots$$

This expression also checks rather well with experimental evidence in the frequency range from zero to ten cycles/sec $\left(\frac{\omega A}{k_\epsilon} < 3.5\right)$ on Northrop systems. If frequencies greater than ten cycles per second are important, the above results are no longer acceptable approximations.

C. Compressible Fluid; Operating Point at Neutral

Oil compressibility must be considered for a more complete analysis of the system when operation is about the neutral point. Considering compressibility (N finite) the transfer functions about the neutral point become

$$(22c) \qquad \frac{X_c\ (s)}{\epsilon\ (s)} = \frac{k_\epsilon\ A}{s\left[\frac{\gamma M}{N} s^2 + \frac{B\gamma}{N} s + \frac{\kappa\gamma}{N} + A^2\right]} \qquad \text{and}$$

$$(23c) \qquad \frac{X_c\ (s)}{X_i\ (s)} = \frac{k_\epsilon\ A}{\frac{\gamma M}{N} s^3 + \frac{B\gamma}{N} s^2 + \frac{K\gamma}{N} + A^2\ s + k_\epsilon\ A}$$

Equation (22c) may be rearranged as follows:

$$(22d) \qquad \frac{X_c\ (s)}{\epsilon\ (s)} = \frac{N\ k_\epsilon\ A}{\gamma\ M}\left[\frac{1}{s\left[s^2 + \frac{B}{M} s + \frac{K}{M} + \frac{A^2\ N}{\gamma\ M}\right]}\right]$$

$$= \frac{K'}{s\left[s^2 + 2\zeta\omega_n\ s + \omega_n^2\right]},$$

where

$$K' = \frac{N\ k_\epsilon\ A}{\gamma\ M}$$

$$(30) \qquad \omega_n^2 = \frac{K}{M} + \frac{A^2\ N}{\gamma\ M}$$

$$\zeta = \frac{B}{2\sqrt{\left(K + \frac{A^2\ N}{\gamma}\right)M}}$$

From the equations above it may be noted that the load is coupled into the system even at the neutral point by the compressibility effect of the hydraulic fluid. ζ, the damping ratio, is normally quite small because it is due almost entirely to the aerodynamic damping of the surface. ω_n, the undamped natural frequency, is high because of the high effective spring rate of oil. Since the bulk modulus of normal hydraulic oil (N) is on the order of 2.5. x 10^5 psi, the hinge-moment term (K/M) in the natural frequency is ordinarily negligible in comparison to the term due to oil compressibility; this fact agrees well with experimental data, and equation (30) may be simplified to

(30a) $$\omega_n^2 \approx \frac{A^2 N}{\gamma M}$$

$$\zeta \approx \frac{B}{2\sqrt{\frac{A^2 N M}{\gamma}}}$$

The error expression using this assumption becomes

(29c)
$$\underset{t \to \infty}{\epsilon(t)} = \left[\frac{1}{k_\epsilon A}\left(\frac{K\gamma}{N} + A^2\right)\right]\frac{d X_i(t)}{d t} + \left[\frac{1}{k_\epsilon A}\left(\frac{B\gamma}{N} + \frac{\left[\frac{K\gamma}{N} + A^2\right]^2}{k_\epsilon A}\right)\right]\frac{d^2 X_i(t)}{d t^2} + \cdots$$

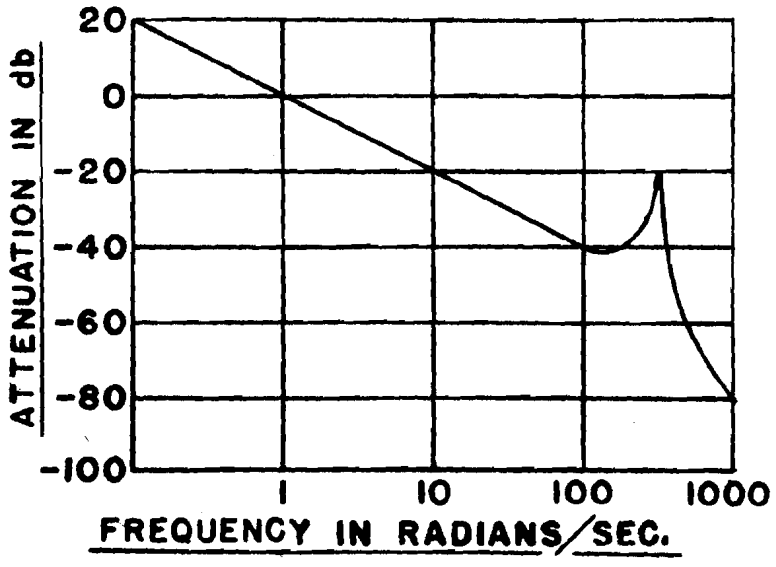

Fig. 5 - Open loop transfer function attenuation plot.

A sketch of a typical frequency-response plot is shown in Figure 5. The gain (K) is fixed so that the second-order peak is well below zero decibels. If this peak is allowed to approach zero decibels, the amplitude of the resulting oscillations are small, and the frequency is very high compared to that of the airplane but of the same order of magnitude as the flutter frequencies. This situation can become rather important on systems where high gain (K) is desired without additional damping also being available. If the peak is greater than zero decibels, the system is unstable.

The real root of the closed-loop transfer function, equation (23c), is very near the value of ω at the gain cross-over point of the open-loop transfer function (Figure 5). The other two roots of the closed-loop transfer function form a complex pair, with an undamped natural frequency near that given by equation 30a. The damping of this complex pair is a function of K'.

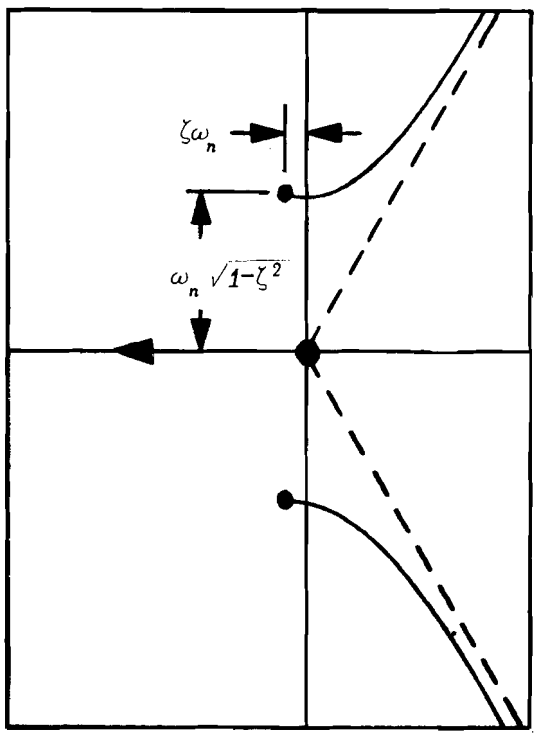

Fig. 6 - Root locus plot.

The behavior of these roots with variation in K' is shown by the root locus plot of Figure 6. The direction of changes in the roots with increase in K' is shown by the arrows; the starting points are the roots of the open loop transfer function.

It should be noted that the analysis prior to this section is quite general, whereas the assumptions and analytical conclusions of this section are dependent upon system design practice. For example, effects of compressibility are minimized on Northrop systems by elimination of most of the free air from the hydraulic oil; yet there are many existing systems where the assumptions of incompressibility and/or no load effect on valve flow would be ridiculous. For these latter systems the analysis of Parts II to IV should be used in its entirety.

***

DISCUSSION

MR. RAHN, Boeing Aircraft: *I notice you took into account the compressibility of the oil. There is no term in your equation for the spring of the oil.*

MCRUER: *In our original development, we ran some tests. Actually the basic assumption is that the way to get that factor is the motion of the cylinder relative to the piston to some point in the airplane which is greater than the motion of the piston to the airplane.*

RAHN: *We have run into trouble with high compressibility, especially with air in the oil.*

MCRUER: *It is a point that shouldn't be neglected.*

DR. CLAUSER, *Douglas Aircraft: I am very much interested in the assumption of compressibility flow. Of course, it bears on the stability, too. We have found that the implication is that if you can neglect it you have stable systems apparently even with your method. Does this mean you have tried to keep the air completely out of the system? We get instability when we put air into the system.*

MCRUER: *All that happens when you put air into the system is that the stability goes down.*

CLAUSER: *With this type of system we would get an unstable system so we have to do more to make it stable.*

MCRUER: *We can't make those assumptions unless we design it that way.*

CLAUSER: *It was mentioned yesterday that you don't have to stabilize them; they come out stable. Is that because you have some unusual technique of bleeding them or what?*

MR. FEENEY, Northrop Aircraft: *We take no particular steps at all in bleeding and what we do do is use this control leakage which keeps the pressure in the cylinder up to about half of system pressure so whatever air is in there is compressed to the point where the bulk modulus is practically that of oil.*

CLAUSER: *We have had some interesting experiences there. We even assembled a complete system under oil so that there would be no possibility of getting air in it and we still found the thing to be pretty well unstable, pretty well flexible. It can easily admit air just by changing the temperature and the solubility. Even when we run the system at pressure, we don't get the system stable.*

FEENEY: *We have purposely by cavitation admitted air into the cylinder, then turned the power on after about half a second or so. It is unstable because you have a terrific amount of vapor in there but it is immediately carried out fully, that is, almost entirely. We have no bleeding procedure beyond normal hydraulic system bleeding procedure.*

CLAUSER: *I don't remember what type packings you use. Is your packing "O" rings?*

FEENEY: *Just "O" rings.*

MCRUER: *Actually as indicated on that last slide, as the bulk modulus goes down, of course, this goes up. Also K changes and we get on our systems which show*

a step response. It wouldn't look nearly as nice as the frequency response because we actually get a small well-damped oscillation out of this thing.

CLAUSER: *What frequency is that?*

MCRUER: *This happens to be on the order of about 250. This happened to be a different system. We really guessed at the value of B but this phenomena has explained some of our earlier troubles in the lab. Of course, compressibility--as I recall some curves in the Franklin Institute Report on some measurements of compressibility--if you have more than 500 psi, the fluid, no matter the amount of air in the lines, is up to as much as 2/10 of 1 per cent, the compressibility is still about the same but below about 500 psi, it changes drastically.*

MR. DREW, Chance-Vought: *How well does your actual test experimental data compare with the last curve?*

MCRUER: *We have not compared them; however, we do have a check on the value of the natural frequency and as I said, I think we come within about 10 per cent. We don't know what the value of compressibility is.*

MR. HILL, Glenn L. Martin: *Do you feel that as a result of your analysis in further designs you can perhaps eliminate the mock-up in testing and let the figures be the criteria for setting up a stable system?*

MCRUER: *No. Actually, we have some people going through using basically this analysis on every system we design. We do make a decided effort from the time the fellow first has it down on paper so that we can get an idea of the masses involved and things of that nature. Obviously, if the first designer draws his first flow curve, we aren't in a position to tell about the stability of the system. If it is going to be stable, you can tell probably what the errors are and so forth quite nicely because as you saw, up to ten cycles, we were pretty close with that very drastic assumption. Of course, unless we know what the compressibility is, plus the inertia of the surface, the effective mass, etc., we may not be able to make a good guess. We are trying to integrate the analysis along with the actual design as far as possible.*

MR. CHATTLER, Bureau of Aeronautics: *Has your analysis helped you any? Have you made any changes?*

MCRUER: *Unfortunately, we didn't make the analysis until the system was almost perfect.*

CHATTLER: *You built a number of systems and, as I understand you, applied this theory to the last few for check purposes.*

MCRUER: *We have applied it almost invariably to systems that have been built in the past to see whether we were right in our first assumption, and in our latest production airplanes we apply it right along.*

MR. BURSTEIN, Consolidated-Vultee: *Have you been neglecting the deflection of the "O" rings in compressibility?*

MCRUER: *We realize that "O" rings act more or less as a spring. "O" rings are another pretty tough nut to crack, like the elasticity of the rubber hose.*

MR. WICK, Syracuse University: *You assume that your equation holds through the whole range of frequencies.*

MCRUER: *I don't assume that. It is all I can do. Another word of explanation on these experimental frequency plots. We were using a surface output displacement on the order of 10 degrees and the only reason we have gone to that model is to get rid of non-linearities in our simulated hinge moment.*

MR. ALTMAN, AMC: *I would like to direct a question if I might to Mr. Rahn of Boeing in connection with the comments he made before, that he experienced a spring effect with high inertia surfaces. What was the inertia of your surface?*

RAHN: *It varies with the airplane, of course, but we have had surfaces from 60,000 pound inches squared to about, I believe, up to something like four million. What was the inertia that you were working with?*

MCRUER: *Actually this experimental stuff was on the order of 89. To tell you the truth, I've forgotten.*

RAHN: *The inertia on the rudder for the B-50 is around 130,000 pounds and on the B-47 is 60,000.*

MCRUER: *Pretty close to the B-37.*

RAHN: *We also found we had to take into account the expansion of the cylinder walls and the compressibility of the springs and the rod itself.*

APPLICATION OF FREQUENCY RESPONSE TECHNIQUES TO THE AILERON CONTROL SYSTEM OF THE F-86A AIRPLANE

By

William R. Monroe

North American Aviation, Inc., Los Angeles, California

Abstract

The methods currently being applied to the stability problem of the artificial feel system of the F-86A aileron control system are presented. The analytical phase consists of setting up differential equations describing the dynamics of the control system and determining the system transfer function. In the experimental phase the method used for determining the transfer function of the airplane system is discussed. The problems encountered in both phases are discussed and proposed solutions are indicated.

The results of the program have not yet been analyzed; consequently no definite stability changes are presented.

Introduction

During recent years, as the power requirements for airplane surface control systems have increased, the standard aircraft design techniques have steadily grown less effective. The most outstanding example of the limitations of a static design approach is that of system oscillation which is also referred to as chatter, buzz, motoring, etc. This kind of oscillation may be very serious and, if unrestrained, may continue to increase in amplitude until the airplane system is destroyed.

The first methods applied at North American Aviation to this problem consisted of cut and try techniques supported by engineering logic. This method, which has proven very effective in solving many problems is not generally successful when applied to a servomechanism such as a boost system. For example, the cut and try approach is limited as follows:

1. Satisfactory results depend to a large extent on engineering experience which is very limited as far as dynamics of boosted surface control systems are concerned.
2. With a boost system, one successful cut and try solution will not necessarily prove successful when applied to a different system.
3. Because of the extremely complicated nature of the system, it is almost impossible to evaluate, classify, and remember all observations. Thus valid engineering experience is difficult to gain.
4. Cut and try techniques do not show the degree of stability. Consequently a near solution might not be recognized and any definite solution obtained by this means might penalize system performance beyond requirements.

In 1948 North American began to investigate the dynamics of the problem by applying Rough's stability criterion to the load feel valve portion of an aileron boost

system. This resulted in the addition of a dash pot to the valve with subsequent elimination of oscillation in the valve alone - but the entire system remained oscillatory. Because of the complexity of the system, no analysis of the entire system was ever completed. During this investigation it had been almost impossible to obtain reliable values of the system constants; many were estimated or roughly determined in the laboratory. Consequently it was evident that if any future work were to be conducted, it would be necessary to conduct a basic research program to determine the fundamental characteristics of hydraulic systems.

A contract for this purpose was obtained from the Air Material Command in July 1948 and this work is still in progress. The general subjects being investigated consist of fluid flow phenomena, system elasticity, damping, and special components such as valves and pumps.

As soon as this basic research program was progressing satisfactorily, emphasis was placed on improving the means for investigating the oscillations in boost systems. At this point application of the frequency response technique was first actively applied to airplane surface control systems at North American Aviation. The work was started early in 1949 with part-time work of one man and was built up gradually to five men in May and to 13 men at the present time.

The Servomechanism Group is at present engaged in analyzing the aileron system of the F-86A and the B-45A airplanes. The backlog of work consists of an analysis of practically all of the control surfaces of all current North American Aviation airplanes.

The activities of the group encompass only the improvement of the stability and performance of present systems. At present, no effort is being made to influence preliminary design. As a consequence no work on designing a new system has been done by the Servomechanism Group.

Description of the F-86A Artificial Feel Aileron Control System

When servomechanism techniques were first applied to the F-86A, the airplane was equipped with an artificial feel aileron system. Subsequently the system was changed to a load feel type which now constitutes the F-86A aileron system. This paper is exclusively concerned with the stability analysis of the artificial feel aileron system which is shown schematically in Fig. 1a.

With the system shown in the figure a downward motion of the stick deflects the artificial feel spring and causes the stick point on the walking beam to move upward. Since the artificial feel valve is balanced no force can be statically applied to the walking beam. Consequently any force at the stick is determined by the artificial feel spring. Thus any force applied by the pilot to the stick is directly changed into a displacement of the stick and the stick point on the walking beam. Once the stick point is shifted, the walking beam must reach a new equilibrium orientation determined by the position of the sector point which is statically equivalent to aileron position. The new equilibrium position is obtained as follows: As the stick is deflected the valve point is rotated about the sector point. The valve, Fig. 1b, is an open center type provided with constant flow rate. Thus the deflection of the valve arm causes a pressure drop to be applied across the actuating piston. The

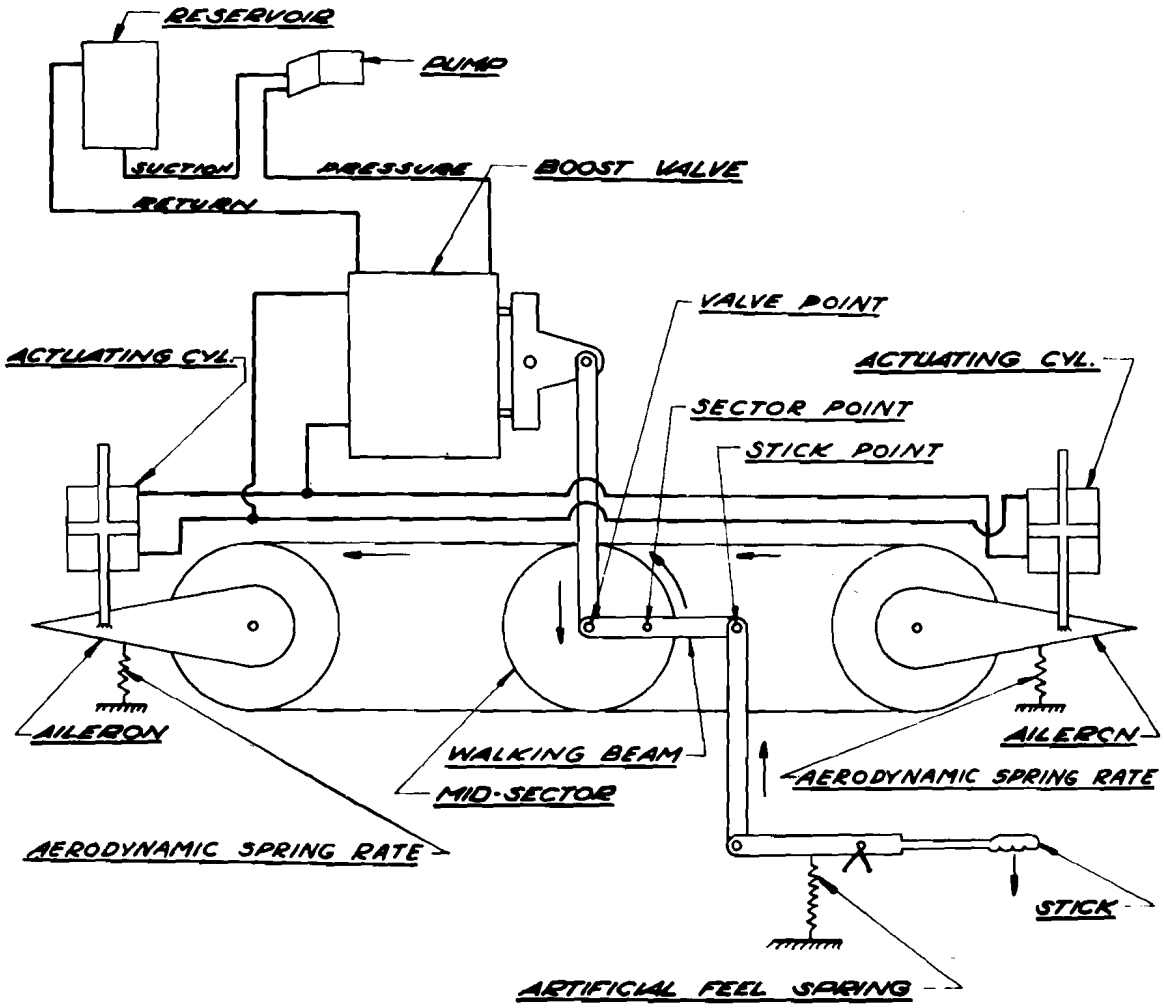

SCHEMATIC DIAGRAM OF
F 86A ARTIFICIAL FEEL AILERON SYSTEM
FIG. 1a

aileron (sector point) then moves the walking beam and with the stick held in a given position this action moves the walking geam valve point until the aileron is in such a position that the load is balanced by the pressure drop across the piston. Under static conditions this action does not affect the stick force or position. However, any new force applied to the aileron moves the aileron (sector point) and the valve causing additional pressure to be applied to the actuating piston until the load is again balanced.

The system described has the following general characteristics:

(1) Artificial Feel - The static force at the stick has no component resulting from output load.

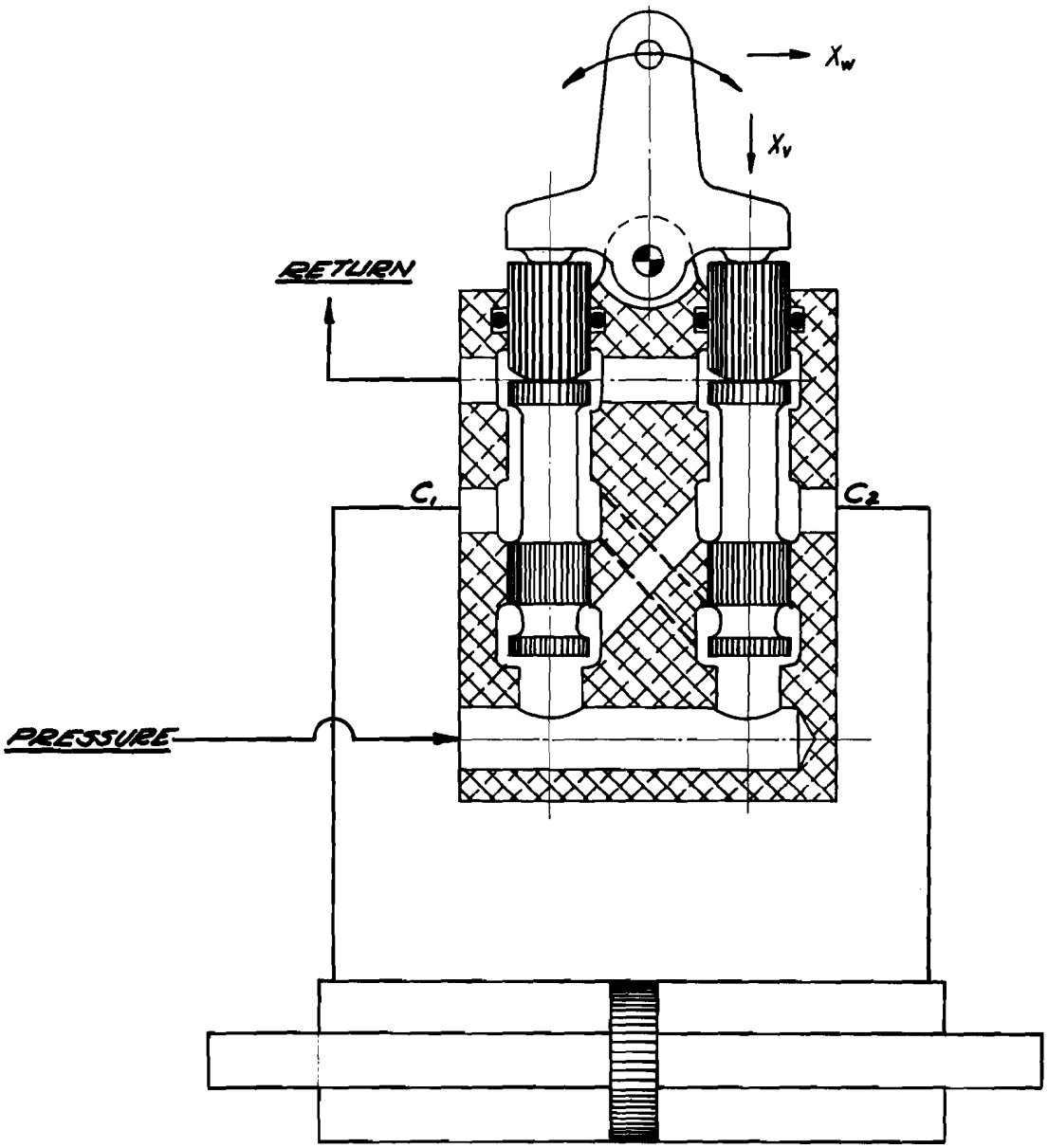

SCHEMATIC DIAGRAM OF BOOST VALVE
FIG. 16

(2) Reversible - The actuating piston is reversible since a change in load can cause the piston to move. The valve is statically irreversible since any change in valve output (pressure) does not affect valve input displacement.

(3) Open Center - With the valve in neutral the hydraulic fluid flows freely through the valve and thus the entire system is at return line pressure unless the ailerons are being operated.

Application of Frequency Response Techniques to the F-86A Airplane

Application of frequency response techniques to the F-86A airplane consists of four phases.

Phase I: Experimental determination of the frequency response characteristics of the airplane system. The purpose of Phase I is to verify the validity of the stability criterion on an actual airplane, to determine the reproducibility of open loop tests, to evaluate and improve instrumentation and equipment, and to determine the frequency response characteristics of the airplane system for comparison with the analysis and simulator results.

Phase II: An analytical study to develop an equation for the frequency response characteristics of the system. This phase includes evaluation of all pertinent system constants. The results of this analysis will facilitate intelligent use of the results of Phase I.

Phase III: Application of the results of Phases I and II to a simulator. This phase will make possible testing of improvements indicated by Phases I and II so that a screening process can be conducted without requiring the use of an airplane.

Phase IV: Application of the results of the first three phases to an airplane for ground and flight tests.

Discussion of Phase I

Experimental Determination of Frequency Response Characteristics of the System

In order to evaluate the stability of the airplane it is necessary to determine in some manner the open loop transfer function of the system. Because of difficulties of opening the servo loop, closed loop tests were first considered. However it was decided that any closed loop tests would either result in exciting the natural mode of oscillation of the system or restrict the system to the extent of altering its characteristics. This conclusion is indicated by two facts:

(1) The only unquestionable point at which a closed cloop system can be driven by a sine wave displacement generator is at some point normally having infinite impedance when seen by the rest of the system, for example, at some point normally grounded.

(2) Driving at a point normally having infinite impedance will not confine an unstable system to follow the sine wave generator but will tend to excite the system and start the natural oscillation.

For these reasons all frequency response tests with the F-86A have been conducted with the system in the open loop configuration.

The major problem of determining a method of opening the servo loop without changing the system characteristics was solved by the arrangement shown in Fig. 2.

SCHEMATIC DIAGRAM OF OPEN LOOP ARRANGEMENT

FIG.2

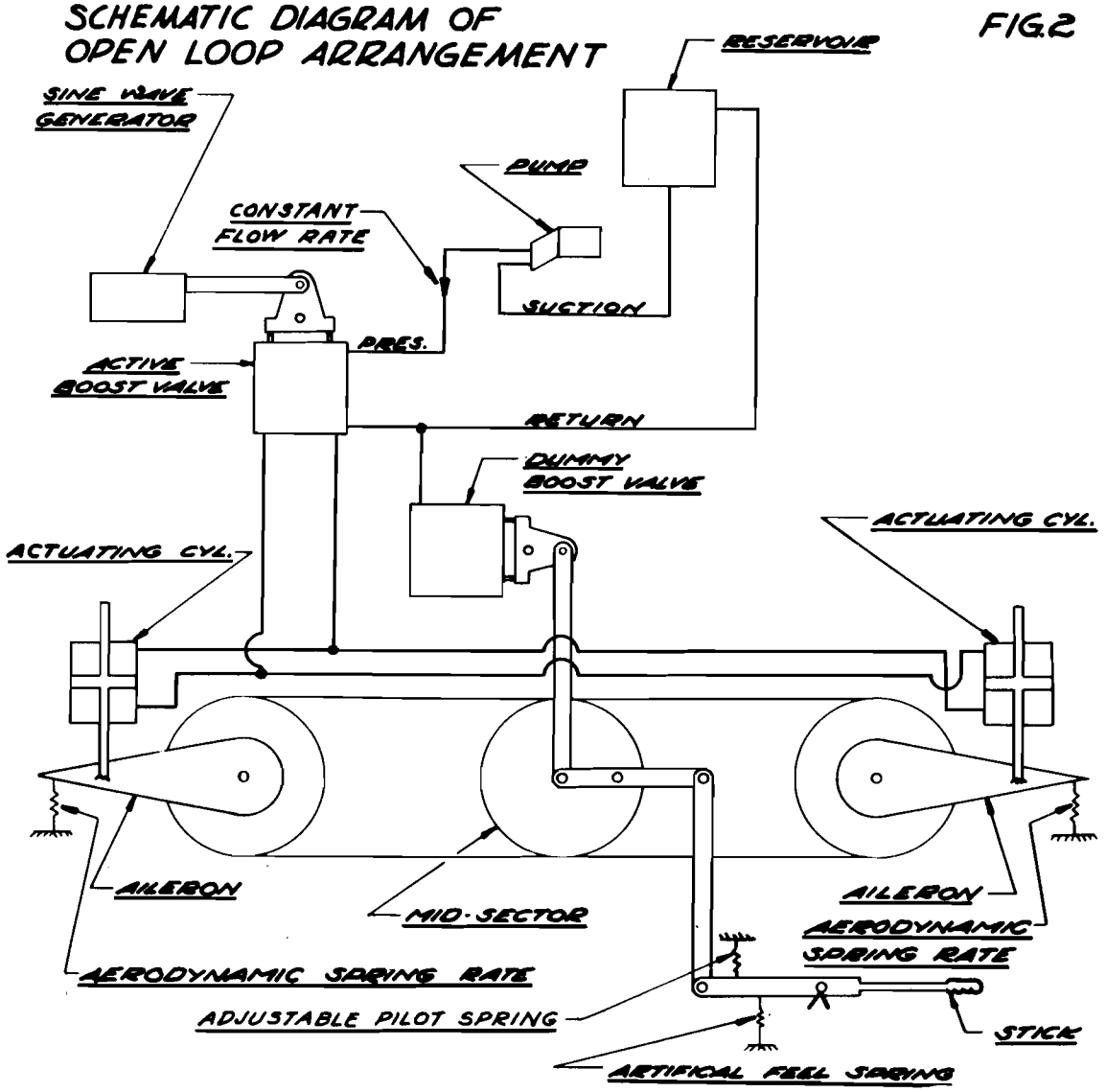

In this figure the system is connected in a normal manner with the following exceptions:

(1) All of the hydraulic lines to the boost valve were removed and connected to a similar "active " boost valve mounted on a sine wave displacement generator.

(2) The "dummy" boost valve remaining in the airplane was connected to the return line so that the "0" rings are pressurized to provide the same damping present in the normal system. All mechanical connections to the dummy valve are the same as in the normal system. This dummy valve is intended to simulate the valve dynamic impedance of the closed loop system.

In order to make open loop tests with any average position of the ailerons other than neutral, it was necessary to simulate the pilot by means of a spring. Without this spring any average position of the aileron except neutral would tend to deflect the artificial feel spring which would in turn cause the dummy valve arm to move until, with an aileron deflection of 0.4 deg, the valve arm contacts the stops. With the pilot spring the stick position can be adjusted to its correct position for a given aileron position and load.

To simulate aerodynamic hinge moment, torsion springs were attached to artificial ailerons having the same moment of inertia as the actual ailerons. This installation is shown in Fig. 3a and 3b. Three sets of springs were provided to cover a range of speeds and altitudes consistent with airplane performance.

Aerodynamic damping was neglected on the basis that as far as stability is concerned, positive output damping would be helpful. Consequently neglecting aerodynamic damping is a conservative assumption.

The sine wave displacement generator for driving the active valve consisted of a scotch yoke driven by a hydraulic power supply. The frequency, average position, and amplitude of the output are adjustable. The active valve mounted on the sine wave generator is shown in Fig. 4a and 4b. Strain gages were used to measure instantaneously stick, sector, active valve, aileron, and dummy valve positions. Dynamic pressure pickups were installed to measure pressures at all valve ports and at both ports of the right hand aileron cylinder.

Airplane tests were conducted as follows:

Part I - Calibration

With the closed loop configuration and with boost power on, the aileron, sector, and boost valve positions were measured for various stick deflections with different load springs and different pump flow rates. This was necessary because of the non-linearities of the system. With this information it was possible to adjust the open loop system so that in all tests correspondence with a closed loop configuration could be assured.

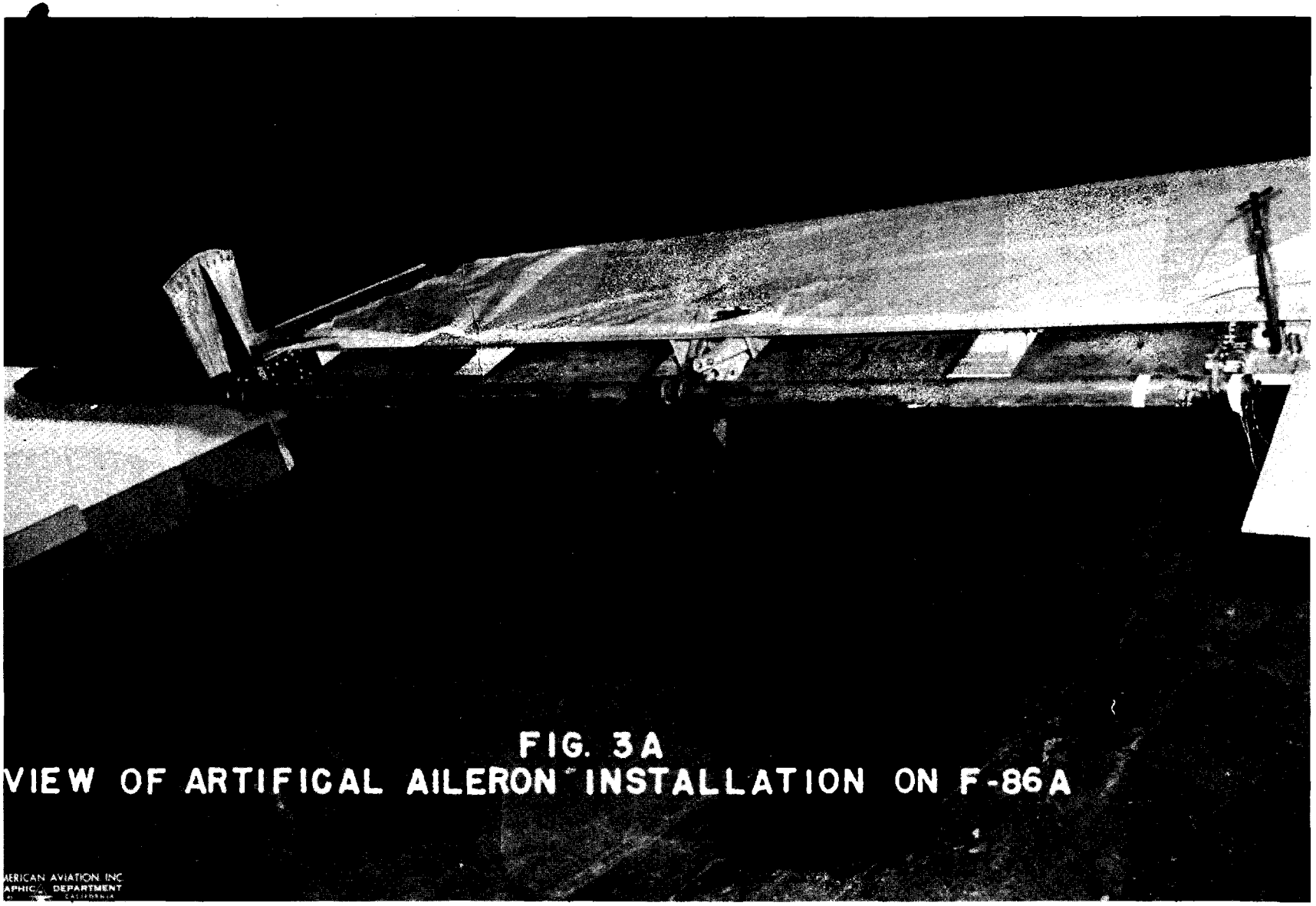

FIG. 3A
VIEW OF ARTIFICAL AILERON INSTALLATION ON F-86A

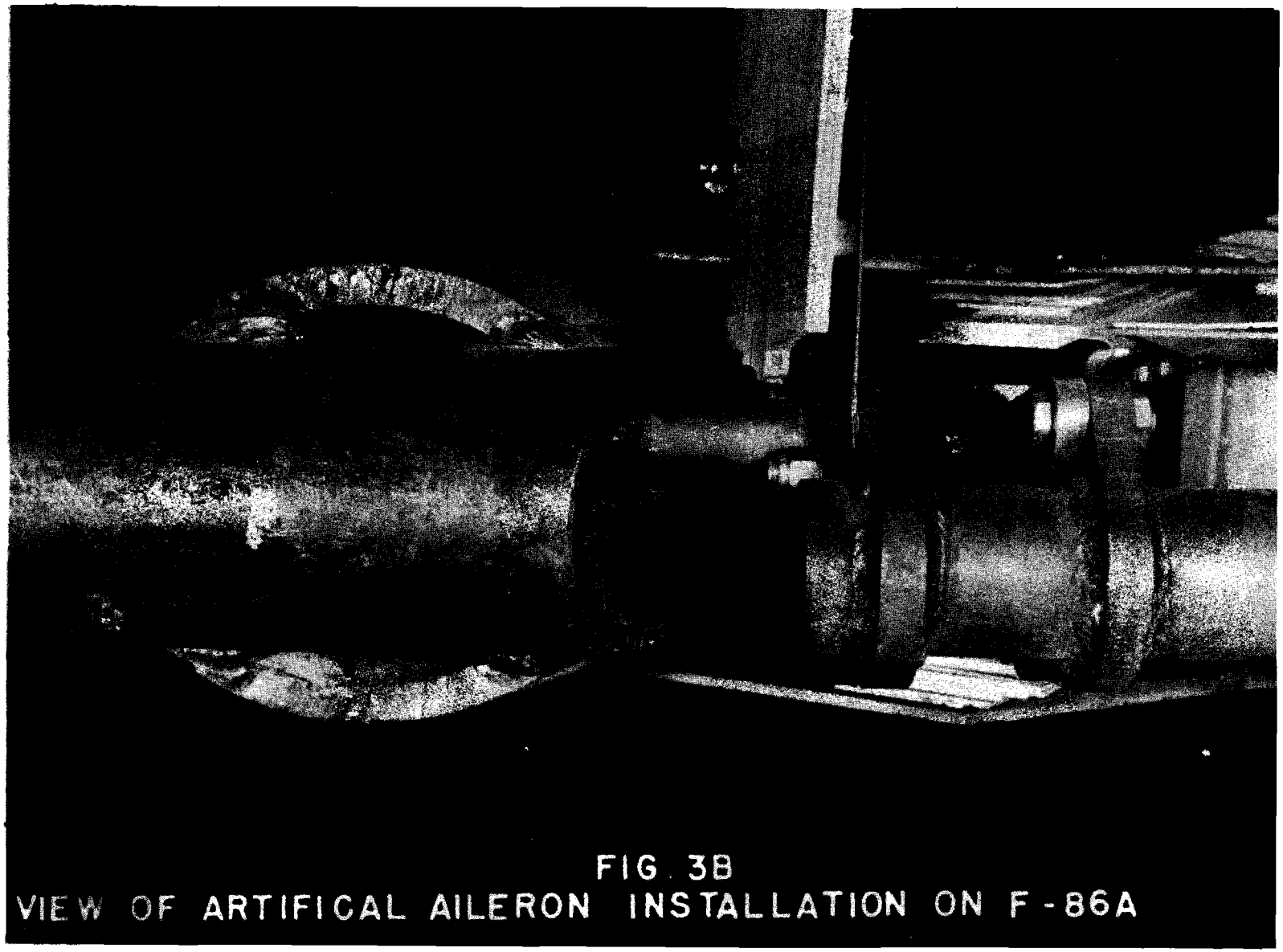

FIG. 38
VIEW OF ARTIFICAL AILERON INSTALLATION ON F-86A

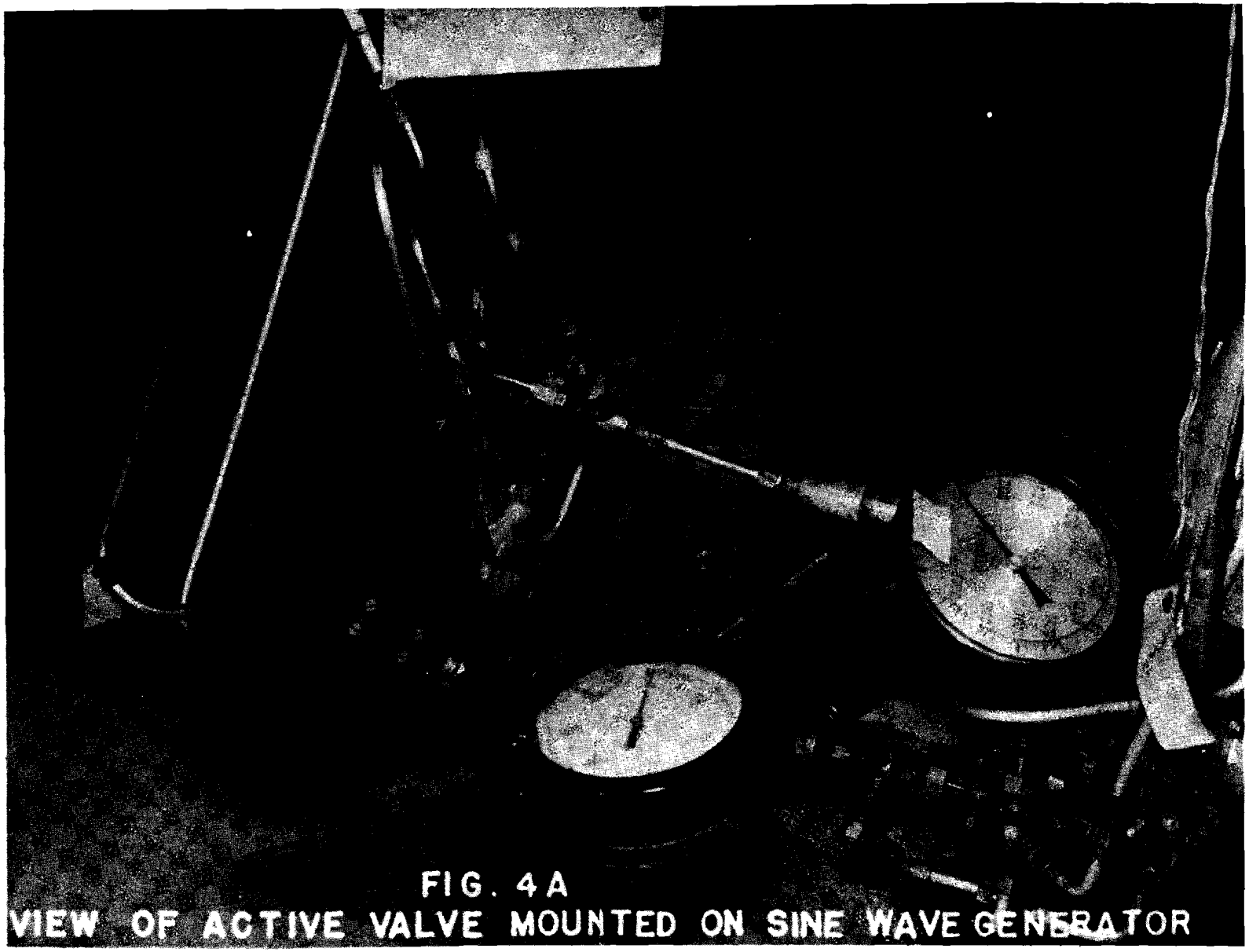

FIG. 4A
VIEW OF ACTIVE VALVE MOUNTED ON SINE WAVE GENERATOR

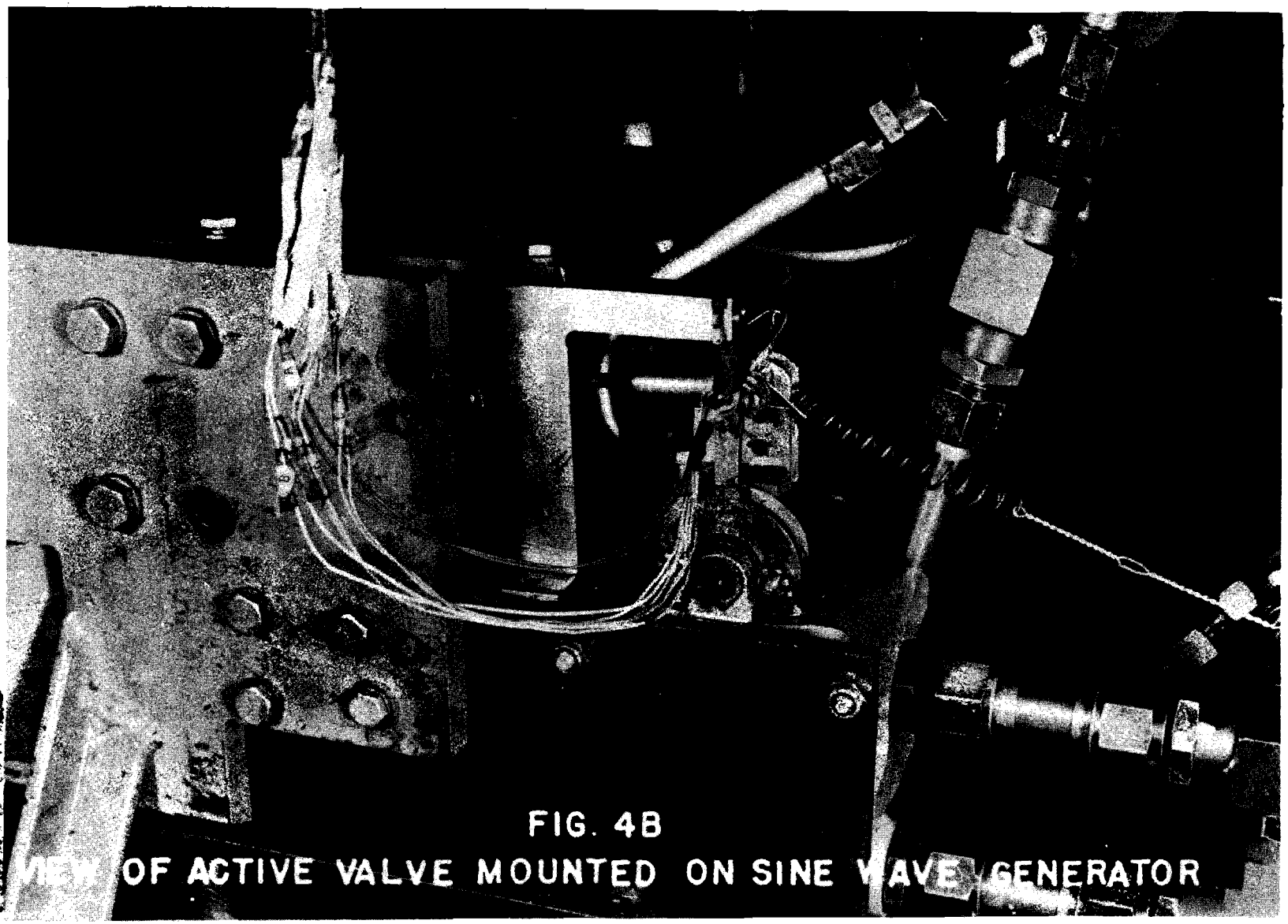

FIG. 4B

VIEW OF ACTIVE VALVE MOUNTED ON SINE WAVE GENERATOR

[redacted]

Part II - Stability Criterion Validity

With the loop closed, the flow rate was reduced until the system would no longer oscillate indefinitely. No precise point separating a stable case from an unstable case can be obtained, but this test was conducted to obtain a rough check of the stability of the closed loop system against the stability criterion obtained with the open loop system.

Part III - Stability Criterion Validity and Reproducibility

This part consisted of several determinations of the open loop frequency response of a slightly stable case observed in Part II. The results of this test (Fig. 5a) indicate that

(1) The open loop tests seem to be reproducible. It may be necessary to modify this statement as additional results are plotted.

(2) The transfer function checks roughly with the results of Part II which are illustrated with the oscillograph record of Fig. 5a.

Part IV - Frequency Response Characteristics

These tests were conducted to determine system transfer functions with different aileron positions, flow rate, hydraulic tubing sizes, stick inertias, pilot spring rates, and aerodynamic spring rates. One unstable configuration is depicted in Fig. 5b where both open loop transfer functions and closed loop oscillograph records are presented. Typical open loop oscillograph records are shown in Fig. 5c.

In addition to these variables, small and large valve amplitudes were used since it was found impractical to restrict the system amplitude to a range that could be considered linear.

In conducting the open loop tests, several difficulties were encountered:

(1) Because of wear, the sine wave generator backlash increased until the sine wave form became so poor that it was necessary to add an anti-backlash spring. In addition to this, any adjustments of amplitude proved to be difficult and awkward. In work of this kind it is essential that the sine wave generator have extremely low backlash and that both amplitude and average position be easily and independently adjustable.

(2) Strain gage failures were frequent and were the cause of serious delays in the test program.

(3) Extreme non-linearities caused by valve and sector stops were troublesome at first but accurate adjustment of the system eliminated this difficulty.

[redacted]

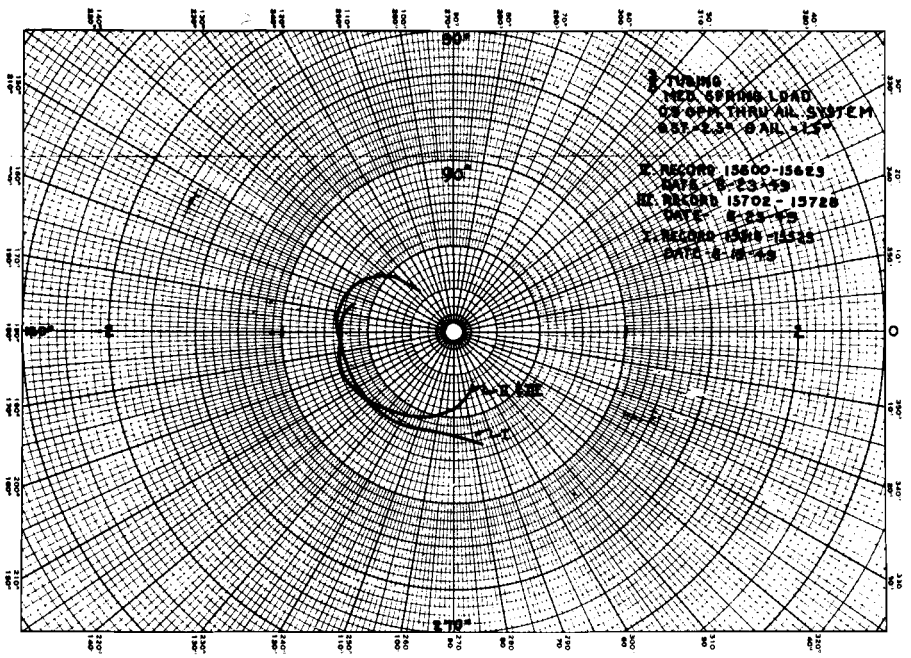

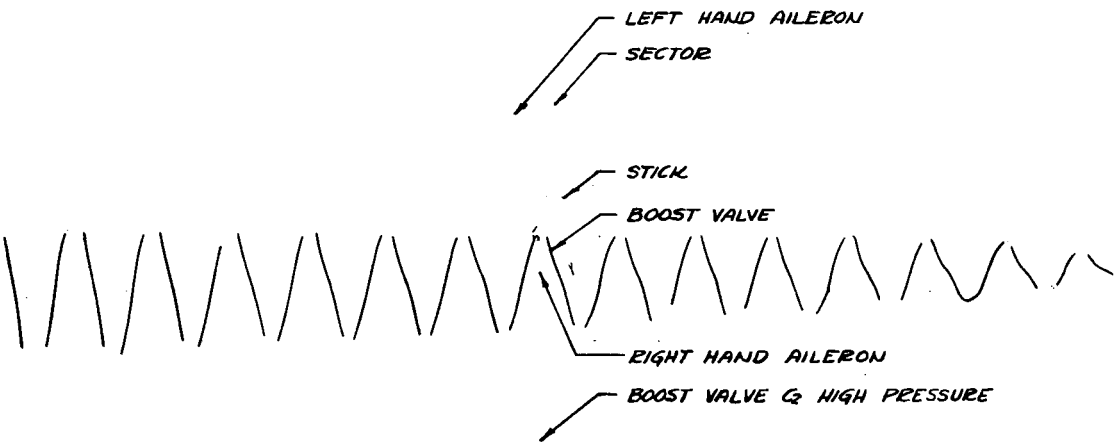

OPEN LOOP EXPERIMENTAL TRANSFER FUNCTION AND
CLOSED LOOP OSILLOGRAPH RECORD
OF A STABLE CONFIGURATION

FIG. 5a

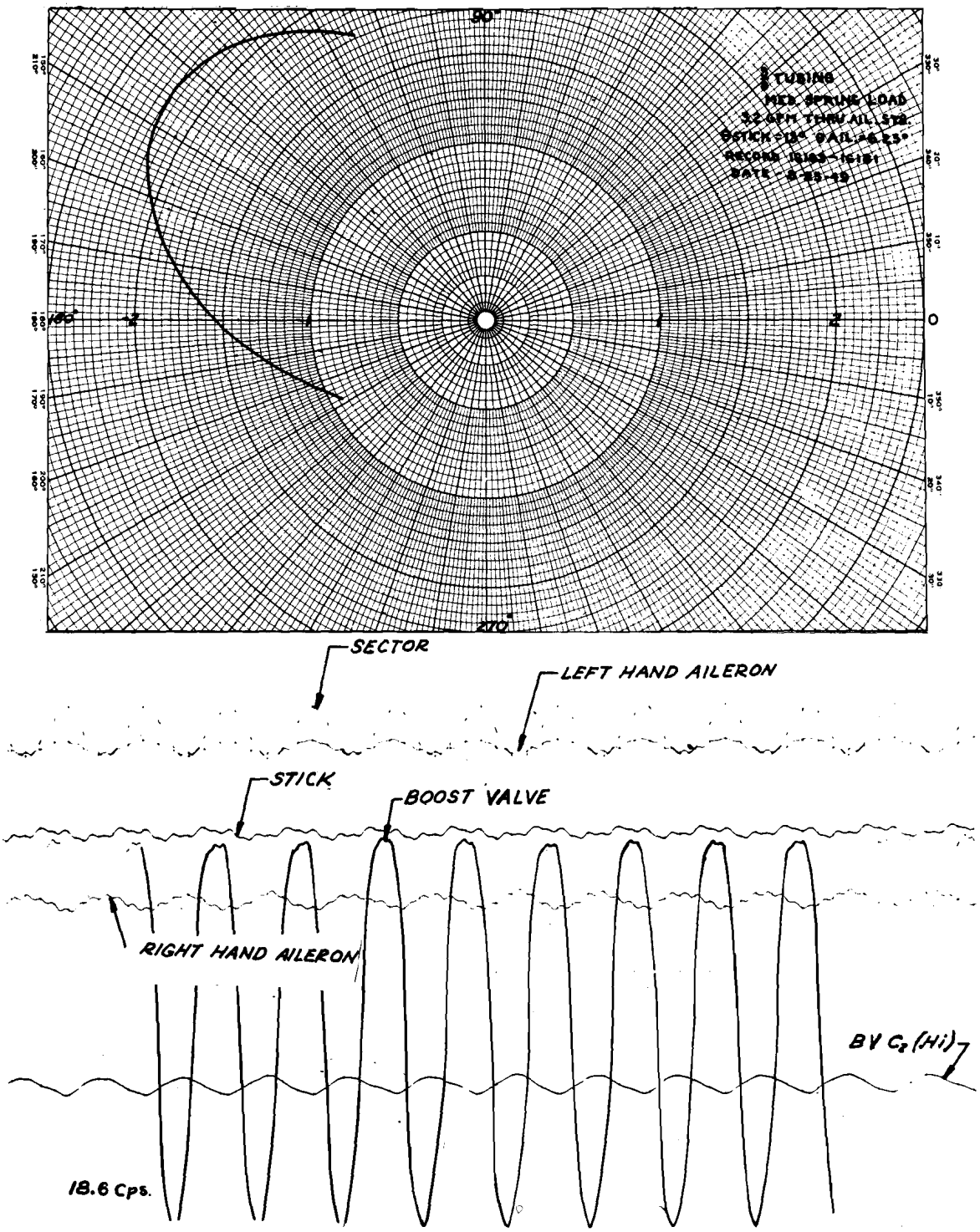

OPEN LOOP EXPERIMENTAL TRANSFER FUNCTION AND CLOSED LOOP OSILLOGRAPH RECORD OF AN UNSTABLE CONFIGURATION

FIG. 5b

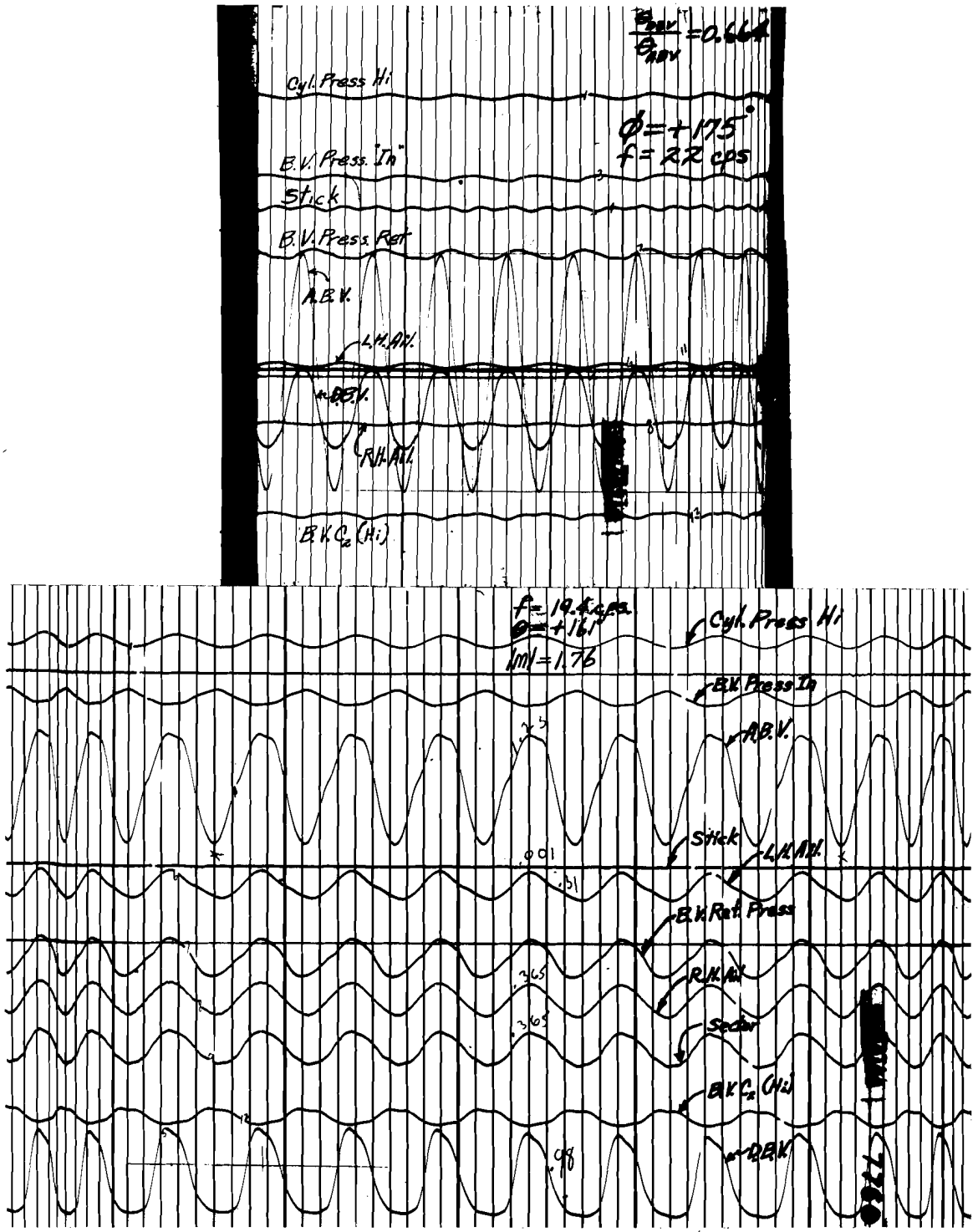

TYPICAL TRANSFER FUNCTION OSCILLOGRAPH RECORDS

FIG. 5c

(4) It was impossible to use input amplitudes small enough to be considered linear since such a small input was absorbed in backlash in the system. This difficulty is inherent in any system with a valve stroke in the order of a thousandth of an inch and with system backlash of the same order of magnitude. Consequently larger amplitudes were used in most tests.

The oscillograph records of these tests are currently being studied and plots of transfer functions have not yet been made.

Analytical Determination of Frequency Response Characteristics of the System

The open loop arrangement of Fig. 2 can be simplified as shown in Fig. 6a and 6b if the ailerons are replaced by a single output member. In Fig. 6b the transfer function relating the aileron angle, θ_a, to input active valve arm position X_{va}, is called μ_1.* The remainder of the open loop can be represented by μ_2, the transfer function relating the dummy valve arm displacement to aileron angle θ_a. Thus the entire open loop transfer function is represented by the function,

$$\mu = \mu_1 \mu_2$$

The following pages of this paper are concerned with determining analytically the transfer functions μ_1 and μ_2 and their product $\mu_1\mu_2$. All variables are considered as variations from average and the LaPlace transform is designated by $f(s)$ except in long equations where the letter s is omitted. Throughout the stability analysis the initial condition operator is neglected.

(1) Determination of $\mu_2(s) = \dfrac{X_{dv}(s)}{\theta_a(s)}$

The transfer function $\mu_2(s)$ describing that part of the system shown between θ_a and X_v in Fig. 3b may be determined from the following equations:

$$F_{se} = F_s + F_v \tag{1}$$

$$l_2 F_s = l_3 F_v \tag{2}$$

$$F_{se} = K_c(C_4 X_{ee} - \theta_a) \tag{3}$$

$$F_s = (K_s + M_s s)\, X_s \quad ; \quad \text{if } D_s = 0 \tag{4}$$

* *The transfer function is a complex function representing the ratio of the LaPlace transform of the two variables. This is discussed thoroughly in several texts such as "Principles of Servomechanisms" by G. S. Brown and D. P. Campbell, John Wiley and Sons, New York, 1948.*

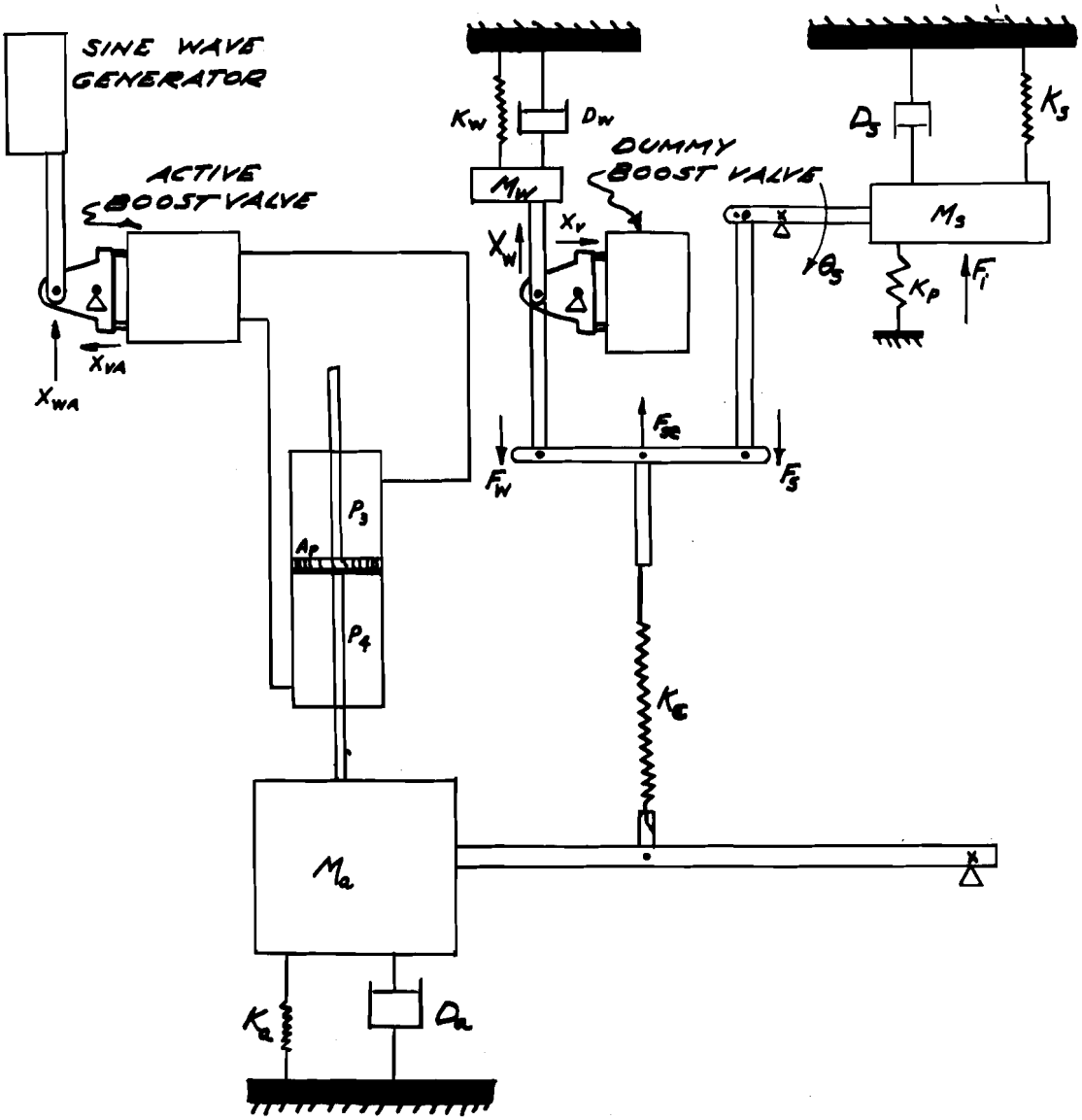

SIMPLIFICATION OF THE OPEN LOOP
ARRANGEMENT OF FIG. 2

FIG.6a

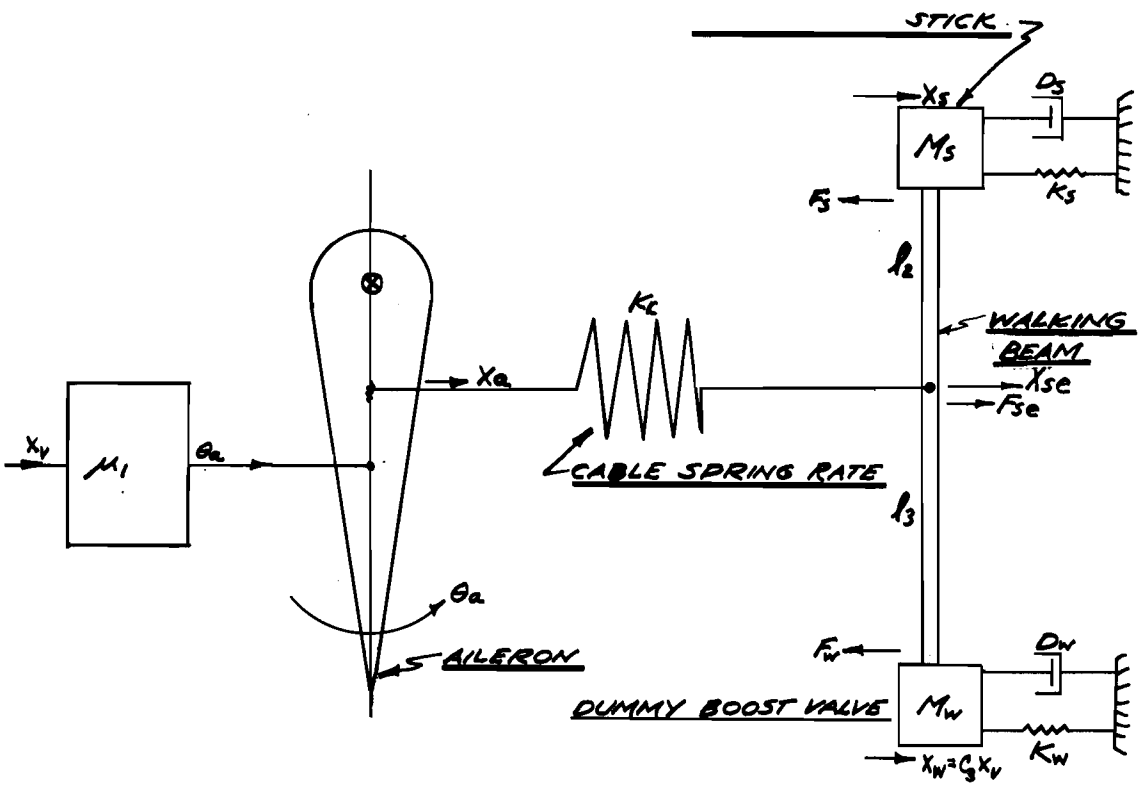

1. $F_{Se} = F_S + F_W$
2. $l_2 F_S = l_3 F_W$
3. $F_{Se} = K_C (C_4 X_{Se} - \theta_a)$
4. $F_S = (K_S + M_S S^2) X_S$ IF $D_S = 0$
5. $F_W = (K_W + D_W S + M_W S^2) X_W$
6. $X_{Se} = \frac{l_3}{l_2 + l_3} X_S + \frac{l_2}{l_2 + l_3} X_W = L_2 X_S + L_1 X_W$

$$\mu_2 = \frac{X_V}{\theta_a} = \frac{C_3 X_W}{\theta_a} = \frac{C_3 K_C (K_S + M_S S^2)}{L_3 (K_C C_4 L_2 - K_S - M_S S^2)(K_W + D_W S + M_W S^2) + (K_C C_4 L_1 - K_W - D_W S - M_W S^2)(K_S + M_S S^2)}$$

FIG. 6b FURTHER SIMPLIFICATION OF FIG. 2 TO SHOW THE μ_2 SYSTEM

$$F_v = (K_v + D_v s + M_v s^2)\, X_v \tag{5}$$

$$X_{ve} = \frac{l_3}{l_2+l_3} X_a + \frac{l_2}{l_2+l_3} X_v = L_2 X_a + L_1 X_v \tag{6}$$

$$X_v = C_3 X_v \tag{7}$$

Solving these seven equations for $X_v(s)/\theta_a(s)$ yields the following:

$$\mu_2 = \frac{C_3 K_c (K_a + M_a s^2)}{L_3 (K_c C_4 L_2 - K_a - M_a s^2)(K_v + D_v s + M_v s^2) + (K_c C_4 L_1 - K_v - D_v s - M_v s^2)(K_a + M_a s^2)}$$

where

$$L_3 = \frac{l_3}{l_2}$$

The constants involved in this equation were determined and the transfer function has been plotted.

(2) Determination of $\mu_1(s) = \dfrac{\theta_a(s)}{X_{va}(s)}$

This part of the system is shown schematically in Fig. 7a where the ailerons are clamped together to indicate that they are treated as a single output member. The network equivalent of the two aileron systems of Fig. 7a is shown in Fig. 7b. This figure shows two ailerons to simplify the determination of the system elements as the reduction to a single output system is carried out. In the figure each hydraulic line has been represented by a single equivalent electrical "T" network consisting of resistance (fluid friction), inductance (fluid inertia), and capacity (elasticity). This representation is an approximation of an infinite number of such "T" networks (APPENDIX I). Calculation has shown that for the lines used in this system this assumption introduces a very small error (APPENDIX II).

The actuating cylinders have been represented by a leakage resistance in parallel with an impedance consisting of an inductance (aileron and piston inertia), resistance (output damping), and capacity (aerodynamic spring rate).

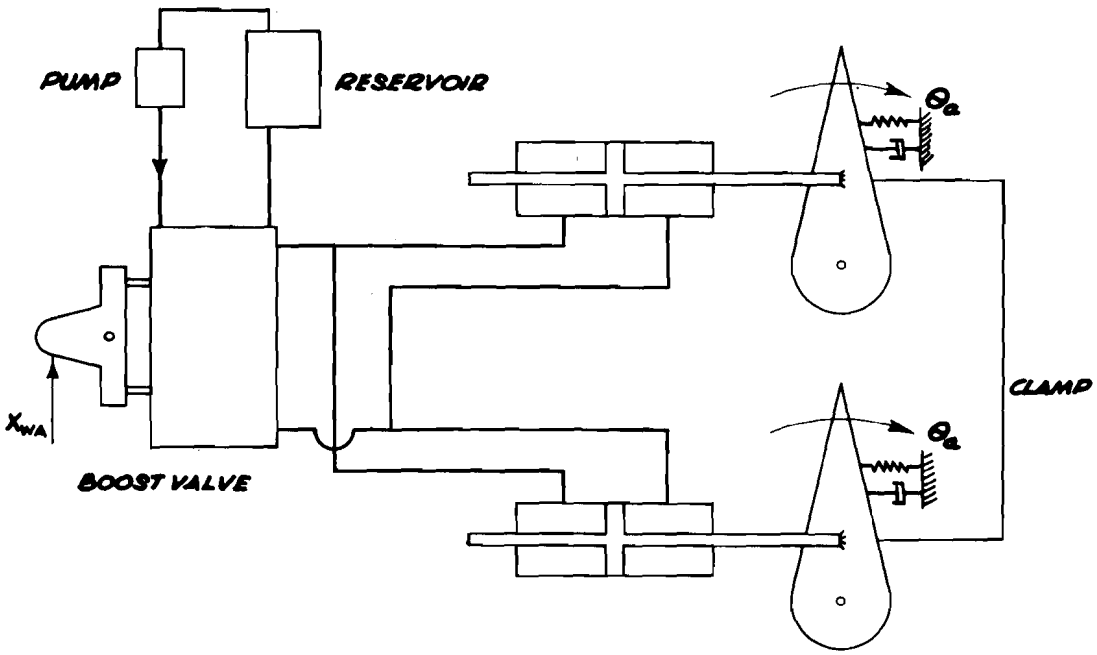

SCHEMATIC DIAGRAM SHOWING μ_1 SYSTEM
FIG. 7a

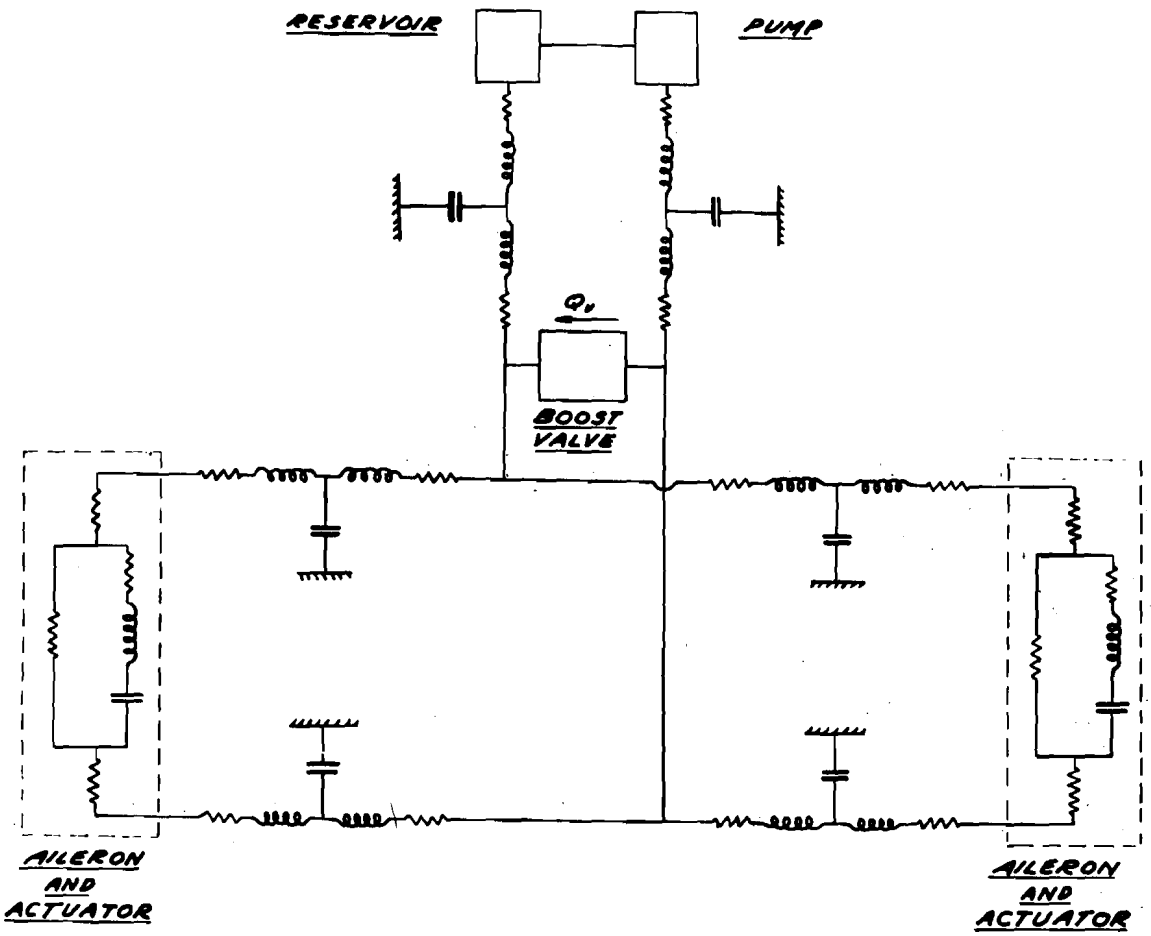

SCHEMATIC DIAGRAM SHOWING NETWORK EQUIVALENT TO M_1 SYSTEM

FIG. 7b

In Fig. 7b the active boost valve is represented by a block. The orifice flow rate as a function of pressure drop and valve displacement is shown in Fig. 8. The constants C_{30} and C_{40} for this valve equation have been evaluated experimentally.

In a further simplification the system has been reduced to that shown in Fig. 9 in which the left and right ailerons have been combined into a single system with proper choice of values of the constants. In this figure the aileron impedance of one aileron is called $2Z_1$.

Conducting a nodal circuit analysis of Fig. 9 and considering variations from average values we obtain the following transform equations:

$$0 = \frac{P_0 - P_1}{Z_9} + C_1 s P_0 \tag{1}$$

(since flow from the pump is constant)

$$\frac{P_0 - P_1}{Z_9} = C_{30}(P_1 - P_3) + C_{40} X_{va} + \frac{P_1 - P_2}{Z_e} \tag{2}$$

$$\frac{P_1 - P_2}{Z_e} = \frac{P_2 - P_3}{2Z_e} + C_2 s P_2 \tag{3}$$

$$\frac{P_2 - P_3}{2Z_e} = \frac{P_3 - P_4}{R_l} + A_p s X_p \tag{4}$$

$$\frac{P_3 - P_4}{R_l} + A_p s X_p = \frac{P_4 - P_5}{Z_e} + C_2 s P_4 \tag{5}$$

$$\frac{P_5 - P_6}{Z_e} = \frac{P_4 - P_5}{Z_e} + C_{30}(P_1 - P_5) + C_{40} X_{va} \tag{6}$$

$$\frac{P_5 - P_6}{Z_e} = \frac{P_6}{Z_e} + C_3 s P_6 \tag{7}$$

$$\frac{P_3 - P_4}{Z_1} = A_p s X_p \tag{8}$$

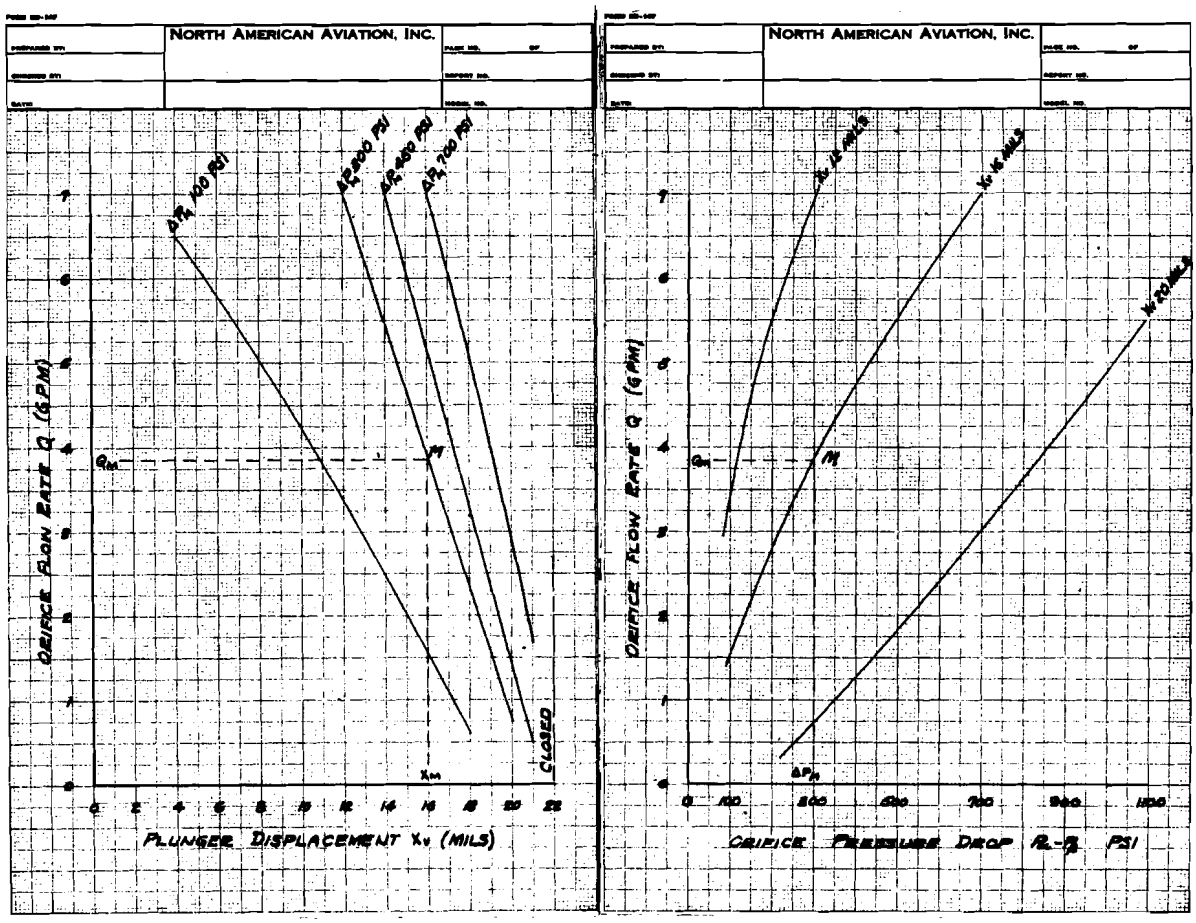

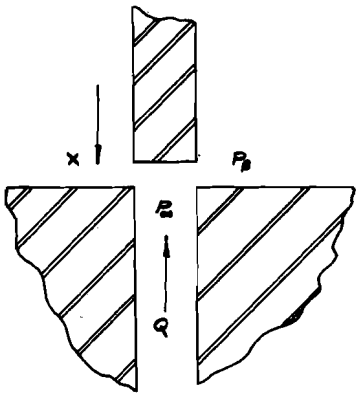

FOR THE VALVE ORIFICE

$Q = f(X, P_a - P_b)$

WITH dQ, dX, $dP_a - dP_b$ REPRESENTED AS q, x AND ΔP

$$q = \left(\frac{\partial Q}{\partial X}\right) x + \left(\frac{\partial Q}{\partial (P_a - P_b)}\right) \Delta P$$

FOR A SMALL RANGE

$q \cong C_{40} x + C_{30} \Delta P$

WHERE $C_{30} = \frac{\partial Q}{\partial (P_a - P_b)}$ AND $C_{40} = -\left(\frac{\partial Q}{\partial X}\right)$

MUST BE EVALUATED AT THE OPERATING POINT, M.

FIG. 8 BOOST VALVE CHARACTERISTICS

SIMPLIFIED NETWORK EQUIVALENT TO M_1 SYSTEM FIG. 9

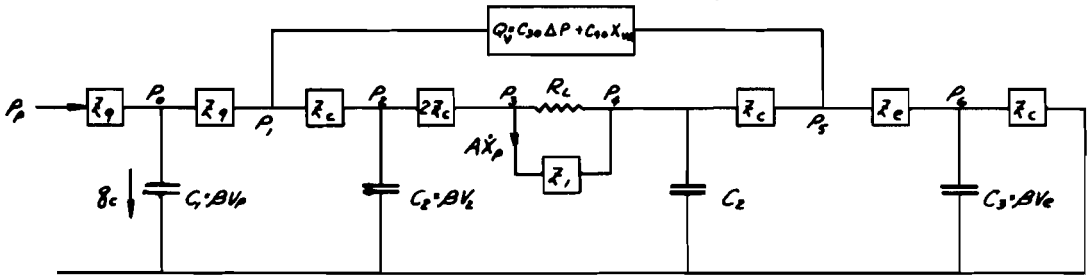

$C = \beta V$ = ELASTICITY OF FLUID IN TUBE
WHERE: $\beta = -\frac{\Delta V}{V}/\Delta P$ = ELASTIC CONSTANT
V = VOLUME OF TUBE

$2Z = 2R + j2L\omega$
WHERE: $2R$ = RESISTANCE OF TUBE
$2L = \frac{\rho}{A}\ell$ = INDUCTANCE OF TUBE OF LENGTH ℓ
WHERE: ρ = MASS DENSITY OF FLUID
A = AREA OF TUBE

$2Z_1$ = IMPEDANCE OF ONE AILERON = $\frac{P_3 - P_4}{A_p S X_p}$

$q_c = \beta V_p P_0^\circ$
$q_c(s) = \beta V_p S P_0(s)$

IN THESE EQUATIONS ALL VARIABLES REPRESENT VARIATIONS FROM AVERAGE VALUES

1. $0 = \frac{P_0 - P}{Z_g} + C_1 S P_0$ SINCE FLOW FROM PUMP IS CONSTANT
2. $\frac{P_0 - P_1}{Z_g} = C_{30}(P_1 - P_3) + C_{e0}X_{in} + \frac{P_1 - P_2}{Z_c}$
3. $\frac{P_1 - P_2}{Z_c} = \frac{P_2 - P_3}{2Z_c} + C_2 S P_2$
4. $\frac{P_2 - P_3}{2Z_c} = \frac{P_3 - P_4}{R_L} + A_p S X_p$
5. $\frac{P_3 - P_4}{R_L} + A_p S X_p = \frac{P_4 - P_5}{Z_c} + C_2 S P_4$
6. $\frac{P_4 - P_5}{R_L} + C_{30}(P_1 - P_5) + C_{e0}X_{in} = \frac{P_5 - P_6}{Z_e}$
7. $\frac{P_5 - P_6}{Z_e} = \frac{P_6}{Z_c} + C_3 S P_6$
8. $A_p S X_p = \frac{P_3 - P_4}{Z_1}$

1. $0 = (1 + C_1 S Z_g) P_0 - (1) P_1$
2. $(C_{e0} Z_g Z_c) X_{in} = (-Z_c) P_0 + (Z_g + Z_c + Z_g Z_c C_{30}) P_1 - (Z_g) P_2 - (Z_g Z_c C_{30}) P_5$
3. $0 = -(2) P_1 + (3 + 2C_2 Z_c S) P_2 - (1) P_3$
4. $0 = -(R_L) P_2 + (2Z_c + R_L) P_3 - (2Z_c) P_4 + (2Z_c R_L A_p S) X_p$
5. $0 = (-Z_c) P_3 + (R_L + Z_c + R_L Z_c C_2 S) P_4 - (R_L) P_5 - (R_L Z_c A_p S) X_p$
6. $(Z_c Z_e C_{e0}) X_{in} = -(Z_c Z_e C_{30}) P_1 - (R_e) P_4 + (R_e + Z_c Z_e C_{30} + Z_e) P_5 - (Z_e) P_6$
7. $0 = (-1) P_5 + (2 + Z_e C_3 S) P_6$
8. $0 = (+1) P_3 - (1) P_4 - (Z_1 A_p S) X_p$

SOLVE FOR $\frac{X_p(s)}{X_{in}(s)} \frac{1}{\alpha_1} = \frac{\theta_w(s)}{X_{in}(s)}$

Simplification of these equations yields the following:

$$0 = (1 + C_1 s Z_9)P_0 - P_1 \tag{1}$$

$$(-C_4 Z_9 Z_e)X_{va} = (-Z_e)P_0 + (Z_9 + Z_e + Z_9 Z_e C_{30})P_1 - (Z_9)P_2 - (Z_9 Z_e C_{30})P_5 \tag{2}$$

$$0 = (-2)P_1 + (3 + 2C_2 Z_e s)P_2 - P_3 \tag{3}$$

$$0 = (-R_L)P_2 + (2Z_e + R_L)P_3 - (2Z_e)P_4 + (2Z_e R_L A_p s)X_p \tag{4}$$

$$0 = (-Z_e)P_3 + (R_L + Z_e + R_L Z_e C_2 s)P_4 - (R_L)P_5 - (R_L Z_e A_p s)X_p \tag{5}$$

$$(Z_e Z_e C_{40})X_{va} = -(Z_e Z_e C_{30})P_1 - (Z_e)P_4 + (Z_e + Z_e Z_e C_{30} + Z_e)P_5 - (Z_e)P_6 \tag{6}$$

$$0 = (-1)P_5 + (2 + Z_e C_3 s)P_6 \tag{7}$$

$$0 = P_3 - P_4 - (Z_1 A_p s)X_p \tag{8}$$

From these eight equations $X_p(s)$ can be determined as a function of $X_v(s)$. Thus the transfer function

$$\mu_1(s) = \frac{\theta_a(s)}{X_{av}(s)} = \frac{\alpha_1 X_p(s)}{X_{av}(s)}$$

can be determined analytically. This analysis is being conducted at present and the final expression for μ_1 is not yet available.

(3) Determination of $\mu(s) = \mu_1(s)\mu_2(s)$

The total transfer function can be determined by multiplying μ_1 and μ_2 graphically.

Discussion of Results

The results obtained to date must be regarded as preliminary; however, several observations can be made at this time.

1. The results of the airplane tests indicate that the ailerons do not always move together but may be out of phase by as much as 150 deg at some frequencies. In addition to this the amplitudes of the left aileron is sometimes different from that

of the right aileron. These characteristics indicate that in the analysis it is necessary to treat the ailerons as part of a dual output system instead of the single output system illustrated in this report. The analysis is at present being extended to include this effect.

2. Recent experimental determinations of the boost valve fixed resistances indicate that these resistances cannot be neglected. Consequently the extension of the analysis will include these additional resistances.

3. Because of the additional complications resulting from this extension, the resulting equations for the system transfer function will not be readily solvable. Consequently it is planned that an analogue or a computer will be used.

4. The experimental results indicate that the system is extremely unstable as shown in Fig. 5b. If the system flow rate is increased to 4 gpm, the system becomes even more unstable and the transfer function passes through the $-4+j0$ point at 21 cps and the $0+j4$ point at 28 cps.

Conclusions

1. An experimental method for determining the transfer function of the F-86A artificial feel aileron system was developed and has provided satisfactory results.

2. An analytical method has been developed and is currently in the process of solution. Several simplified methods have been eliminated as unsound.

3. The greatest difficulty encountered in the entire program was the unreliable nature of the strain gages used for displacement and pressure measurements. This problem has not yet been solved satisfactorily.

4. Experience gained during this investigation indicated that much time can be saved if all original designs are based on the results of a frequency response analysis. The ideal and possibly the only satisfactory way to obtain a good surface control system is by a combination analytical and experimental development.

***

APPENDIX I

Electrical Network Equivalent to Hydraulic Transmission Line

The total pressure drop per unit length of a tube is

Total Pressure Change per Unit Length		Flow Friction		Inertia
$-\frac{\partial p}{\partial x}$	$=$	$R_s q$	$+$	$\frac{\rho}{A} \cdot \frac{\partial q}{\partial t}$

where R_x = Resistance per unit length

ρ = Density of fluid

A = Area of tubing

Because of elasticity flow is lost. This lost flow per unit length, is

$$-\frac{\partial q}{\partial x} = \beta V \frac{\partial p}{\partial t}$$

where $\beta = \frac{\Delta V}{V} \cdot \frac{1}{\Delta p}$ = elastic constant for fluid

and V = volume of tubing

The equations for an electrical transmission line with no leakage are

$$-\frac{\partial e}{\partial x} = R_x i + L_x \frac{\partial i}{\partial t}$$

and

$$-\frac{\partial i}{\partial x} = C_x \frac{\partial e}{\partial t}$$

where R_x = Resistance per unit length,

L_x = Inductance per unit length, and

C_x = Capacity per unit length.

By comparison of these two sets of equations it is obvious that hydraulic tubing can be represented by an electrical transmission line with

$$R_x = R_x$$

$$L_x = \rho/A$$

$$C_x = \beta V$$

Thus the hydraulic transmission line can be reduced to an infinite number of "T" networks such as

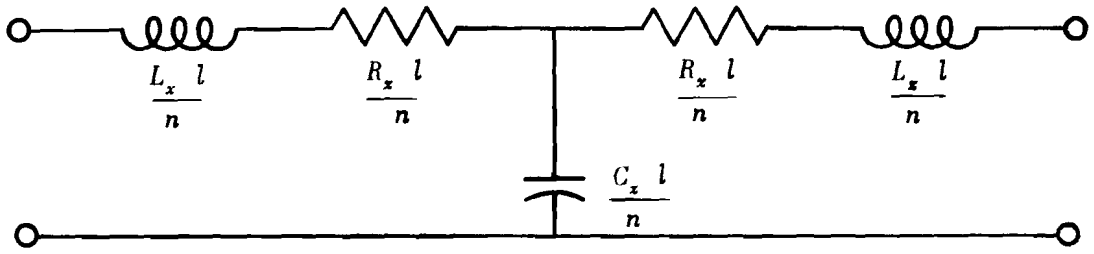

APPENDIX II

Error Introduced by Using Only One "T" Network to Represent A Hydraulic Transmission Line

The characteristic impedance of a transmission line is

$$Z_0 = \sqrt{\frac{R_x l + jwL_x l}{jwC_x l}}$$

while the characteristic impedance of a single "T" network is

$$Z_t = Z_1 Z_2 \left(1 + \frac{Z_1}{4Z_2}\right)$$

where $Z_1 = R_x l + jwL_x l$

$$Z_2 = \frac{1}{jwC_x l}$$

The error introduced by using only one "T" network is

$$\delta_x = \frac{Z_0 - Z_t}{Z_0} = 1 - \frac{Z_t}{Z_0} = 1 - \sqrt{1 + \frac{Z_1}{2Z_2}}$$

Using the first two terms of the binomial expansion of this expression we obtain the expressions

$$\delta_x = 1 - \left(1 + \frac{Z_1}{8Z_2}\right) = \frac{Z_1}{8Z_2}$$

$$\delta_x = \frac{1}{8}(R_x l + jwL_x l)(jwC_x l)$$

$$\delta_x = \frac{l^2}{8}(-w^2 L_x C_x + jwR_x C_x)$$

For 3/8 x .028 tubing

$R_x = 8.0 \times 10^{-3}$ Lb Sec $In.^{-6}$, $L_x = 9.6 \times 10^{-4}$ Lb Sec^2 $In.^{-6}$, $C_x = 3.7 \times 10^{-7}$ $Lb^{-1} In.^4$

Thus at 25 cps, $\omega = 1.57 \times 10^2$ *Rad. Sec.*$^{-1}$

$$\delta_z = l^2(-1.08 \times 10^{-6} + j\ 5.83 \times 10^{-8})$$

For $l = 320$ in.

$$\delta_z = (-0.011 + j\ 0.0059)$$

which means that by using a single "T" network, errors of 1.1% and of 0.59% are introduced into the real and imaginary parts of the characteristic impedance. For shorter lines these errors will be less.

The error in the attenuation factor is less than the error in characteristic impedance. A discussion of transmission line theory is presented in Volume II of "The Classical Theory of Long Line, Filters and Related Networks" by E. A. Guillemin published by John Wiley and Sons (1947).

APPENDIX III

Impedance, Z_1, of Aileron and Actuating Cylinders

In Fig. 10 the drop pressure, $P_3 - P_4$, across the piston causes the piston and aileron to accelerate, the spring to deflect, and the damper to move. Thus with the application of Newton's Laws we obtain the expression

$$\alpha_1 A_p(P_3 - P_4) = I_a\ddot{\theta}_a + \delta_a\dot{\theta}_a + k_a\theta_a$$

where I_a, δ_a, and k_a are the moment of inertia, damping, and spring rate of the aileron and actuating piston about the axis of rotation. Taking the LaPlace transform and neglecting the initial condition operator, we obtain the expression

$$\alpha_1 A_p[P_3(s) - P_4(s)] = [I_a s^2 + \delta_a s + k_a]\theta_a(s)$$

By definition the impedance of one aileron is given by

$$2Z_1(s) = \frac{P_3(s) - P_4(s)}{A_p s X_p(s)}$$

Thus since $X_p = \alpha_1\theta_a$

$$Z_1(s) = \frac{1}{2\alpha_1^2 A_p^2}\left[I_a s + \delta_a + \frac{k_a}{s}\right]$$

IMPEDANCE OF AILERON AND ACTUATING CYLINDER FIG. 10

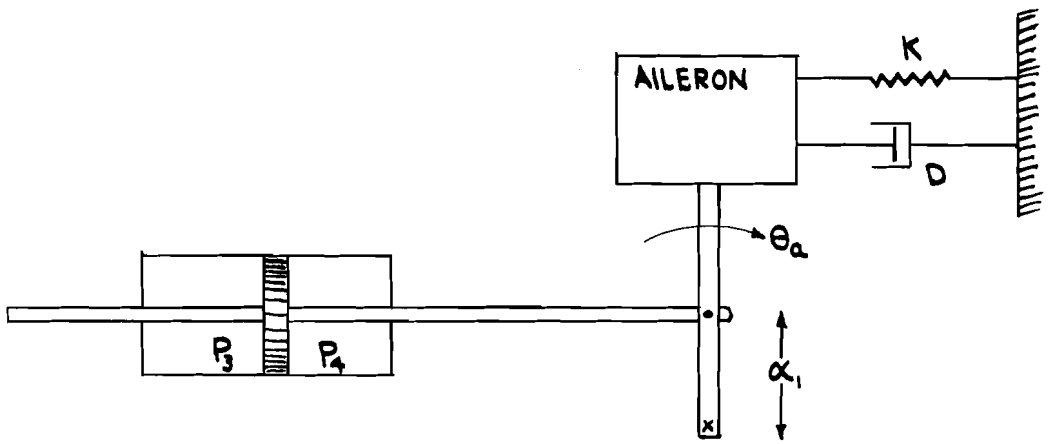

$$T = I\ddot{\theta}$$

$$\alpha_1 A_p (P_3 - P_4) = I_a \ddot{\theta}_a + \delta_a \dot{\theta}_a + k_a \theta_a$$

$$\alpha_1 A_p [P_3(s) - P_4(s)] = [I_a s^2 + \delta_a s + k_a] \theta_a(s)$$

BY DEFINITION

$$2 Z_1(s) = \frac{P_3(s) - P_4(s)}{A_p s X_p(s)} = \frac{P_3(s) - P_4(s)}{A_p \alpha_1 s \theta_p(s)}$$

$$Z_1(s) = \frac{1}{2\alpha_1^2 A_p^2} \left[I_a s + \delta + \frac{k_a}{s} \right]$$

DISCUSSION

MR. HARRIS, Chance-Vought Aircraft: *I notice you use the actual wing panel for your tests. Why did you do that rather than some type of mock-up?*

MONROE: *That eliminated one problem; that is, how good is the mock-up. Of course, we had to worry about how good is one airplane like the other. We had one airplane. Although we had a simulator constructed, we decided since the airplane was available, we had better use it. Actually we intend to use a simulator, but when we do, we would check the results of that against the airplane tests, just to be sure.*

MR. MCRUER, Northrop Aircraft: *As a matter of curiosity, what value did you use for the spring rate of the pilot?*

MONROE: *We didn't really attempt to simulate the pilot dynamically but we decided if the pilot were to move the stick, he would have to go according to the aerodynamic, well, the artificial spring rate so we made it equal to that.*

MR. FOLSE, Bureau of Aeronautics: *In connection with the study of the reproducibility of the transfer function, have you used the method of least squares as a means of adjusting data to supplement conventional servo theory? So far as I am concerned that is the most rigorous method, at least one of the most rigorous methods if not the most. I suggest that it might be useful.*

MONROE: *We have considered such an action with regard to eliminating some of the difficulties. In other words, we would like to check the theory against our experimental work to see what can really be legitimately eliminated from the analysis, so I think that is something in line with what you were saying.*

MR. RICHOLT, Lockheed Aircraft: *Since you say this system was unstable and I know the airplanes are flying, what did you do to them? What kind of system do you have?*

MONROE: *We have a load feel system on the airplane.*

RICHOLT: *It was just a modification to this system?*

MONROE: *We have a different system but it is quite similar in general arrangement to this. I think the only substantial difference is that we don't have an artificial feel spring and we have a load feel valve.*

RICHOLT: *You get the load feel through hydraulic pressure?*

MONROE: *Yes. Incidentally, that is pretty complicated because that introduces another loop in the servo. The valve itself can be unstable.*

STABILITY AND PERFORMANCE CHARACTERISTICS OF AN IRREVERSIBLE SURFACE BOOST SYSTEM, CHANCE VOUGHT AIRCRAFT

By

E. R. Harris and J. Drew

Chance Vought Aircraft, Dallas, Texas

PART I

Introduction

The power boosted surface control is a mechanism that has been developed concurrently with the progress and development of high performance aircraft. Nothing new has been added to the basic control configuration; the development of the mechanism reflects primarily the pilot's limited ability to deliver power. Means for supplementing the pilot's effort could be provided by mechanical, electrical, hydraulic or pneumatic devices. The major efforts in this field, however, have been with hydraulic devices and this symposium is assembled to discuss the means and methods used in the development of hydraulic power boost surface control equipment.

The "irreversible boost system" is receiving a considerable amount of attention and interest in the aircraft industry at the present time. This device offers a means of supplying supplementaty power for the pilot and in addition has the desirable characteristic of isolating the surface forces from the pilot's control devices. A successful installation of this type alleviates the aerodynamiscists concern over peculiar hinge moment characteristics and pilot effort problems of high speed flight, but presents the additional problem of requiring an installation of artificial "pilot feel".

The basic requirements and the basic mechanisms of power boost equipment are evidently established, but the unfortunate fact of the matter is that a completely satisfactory system is not in hand. The systems show a tendency to instability and the pilot's characterize the operation of the equipment as "over sensitive."

In this paper, an effort will be made to discuss the "irreversible boost system" with particular emphasis on the stability and performance characteristics. Force feedback systems, the "over-sensitivity" problem, artificial feel, etc., will not be discussed. Part I is devoted to the application of servo-theory to the mechanism and Part II, to a discussion of laboratory results and techniques determined at Chance Vought.

Development of the Theory

Figure I has been prepared to illustrate the mechanism under consideration and to define the parameters. The displacement X_i represents the motion received from the pilot's control; X_o represents the motion imparted to the controlled surface; and X_ϵ represents the difference between X_i and X_o and is the valve opening. This configuration is known as a closed-center irreversible power boost and requires an external

FIG. I

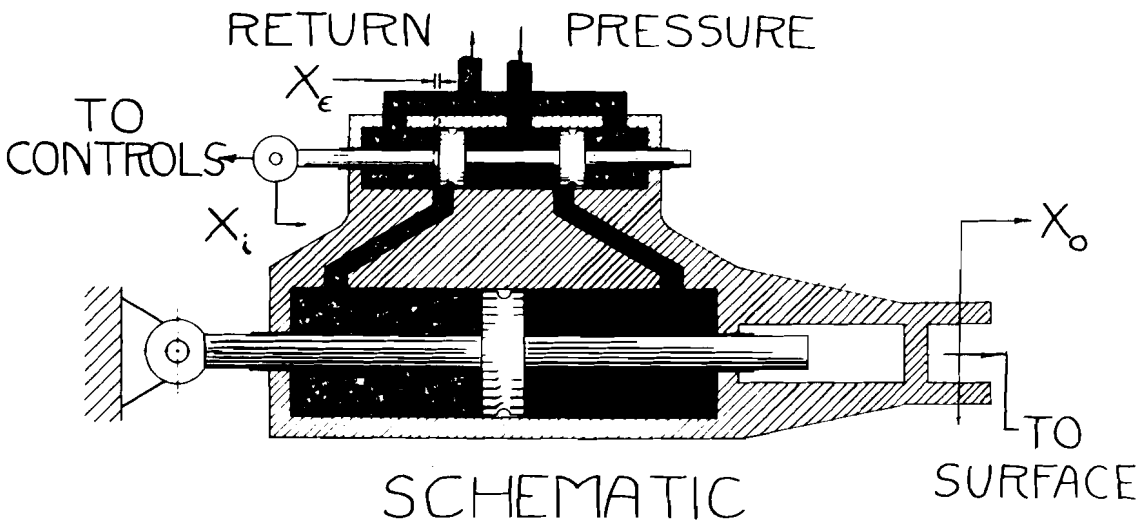

CLOSED CENTER IRREVERSIBLE BOOST SYSTEM

hydraulic circuit to supply pressure at a constant flow consistent with the maximum speed requirements of the operator. Figures Ia and Ib have been prepared to illustrate other configurations that satisfy the same definitions. These configurations are basically the same as that of Figure I, and mathematical expressions developed for any one of them can be applied directly to another. The configuration of Figure I has been selected for discussion because it is the most elementary and it is the configuration with which we have had the most experience. Let it suffice to say that the configurations differ only in geometry and these properties appear as multiplying factors in the open-loop transfer function.

As in most servo theory, it is convenient to revert directly to an examination of the relationship between the output X_o and the error X_ϵ. In this case, the valve characteristics dominate the considerations. Pressures and flows are excited by valve error which in turn direct output motion. Since the output pressure is totally dependent on the character of the "load", it is evident that an expression relating valve motion to output motion for an arbitrary load must first be developed.

There are two significant characteristics of a valve which can be used to develop the expression. The first is the flow-stroke characteristic and the second is the pressure-stroke characteristic. Figure II has been prepared to illustrate suitable test methods for determining these characteristics for any given valve. Over a short range and particularly near $X_\epsilon = 0$, the following equations may be used:

$$P_\epsilon = K X_\epsilon$$

and

$$Q_{sc} = K_1 X_\epsilon$$

FIG. Ia

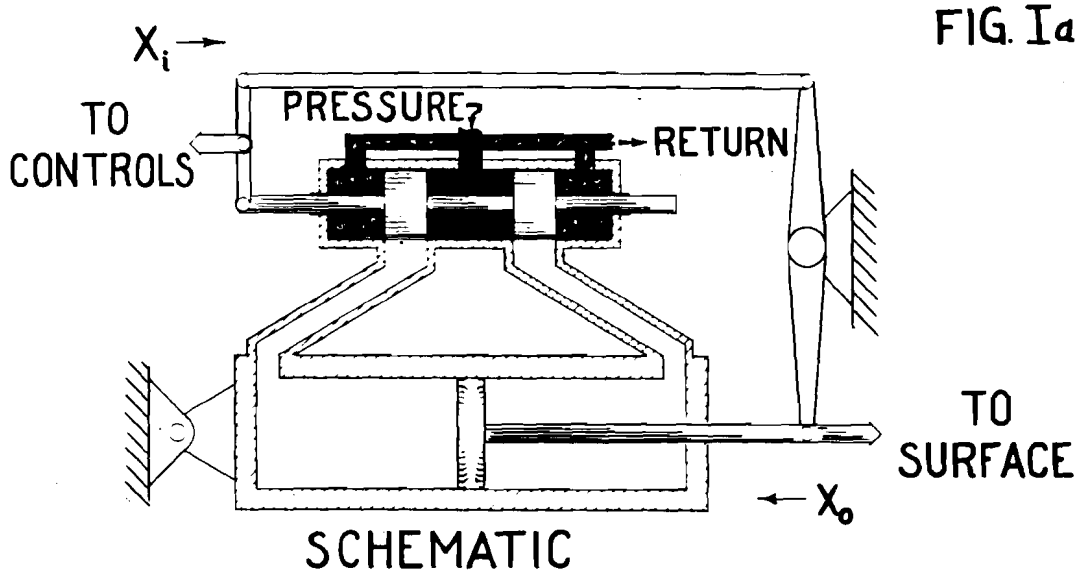

SCHEMATIC

CLOSED CENTER IRREVERSIBLE BOOST SYSTEM

DIFFERENTIAL BAR FOLLOW-UP

FIG. Ib

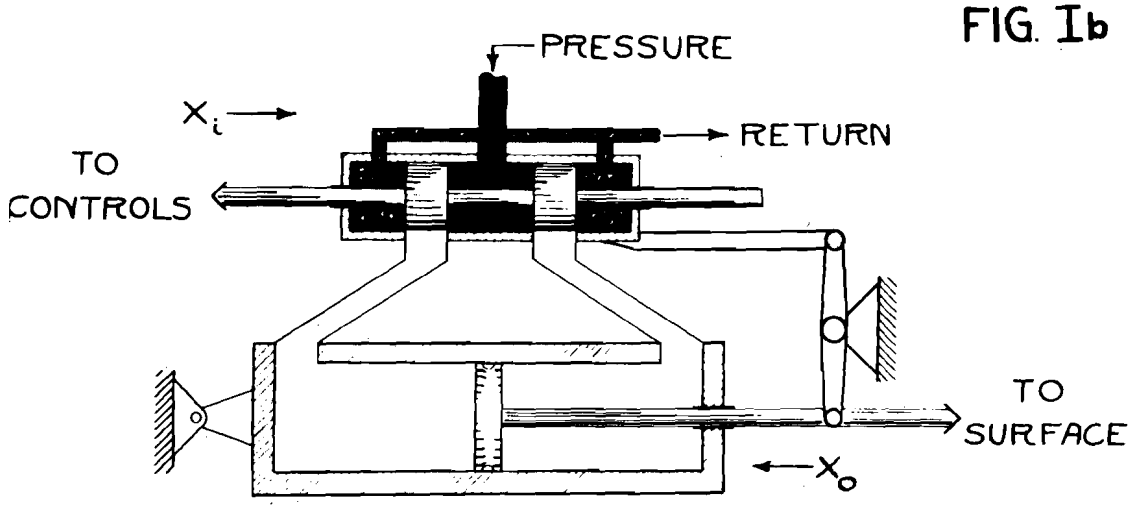

SCHEMATIC

CLOSED CENTER IRREVERSIBLE BOOST SYSTEM

VALVE CASE OR VALVE SLEEVE FOLLOW-UP

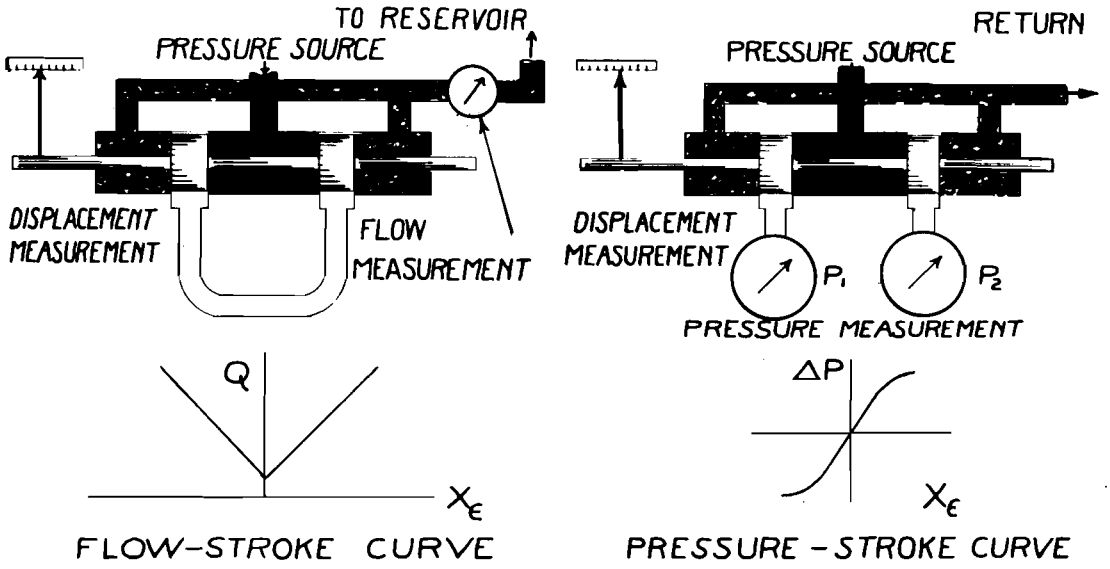

FIGURE II

FIG. III

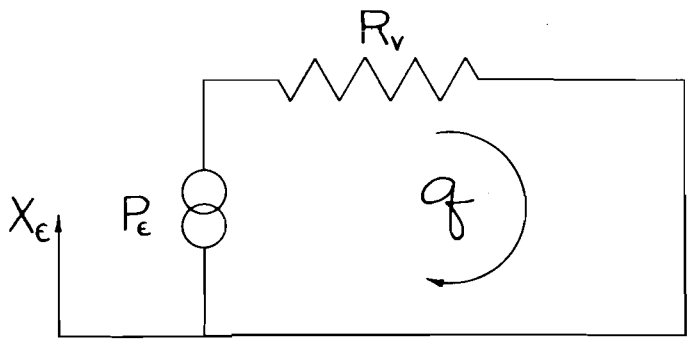

FOUR-WAY VALVE EQUIVALENT CIRCUIT

Now, if methods of the electrical engineers are borrowed, an equivalent hydraulic circuit can be assumed. Figure III illustrates an equivalent circuit that satisfies the assumed proportional characteristics of the valve. Using the schematic, a pressure drop equation can be written as follows:

$$P_\epsilon = R_v Q_{sc}$$

Where P_ϵ is the pressure rise and $R_v Q_{sc}$ is the pressure drop. When the expressions for the flow-stroke and pressure-stroke are substituted, for P_ϵ and Q_{sc}, R_v is expressed in terms of constants.

$$K X_\epsilon = R_v K_1 X_\epsilon \quad ; \qquad R_v = \frac{K}{K_1}$$

or

$$R_v = \frac{\textit{Pressure - stroke slope}}{\textit{Flow - stroke slope}}$$

This method of determining the internal "resistance" of the valve is analogous to methods used to determine generator internal impedance, electronics amplifier output imedance, etc. Having established an equivalent circuit for the valve, it is now possible to develop an expression relating X_o and X_ϵ for an arbitrary "load". Again, using electrical engineering terminology, the load will be called an "impedance" Z_L and will have dimensions of pressure per unit flow. The impedance may be added to the basic equivalent circuit as shown in Figure IV.

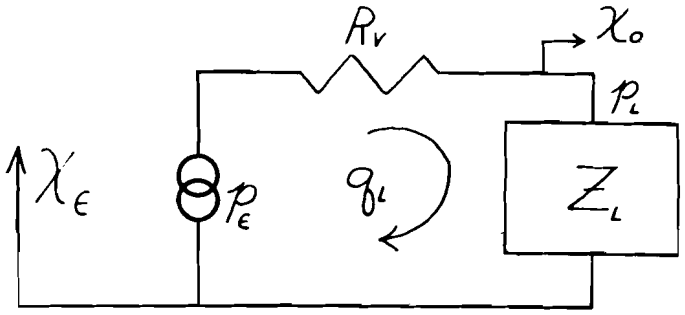

FIG. IV

$$\frac{X_o}{X_\epsilon} = \frac{k}{AR_v} \times \frac{1}{S} \times \frac{1}{1 + Z_L\left(\frac{1}{R_v}\right)}$$

Four-Way Valve
Equivalent Circuit Including
Load Impedance

Equating pressure rises to pressure drops,

$$P_\epsilon = R_v\, q_L + Z_L\, q_L$$

and substituting:

$$P_\epsilon = K\, X_\epsilon$$

and

$$q_L = A\, X_o\, s$$

The ratio of X_o to X_ϵ is developed.

$$\frac{X_o}{X_\epsilon} = \frac{K}{A\, R_v} \cdot \frac{1}{s} \cdot \frac{1}{1 + Z_L\left(\frac{1}{R_v}\right)}$$

This expression may be called the open loop transfer function for an arbitrary load. Without considering the effects of Z_L, the expression has the characteristics of a zero position servomechanism.

Before proceeding to a detailed examination of load impedance and its effect on the transfer function, a word or two must be said about an alternate equivalent circuit. Under most circumstances, the compressibility of the fluid and deformation of lines and cylinders must be taken into account. In this case a two-loop equivalent

FIG. V

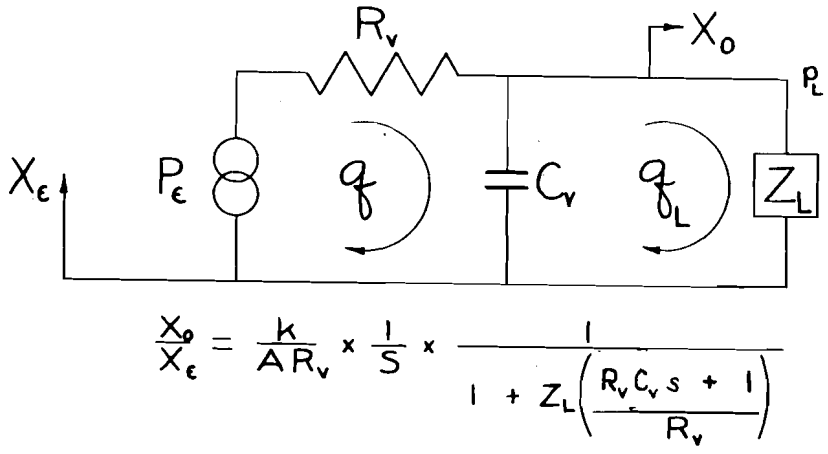

$$\frac{X_o}{X_\epsilon} = \frac{k}{A R_v} \times \frac{1}{S} \times \frac{1}{1 + Z_L\left(\frac{R_v C_v s + 1}{R_v}\right)}$$

FOUR-WAY VALVE EQUIVALENT CIRCUIT
INCLUDING
LOAD AND COMPRESSIBILITY EFFECTS

circuit must be assumed as shown in Figure V. The expression for the transfer function may be solved in the same manner as before, giving

$$\frac{X_o}{X_\epsilon} = \frac{K}{A R_v} \cdot \frac{1}{s} \cdot \frac{1}{1 + Z_L\left(\frac{R_v C_v s + 1}{R_v}\right)}$$

For the moment, it will be convenient to abandon the generalized transfer functions and examine the character of the load impedance Z_L in detail. The load pressure p_L resulting from flow q_L is due to mechanical phemonena such as hinge moment, surface mass, friction, etc., and consequently a conversion factor is necessary to relate hydraulic to mechanical phenomena. The impedance Z_L has been defined as the ratio of p_L to q_L :

$$Z_L = \frac{p_L}{q_L}$$

but since

$$p_L = \frac{F_o}{A}$$

and

$$q_L = A X_o s$$

$$Z_L = \frac{1}{A^2} \cdot \frac{F_o}{s X_o}$$

The hydraulic load impedance Z_L can be determined by solving for the mechanical impedance and multiplying by $1/A^2$, the conversion factor.

Figures VIa, VIb, VIc & VId have been prepared to illustrate solutions of the hydraulic load impedance for increasingly complex systems. The next step is to combine the equivalent valve circuit and the load impedance and examine progressively the effects on the open and closed transfer functions and the closed loop transient response.

Figure VII illustrates the case of $Z_L = 0$. The open loop transfer function plots along the $-j$ axis, the closed loop has the pure time lag characteristic and the transient solution is shown accordingly. It is interesting to note that it is impossible to make this system unstable. An increase in the flow stroke curve K/R_v or a decrease in the piston area A both serve to decrease the time of response, but extension to limits simply reduces or increases the speed of the system. It is also evident that the steady state response of the mechanism is independent of the parameters.

Figure VIIa illustrates the condition in which the load is composed of mass only. This particular condition illustrates some of the confusing aspects of this type of mechanism. For example, by examination of the expressions for ω_o and ζ_o it is evident that the natural frequency and the damping are both increased for an increase of the piston area. It is contradictory in a sense, since an increase in the piston area intuitively decreases the speed! The explanation is however, that the damping increases much faster than the natural frequency and affects a net decrease. The effect

Hydraulic Impedance

FIG. VI a

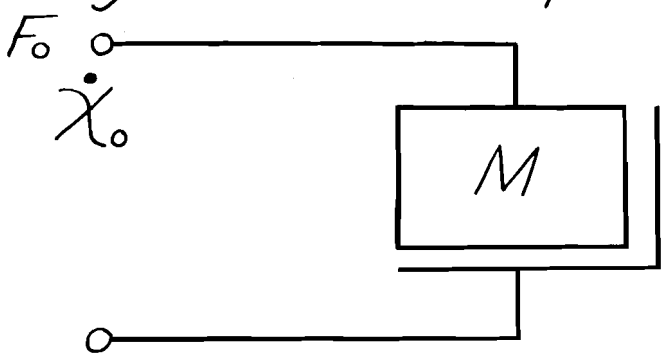

$$Z_L = \frac{1}{A^2} \times \frac{F_o}{\dot{x}_o} = \frac{1}{A^2} MS$$

Mass Load

FIG. VI b

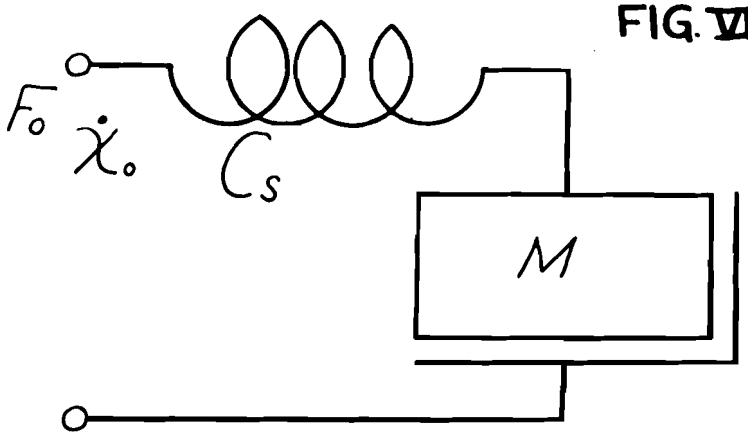

$$Z_L = \frac{1}{A^2} \times \frac{F_o}{\dot{x}_o} = \frac{1}{A^2}\left[\frac{C_s M}{C_s/S + MS}\right]$$

Mass & Structural Load

Hydraulic Impedance

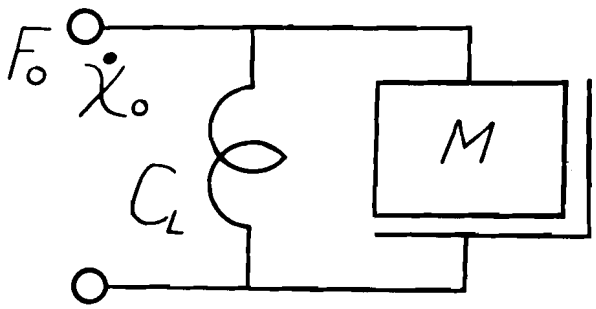

FIG VI c

$$Z_L = \frac{1}{A^2} \times \frac{F_o}{\dot{x}_o} = \frac{1}{A^2}\left[MS + \frac{C_L}{S}\right]$$

Mass & Hinge Moment

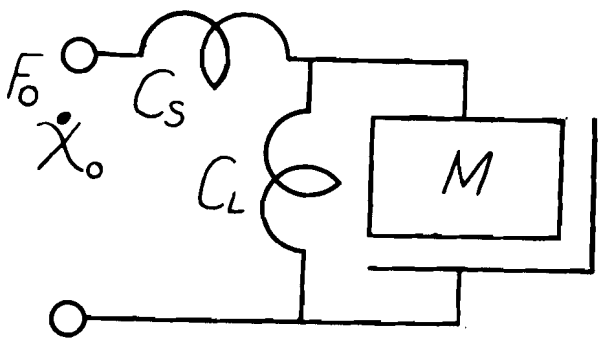

FIG VI d

$$Z_L = \frac{1}{A^2} \times \frac{F_o}{\dot{x}_o} = \frac{1}{A^2}\left[\frac{\frac{C_S C_L}{S^2} + C_S M}{\frac{C_S + C_L}{S} + MS}\right]$$

Mass, Hinge Moment & Structural Load

FIG. VII

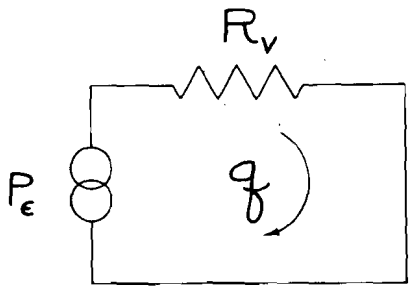

$$\frac{X_o}{X_\epsilon} = \frac{k}{R_v A} \times \frac{1}{P}$$

$$\frac{X_o}{X_i} = \frac{1}{1 + \frac{R_v A}{k} S}$$

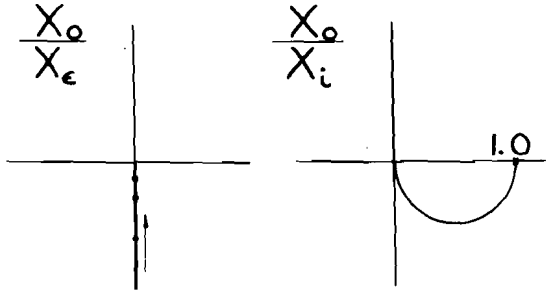

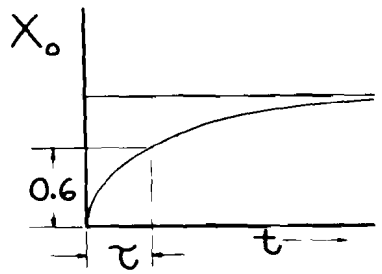

FIG. VII a

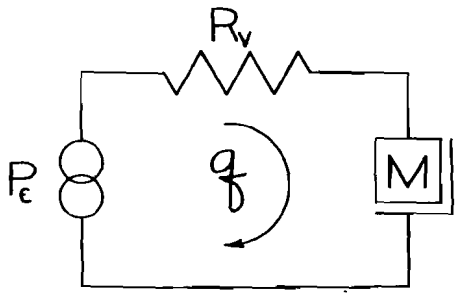

$$\frac{X_o}{X_\epsilon} = \frac{k}{AR_v} \times \frac{1}{S} \times \frac{1}{\left(1 + \frac{M}{A^2 R_v} S\right)}$$

$$\frac{X_o}{X_i} = \frac{1}{\frac{M}{kA} S^2 + \frac{R_v A}{k} + 1}$$

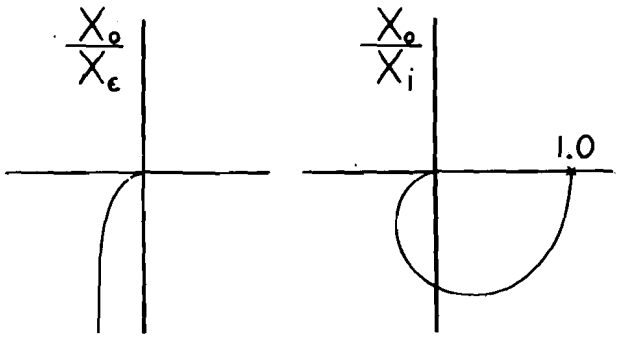

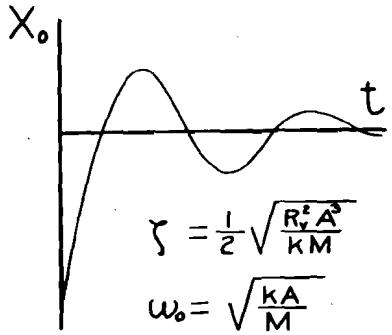

$$\zeta = \frac{1}{2}\sqrt{\frac{R_v^2 A^3}{kM}}$$

$$\omega_o = \sqrt{\frac{kA}{M}}$$

of changes in the mass M is more evident. An increase in the mass of the system decreases the natural frequency and the damping and should be avoided if at all possible. The best control of the amount of damping is provided by K/R_v. The flow-stroke curve which appears in the open loop transfer function as a gain factor. A reduction of the flow stroke curve will increase the damping factor and not alter the natural frequency. Again the assumed configuration is stable and self-sustained oscillation is not possible.

Figure VIIb illustrates the case in which it is assumed that structural deflections take place between the output piston and the surface mass. The addition of the structural deflection term alters the dynamic characteristics of the system, but leaves the steady-state unaltered. Of particular interest again is the fact that this system cannot become unstable by any manipulation of parameters. The open-loop transfer function does not cross the $-180°$ axis. One particularly interesting feature of this configuration is the appearance of terms in the numerator of the closed-loop transfer function. This introduces a zero or null into the transfer function plot and means that X_0 does not respond to X_ϵ or X_1 at this frequency. Another interesting feature of this configuration is that the natural frequency term associated with the system mass and the valve pressure-stroke curve becomes unimportant. To illustrate, typical values of M/C and M/KA are 100×10^{-6} and 10×10^{-6} respectively. The ratio of these numbers is independent of the mass of the system and the implication is that the force per-unit motion of the valve is high compared to the stiffness of efficient structural design. If the M/KA term is neglected compared to the M/C term, the natural frequency of the system becomes independent of valve characteristics and the effective damping is dependent only on the flow-stroke characteristic of the valve. Piston area and system mass have the same effects as before.

FIG. VII b

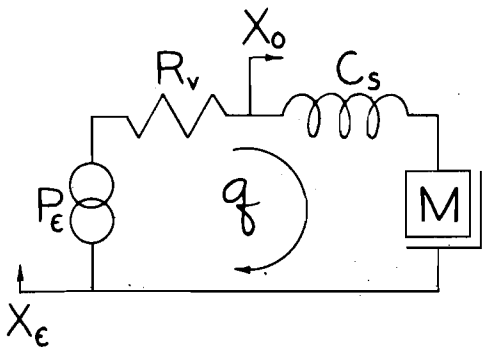

$$\frac{X_0}{X_\epsilon} = \frac{K}{AR_v} \times \frac{1}{S} \times \frac{\frac{M}{C_s}S^2 + 1}{\frac{M}{C_s}S^2 + \frac{M}{A^2R_v}S + 1}$$

$$\frac{X_0}{X_i} = \frac{\frac{M}{C}S^2 + 1}{\frac{AR_v}{K} \times \frac{M}{C}S^3 + \left(\frac{M}{kA} + \frac{M}{C}\right)S^2 + \frac{AR_v}{K}S + 1}$$

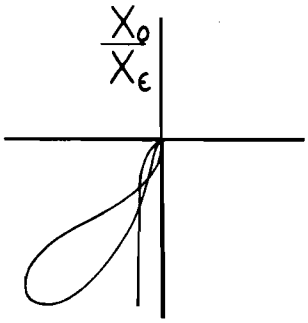

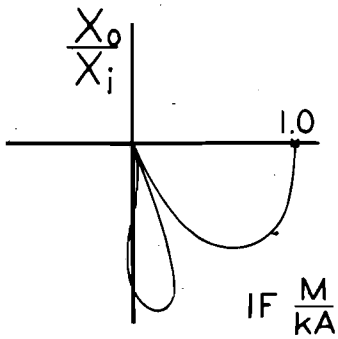

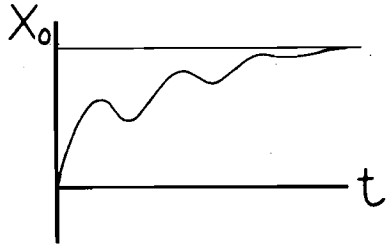

IF $\frac{M}{kA} < \frac{M}{C}$ $\quad \zeta \sim \frac{AR_v}{k}\frac{1}{2}\sqrt{\frac{C}{M}}$

FIG VIIc

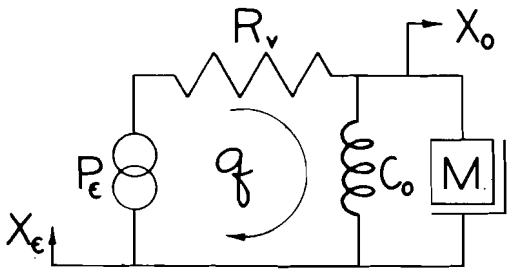

$$\frac{X_o}{X_\epsilon} = \frac{k}{AR_v} \times \frac{1}{\frac{C_o}{A^2R_v}\left(S^2\frac{M}{C_o} + S\frac{A^2R_v}{C} + 1\right)}$$

$$\frac{X_o}{X_i} = \frac{kA}{C_o + kA} \times \frac{1}{S^2\left(\frac{M}{C_o+kA}\right) + S\left(\frac{A^2R_v}{C_o+kA}\right) + 1}$$

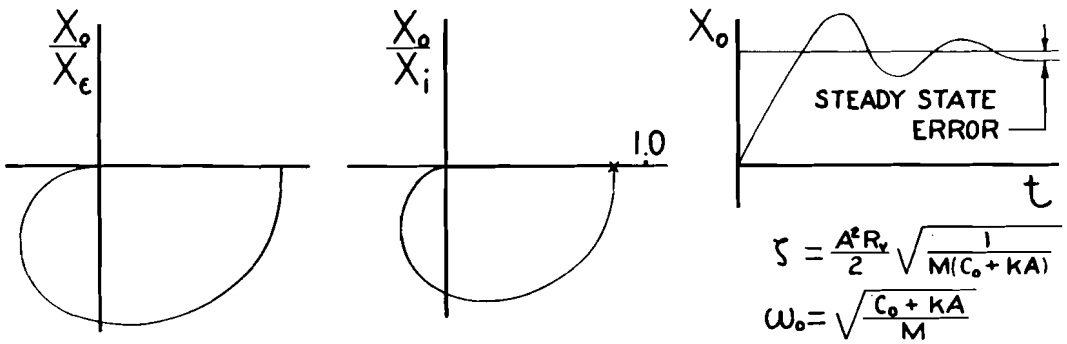

$$\zeta = \frac{A^2R_v}{2}\sqrt{\frac{1}{M(C_o+kA)}}$$

$$\omega_o = \sqrt{\frac{C_o + kA}{M}}$$

When the effects of "load" or hinge moment are considered, another change is introduced in the system. Figure VIIc illustrates this configuration. One property of the system is of particular interest. The system is no longer a zero error servomechanism. This is due to the fact that a finite valve error is required to hold a hinge moment and results in a smaller deflection of the surface than is called for by the control column. This property is sometimes called "droop" in regulators and in this particular case is only of importance when the controlability of the aircraft is considered. It is not significant or important as a property of the boost itself.

The final illustration of loads with the simple hydraulic equation is given on Figure VIId. The complexity of the characteristic equation and the parameters have increased to the point where it is indeed difficult if not impossible to casually evaluate the effects of number changes. It should be noted, however, that these characteristics possess all the properties of the systems previously discussed. The steady-state has "droop" and the dynamic characteristics are of the same order as the configuration using structural deflection and mass parameters for the load. One property appears that should be very heartening to irreversible boost system designers:-- The addition of hinge-moment tends to make the system more stable. In other words, a system that is stable on the ground will not develop self-oscillations in flight.

The dominant feature of the analysis so far is that none of the assumptions made indicate a tendency toward instability in the characteristic equations. If such is the case, it is evident that the theory is in error or that sufficient parameters

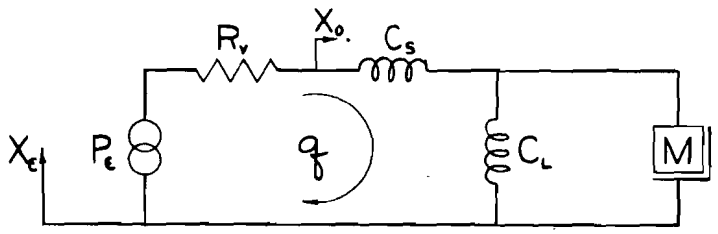

FIG VII d

$$\frac{X_o}{X_i} = \frac{k}{AR_v} \times \frac{A^2R_v(C_s + C_L)}{C_sC_L} \times \frac{S^2\left(\frac{M}{C_s + C_L}\right) + 1}{S^3\frac{A^2R_vM}{C_sC_L} + S^2\frac{M}{C_L} + SA^2R_v\left(\frac{C_s + C_L}{C_sC_L}\right) + 1}$$

$$\frac{X_o}{X_i} = \frac{kA(C_s + C_L)}{C_sC_L + kA(C_s + C_L)} \times \frac{S^2\left(\frac{M}{C_s + C_L}\right) + 1}{S^3\left[\frac{AR_vM}{C_sC_L + kA(C_s + C_L)}\right] + S^2\left[\frac{C_sC_L}{C_sC_L + kA(C_s + C_L)}\left(\frac{M}{C_L} + \frac{kMA}{C_sC_L}\right)\right] + S\left[\frac{(C_s + C_L)A^2R_v}{C_sC_L + kA(C_s + C_L)}\right] + 1}$$

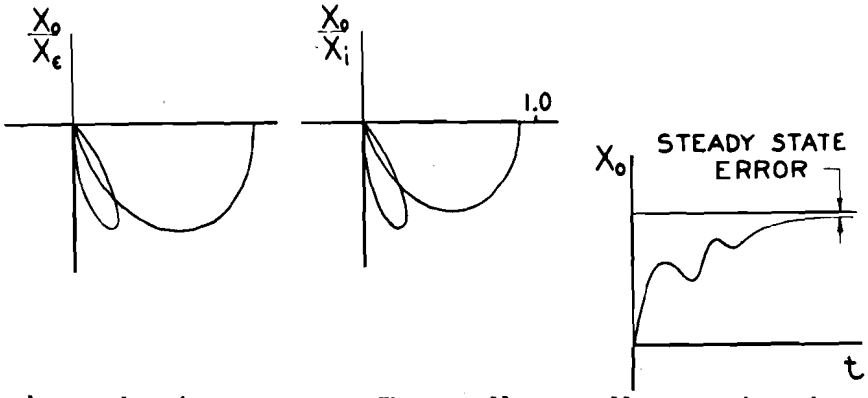

have not been taken into account. We are all too well aware that the mechanisms do oscillate. Actually, it is essential to assume oil compressibility or cylinder expansion to account for the unstable properties of this mechanism. The next set of illustrations have been prepared to contrast with those already illustrated. The same load impedances will be added to the second equivalent hydraulic circuit in the same order.

Figure VIIIa illustrates the combination of the equivalent hydraulic circuit including compressibility effects and a simple mass load. When compared to Figure VIIa, it is immediately apparent that this system can be unstable even with a very simplified load. This is the first illustration in which the open-loop transfer function crosses the -180° axis.

Figure VIIIb illustrates the above configuration with hinge-moment added. As before, the open-loop transfer function crosses the -180° axis and the addition of the load introduces "droop" in the same fashion as with the simple circuit.

Figure VIIIc illustrates the compressibility configuration with a load consisting of structural deflection and mass. Again, we have an open-loop transfer function that crosses the -180° axis and is therefore subject to self-oscillation.

FIG VIII a

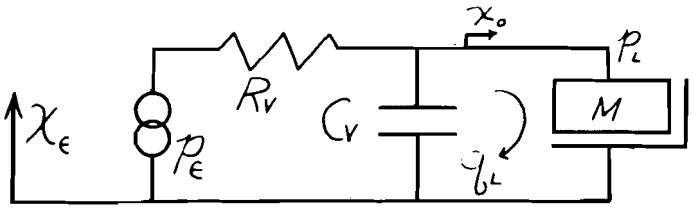

$$\frac{X_o}{X_\epsilon} = \frac{k}{AR_V} \times \frac{1}{S} \times \frac{1}{S^2\left(\frac{M}{A^2C_V}\right) + S\left(\frac{M}{A^2R_V}\right) + 1}$$

$$\frac{X_o}{X_i} = \frac{1}{S^3\left(\frac{MR_V}{ACVk}\right) + S^2\frac{M}{Ak} + S\frac{AR_V}{k} + 1}$$

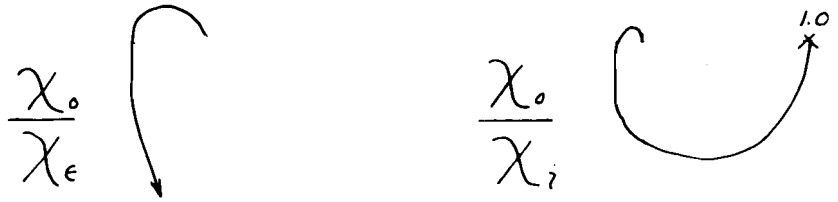

FIG VIII b

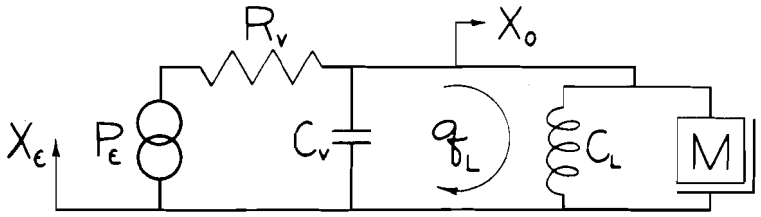

$$\frac{X_o}{X_\epsilon} = \frac{kA}{C_L} \times \frac{1}{S^3\frac{MR_V}{C_VC_L} + S^2\frac{M}{C_L} + S\left(\frac{C_L}{A^2C_V} + 1\right)\left(\frac{A^2R_V}{C_L}\right) + 1}$$

$$\frac{X_o}{X_i} = \frac{kA}{kA + C_L} \times \frac{1}{S^3\frac{MR_V}{C_VC_L}\left(\frac{1}{\frac{kA}{C_L} + 1}\right) + S^2\frac{M}{C_L}\left(\frac{1}{\frac{kA}{C_L} + 1}\right) + S\left(\frac{C_L}{A^2C_V} + 1\right)\left(\frac{A^2R_V}{C_L}\right)\left(\frac{1}{\frac{kA}{C_L} + 1}\right) + 1}$$

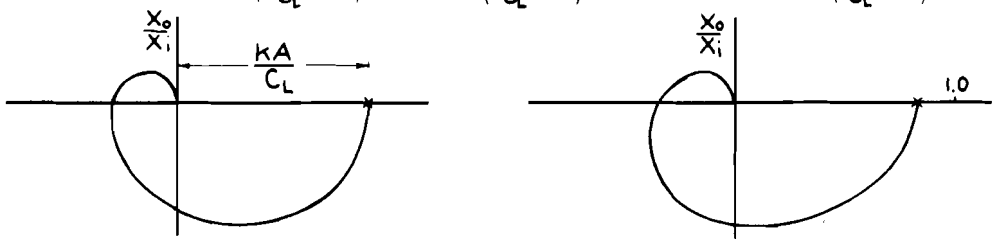

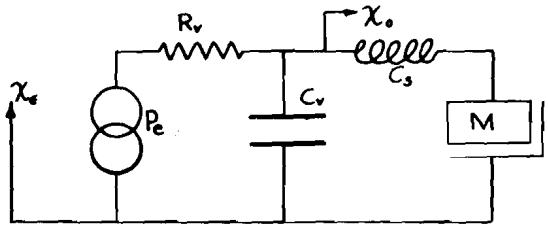

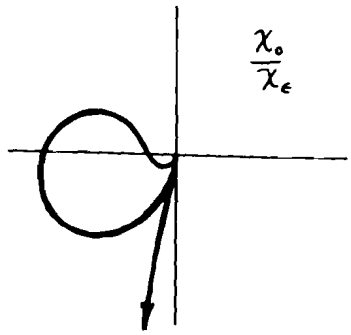

$$\frac{\chi_o}{\chi_\epsilon} = \frac{k}{AR_v} \times \frac{1}{S} \times \frac{\left(\frac{M}{C_s}\right)S^2+1}{S^2\left(\frac{M}{C_s}+\frac{M}{A^2C_v}\right)+S\frac{M}{A^2R_v}+1}$$

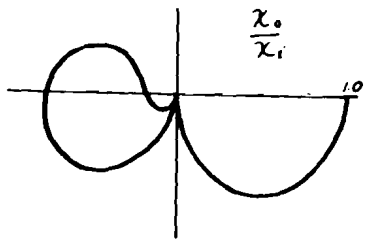

$$\frac{\chi_o}{\chi_i} = \frac{\left(\frac{M}{C_s}\right)S^2+1}{S^3\frac{AR_v}{k}\left(\frac{M}{C_s}+\frac{M}{A^2C_v}\right)+S^2\left(\frac{M}{kA}+\frac{M}{C_s}\right)+\frac{AR_v}{k}S+1}$$

FIG VIII c

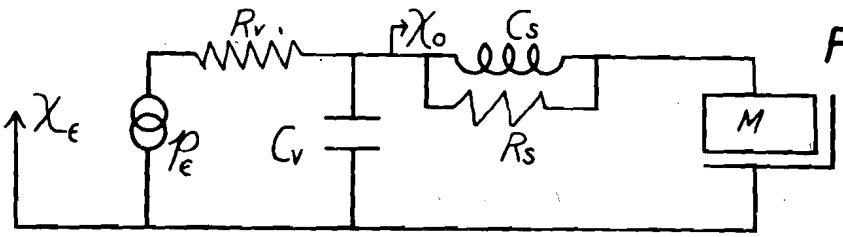

FIG VIII d

$$\frac{\chi_o}{\chi_\epsilon} = A\,\frac{B\mu^2+C\mu+1}{\mu\left[D\mu^3+E\mu^2+F\mu+1\right]}$$

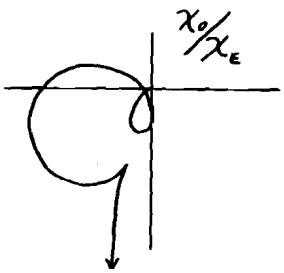

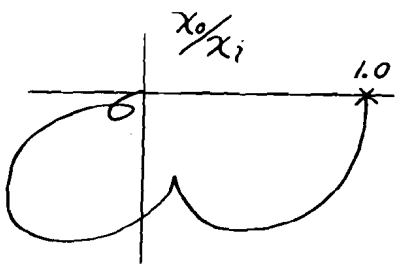

A final illustration, Figure VIIId, is now presented which has proven to be the minimum configuration necessary to check experimental data. This configuration includes the mass and structural deflection term and requires the more complicated hydraulic equivalent circuit. In addition, it has been found necessary to include a term representing structural damping. The hinge moment term has been left out since it generally improves the stability.

Now that a series of progressively more complicated configurations has been developed, it is necessary to summarize the importance and significance of the various parameters that appear in the equations.

a. Pressure-Stroke Curve -- The pressure-stroke curve must be selected as a compromise. If the value is too low, an excessive amount of "droop" is introduced to the system when hinge moment is applied. If the value is too high, self-oscillation will be encountered. A closer examination will show that, for stable operation, $KA < C_v A^2$.

b. Flow-Stroke Curve -- The flow-stroke curve dominates the speed of response of the system. The term $\frac{AR_v}{K}$ appears as the coefficient of the s term in the denominator of all configurations. An increase in the flow-stroke curve decreases the time constant. This term also has an effect on the stability of the system since it always appears as a multiplying factor in the open-loop transfer function. The value of this term should be selected on a basis of closed-loop time of response requirements, if feasible.

c. System Mass -- The systems examined cannot become unstable without the mass term. An increase in mass always tends to decrease the stability.

d. Piston Area -- Changes to the piston area affect the system operation in a manner quite similar to changes in the flow-stroke curve. An increase in piston area is generally stabilizing but tends to decrease the speed of response of the system. Changes in piston area are not considered a satisfactory method of increasing stability.

e. Aerodynamic Load -- From the stability point of view, the aerodynamic load usually has a stabilizing effect and is generally ignored for stability studies.

f. Structural Effects -- The structural stiffness term, together with the mass, usually define the natural frequency of oscillations or overshoot. As long as the resulting natural frequency is high compared to the speeds of response required of the system, the term is not important. If very high speed servos, such as missile servos, are required, this term becomes significant in the stability considerations.

g. Oil Compressibility and Cylinder and Line Expansion -- As demonstrated in the illustrations, instability is not possible without this term. To avoid the effects of this parameter, it is necessary to use strong short lines, a minimum of piston chamber volume and take considerable care to assure that the fluid is not full of air.

h. Structural and Aerodynamic Damping -- These terms are generally stabilizing, but do not offer a good means to improve stability since it is not possible to control them.

PART II

Application and Test Results

Part I of this paper was devoted to the application of servomechanism theory to the irreversible hydraulic boost system. This section of the paper will be confined to a description of an application of the theory to the ailavator boost system of the Chance Vought experimental Cutlass, XF7U-1. Actually, the theoretical expressions could not have been developed or refined without parallel and supporting laboratory investigation.

Development of the complete hydraulic system for the Cutlass included the construction of a full scale dimensional hydraulic mock-up. In the original planning, the mock-up was intended for operational and other routine hydraulic tests. The availability of the hydraulic mock-up offered the possibility of investigating the stability characteristics of the boost system prior to installation in the first flight article. The possibility of avoiding delays to the flight test program by qualifying the boost system dynamically prior to flight was attractive and actively prosecuted thereafter.

It was necessary to simulate parameters of the aircraft to a certain extent and additions and changes were made to the mock-up accordingly. Airloads were simulated by a family of torque tubes producing hinge moments from zero to 1000 foot pounds per degree which were calibrated in terms of airspeed at given altitudes. The mass of the control surface was represented by a rotating steel body with the same moment of inertia as that of the control surface with the same radius arm coupling it to the boost cylinder. The load can best be pictured as a concentrated mass of 1,700 pounds attached directly to the boost cylinder. This inertia load assumed a concentrated mass rather than the actual case of mass distributed along the torque box of the surface with a concentrated mass terminating the torque box. At the time of construction of the inertia load, the surface was assumed to be rigid insofar as its dynamic characteristics at the boost system's resonant frequencies were concerned. In order that as many of the aircraft components as possible would be checked in the tests, actual parts were used to couple the boost cylinder rod end to the mock-up structure and the boost cylinder to the simulated inertia and aerodynamic spring loads.

The boost cylinder and integral valve housing are shown schematically in Figure I. It can be seen that positional follow-up is obtained by attaching the rod end to the structure and the cylinder housing to the load. In this way, once a valve input signal is received, movement of the housing is initiated and as controlled by the error between the input signal and the position of the output will continue to move until the error between the two is brought to zero. Forging of the valve housing and the cylinder housing as one unit insures a minimum possibility of error entering into the feedback linkage.

The physical dimensions of the unit were more or less dictated by the extreme aerodynamic requirements. For example, approximately nine square inches of piston area were required at a line pressure of 3300 pounds per square inch to match the hinge moments anticipated as well as a flow of 20 gallons per minute maximum for each unit. Since the boost system dimensions were not variable, the entire problem of stability required the determination of valve characteristics as a possible means of

control. Mr. Harris has already discussed the contribution of the valve characteristics to the analytical approach.

The test program on the irreversible boost system was divided into two distinct phases, static and dynamic.

The first or static phase entailed the determination of static valve characteristics and calibration of the instrumentation and was performed in the hydraulic and electronic test laboratories.

The second or dynamic phase checked the boost system's open-loop response to a variable frequency sinusoidal input, emphasized the important role the valve characteristics play in the stability of such a system, and was performed on the hydraulic mock-up and the aircraft.

The valve under test was of the two land linear slide type with a basic configuration as shown in Figure I. Pressure is introduced as indicated and metered through an orifice into one cylinder port when the valve slider is displaced. The flow out of the cylinder caused by pixton motion is metered through a similar orifice to the return line.

The equipment used in the determination of the valve characteristics was of the standard hydraulic laboratory type, consisting of a power source similar to that used in the aircraft, pressure gauges, flow meters, and a test jig for the valve and fittings.

The total flow versus valve stroke curve was obtained by setting up a hydraulic circuit as illustrated in Figure II. and obtaining flow measurements for specific valve slider positions as determined by an accurate dial gauge. By adjusting the bypass valve, it was possible to simulate a given differential pressure across the piston, thus producing the effect of flow controlled by the valve with the piston subjected to a load. Results of the test are shown in Figure IXa. By removing the effect of neutral leakage (flow through the valve when the flow to the cylinder is zero), the resultant curves, Figure IXb, are seen to be similar to vacum tube dynamic characteristics of plate current versus grid voltage for a family of resistive load impedances.

The differential pressure versus valve stroke curve was determined by use of hydraulic circuitry as illustrated in Figure II. Results of the test are shown in Figure X. Although the flow versus valve stroke curve was determined to be a function of orifice configuration and line pressure solely, the differential pressure versus valve stroke curve was found to be affected by orifice configuration, valve land underlap with respect to the orifice, and the clearance between the valve slider and the valve sleeve.

Methods of control of the valve characteristics were required, since they effectively determined the internal resistance of the valve R_v which is represented by the slope of the differential pressure versus valve stroke curve divided by the slope of the flow versus valve stroke curve.

Change of the slope of the flow versus valve stroke curve was a straight forward correction of the delta area for a given valve slider displacement increment.

The Cutlass valve had two orifices per land with its total stroke (orifice length) fixed at 0.4 inches. This, perforce, left the only delta area per valve stroke increment variation possible that of orifice width. The mock-up valve orifices were designed with a width of 0.040 inches whereas the aircraft valve orifices had tips 0.025

FIG IX a

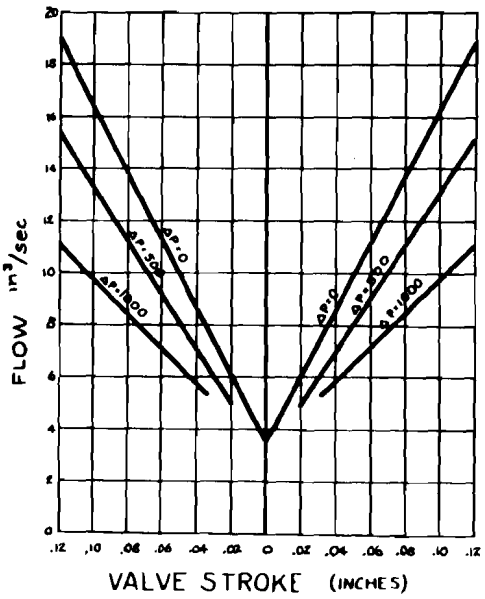

TOTAL FLOW vs VALVE STROKE

FIG. IX b

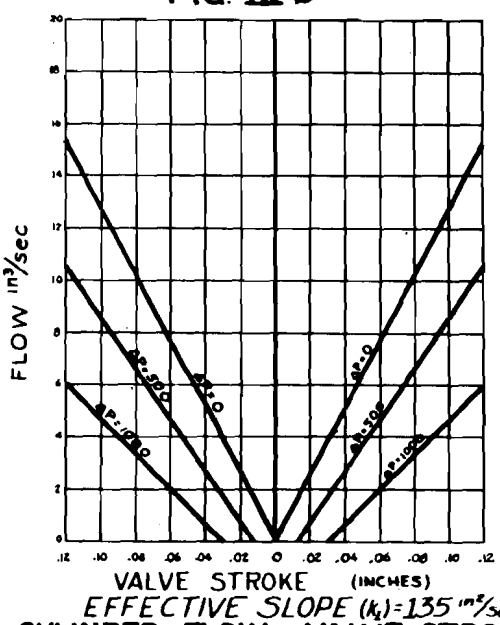

EFFECTIVE SLOPE (k_1) = 135 in³/sec

CYLINDER FLOW vs VALVE STROKE

FIG. X

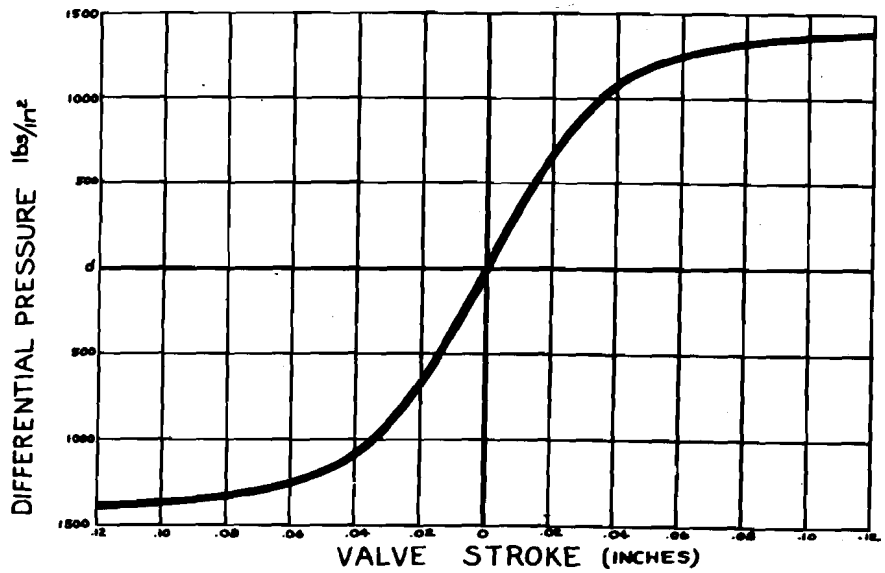

EFFECTIVE SLOPE (k) = 47,500 $\frac{lb}{in^3}$

DIFFERENTIAL PRESSURE vs VALVE STROKE

inches wide and gradually broadened to 0.080 near maximum valve excursion.

Control of the differential pressure versus valve stroke curve was more difficult, and was obtained finally by choosing an orifice to fit the flow requirements, holding the valve land overlap to a definite value, in this case, 0.002 inches, and then varying the clearance between the valve sleeve and slider until the desired slope was obtained.

The static tests, then, were useful in obtaining actual values for the slope of the flow-stroke curve K, the slope of the pressure-stroke curve K_1, and the internal resistance of the valve R_v. These tests also disclosed practical means of varying the valves' dimensions to obtain the required parameters.

Proceeding with the test program, a sinusoidal input device was designed and fabricated. This input system consisted of a hydraulic motor driving a variable amplitude scotch yoke through a series of gears with stabilization provided by a flywheel. The frequency of the unit was varied by adjusting the flow from a hydraulic power source to the hydraulic motor which was the fixed volumetric displacement type. This flexibility of control enabled the reduction of operational test time to a minimum.

Instrumentation for the tests consisted of two displacement pick-ups. One recorded the position of the valve slider with respect to the valve cylinder housing (valve error) and the other recorded the position of the cylinder housing with respect to a structural reference which was located adjacent to the point at which the input member fastened to the structure when closing the servo loop. The pick-ups used were geared up potentiometers in bridge circuits which supplied signals to the recording apparatus. An oscillograph was used as the recording means which supplied a stable reference line for measurement of the traces and an electrically driven tuning fork trace for a dependable time reference in addition to the output and error traces. Figure XI illustrates a sample test record. This test record graphically illustrates the phase lag and amplitude ratio phenomena associated with dynamic tests. Reduction of the data by use of calibration charts permits the calculation of output amplitude divided by error amplitude (amplitude ratio) and of percentage lag of the output to error which when multiplied by 360° produces the phase lag. Comparison of the error signal trace with the 60 cycles per second timing trace allowed the calculation of the period and the frequency of the error signal. Two output traces were recorded during this run, which brings up one difficulty encountered. The original tests on the mock-up measured output as picked up from motion of the axle on which the output mass was supported. Examination of the test results indicated very poor agreement with the analytical solution both in phase and amplitude ratio. It was learned that the errors were introduced largely by deflection of the axle which produced translational motion of the pick-up element as well as rotation. To improve our recording technique and also to verify our interpretation of the discrepancies, both output traces were recorded, the one from the original pick-up, and one from a pick-up recording the translational motion of the cylinder housing. The latter resulted in much less scatter of the test points and fairly close agreement with the analytical predictions.

As each test run was completed, the records were interpreted and plotted in polar form, phase and amplitude ratio for various frequencies up to 30 cycles per second. These test results made possible the revision of the analytical parameters. Test results produced the system's damped natural frequency and the phase and

FIG XI

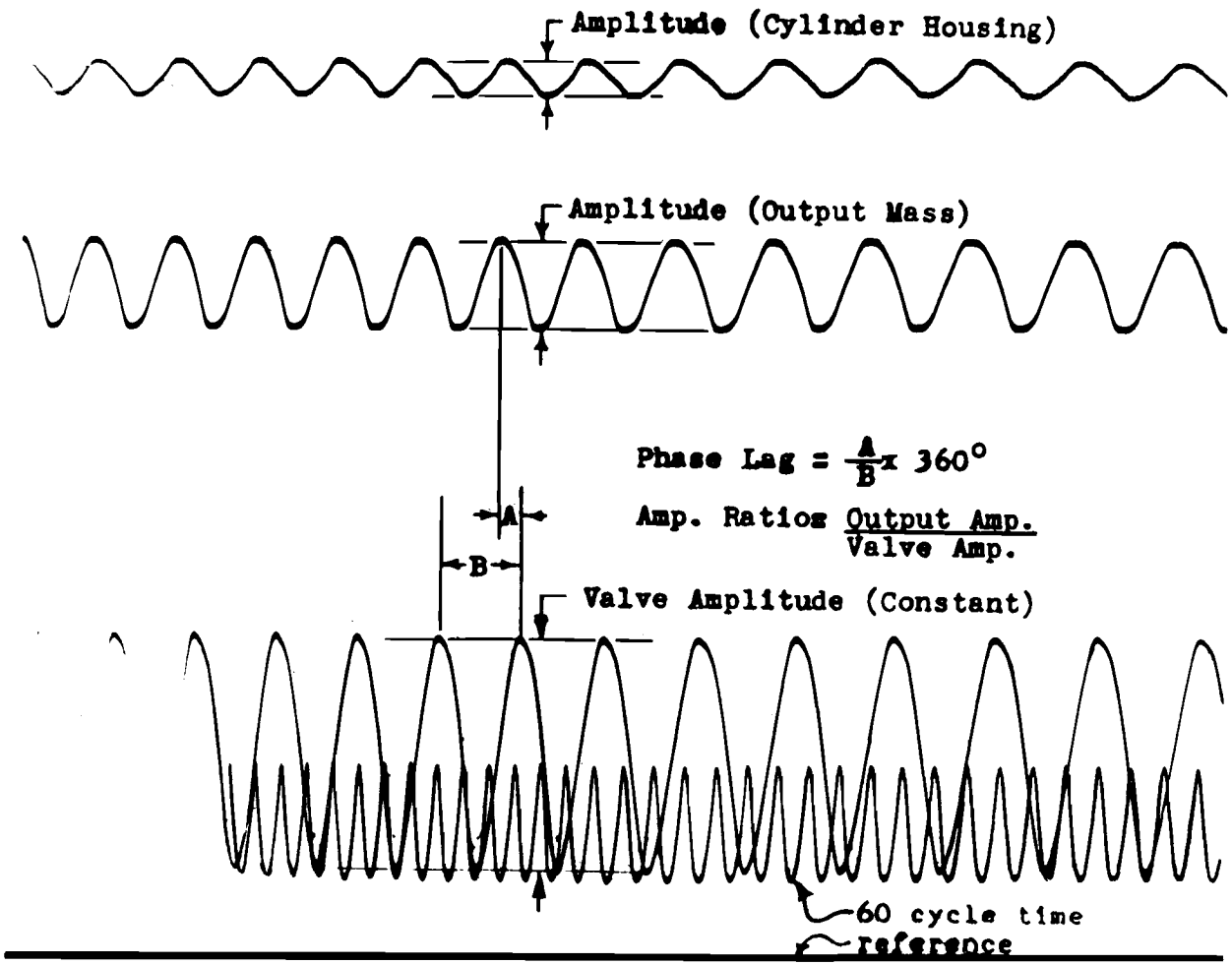
Amplitude (Cylinder Housing)
Amplitude (Output Mass)
Phase Lag = A/B x 360°
Amp. Ratio = Output Amp. / Valve Amp.
A
B
Valve Amplitude (Constant)
60 cycle time
reference

amplitude ratios for definite frequencies. These figures allowed the analyst to vary the parameters originally assumed. At this point, there was enough information available upon which to base a new set of valve characteristics designed to deliver optimum performance of the unit under test. Using the revised differential equations, and applying Nyquist's stability criteria, valve characteristics were assigned that would result in such performance.

In this test case, the flow versus valve stroke characteristics were already satisfactory which then indicated that a change in differential pressure versus valve stroke slope would be the only alteration necessary. This was done by honing out the valve sleeve which effectively altered the characteristics to a small extent which was all that was indicated to be necessary. This particular valve required removal of 0.0005 inches in diameter. Upon completion of this rework, the tests were repeated and it was ascertained that for the given condition of operations, no further improvement through rework of the valve could be expected or desired.

The final test results in polar diagram form as compared to the analytically predicted curve are presented in Figure XII. Although the resonant frequency matches in phase angle and amplitude ratio, it can be seen that the predicted curve has a sharper resonant peak and that some of the damping terms appear to differ from the actual case. However, the correlation was acceptable for the establishment of design parameters for stability purposes.

Operation of the boost system was then checked by closing the feed-back loop which in this case meant coupling the valve slider to the control stick system and introducing random input disturbances. The boost system operated as anticipated and was considered to be acceptable for use on the aircraft.

FIG XII

COMPARISON OF CALCULATED AND TEST TRANSFER FUNCTIONS

$$K = 0.06135$$

$$\mu = \frac{j\omega}{424.04}$$

$$G(\mu) = \frac{7.0331\mu^2 + 0.14\mu + 1}{\mu[0.14\mu^3 + 8.0404\mu^2 + 0.1924\mu + 1]}$$

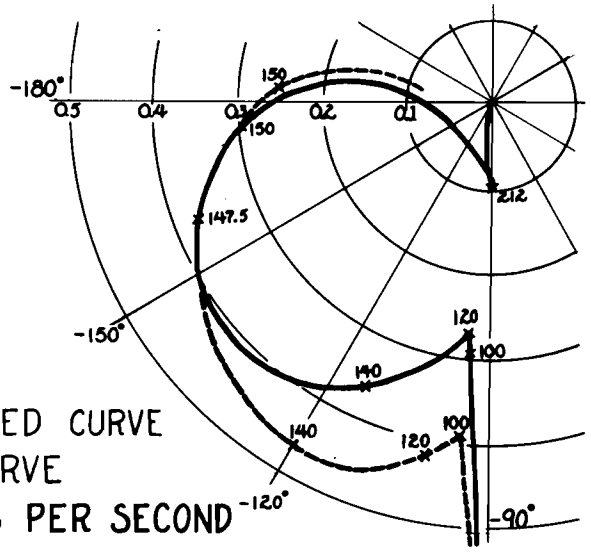

— REPRESENTS CALCULATED CURVE
-- REPRESENTS TEST CURVE
FREQUENCIES IN RADIANS PER SECOND

[redacted]

At this time, the fallacy of a basic assumption became apparent. Upon installation of the boost system in the aircraft, it was found to be dynamically unstable. This, of course, indicated a marked difference between the mock-up and the aircraft. Since the same boost system was involved, the difference had to be attributed to the supporting structure and to the dynamic characteristics of the control surface. A detailed structural study at this time would have been too lengthy, therefore, tests were continued with the boost system mounted in an outer wing panel from the aircraft. Operation of this assembly indicated visually that the control surface was not rigid as had been assumed and was undoubtedly contributing to the excessive energy storage problem as was the structure supporting the boost system. Since any rework of the structure and the surface to improve their dynamic characteristics would have required considerable time, and since the likelihood of sufficient improvement was slight, it was decided that the valve again appeared to provide the most direct means of obtaining an acceptable system. Space limitations precluded the use of the sinusoidal input device which was utilized in the mock-up tests so that transient response studies were substituted. Results of the tests on the wing panel assembly indicated that the change in valve characteristics would be too great to be controlled by alteration of the differential pressure versus valve stroke curve alone. Therefore, the orifice width was reduced to the next small engraving cutter size which reduced the slope of the flow versus valve stroke curve. The differential pressure versus valve stroke curve slope was also reduced to the desired value.

Reduction of the flow-stroke curve slope meant in this case that there would be a considerable restriction to flow at maximum valve excursion. The hydraulic power source was not a linear device instead giving increased flow at a reduced pressure. Thus, it was justifiable to open the valve orifice width near maximum valve excursion making the flow response curve more nearly linear. Upon installation of the reworked valve in the wing panel assembly, it was found to operate satisfactorily under all input conditions and was approved for flight.

One last precautionary stability check was made prior to flight, and that was the determination of the allowable clearances in the boost system couplings that would still permit normal operation. The previous tests had all been conducted with honed and lapped pins, bushings, and bearing races. The last check was of the boost system response to random input disturbances as the clearances in all couplings were progressively increased. With the particular system under test, 0.004 inch was found to make the system marginally stable. This figure was the total clearance for all the joints. In view of this data, recommendations as to allowable tolerances for the clearance at each joint were released and the system considered complete.

The usefulness of the frequency response method of analysis was apparent when it was determined that only minor adjustments of the valve were necessary for optimum performance when designed from analytically derived parameters.

The actual test program verified the usefulness of the frequency response method and also pointed out some of its limitations.

The limitations result from the necessity of assumption of certain parameters such as structural damping. Undoubtedly, errors resulting from such assumptions could be minimized by careful structural studies of the elements involved. Secondly, analysis will always be subject to some error through the introduction of unpredictable non-linear characteristics and possibility of variations due to fabrication processes.

[redacted]

STABILITY AND PERFORMANCE CHARACTERISTICS OF AN IRREVERSIBLE SURFACE BOOST SYSTEM, CHANCE VOUGHT AIRCRAFT

By

E. R. Harris and J. Drew

Chance Vought Aircraft, Dallas, Texas

PART I

Introduction

The power boosted surface control is a mechanism that has been developed concurrently with the progress and development of high performance aircraft. Nothing new has been added to the basic control configuration; the development of the mechanism reflects primarily the pilot's limited ability to deliver power. Means for supplementing the pilot's effort could be provided by mechanical, electrical, hydraulic or pneumatic devices. The major efforts in this field, however, have been with hydraulic devices and this symposium is assembled to discuss the means and methods used in the development of hydraulic power boost surface control equipment.

The "irreversible boost system" is receiving a considerable amount of attention and interest in the aircraft industry at the present time. This device offers a means of supplying supplementaty power for the pilot and in addition has the desirable characteristic of isolating the surface forces from the pilot's control devices. A successful installation of this type alleviates the aerodynamiscists concern over peculiar hinge moment characteristics and pilot effort problems of high speed flight, but presents the additional problem of requiring an installation of artificial "pilot feel".

The basic requirements and the basic mechanisms of power boost equipment are evidently established, but the unfortunate fact of the matter is that a completely satisfactory system is not in hand. The systems show a tendency to instability and the pilot's characterize the operation of the equipment as "over sensitive."

In this paper, an effort will be made to discuss the "irreversible boost system" with particular emphasis on the stability and performance characteristics. Force feedback systems, the "over-sensitivity" problem, artificial feel, etc., will not be discussed. Part I is devoted to the application of servo-theory to the mechanism and Part II, to a discussion of laboratory results and techniques determined at Chance Vought.

Development of the Theory

Figure I has been prepared to illustrate the mechanism under consideration and to define the parameters. The displacement X_i represents the motion received from the pilot's control; X_o represents the motion imparted to the controlled surface; and X_ϵ represents the difference between X_i and X_o and is the valve opening. This configuration is known as a closed-center irreversible power boost and requires an external

FIG. I

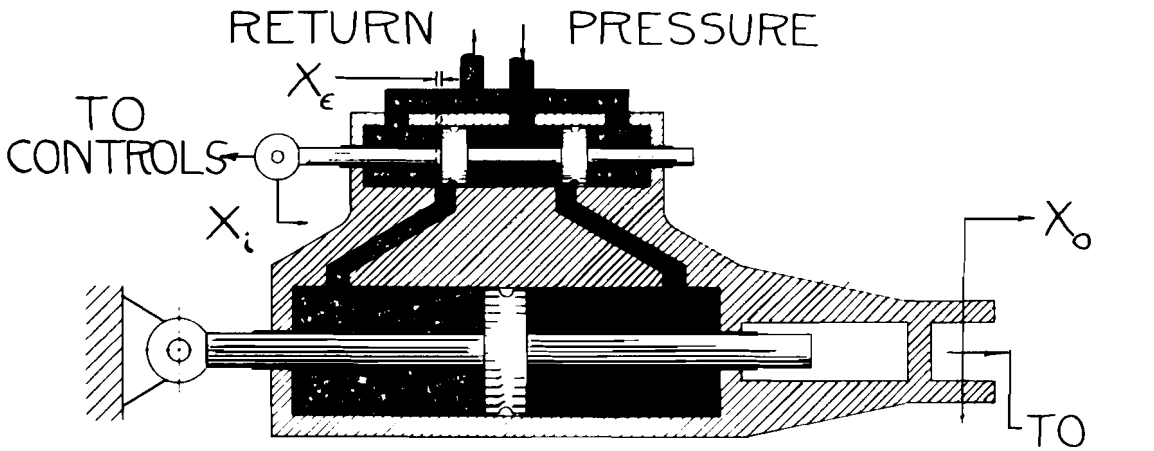

SCHEMATIC

CLOSED CENTER IRREVERSIBLE BOOST SYSTEM

hydraulic circuit to supply pressure at a constant flow consistent with the maximum speed requirements of the operator. Figures Ia and Ib have been prepared to illustrate other configurations that satisfy the same definitions. These configurations are basically the same as that of Figure I, and mathematical expressions developed for any one of them can be applied directly to another. The configuration of Figure I has been selected for discussion because it is the most elementary and it is the configuration with which we have had the most experience. Let it suffice to say that the configurations differ only in geometry and these properties appear as multiplying factors in the open-loop transfer function.

As in most servo theory, it is convenient to revert directly to an examination of the relationship between the output X_o and the error X_ϵ. In this case, the valve characteristics dominate the considerations. Pressures and flows are excited by valve error which in turn direct output motion. Since the output pressure is totally dependent on the character of the "load", it is evident that an expression relating valve motion to output motion for an arbitrary load must first be developed.

There are two significant characteristics of a valve which can be used to develop the expression. The first is the flow-stroke characteristic and the second is the pressure-stroke characteristic. Figure II has been prepared to illustrate suitable test methods for determining these characteristics for any given valve. Over a short range and particularly near $X_\epsilon = 0$, the following equations may be used:

$$P_\epsilon = K X_\epsilon$$

and

$$Q_{sc} = K_1 X_\epsilon$$

FIG. Ia

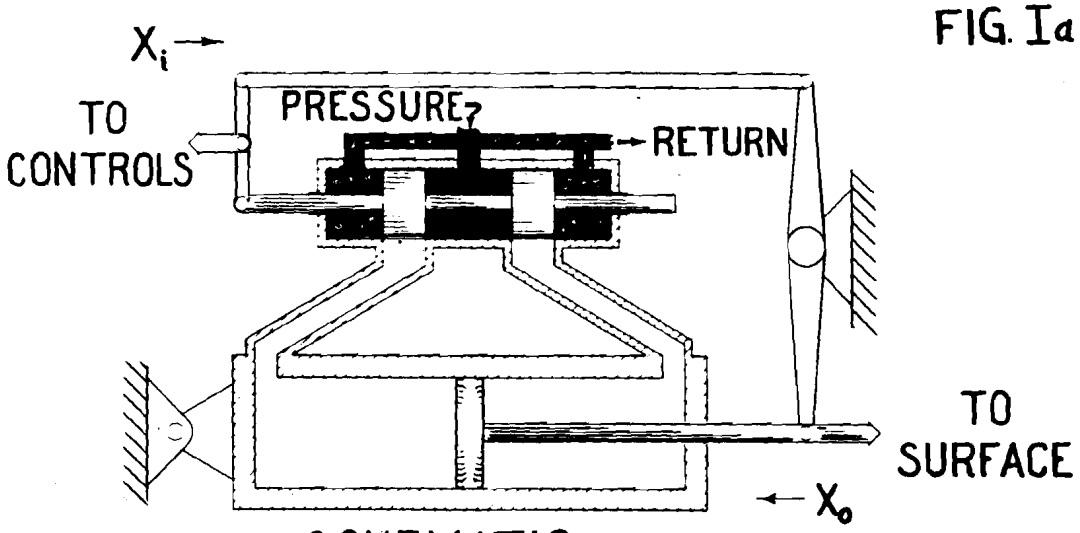

SCHEMATIC

CLOSED CENTER IRREVERSIBLE BOOST SYSTEM

DIFFERENTIAL BAR FOLLOW-UP

FIG. Ib

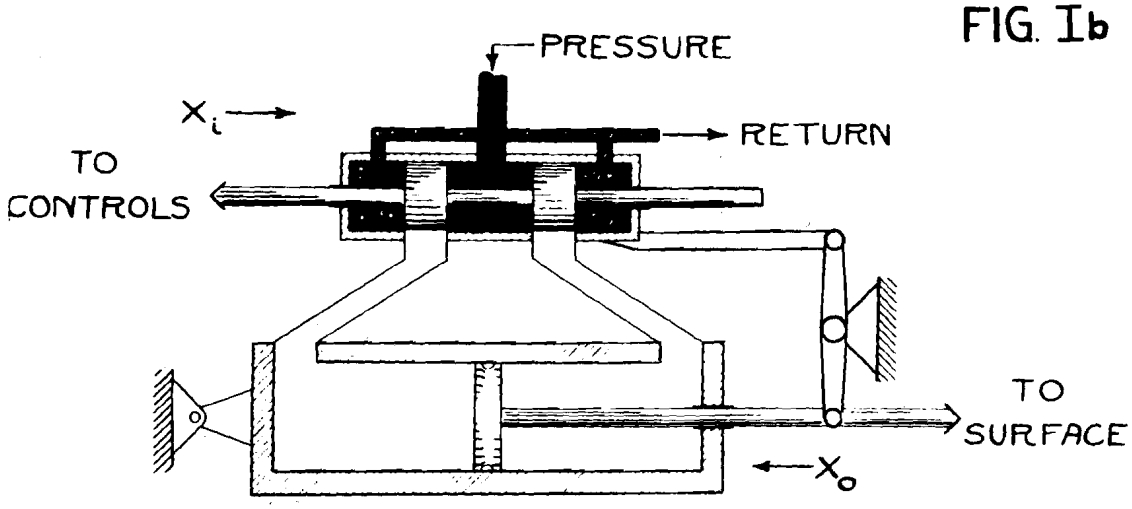

SCHEMATIC

CLOSED CENTER IRREVERSIBLE BOOST SYSTEM

VALVE CASE OR VALVE SLEEVE FOLLOW-UP

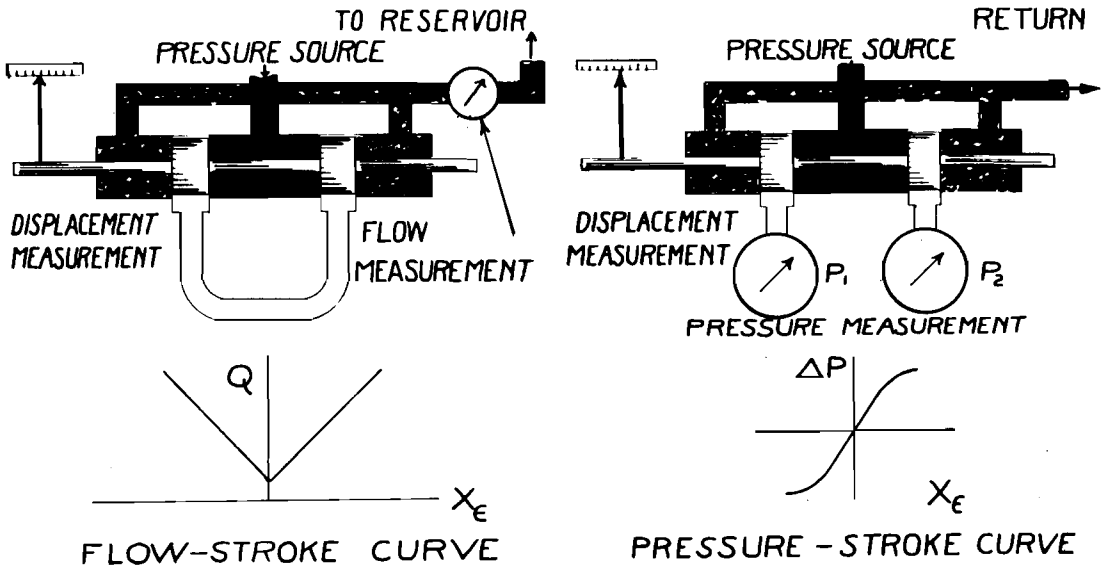

FIGURE II

FIG. III

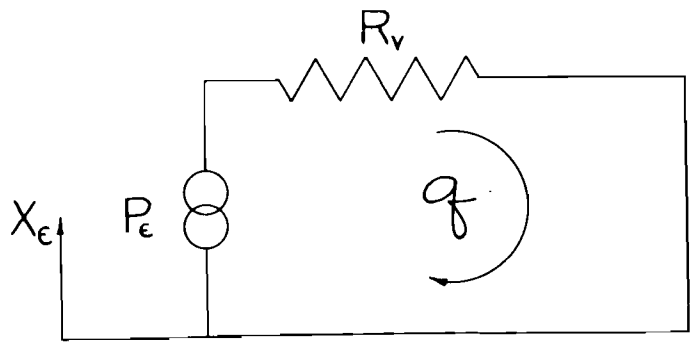

FOUR-WAY VALVE EQUIVALENT CIRCUIT

Now, if methods of the electrical engineers are borrowed, an equivalent hydraulic circuit can be assumed. Figure III illustrates an equivalent circuit that satisfies the assumed proportional characteristics of the valve. Using the schematic, a pressure drop equation can be written as follows:

$$P_\epsilon = R_v Q_{sc}$$

Where P_ϵ is the pressure rise and $R_v Q_{sc}$ is the pressure drop. When the expressions for the flow-stroke and pressure-stroke are substituted, for P_ϵ and Q_{sc}, R_v is expressed in terms of constants.

$$K X_\epsilon = R_v K_1 X_\epsilon \quad ; \qquad R_v = \frac{K}{K_1}$$

or

$$R_v = \frac{Pressure\ -\ stroke\ slope}{Flow\ -\ stroke\ slope}$$

This method of determining the internal "resistance" of the valve is analogous to methods used to determine generator internal impedance, electronics amplifier output imedance, etc. Having established an equivalent circuit for the valve, it is now possible to develop an expression relating X_o and X_ϵ for an arbitrary "load". Again, using electrical engineering terminology, the load will be called an "impedance" Z_L and will have dimensions of pressure per unit flow. The impedance may be added to the basic equivalent circuit as shown in Figure IV.

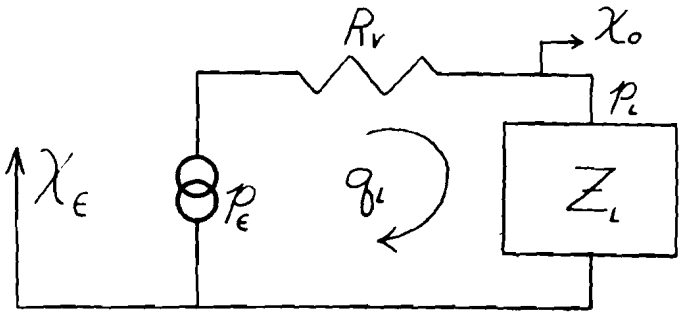

FIG. IV

$$\frac{X_o}{X_\epsilon} = \frac{k}{AR_v} \times \frac{1}{S} \times \frac{1}{1 + Z_L\left(\frac{1}{R_v}\right)}$$

Four-Way Valve
Equivalent Circuit Including
Load Impedance

Equating pressure rises to pressure drops,

$$P_\epsilon = R_v\, q_L + Z_L\, q_L$$

and substituting:

$$P_\epsilon = K\, X_\epsilon$$

and

$$q_L = A\, X_o s$$

The ratio of X_o to X_ϵ is developed.

$$\frac{X_o}{X_\epsilon} = \frac{K}{A\, R_v} \cdot \frac{1}{s} \cdot \frac{1}{1 + Z_L\left(\frac{1}{R_v}\right)}$$

This expression may be called the open loop transfer function for an arbitrary load. Without considering the effects of Z_L, the expression has the characteristics of a zero position servomechanism.

Before proceeding to a detailed examination of load impedance and its effect on the transfer function, a word or two must be said about an alternate equivalent circuit. Under most circumstances, the compressibility of the fluid and deformation of lines and cylinders must be taken into account. In this case a two-loop equivalent

FIG V

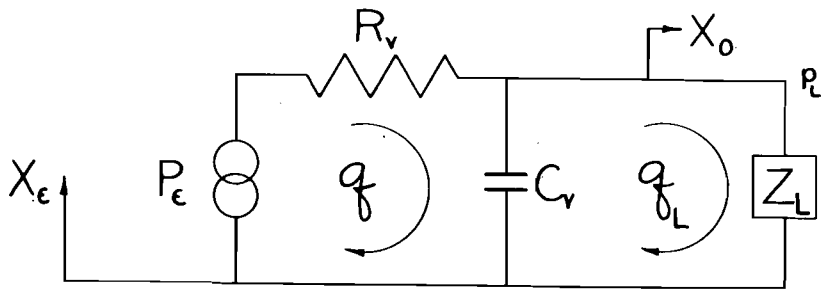

$$\frac{X_o}{X_\epsilon} = \frac{k}{A R_v} \times \frac{1}{S} \times \frac{1}{1 + Z_L\left(\frac{R_v C_v s + 1}{R_v}\right)}$$

FOUR-WAY VALVE EQUIVALENT CIRCUIT
INCLUDING
LOAD AND COMPRESSIBILITY EFFECTS

circuit must be assumed as shown in Figure V. The expression for the transfer function may be solved in the same manner as before, giving

$$\frac{X_o}{X_\epsilon} = \frac{K}{A R_v} \cdot \frac{1}{s} \cdot \frac{1}{1 + Z_L\left(\frac{R_v C_v s + 1}{R_v}\right)}$$

For the moment, it will be convenient to abandon the generalized transfer functions and examine the character of the load impedance Z_L in detail. The load pressure p_L resulting from flow q_L is due to mechanical phemonena such as hinge moment, surface mass, friction, etc., and consequently a conversion factor is necessary to relate hydraulic to mechanical phenomena. The impedance Z_L has been defined as the ratio of p_L to q_L :

$$Z_L = \frac{p_L}{q_L}$$

but since

$$p_L = \frac{F_o}{A}$$

and

$$q_L = A X_o s$$

$$Z_L = \frac{1}{A^2} \cdot \frac{F_o}{s X_o}$$

The hydraulic load impedance Z_L can be determined by solving for the mechanical impedance and multiplying by $1/A^2$, the conversion factor.

Figures VIa, VIb, VIc & VId have been prepared to illustrate solutions of the hydraulic load impedance for increasingly complex systems. The next step is to combine the equivalent valve circuit and the load impedance and examine progressively the effects on the open and closed transfer functions and the closed loop transient response.

Figure VII illustrates the case of $Z_L = 0$. The open loop transfer function plots along the $-j$ axis, the closed loop has the pure time lag characteristic and the transient solution is shown accordingly. It is interesting to note that it is impossible to make this system unstable. An increase in the flow stroke curve K/R_v or a decrease in the piston area A both serve to decrease the time of response, but extension to limits simply reduces or increases the speed of the system. It is also evident that the steady state response of the mechanism is independent of the parameters.

Figure VIIa illustrates the condition in which the load is composed of mass only. This particular condition illustrates some of the confusing aspects of this type of mechanism. For example, by examination of the expressions for ω_o and ζ_o it is evident that the natural frequency and the damping are both increased for an increase of the piston area. It is contradictory in a sense, since an increase in the piston area intuitively decreases the speed! The explanation is however, that the damping increases much faster than the natural frequency and affects a net decrease. The effect

Hydraulic Impedance

FIG. VI a

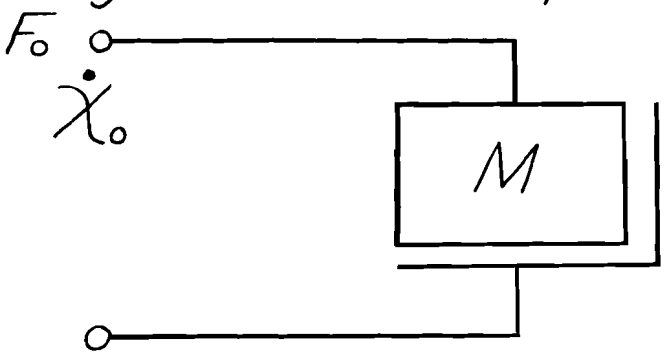

$$Z_L = \frac{1}{A^2} \times \frac{F_o}{\dot{x}_o} = \frac{1}{A^2} MS$$

Mass Load

FIG. VI b

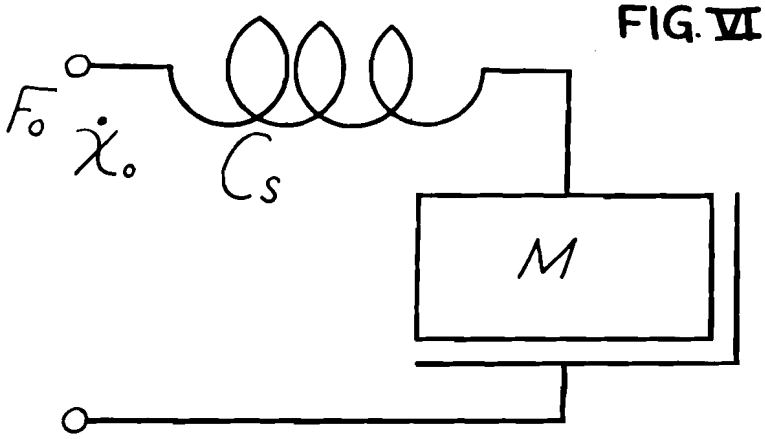

$$Z_L = \frac{1}{A^2} \times \frac{F_o}{\dot{x}_o} = \frac{1}{A^2}\left[\frac{C_s M}{C_s/S + MS}\right]$$

Mass & Structural Load

Hydraulic Impedance

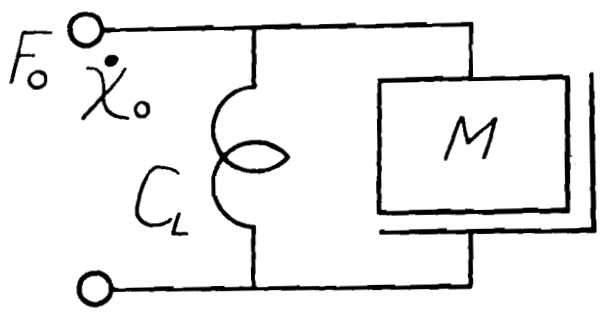

FIG VI c

$$Z_L = \frac{1}{A^2} \times \frac{F_o}{\dot{X}_o} = \frac{1}{A^2}\left[MS + \frac{C_L}{S}\right]$$

Mass & Hinge Moment

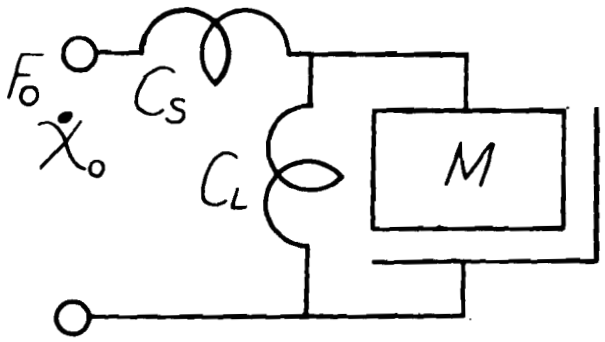

FIG VI d

$$Z_L = \frac{1}{A^2} \times \frac{F_o}{\dot{X}_o} = \frac{1}{A^2}\left[\frac{\frac{C_S C_L}{S^2} + C_S M}{\frac{C_S + C_L}{S} + MS}\right]$$

Mass, Hinge Moment & Structural Load

FIG. VII

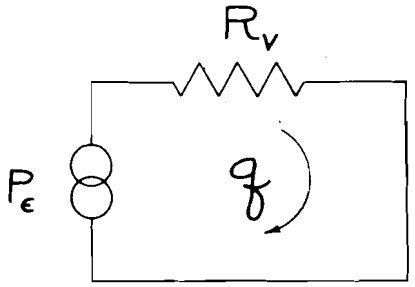

$$\frac{X_o}{X_\epsilon} = \frac{k}{R_v A} \times \frac{1}{P}$$

$$\frac{X_o}{X_i} = \frac{1}{1 + \frac{R_v A}{k} S}$$

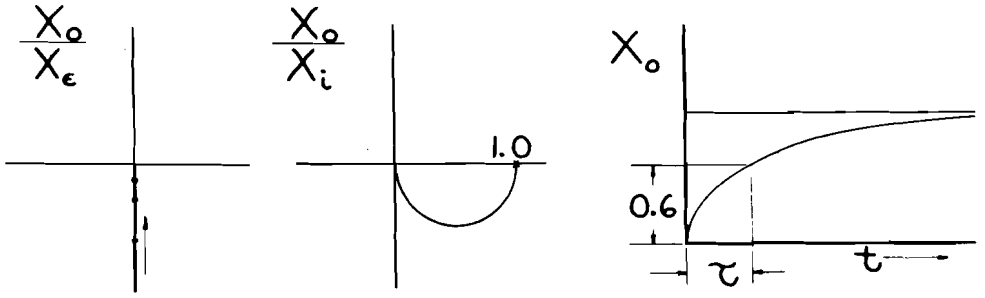

FIG. VII a

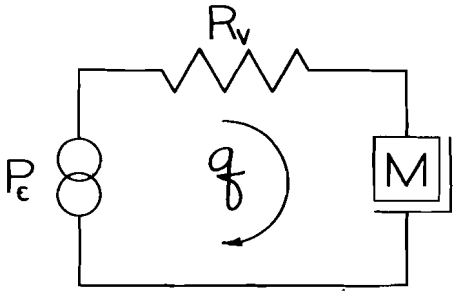

$$\frac{X_o}{X_\epsilon} = \frac{k}{AR_v} \times \frac{1}{S} \times \frac{1}{\left(1 + \frac{M}{A^2 R_v} S\right)}$$

$$\frac{X_o}{X_i} = \frac{1}{\frac{M}{kA} S^2 + \frac{R_v A}{k} + 1}$$

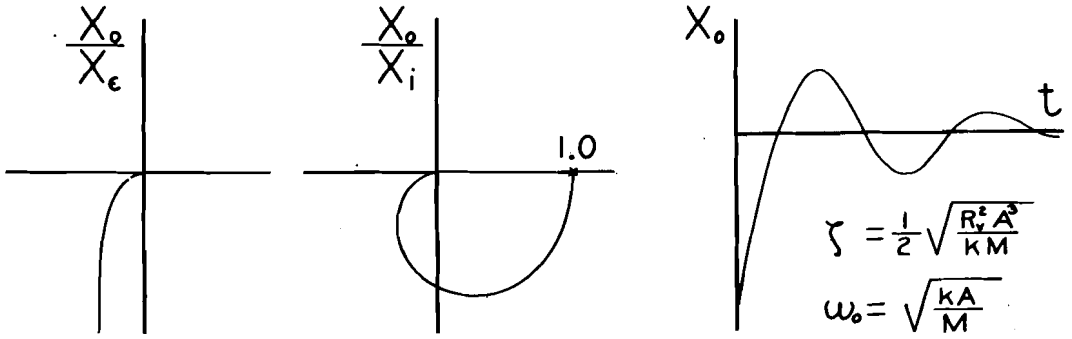

of changes in the mass M is more evident. An increase in the mass of the system decreases the natural frequency and the damping and should be avoided if at all possible. The best control of the amount of damping is provided by K/R_v. The flow-stroke curve which appears in the open loop transfer function as a gain factor. A reduction of the flow stroke curve will increase the damping factor and not alter the natural frequency. Again the assumed configuration is stable and self-sustained oscillation is not possible.

Figure VIIb illustrates the case in which it is assumed that structural deflections take place between the output piston and the surface mass, The addition of the structural deflection term alters the dynamic characteristics of the system, but leaves the steady-state unaltered. Of particular interest again is the fact that this system cannot become unstable by any manipulation of parameters. The open-loop transfer function does not cross the -180° axis. One particularly interesting feature of this configuration is the appearance of terms in the numerator of the closed-loop transfer function. This introduces a zero or null into the transfer function plot and means that X_0 does not respond to X_ϵ or X_i at this frequency. Another interesting feature of this configuration is that the natural frequency term associated with the system mass and the valve pressure-stroke curve becomes unimportant. To illustrate, typical values of M/C and M/KA are 100×10^{-6} and 10×10^{-6} respectively. The ratio of these numbers is independent of the mass of the system and the implication is that the force per-unit motion of the valve is high compared to the stiffness of efficient structural design. If the M/KA term is neglected compared to the M/C term, the natural frequency of the system becomes independent of valve characteristics and the effective damping is dependent only on the flow-stroke characteristic of the valve. Piston area and system mass have the same effects as before.

FIG. VII b

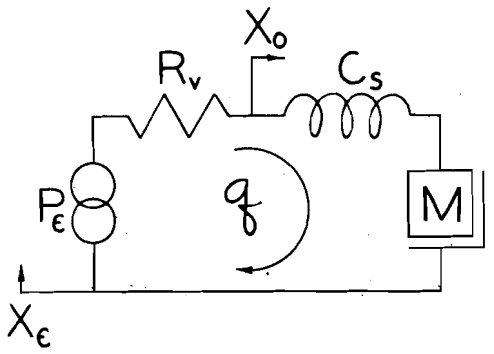

$$\frac{X_0}{X_\epsilon} = \frac{k}{AR_v} \times \frac{1}{S} \times \frac{\frac{M}{C_s}S^2 + 1}{\frac{M}{C_s}S^2 + \frac{M}{A^2R_v}S + 1}$$

$$\frac{X_0}{X_i} = \frac{\frac{M}{C}S^2 + 1}{\frac{AR_v}{k} \times \frac{M}{C}S^3 + \left(\frac{M}{kA} + \frac{M}{C}\right)S^2 + \frac{AR_v}{k}S + 1}$$

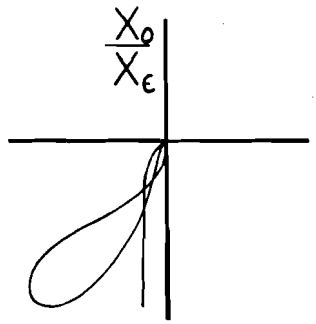

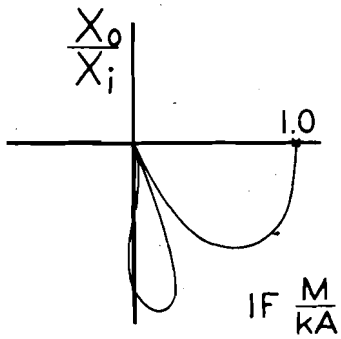

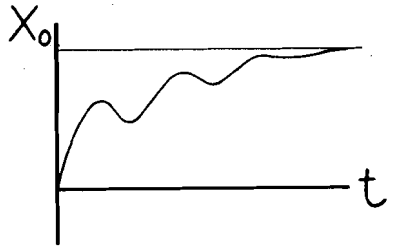

IF $\frac{M}{kA} < \frac{M}{C}$ $\quad \zeta \sim \frac{AR_v}{k}\frac{1}{2}\sqrt{\frac{C}{M}}$

FIG VII c

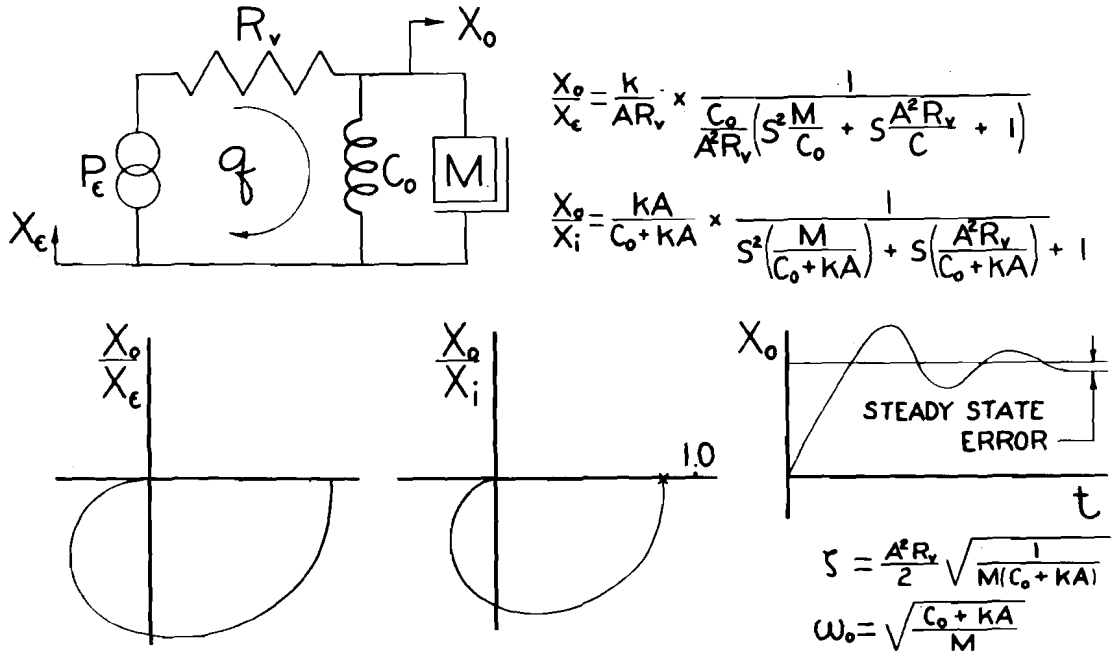

When the effects of "load" or hinge moment are considered, another change is introduced in the system. Figure VIIc illustrates this configuration. One property of the system is of particular interest. The system is no longer a zero error servomechanism. This is due to the fact that a finite valve error is required to hold a hinge moment and results in a smaller deflection of the surface than is called for by the control column. This property is sometimes called "droop" in regulators and in this particular case is only of importance when the controlability of the aircraft is considered. It is not significant or important as a property of the boost itself.

The final illustration of loads with the simple hydraulic equation is given on Figure VIId. The complexity of the characteristic equation and the parameters have increased to the point where it is indeed difficult if not impossible to casually evaluate the effects of number changes. It should be noted, however, that these characteristics possess all the properties of the systems previously discussed. The steady-state has "droop" and the dynamic characteristics are of the same order as the configuration using structural deflection and mass parameters for the load. One property appears that should be very heartening to irreversible boost system designers:-- The addition of hinge-moment tends to make the system more stable. In other words, a system that is stable on the ground will not develop self-oscillations in flight.

The dominant feature of the analysis so far is that none of the assumptions made indicate a tendency toward instability in the characteristic equations. If such is the case, it is evident that the theory is in error or that sufficient parameters

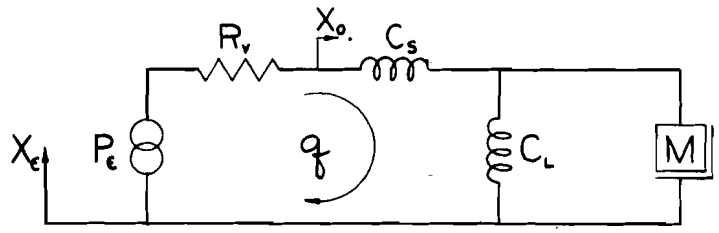

FIG VII d

$$\frac{X_o}{X_\epsilon} = \frac{k}{AR_v} \times \frac{A^2R_v(C_s + C_L)}{C_sC_L} \times \frac{S^2\left(\frac{M}{C_s + C_L}\right) + 1}{S^3\frac{A^2R_vM}{C_sC_L} + S^2\frac{M}{C_L} + SA^2R_v\left(\frac{C_s + C_L}{C_sC_L}\right) + 1}$$

$$\frac{X_o}{X_i} = \frac{kA(C_s + C_L)}{C_sC_L + kA(C_s + C_L)} \times \frac{S^2\left(\frac{M}{C_s + C_L}\right) + 1}{S^3\left[\frac{AR_vM}{C_sC_L + kA(C_s + C_L)}\right] + S^2\left[\frac{C_sC_L}{C_sC_L + kA(C_s + C_L)}\left(\frac{M}{C_L} + \frac{kMA}{C_sC_L}\right)\right] + S\left[\frac{(C_s + C_L)A^2R_v}{C_sC_L + kA(C_s + C_L)}\right] + 1}$$

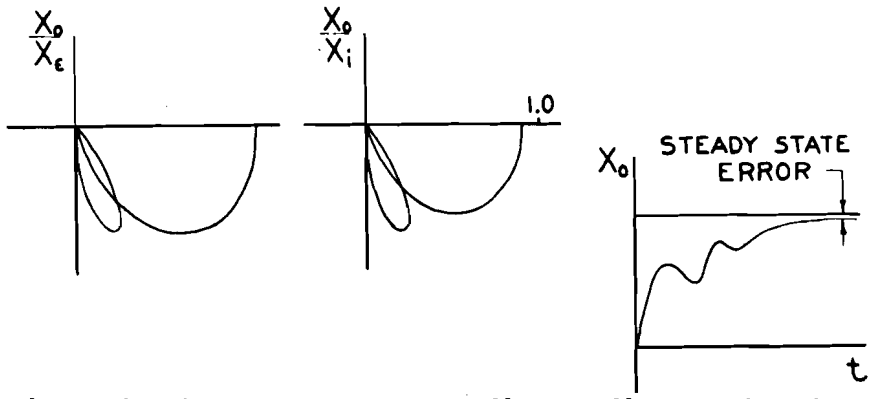

have not been taken into account. We are all too well aware that the mechanisms do oscillate. Actually, it is essential to assume oil compressibility or cylinder expansion to account for the unstable properties of this mechanism. The next set of illustrations have been prepared to contrast with those already illustrated. The same load impedances will be added to the second equivalent hydraulic circuit in the same order.

Figure VIIIa illustrates the combination of the equivalent hydraulic circuit including compressibility effects and a simple mass load. When compared to Figure VIIa, it is immediately apparent that this system can be unstable even with a very simplified load. This is the first illustration in which the open-loop transfer function crosses the -180° axis.

Figure VIIIb illustrates the above configuration with hinge-moment added. As before, the open-loop transfer function crosses the -180° axis and the addition of the load introduces "droop" in the same fashion as with the simple circuit.

Figure VIIIc illustrates the compressibility configuration with a load consisting of structural deflection and mass. Again, we have an open-loop transfer function that crosses the -180° axis and is therefore subject to self-oscillation.

FIG VIII a

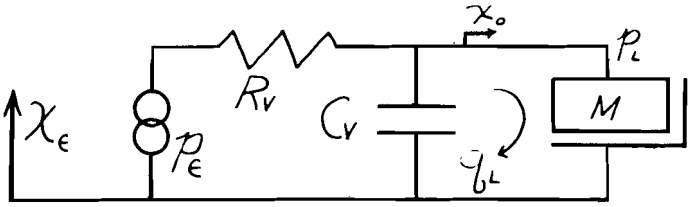

$$\frac{x_o}{x_\epsilon} = \frac{k}{AR_v} \times \frac{1}{S} \times \frac{1}{S^2\left(\frac{M}{A^2C_v}\right) + S\left(\frac{M}{A^2R_v}\right) + 1}$$

$$\frac{x_o}{x_i} = \frac{1}{S^3\left(\frac{MR_v}{ACvk}\right) + S^2\frac{M}{Ak} + S\frac{AR_v}{k} + 1}$$

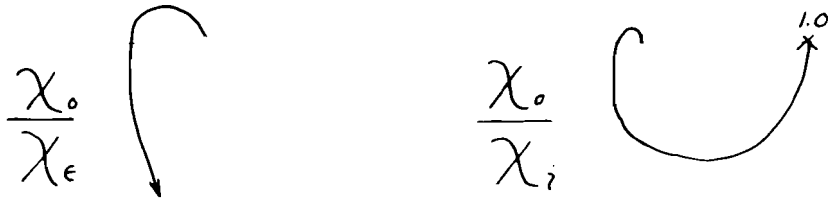

FIG VIII b

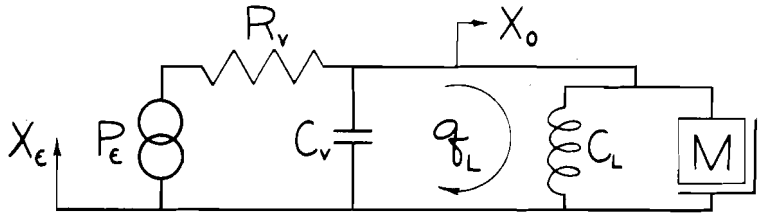

$$\frac{X_o}{X_\epsilon} = \frac{kA}{C_L} \times \frac{1}{S^3\frac{MR_v}{C_vC_L} + S^2\frac{M}{C_L} + S\left(\frac{C_L}{A^2C_v} + 1\right)\left(\frac{A^2R_v}{C_L}\right) + 1}$$

$$\frac{X_o}{X_i} = \frac{kA}{kA + C_L} \times \frac{1}{S^3\frac{MR_v}{C_vC_L}\left(\frac{1}{\frac{kA}{C_L} + 1}\right) + S^2\frac{M}{C_L}\left(\frac{1}{\frac{kA}{C_L} + 1}\right) + S\left(\frac{C_L}{A^2C_v} + 1\right)\left(\frac{A^2R_v}{C_L}\right)\left(\frac{1}{\frac{kA}{C_L} + 1}\right) + 1}$$

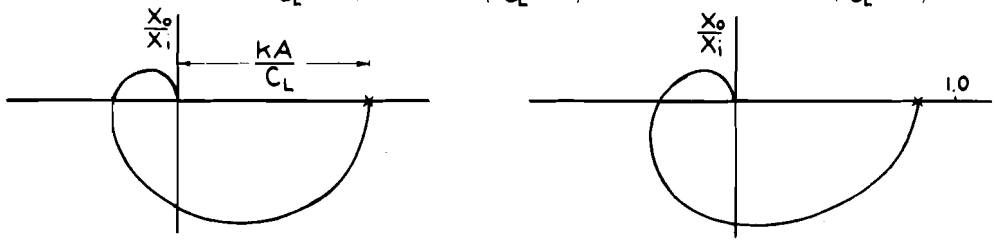

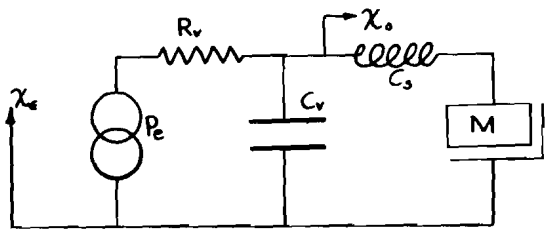

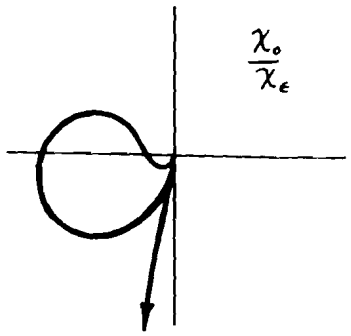

$$\frac{\chi_o}{\chi_\epsilon} = \frac{k}{AR_v} \times \frac{1}{S} \times \frac{\left(\frac{M}{C_s}\right)S^2+1}{S^2\left(\frac{M}{C_s}+\frac{M}{A^2C_v}\right)+S\frac{M}{A^2R_v}+1}$$

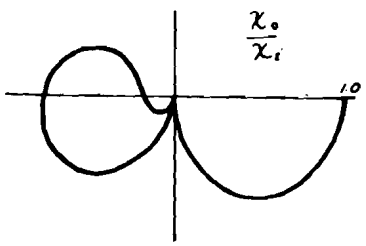

$$\frac{\chi_o}{\chi_i} = \frac{\left(\frac{M}{C_s}\right)S^2+1}{S^3\frac{AR_v}{K}\left(\frac{M}{C_s}+\frac{M}{A^2C_v}\right)+S^2\left(\frac{M}{kA}+\frac{M}{C_s}\right)+\frac{AR_v}{K}S+1}$$

FIG VIII c

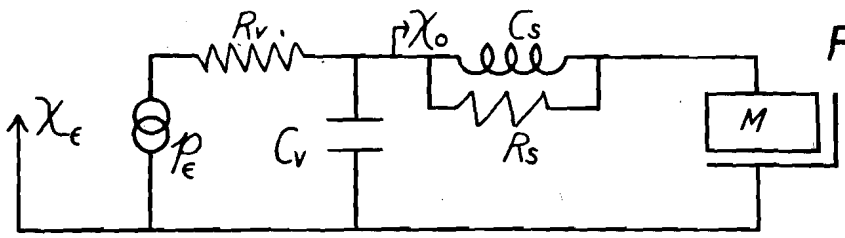

FIG VIII d

$$\frac{\chi_o}{\chi_\epsilon} = A\,\frac{B\mu^2+C\mu+1}{\mu\left[D\mu^3+E\mu^2+F\mu+1\right]}$$

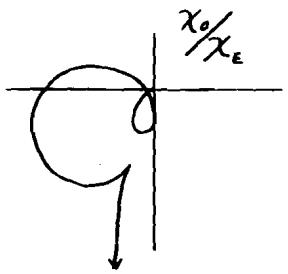

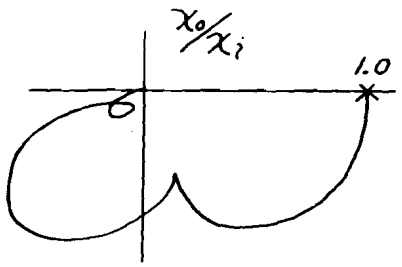

[redacted]

PART II

Application and Test Results

Part I of this paper was devoted to the application of servomechanism theory to the irreversible hydraulic boost system. This section of the paper will be confined to a description of an application of the theory to the ailavator boost system of the Chance Vought experimental Cutlass, XF7U-1. Actually, the theoretical expressions could not have been developed or refined without parallel and supporting laboratory investigation.

Development of the complete hydraulic system for the Cutlass included the construction of a full scale dimensional hydraulic mock-up. In the original planning, the mock-up was intended for operational and other routine hydraulic tests. The avail ability of the hydraulic mock-up offered the possibility of investigating the stability characteristics of the boost system prior to installation in the first flight article. The possibility of avoiding delays to the flight test program by qualifying the boost system dynamically prior to flight was attractive and actively prosecuted thereafter.

It was necessary to simulate parameters of the aircraft to a certain extent and additions and changes were made to the mock-up accordingly. Airloads were simulated by a family of torque tubes producing hinge moments from zero to 1000 foot pounds per degree which were calibrated in terms of airspeed at given altitudes. The mass of the control surface was represented by a rotating steel body with the same moment of inertia as that of the control surface with the same radius arm coupling it to the boost cylinder. The load can best be pictured as a concentrated mass of 1,700 pounds attached directly to the boost cylinder. This inertia load assumed a concentrated mass rather than the actual case of mass distributed along the torque box of the surface with a concentrated mass terminating the torque box. At the time of construction of the inertia load, the surface was assumed to be rigid insofar as its dynamic characteristics at the boost system's resonant frequencies were concerned. In order that as many of the aircraft components as possible would be checked in the tests, actual parts were used to couple the boost cylinder rod end to the mock-up structure and the boost cylinder to the simulated inertia and aerodynamic spring loads.

The boost cylinder and integral valve housing are shown schematically in Figure I. It can be seen that positional follow-up is obtained by attaching the rod end to the structure and the cylinder housing to the load. In this way, once a valve input signal is received, movement of the housing is initiated and as controlled by the error between the input signal and the position of the output will continue to move until the error between the two is brought to zero. Forging of the valve housing and the cylinder housing as one unit insures a minimum possibility of error entering into the feedback linkage.

The physical dimensions of the unit were more or less dictated by the extreme aerodynamic requirements. For example, approximately nine square inches of piston area were required at a line pressure of 3300 pounds per square inch to match the hinge moments anticipated as well as a flow of 20 gallons per minute maximum for each unit. Since the boost system dimensions were not variable, the entire problem of stability required the determination of valve characteristics as a possible means of

[redacted]

control. Mr. Harris has already discussed the contribution of the valve characteristics to the analytical approach.

The test program on the irreversible boost system was divided into two distinct phases, static and dynamic.

The first or static phase entailed the determination of static valve characteristics and calibration of the instrumentation and was performed in the hydraulic and electronic test laboratories.

The second or dynamic phase checked the boost system's open-loop response to a variable frequency sinusoidal input, emphasized the important role the valve characteristics play in the stability of such a system, and was performed on the hydraulic mock-up and the aircraft.

The valve under test was of the two land linear slide type with a basic configuration as shown in Figure I. Pressure is introduced as indicated and metered through an orifice into one cylinder port when the valve slider is displaced. The flow out of the cylinder caused by pixton motion is metered through a similar orifice to the return line.

The equipment used in the determination of the valve characteristics was of the standard hydraulic laboratory type, consisting of a power source similar to that used in the aircraft, pressure gauges, flow meters, and a test jig for the valve and fittings.

The total flow versus valve stroke curve was obtained by setting up a hydraulic circuit as illustrated in Figure II. and obtaining flow measurements for specific valve slider positions as determined by an accurate dial gauge. By adjusting the bypass valve, it was possible to simulate a given differential pressure across the piston, thus producing the effect of flow controlled by the valve with the piston subjected to a load. Results of the test are shown in Figure IXa. By removing the effect of neutral leakage (flow through the valve when the flow to the cylinder is zero), the resultant curves, Figure IXb, are seen to be similar to vacum tube dynamic characteristics of plate current versus grid voltage for a family of resistive load impedances.

The differential pressure versus valve stroke curve was determined by use of hydraulic circuitry as illustrated in Figure II. Results of the test are shown in Figure X. Although the flow versus valve stroke curve was determined to be a function of orifice configuration and line pressure solely, the differential pressure versus valve stroke curve was found to be affected by orifice configuration, valve land underlap with respect to the orifice, and the clearance between the valve slider and the valve sleeve.

Methods of control of the valve characteristics were required, since they effectively determined the internal resistance of the valve R_v which is represented by the slope of the differential pressure versus valve stroke curve divided by the slope of the flow versus valve stroke curve.

Change of the slope of the flow versus valve stroke curve was a straight forward correction of the delta area for a given valve slider displacement increment.

The Cutlass valve had two orifices per land with its total stroke (orifice length) fixed at 0.4 inches. This, perforce, left the only delta area per valve stroke increment variation possible that of orifice width. The mock-up valve orifices were designed with a width of 0.040 inches whereas the aircraft valve orifices had tips 0.025

FIG IX a

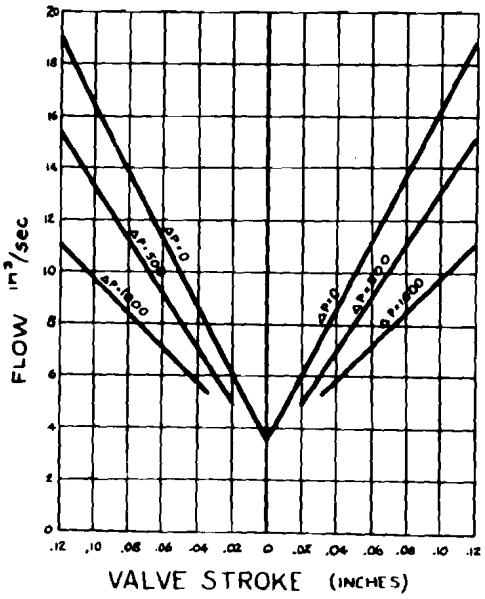

TOTAL FLOW vs VALVE STROKE

FIG. IX b

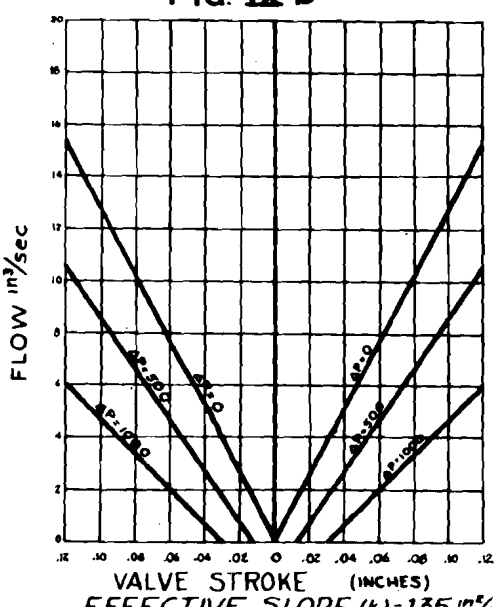

EFFECTIVE SLOPE (K_f)=135 in⁵/sec

CYLINDER FLOW vs VALVE STROKE

FIG. X

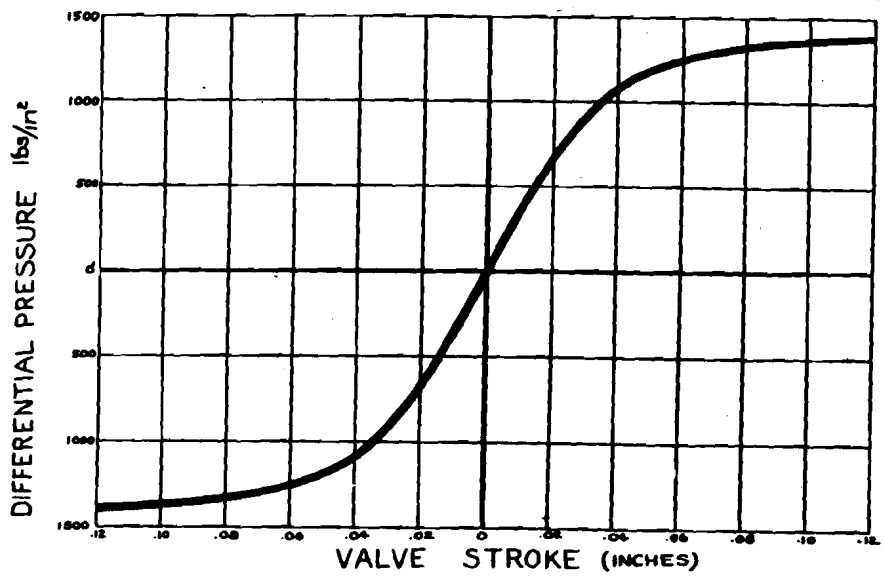

EFFECTIVE SLOPE (K)=47,500 $\frac{lb}{in^5}$

DIFFERENTIAL PRESSURE vs VALVE STROKE

inches wide and gradually broadened to 0.080 near maximum valve excursion.

Control of the differential pressure versus valve stroke curve was more difficult, and was obtained finally by choosing an orifice to fit the flow requirements, holding the valve land overlap to a definite value, in this case, 0.002 inches, and then varying the clearance between the valve sleeve and slider until the desired slope was obtained.

The static tests, then, were useful in obtaining actual values for the slope of the flow-stroke curve K, the slope of the pressure-stroke curve K_1, and the internal resistance of the valve R_v. These tests also disclosed practical means of varying the valves' dimensions to obtain the required parameters.

Proceeding with the test program, a sinusoidal input device was designed and fabricated. This input system consisted of a hydraulic motor driving a variable amplitude scotch yoke through a series of gears with stabilization provided by a flywheel. The frequency of the unit was varied by adjusting the flow from a hydraulic power source to the hydraulic motor which was the fixed volumetric displacement type. This flexibility of control enabled the reduction of operational test time to a minimum.

Instrumentation for the tests consisted of two displacement pick-ups. One recorded the position of the valve slider with respect to the valve cylinder housing (valve error) and the other recorded the position of the cylinder housing with respect to a structural reference which was located adjacent to the point at which the input member fastened to the structure when closing the servo loop. The pick-ups used were geared up potentiometers in bridge circuits which supplied signals to the recording apparatus. An oscillograph was used as the recording means which supplied a stable reference line for measurement of the traces and an electrically driven tuning fork trace for a dependable time reference in addition to the output and error traces. Figure XI illustrates a sample test record. This test record graphically illustrates the phase lag and amplitude ratio phenomena associated with dynamic tests. Reduction of the data by use of calibration charts permits the calculation of output amplitude divided by error amplitude (amplitude ratio) and of percentage lag of the output to error which when multiplied by 360° produces the phase lag. Comparison of the error signal trace with the 60 cycles per second timing trace allowed the calculation of the period and the frequency of the error signal. Two output traces were recorded during this run, which brings up one difficulty encountered. The original tests on the mock-up measured output as picked up from motion of the axle on which the output mass was supported. Examination of the test results indicated very poor agreement with the analytical solution both in phase and amplitude ratio. It was learned that the errors were introduced largely by deflection of the axle which produced translational motion of the pick-up element as well as rotation. To improve our recording technique and also to verify our interpretation of the discrepancies, both output traces were recorded, the one from the original pick-up, and one from a pick-up recording the translational motion of the cylinder housing. The latter resulted in much less scatter of the test points and fairly close agreement with the analytical predictions.

As each test run was completed, the records were interpreted and plotted in polar form, phase and amplitude ratio for various frequencies up to 30 cycles per second. These test results made possible the revision of the analytical parameters. Test results produced the system's damped natural frequency and the phase and

FIG XI

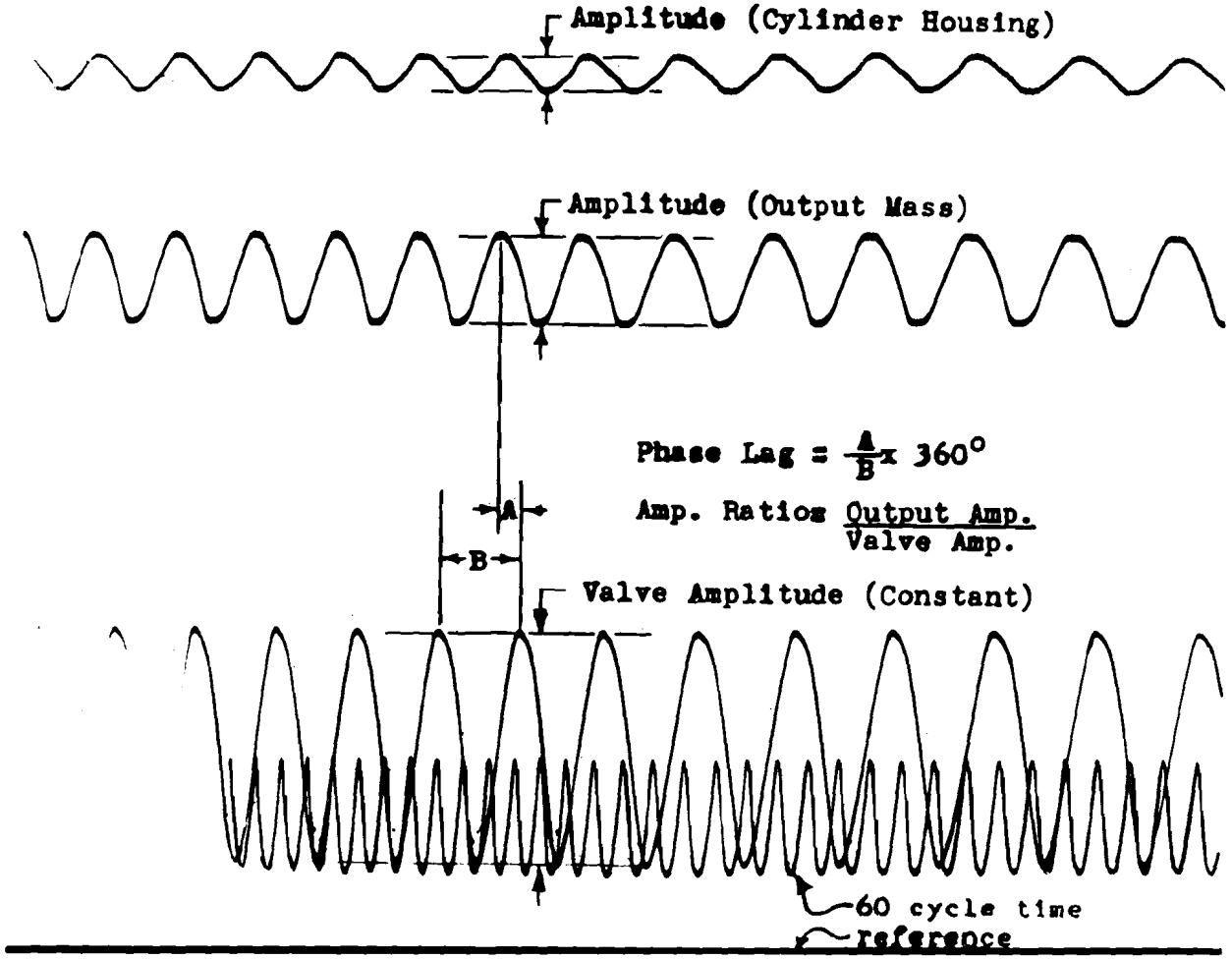
Amplitude (Cylinder Housing)
Amplitude (Output Mass)
Phase Lag = A/B x 360°
Amp. Ratio Output Amp. / Valve Amp.
A
B
Valve Amplitude (Constant)
60 cycle time reference

amplitude ratios for definite frequencies. These figures allowed the analyst to vary the parameters originally assumed. At this point, there was enough information available upon which to base a new set of valve characteristics designed to deliver optimum performance of the unit under test. Using the revised differential equations, and applying Nyquist's stability criteria, valve characteristics were assigned that would result in such performance.

In this test case, the flow versus valve stroke characteristics were already satisfactory which then indicated that a change in differential pressure versus valve stroke slope would be the only alteration necessary. This was done by honing out the valve sleeve which effectively altered the characteristics to a small extent which was all that was indicated to be necessary. This particular valve required removal of 0.0005 inches in diameter. Upon completion of this rework, the tests were repeated and it was ascertained that for the given condition of operations, no further improvement through rework of the valve could be expected or desired.

The final test results in polar diagram form as compared to the analytically predicted curve are presented in Figure XII. Although the resonant frequency matches in phase angle and amplitude ratio, it can be seen that the predicted curve has a sharper resonant peak and that some of the damping terms appear to differ from the actual case. However, the correlation was acceptable for the establishment of design parameters for stability purposes.

Operation of the boost system was then checked by closing the feed-back loop which in this case meant coupling the valve slider to the control stick system and introducing random input disturbances. The boost system operated as anticipated and was considered to be acceptable for use on the aircraft.

FIG XII

COMPARISON OF CALCULATED AND TEST TRANSFER FUNCTIONS

$$K = 0.06135$$

$$\mu = \frac{j\omega}{424.04}$$

$$G(\mu) = \frac{7.0331\mu^2 + 0.14\mu + 1}{\mu[0.14\mu^3 + 8.0404\mu^2 + 0.1924\mu + 1]}$$

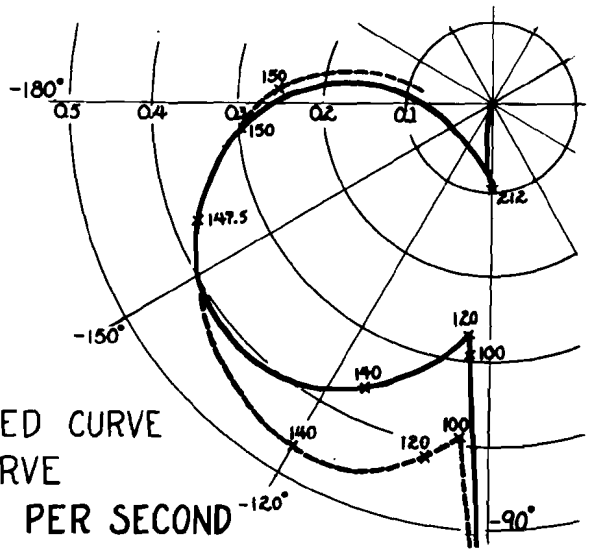

— REPRESENTS CALCULATED CURVE
-- REPRESENTS TEST CURVE
FREQUENCIES IN RADIANS PER SECOND

At this time, the fallacy of a basic assumption became apparent. Upon installation of the boost system in the aircraft, it was found to be dynamically unstable. This, of course, indicated a marked difference between the mock-up and the aircraft. Since the same boost system was involved, the difference had to be attributed to the supporting structure and to the dynamic characteristics of the control surface. A detailed structural study at this time would have been too lengthy, therefore, tests were continued with the boost system mounted in an outer wing panel from the aircraft. Operation of this assembly indicated visually that the control surface was not rigid as had been assumed and was undoubtedly contributing to the excessive energy storage problem as was the structure supporting the boost system. Since any rework of the structure and the surface to improve their dynamic characteristics would have required considerable time, and since the likelihood of sufficient improvement was slight, it was decided that the valve again appeared to provide the most direct means of obtaining an acceptable system. Space limitations precluded the use of the sinusoidal input device which was utilized in the mock-up tests so that transient response studies were substituted. Results of the tests on the wing panel assembly indicated that the change in valve characteristics would be too great to be controlled by alteration of the differential pressure versus valve stroke curve alone. Therefore, the orifice width was reduced to the next small engraving cutter size which reduced the slope of the flow versus valve stroke curve. The differential pressure versus valve stroke curve slope was also reduced to the desired value.

Reduction of the flow-stroke curve slope meant in this case that there would be a considerable restriction to flow at maximum valve excursion. The hydraulic power source was not a linear device instead giving increased flow at a reduced pressure. Thus, it was justifiable to open the valve orifice width near maximum valve excursion making the flow response curve more nearly linear. Upon installation of the reworked valve in the wing panel assembly, it was found to operate satisfactorily under all input conditions and was approved for flight.

One last precautionary stability check was made prior to flight, and that was the determination of the allowable clearances in the boost system couplings that would still permit normal operation. The previous tests had all been conducted with honed and lapped pins, bushings, and bearing races. The last check was of the boost system response to random input disturbances as the clearances in all couplings were progressively increased. With the particular system under test, 0.004 inch was found to make the system marginally stable. This figure was the total clearance for all the joints. In view of this data, recommendations as to allowable tolerances for the clearance at each joint were released and the system considered complete.

The usefulness of the frequency response method of analysis was apparent when it was determined that only minor adjustments of the valve were necessary for optimum performance when designed from analytically derived parameters.

The actual test program verified the usefulness of the frequency response method and also pointed out some of its limitations.

The limitations result from the necessity of assumption of certain parameters such as structural damping. Undoubtedly, errors resulting from such assumptions could be minimized by careful structural studies of the elements involved. Secondly, analysis will always be subject to some error through the introduction of unpredictable non-linear characteristics and possibility of variations due to fabrication processes.

In conclusion then, it may be said that the frequency response method of analysis presents a powerful design tool for the development of power boost systems and that its use should result in a valuable reduction in test time and the possibility of eliminating the need of mock-up tests.

***

DISCUSSION

PROFESSOR GROSSER, Syracuse University: *In the light of Mr. Harris' general comments about the effects of varying the different quantities involved, it might be interesting to review some work that was done some time ago on a microscopic basis with many assumptions made which invalidate the results to some degree. However, one conclusion that was reached on the basis of writing a differential equation of second order assuming incompressibility, and assuming no leakage either in the valve or at the piston. A non-dimensional parameter was found that indicated that instability can occur in the presence of rigidity either of the fluid or the mechanical members. In that parameter appears a mass term and checks your statement that increase of output mass reduces stability to the first order. Cylinder diameter increased stability to the third degree. The size of the valve operation, the valve ports decreased stability to the first degree. The size of the signal, which in the non-linear analysis came in importantly, showed that the amplitude of motion decreased stability to the first degree and the response ratio or the ratio of the movement of the valves to the cylinder reduced stability to the second degree. The ratio of the movement of the valve to the movement of the cylinder, the linkage ratio, decreased stability to the second degree. I thought that perhaps might be interesting.*

MR. RICHOLT, Lockheed Aircraft: *I wonder if he can go over that fixing valve again. What modifications were made to take care of that?*

MR. DREW: *When we switched over to the actual aircraft itself we found it necessary to reduce the flow slope. Our original valve had orifices, and to reduce the stroke of the flow curve, we found it necessary to reduce this width near neutral, which was .025". However, that meant that we had too great a restriction of flow in it so we couldn't meet aerodynamic requirements, and since its power source was non-linear, we felt we were justified in opening it up so that once we got the surface moving, we would have effectively no restrictions as we opened the valve up wide. That was sticking our neck out a little. We did all the calculations we could but it is a little hard to specify the characteristics of the non-linear orifice.*

RICHOLT: *You are uncovering successive portions of the valve.*

[redacted]

DREW: *Yes, you could assume the closed position was gradually opened.*

MR. GRANT, Hughes Aircraft: *I don't want to argue about the future possibilities of theory application but if you hadn't done any of these calculations and analyses and just started out to build an irreversible booster and went by your own and other people's experience, what could the results have been? In other words, all you got out of those calculations was that opening.*

DREW: *That is all that is necessary to go from stable to unstable.*

GRANT: *We assume we know in advance in other designs. Do you think you saved anything by going through the calculations?*

DREW: *The original design was not on the .040 linear orifice. Before the group was formed, they designed this thing. They had something that nearly tore the mock-up right out of the lab, so at that time we were just entering the work and on the basis of our recommendation, we got the .040 orifice and when that was installed, it was marginally stable because we hadn't assumed the proper damping characteristics. Then revising those figures in our analysis, we were able to determine that all we would have to do is change the pressure slope stroke. If we hadn't been able to predict where we were going, we would have had to make new valves, and the engraving process involved would have meant $500,000 per valve. This way it was just a matter of time.*

GRANT: *You feel then that the analysis time cost less than making that series of valves?*

DREW: *Very definitely. Of course, now I should say it will become cheaper as far as analyzing but the valves still cost the same.*

[redacted]

DESIGN OF A POWER CONTROL SYSTEM FOR A TRANSONIC AIRPLANE

By

M. V. Clauser

Douglas Aircraft Company, Inc., El Segundo, California

1. Summary

This report is a description of the design of a power servomechanism for controlling the elevon of the XF4D-1 airplane. The report was made for delivery at a conference on power control systems sponsored by the Bureau of Aeronautics. A general discussion is given of the aerodynamic and structural factors which determine the type of power system. The hydraulic system is described and the control valve shown. The artificial feel generator for providing pilot's feel is described. The dynamic stability problem of the servomechanism is presented in detail. The test results of a dynamic model of the servo system are given and discussed. Recommendations for future development of hydraulic control systems are made.

2. Introduction

The problem treated here is that of designing a control system for the elevon of a supersonic interceptor. Fig. 1 shows the type of airplane and elevon considered. The hinge moments of the surface increases abruptly for $.93 < M < 1.1$. This increased hinge moment produces about the same rolling moment as the lower hinge moment for $M < .93$. The hinge moment required for $M > .93$ precludes the possibility of direct pilot control. With the addition of a power servomechanism to the control system, the following problems have to be considered:

1. The lightest type of power system.

2. Influence of the structural strength of the wing on the power system; or conversely, the effect of the power system on the strength of the wing.

3. Feel for the pilot.

4. Dynamic stability of the servomechanism.

3. Determination of the Type of System

Aerodynamic Requirements

The principal performance characteristic of the airplane considered here which determines the design of the elevon control system is high maneuverability at Mach numbers up to 1.5.

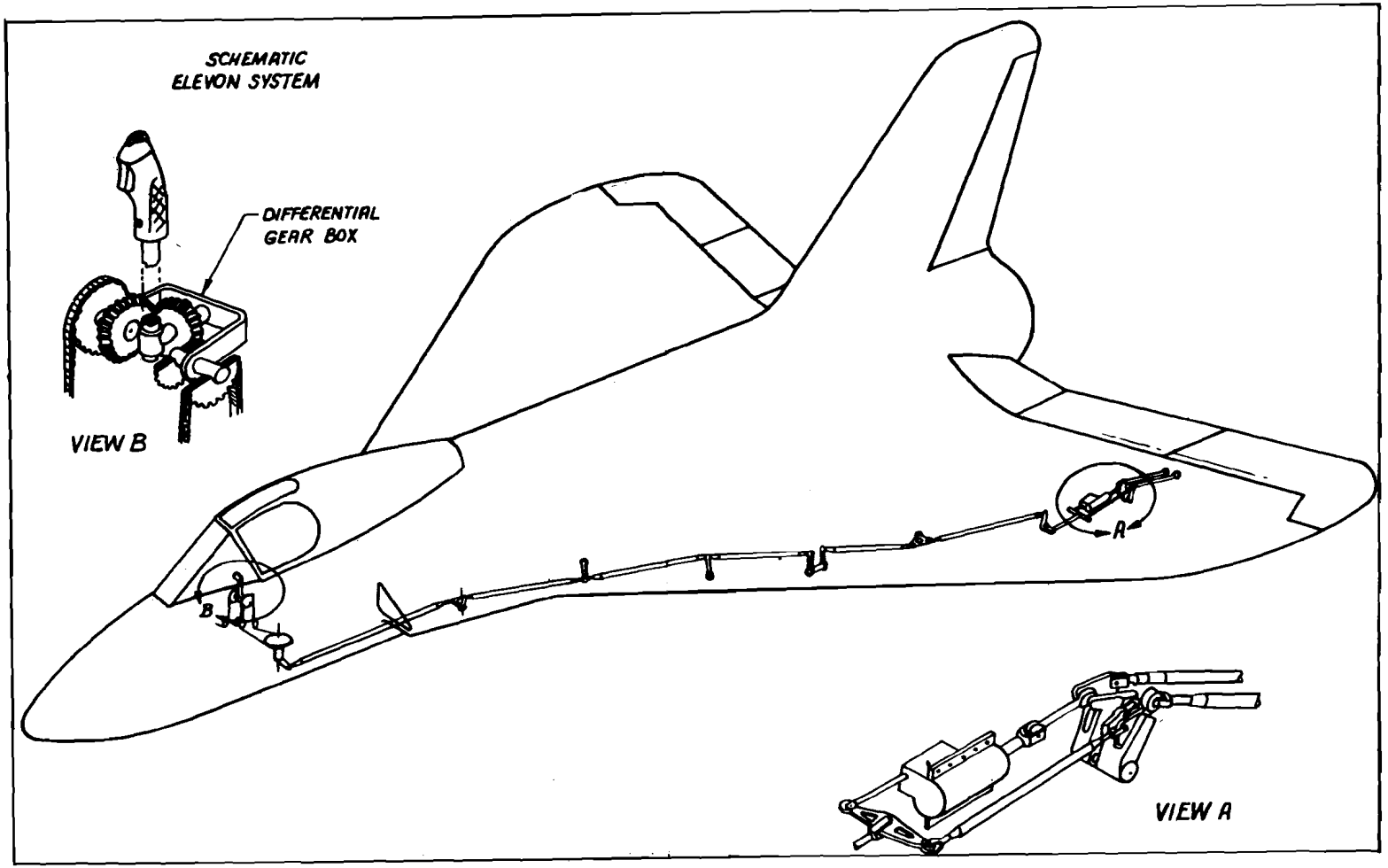
SCHEMATIC
ELEVON SYSTEM
DIFFERENTIAL
GEAR BOX
VIEW B
A
B
VIEW A

Fig. 1

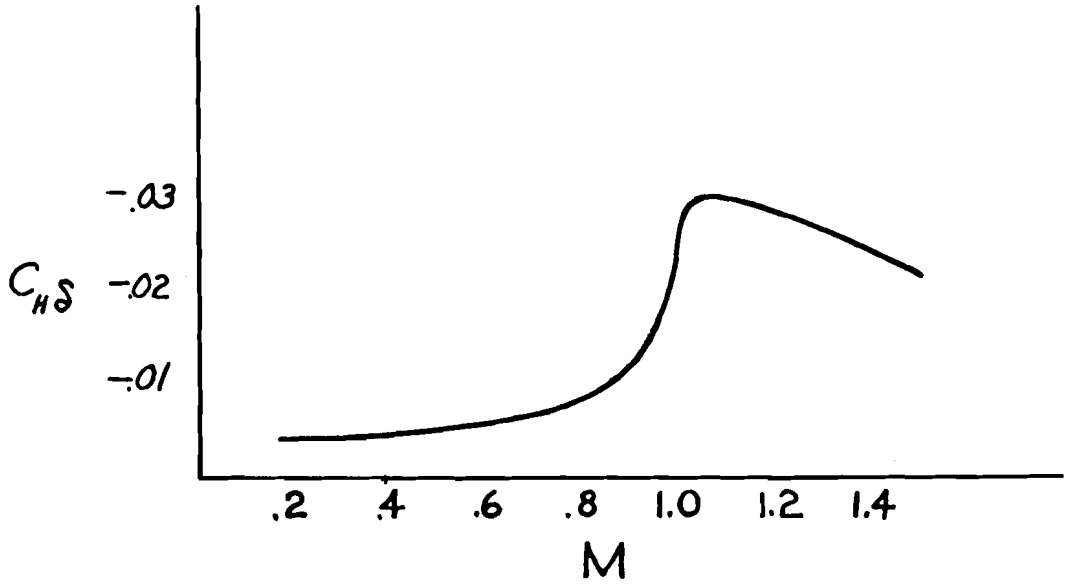

Fig. 2

Fig. 2 shows the variation of the elevon hinge moment coefficient slope with Mach number for the wing-elevon combination chosen to meet the performance specifications. The maximum hinge moment that the control system has to produce is determined by the high Mach number condition and the rate of roll required at this Mach number. This rate of roll is the same as that required below $M = .93$. The maximum power required from the control system is also determined by the high Mach number condition. Table I lists several representative performance conditions for the control system.

The angular velocities of the surface are determined by the arbitrary condition that the time to deflect the surface to one-half its final angle shall be no more than 20% of the time which would be required to roll 45° if the surface had been deflected instantaneously. From Table I it can be seen that at $M < .93$, the system should be able to deliver moderate powers at high angular velocities. At $M > .93$ maximum power is required but can be delivered at a lower velocity because the required maximum displacements are small.

Type of Power System

The lightest type of system for delivering horsepowers in the order of 12 H. P. is an hydraulic system. An hydraulic system can be designed so that the pump is picked for the maximum horsepower condition at $M > .93$. An accumulator can be used to supply the high velocities required at $M < .93$. Fig. 3 is a schematic of the basic control system.

TABLE I

DETERMINATION OF MAXIMUM RATE OF ELEVON MOTION

	M	Alt.	∂_A	Time to 45°	.2 to 45	Time for Full Disp.	Rate °/SEC	H.P. Max.
1.	.29	20,000	20.	.75	.15	.30	66.7	1.36
2.	.40	20,000	9.2	.75	.15	.30	30.6	.56
3.	.54	20,000	8.7	.55	.110	.22	39.5	1.40
4.	.79	20,000	6.5	.44	.088	.176	37.0	2.48
5.	.46	40,000	20.	.70	.14	.28	71.4	1.58
6.	.63	40,000	9.0	.71	.142	.284	31.7	.66
7.	.85	40,000	6.3	.61	.122	.244	25.8	.92
8.	.20	S.L.	16.	.86	.172	.344	46.5	5.44
9.	.56	S.L.	9.5	.39	.078	.156	60.8	2.72
10.	.90	S.L.	3.5	.47	.094	.188	18.6	.70

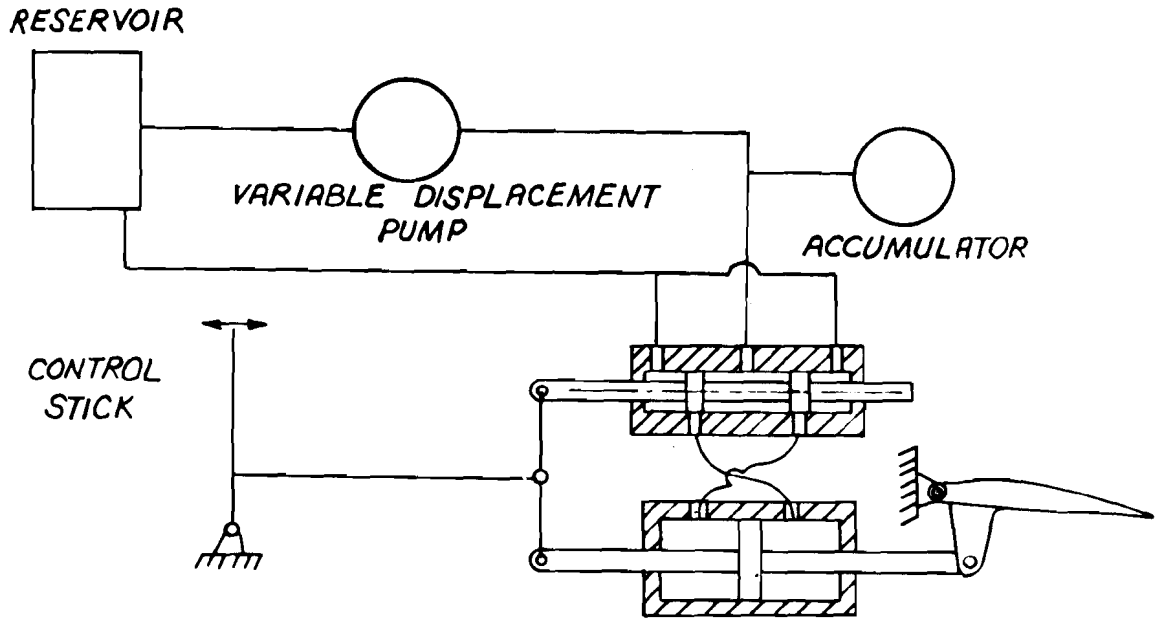

Fig. 3

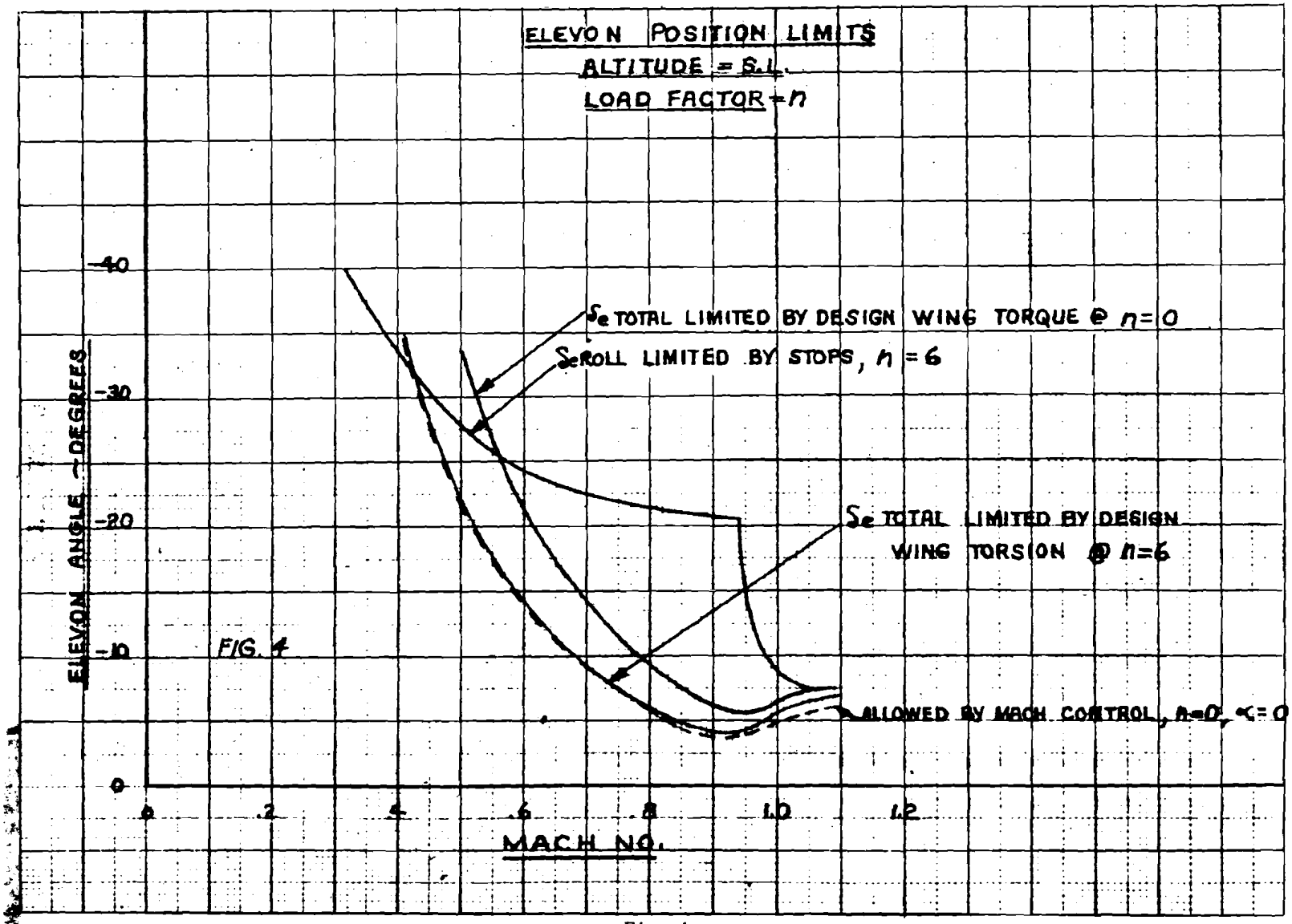
ELEVON POSITION LIMITS
ALTITUDE = S.L.
LOAD FACTOR = n
ELEVON ANGLE - DEGREES
-40
-30
-20
-10
0
Se TOTAL LIMITED BY DESIGN WING TORQUE @ n=0
Se ROLL LIMITED BY STOPS, n = 6
Se TOTAL LIMITED BY DESIGN WING TORSION @ n=6
ALLOWED BY MACH CONTROL, n=0, α=0
FIG. 4
.4
.6
.8
1.0
1.2
MACH NO.

Fig. 4

It can be seen that the system is irreversible and has position feedback only. Since there is no force feedback, an artificial feel generator has to be provided. This feel generator will be discussed later.

Structural Limitation

The rapid change in $C_{H\delta}$ for $.93 < M < 1.1$ complicates the control problem. A capacity for producing a high hinge moment must be provided for $M > 1.1$. This moment, however, is sufficient to fail the wing for $M < 1.1$. Fig. 4 shows the elevon angle for developing design wing torque for $n = 0$ and $n = 6$ (n = airplane load factor); and the angle available, limited by stops and maximum hinge moment. One possible method for protecting the wing would be to control the feel generator such that the force gradient at the stick would limit the surface angles that the pilot can produce to fall within the envelope of Fig. 4. However, pitching forces as well as rolling forces load the wing and the force gradients at the stick for pitching and rolling must be controlled independently. Thus, the total surface angle for maximum pilot's force in both pitch and roll would have to be less than the allowable as shown by Fig. 4. If this were done, the performance in pitch alone or the performance in roll alone or both would not be met. Also, it is felt that limiting the angle by pilot's force is not desirable because of the small surface deflection for wing failure. Possible time lags in the feel generator might allow overshoot of the safe angle.

Several methods of limiting the elevon angle as a function of Mach number were studied. Varying the hydraulic system pressure with Mach number appears to be the best compromise. The variation of hinge moment with Mach number that is used is shown in Fig. 5.

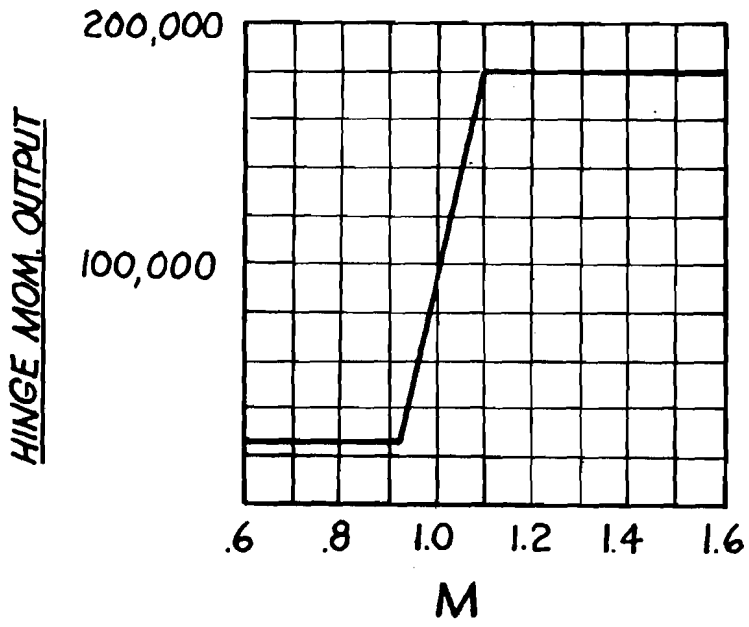

Fig. 5

The elevon angle that can be produced with this type of control is shown on Fig. 4 and follows the desired curve very closely. This angle relation (at sea level) depends primarily on Mach number only.

Hydraulic System

Since condition 5 of Table I has the maximum rate and maximum deflection, it determines the accumulator capacity required. Conditions 5 and 9 determine the pressure drop allowable across the valve and through the lines. The maximum Mach number condition determines the cylinder size and the pump capacity.

Since the accumulators are used for high velocities, the hydraulic system has to be of the pressurized-in-flight type. A valve of the type shown schematically by Fig. 6 was considered for the elevon control. The error signal moves a pilot valve "*A*" which meters a steady bleed flow through orifices "*C*". The pressure differential caused by the metering of valve "*A*" acts on control valves "*B*". Valves "*B*" meter the main system pressure to the actuating cylinder. The pressure in the cylinder feeds back a force to valves "*B*". This type of valve produces a pressure in the cylinder that is proportional to error signal. In the interest of simplicity, it was decided to use a conventional balanced type slide valve. However, it is felt that a valve such as Fig. 6 warrants further study.

Fig. 7 is a schematic of the control valve that is to be used. Valve "*A*" is the selector valve. The damper "*B*" and the springs K_1 and K_2 form a stabilizing device by attenuating the error signal at high frequencies.

It can be seen that at very low frequencies, the damper force is negligible and the valve amplitude is the same as the error signal. At high frequencies, the damper is essentially motionless and the valve amplitude is $K_1/(K_2 + K_1)$ times the amplitude of the error signal. Valve "*C*" is a pressure reducing valve to reduce the system pressure at $M < 1.1$. Valve "*C*" is controlled by the pilot valve "*D*" which in turn is actuated by the Mach meter. At $M < .93$, the pressure available at the valve "*A*" is only 400 p.s.i.; but the high flow conditions occur for $M < .93$ (Ref. Table I). In order to obtain the flows required and to compensate for the pressure drop through the valve and lines, it is necessary to increase the pressure at "*A*" as a function of flow. This is done by feeding back the pressure drop across the orifice "*F*" to the pressure reducing pilot "*D*". Valve "*G*" is a switching valve to switch from the elevon pressure system to the airplane utility system in case of failure of the elevon pressure.

In order to design the control valve and pick the line sizes, it was necessary to find the maximum pressure drop characteristic through the valve that would allow the conditions of Table I to be met. It was assumed that the moment delivered to the elevon would be a parabolic function of the form $M = M_0 - C\beta^2$, where β is the angular velocity of the surface. From this assumption, the equation of motion for

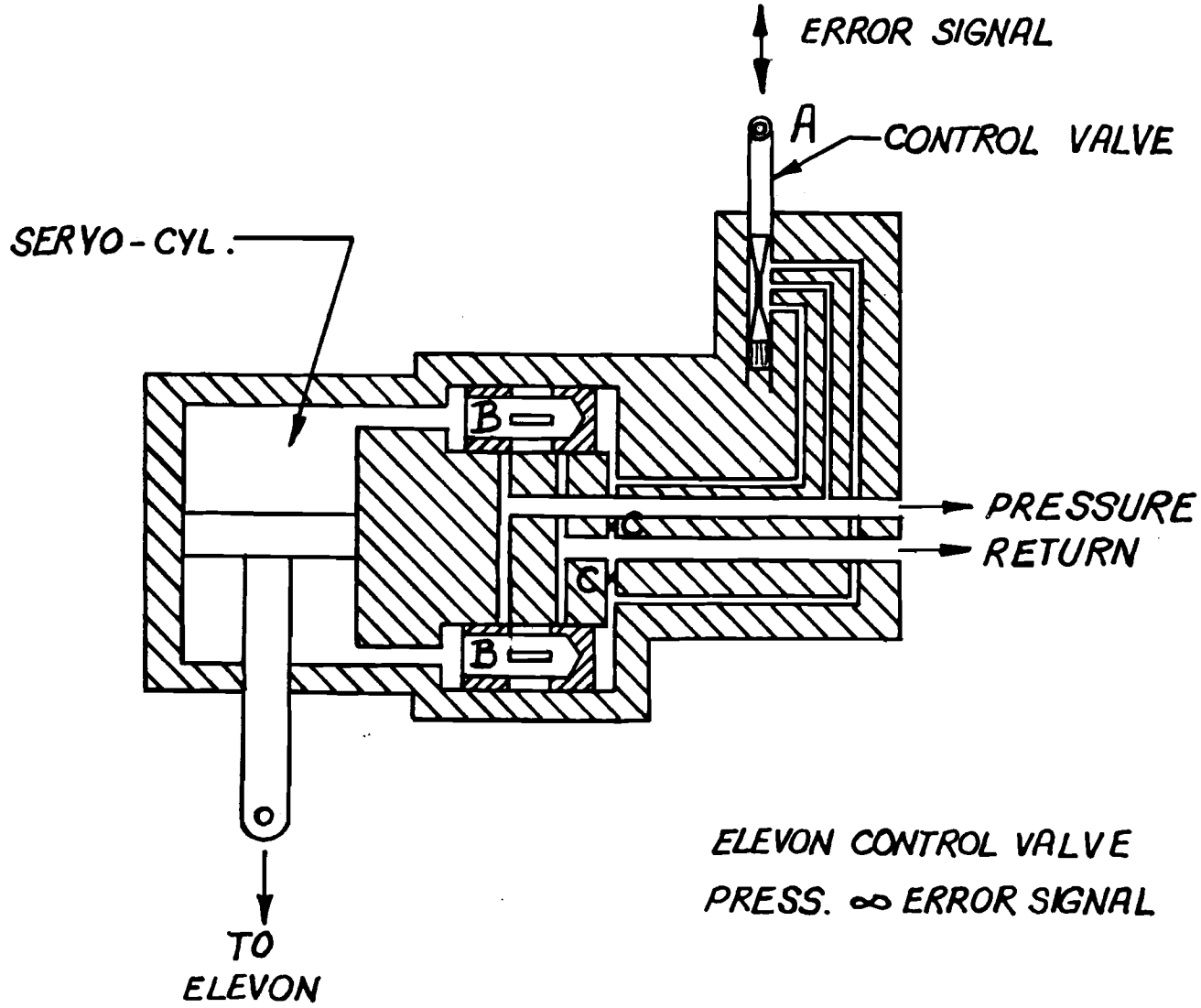
ERROR SIGNAL
A
CONTROL VALVE
SERVO - CYL.
B
C
C
B
PRESSURE
RETURN
TO
ELEVON
ELEVON CONTROL VALVE
PRESS. ∞ ERROR SIGNAL

Fig. 6

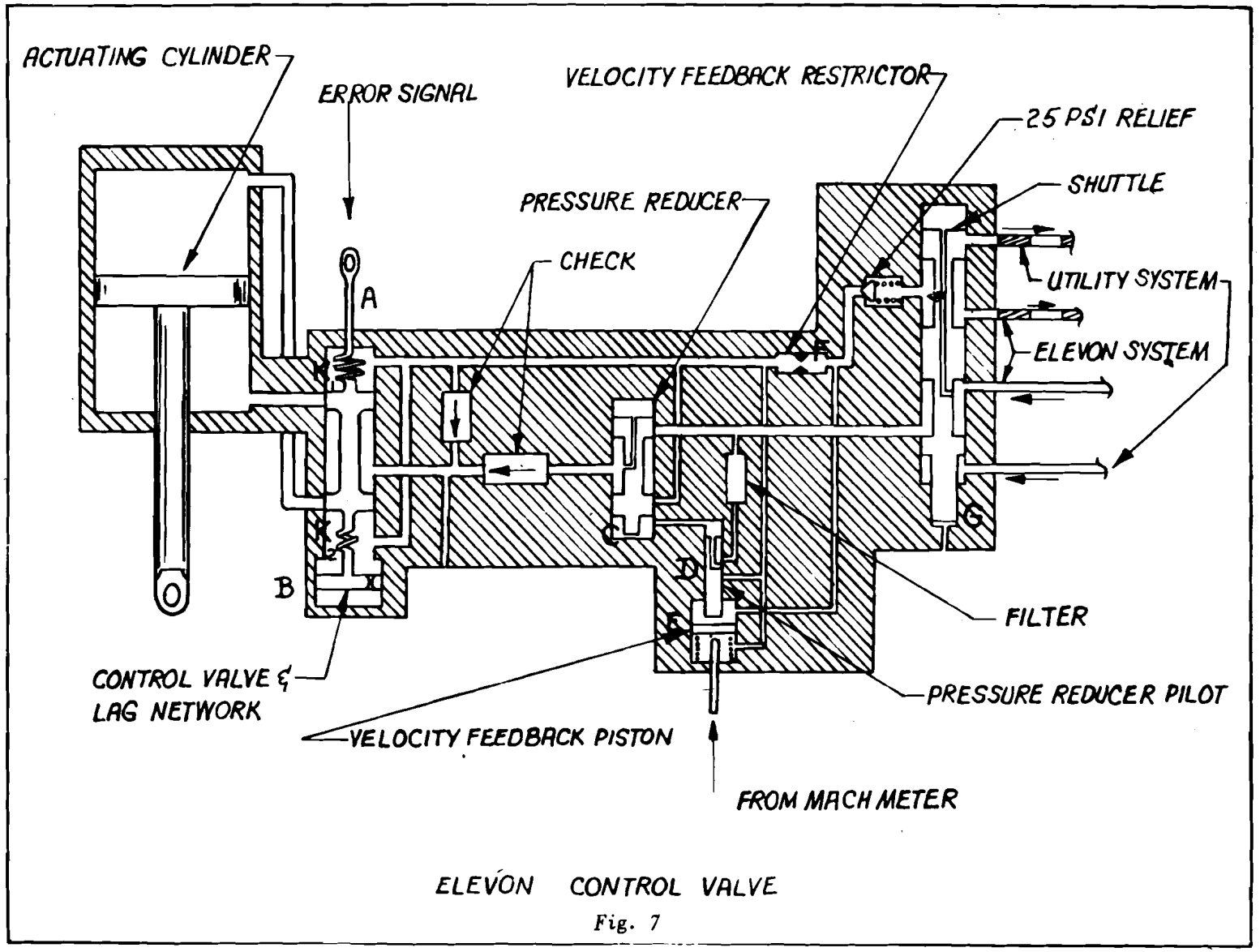

ELEVON CONTROL VALVE

Fig. 7

the elevon was integrated and the coefficient C computed for each condition of Table I. It was desired that C be as large as possible yet a minimum value would be fixed by the critical condition of Table I. Condition 9 gave the smallest value of C. (See Fig. 8).

Fig. 8 shows the angle vs. time curve for condition 9. This condition also determines the maximum error between the stick and the corresponding surface angle since it is a requirement that the surface never lag the stick by more than .05 seconds. The maximum allowable valve travel thus corresponds to 2.1° of elevon.

Curve "A" of Fig. 9 shows the minimum required Moment curve computed using the critical value of K. Condition 5 of Table I designs the pressure drop characteristics of the system. It can be seen from Fig. 9 that performance conditions such as 1 and 5 of Table I, where large deflections at high average angular velocities are desired, will require large lines if they are to be made at low temperatures. The lines of constant temperature, shown on Fig. 9, are for one particular line size. Fig. 9 clearly shows that a compromise must be made between weight of lines and the temperature at which the maneuvers 1 and 5 of Table I can be made. Since conditions 1 and 5 are both low Mach number maneuvers, it is felt that the time for full deflection at low temperatures can be sacrificed for line weight.

Feel Generator

Fig. 10 shows schematically the feel generator for aileron motion. An identical unit is used for elevator motion. Fig. 11 shows the desired variation of stick force gradient as a function of dynamic pressure, q_c.

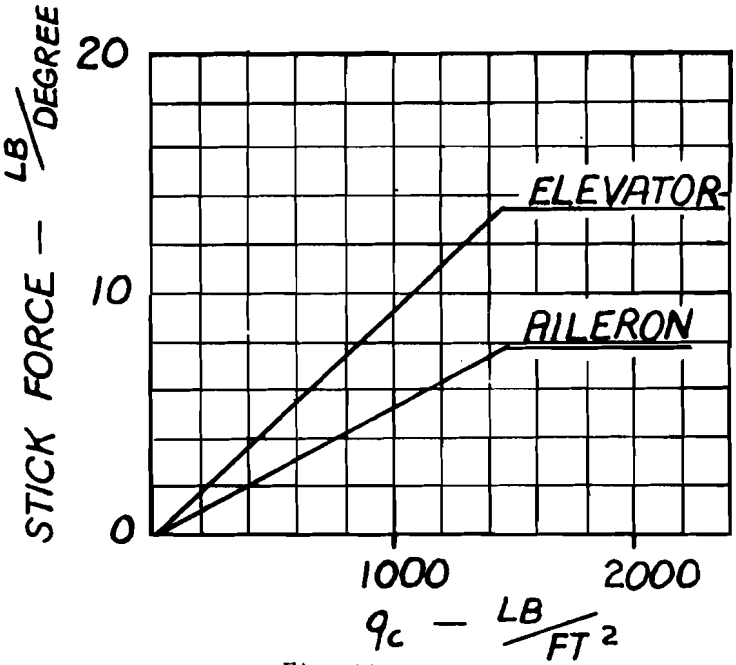

Fig. 11

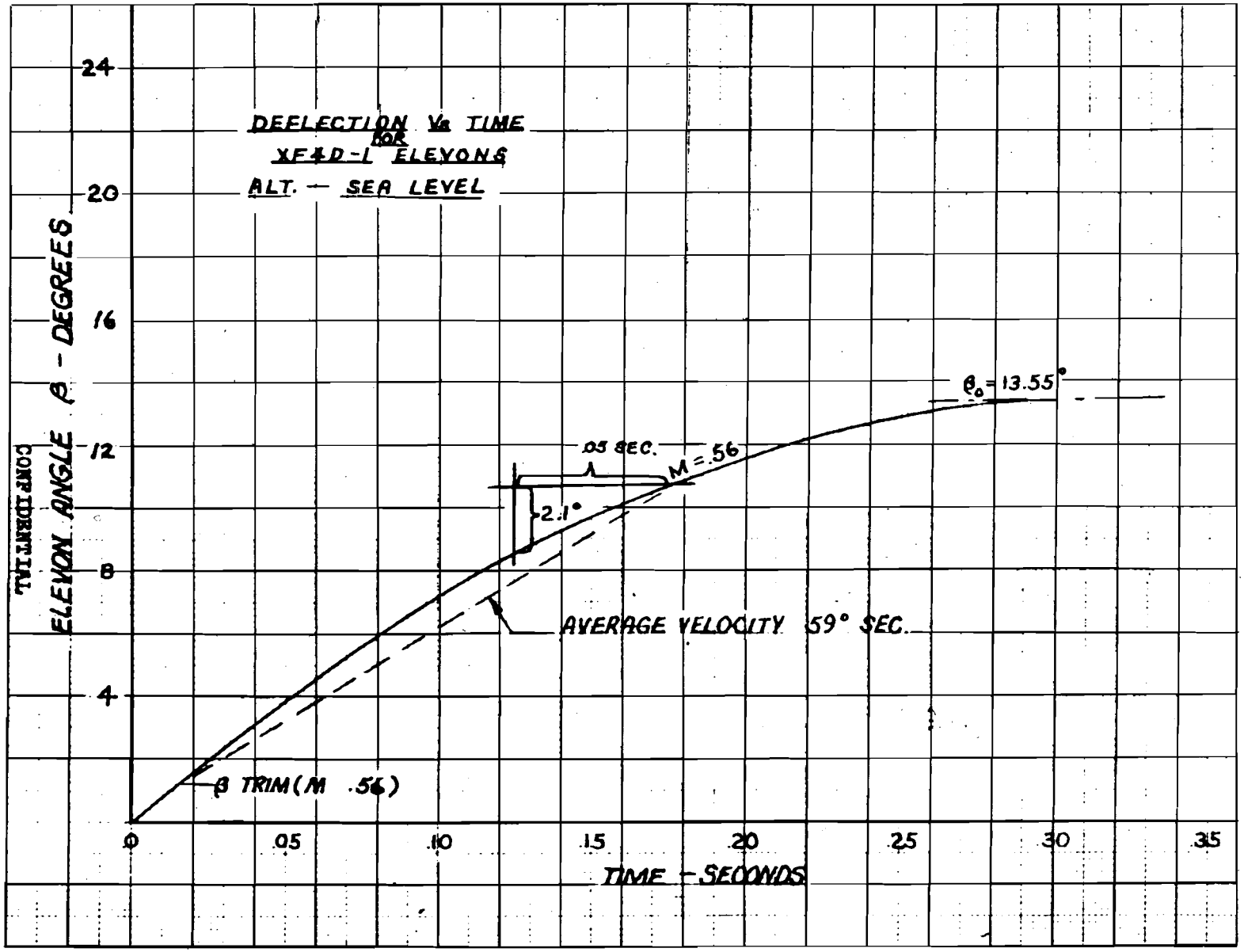
DEFLECTION Vs TIME
FOR
XF4D-1 ELEVONS
ALT. — SEA LEVEL
ELEVON ANGLE β - DEGREES
CONFIDENTIAL
24
20
16
12
8
4
0
.05
.10
.15
.20
.25
.30
.35
TIME - SECONDS
β_o = 13.55°
.05 SEC.
M = .56
2.1°
AVERAGE VELOCITY 59° SEC.
β TRIM (M .56)

Fig. 8

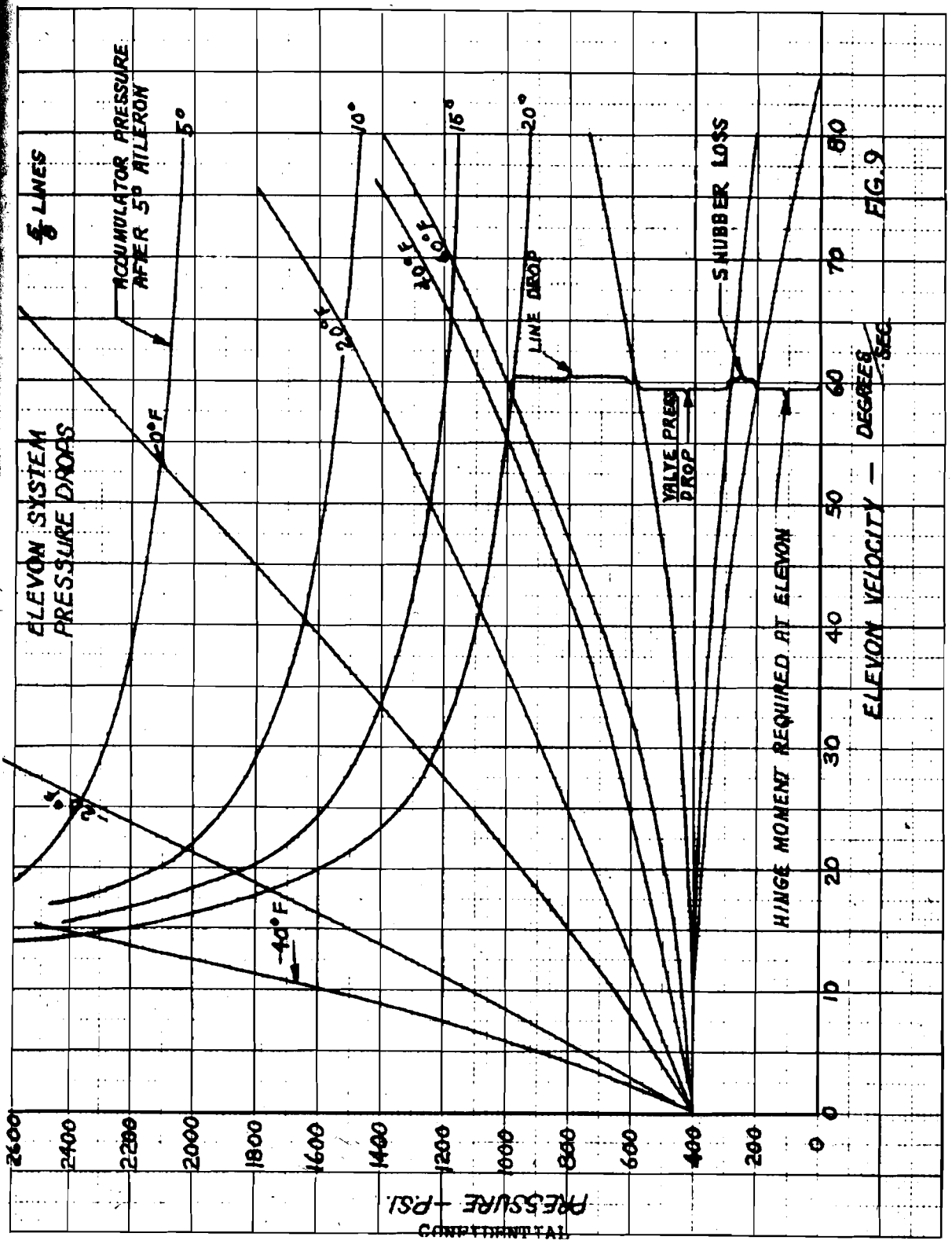

Fig. 9

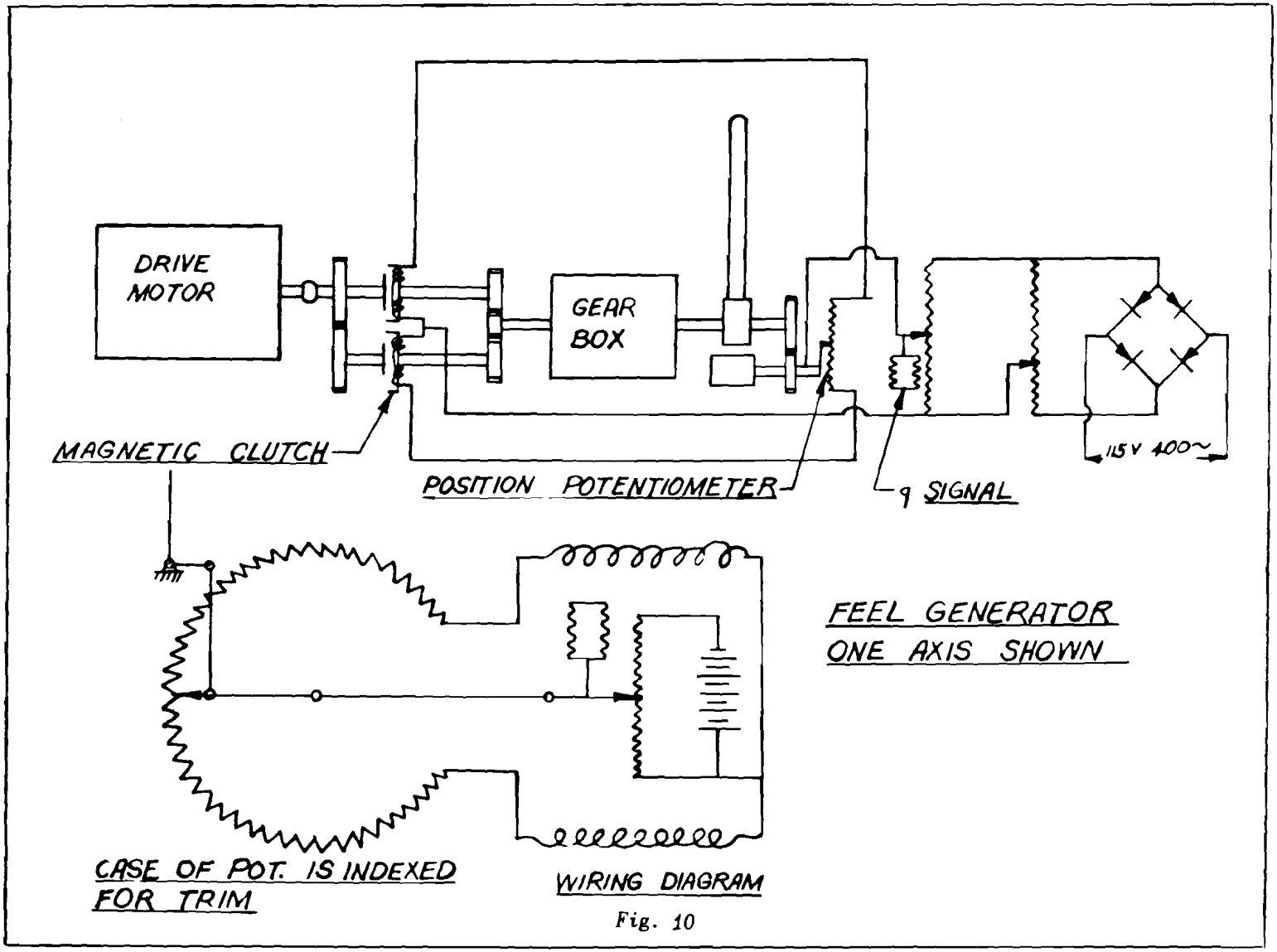
DRIVE MOTOR
GEAR BOX
MAGNETIC CLUTCH
POSITION POTENTIOMETER
q SIGNAL
115 V 400~
FEEL GENERATOR
ONE AXIS SHOWN
CASE OF POT. IS INDEXED FOR TRIM
WIRING DIAGRAM

Fig. 10

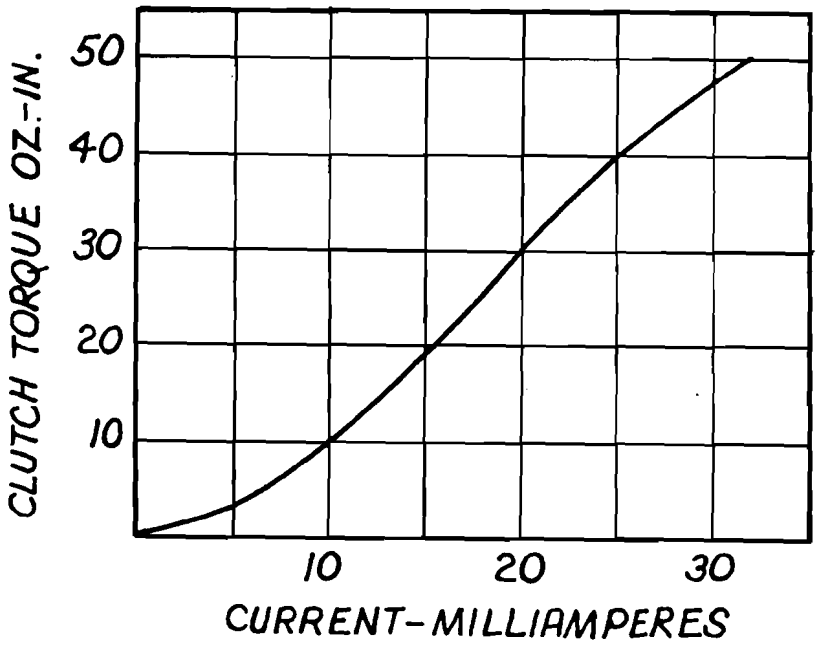

Fig. 12

The torque-current characteristic of a typical clutch is as shown by Fig. 12. Two of the clutches are geared together and are driven by a continuously rotating motor. The output shafts mesh with a common gear attached to a shaft that feeds motion back to the stick. The stick also drives a potentiometer. The potentiometer and the clutch coils are connected as shown in the circuit diagram. When the potentiometer is centered, a small, equal current flows in each clutch coil. If the current in each clutch coil is equal, no torque is delivered to the stick shaft. As the potentiometer is displaced from neutral, a torque proportional to displacement is fed back to the stick. A pressure sensing element drives another potentiometer to vary the force gradient with q_c. Trim adjustment is accomplished by a motor that drives the case of the torque potentiometer. It is felt that this type of feel generator has better flexibility and compactness than any other system studied.

4. Dynamic Stability

Transfer Function of the Basic System

Fig. 13 (a) shows a schematic diagram of the elevon servomechanism. The frequency response method using the LaPlace transformation of the linear differential equations of motion as outlined in Ref. 1, seems to be the most effective method of studying the stability of a servomechanism. From Fig. 13 (b) it can be seen that

$$\delta_s = \frac{b}{a}(\delta_i - \delta_0) = \frac{b}{a}\,\epsilon = K_A\epsilon \qquad (1)$$

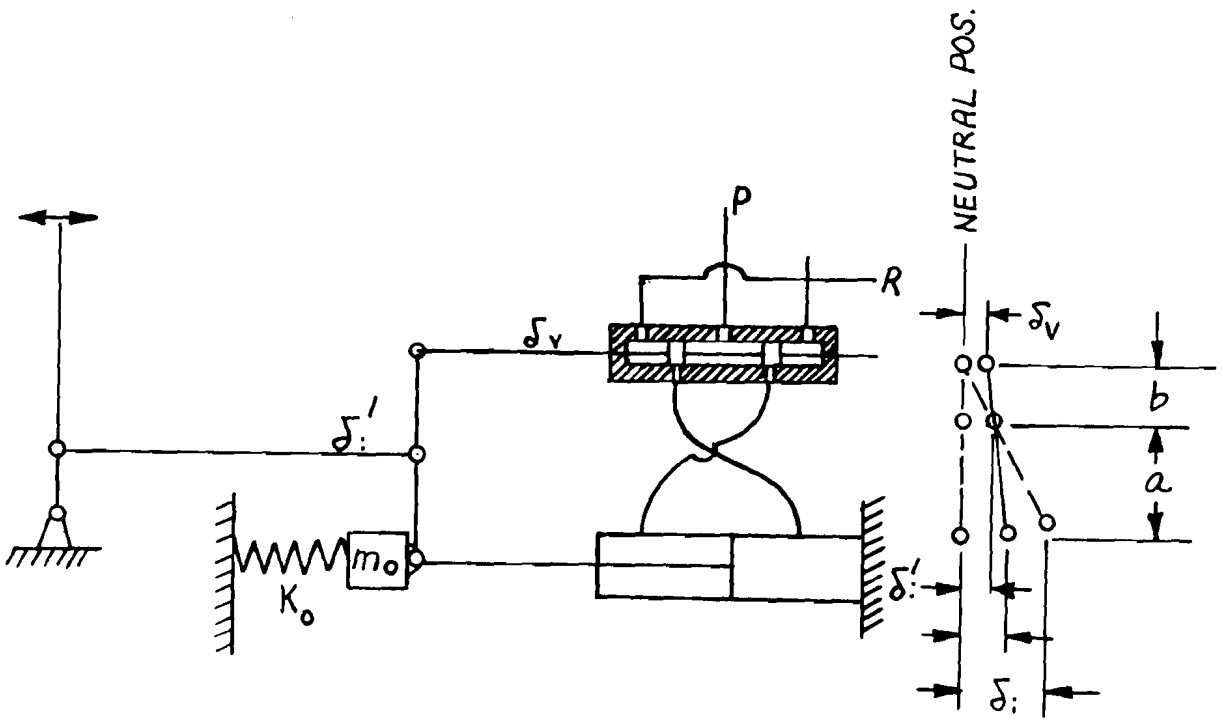

Fig. 13

b/a is a gain constant which can be represented by K_a and ϵ is the error signal.

The block diagram of the servomechanism is shown by Fig. 14. The function $G_v(i\omega)$ is the response of the valve-cylinder combination to an error signal ϵ.

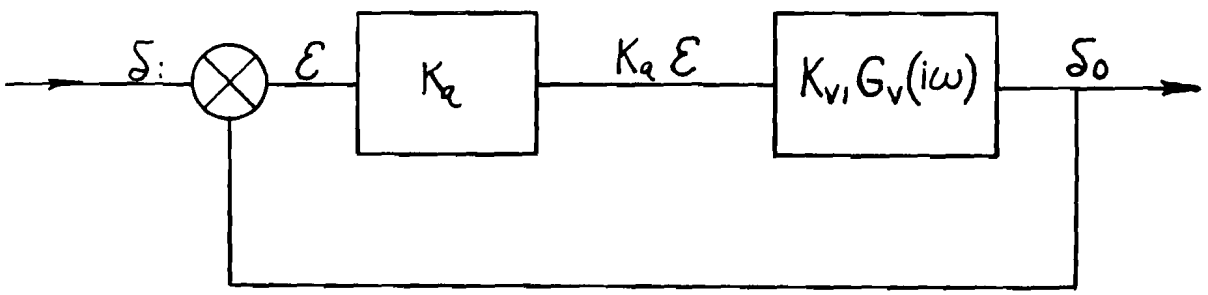

Fig. 14

The determination of the valve characteristic is one of the most important parts of the analysis since there appears to be the least information available on this subject.

With a displacement of the valve slide, an area is opened to admit fluid as well as exhaust fluid from the cylinder. If the resulting rate of flow of fluid through these areas is Q then the total pressure drop across the valve is

$$\Delta P = f (A_1, A_2, Q)$$

where A_1 and A_2 are the entrance and exhaust areas of the valve

and $A_1 = f_1 (\delta_v)$ $\quad A_2 = f_2 (\delta_v)$

To determine the nature of the functions f, f_1, and f_2 would require a knowledge of the nature of the flow through the valve and lines. Since these undoubtedly are not linear functions, they would not be usable in the analysis of the differential equation which must be linear for solution by the method of the LaPlace transform. Keeping this in mind, an approximation will be made which is linear.

Assume that $A_1 = k_1 \delta_v$

$$A_2 = k_2 \delta_v$$

and that $\Delta P = k_3 \frac{Q}{A_1} + k_4 \frac{Q}{A_2}$

This means that the areas increase approximately linearly as the valve position increases and that the pressure drop is approximately due to viscous losses.

From above $\Delta P = k_0 \frac{Q}{\delta_v}$

The pressure on the piston is equal to the pump output pressure minus pressure drop across the valve.

$$P = P_0 - k \frac{Q}{\delta_v} = (P_0 \delta_v - kQ) \frac{1}{|\delta_v|}$$

The absolute value $|\delta_v|$ is used to get proper signs for positive and negative value of δ_v and Q. This expression is also non-linear in $|\delta_v|$ but if we use an average value for $|\delta_v|$ then it can be made linear. This means that the coefficient of the expression $(P_0 \delta_v - kQ)$ will vary for different amplitudes (i.e., the gain will be a function of the amplitude).

Therefore $P = K'_{v1} \delta_v - k_{v_2} Q$ (2)

The adequacy of this approximation will be discussed when the test results are presented.

Another important effect has been found from testing to be the compressibility effect of the oil. It appears that equilibrium is almost inevitably reached with some air in the oil being supplied.

If V is the volume of oil in the pressure side of the cylinder

$$\frac{\Delta V}{V} = \frac{\Delta P}{E}$$

E is bulk modulus of elasticity.

The total change in volume due to compressibility and fluid entering is:

$$\frac{dV}{dt} = -A\dot{\delta}_0 + Q$$

$$\frac{dP}{dt} = \frac{E}{V}(-A\dot{\delta}_0 + Q)$$

substituting for Q from Equation 2

$$\dot{P} = \frac{E}{V}\left(-A\dot{\delta}_0 + \frac{K_{v_1}}{k_{v_2}}\delta_v - \frac{P}{k_{v_2}}\right)$$

Using force F instead of pressure P and reassigning constants

$$\dot{F} = -K_E\dot{\delta}_0 + \frac{K_{v_1}K_E\delta_v}{K_{v_3}} - \frac{FK_E}{K_{v_3}} \qquad (3)$$

and Equation 2 becomes

$$F = K_{v_1}\delta_v - \frac{K_{v_3}Q}{A}$$

K_{v_1} and K_{v_3} can be defined as :

$$K_{v_1} = \frac{\partial F}{\partial \delta_v} \quad \text{and} \quad K_{v_3} = A\frac{\partial F}{\partial Q}$$

Constants K_{v_1} and K_{v_3} are kept distinct in Equation 3 since the effect of these constants on the results are of importance.

It should be noted that K_E is the spring rate of the system due to the compressibility of the oil but is extended to include all effects such as deflection of supports, etc.

The equation of motion of the piston may be written:

$$m_0\ddot{\delta}_0 + K_D\dot{\delta}_0 + K_0\delta_0 = F \tag{4}$$

Where K_D is the damping coefficient and linear damping is assumed.

K_0 is the spring rate of the aerodynamic forces.

Combining Equations 1, 3 and 4

$$m_0\delta_0 + \left[K_0 + \frac{K_E m_0}{K_{v_3}}\right]\ddot{\delta}_0 + \left[K_0 + \frac{K_E K_D}{K_{v_3}} + K_E\right]\dot{\delta}_0 + \frac{K_E K_0}{K_{v_3}}\delta_0 = \frac{K_E K_{v_1} K_A}{K_{v_3}}\epsilon$$

Using the LaPlace transform we have

$$K_v G_v\,(i\omega) = \frac{\delta_0}{\epsilon}\,(i\omega) = \frac{K_A K_{v_1}}{-\frac{m_0 K_{v_3}}{K_E}\, i\omega^3 - \left[\frac{K_D K_{v_3}}{K_E} + m_0\right]\omega^2 + \left[\frac{K_0 K_{v_3}}{K_E} + K_D + K_{v_3}\right] i\omega + K_0} \tag{5}$$

Stability Criterion

The Nyquist stability criterion is that $\left|\frac{\delta_0}{\epsilon}\right| < 1$ when the phase angle between δ_0 and ϵ is 180°, i.e., when the imaginary part of the function is zero.

Therefore, the stability condition for Equation 5 is

$$\frac{\left[\frac{K_D K_{v_3}}{K_E} + m_0\right]\left[\frac{K_0 K_{v_3}}{K_E} + K_D + K_{v_3}\right]}{\frac{m_0 K_{v_3}}{K_E}} - K_0 > K_A K_{v_i} \tag{6}$$

For the special case of $K_D = 0$ (zero damping), the stability condition reduces to $K_D = 0$ From Equation 6 it can be seen that K_0, the air load spring, has a

stabilizing effect for positive values. K_0 is a function of Mach number and increases positively with increasing Mach number. Therefore, zero airplane speed or $K_0 = 0$ will be the most critical condition for stability. The system pressure is reduced at M < 1.1 and consequently the value of K_0 at $M = 1.1$ will be the most critical for operating conditions. However, in view of the fact that at some time in the future it may be desired to fly the airplane with full system pressure at all speeds, all stability studies are made for $K_0 = 0$.

Static Gain

The loop static gain, $K_v = K_A K_{v_1}$, is a measure of the ratio of

$$\frac{\text{restoring force}}{\text{unit error}}$$

or

$$\frac{\text{restoring hinge moment.}}{\text{unit angular error}}$$

The larger the gain, the more unstable the system becomes or the smaller is the stability margin. The maximum hinge moment is fixed by aerodynamic requirements. The static gain of the system is then determined by the maximum allowable error. Since the ratio from the stick to the surface is fixed, the gain can be changed only by changing the ratio from the stick to the valve. Considering the surface fixed, the amount of stick movement required to fully open the valve is a measure of gain. Considering the stick fixed, the angle of rotation of the surface required to fully open the valve is also a measure of the system gain. The limiting value of maximum error allowable is determined by Fig. 8 and the maximum allowable time lag of .05 seconds. There may be other limits to the maximum error, however, such as: free play in the emergency condition with hydraulic power off; space in the cockpit; percent of total angle at high Mach number. The valve characteristic curves are actually non-linear and a change in effective gain can be produced without affecting the stability by changing the valve characteristic curves at constant maximum error. This effect is discussed further below.

Stability of the Airplane System

The stability condition Equation 6 is shown in Figs. 15, 16 and 17. In each figure, one of the coefficients K_D, the external damping coefficient; K_E, the cylinder and structure elasticity; and K_V, the valve pressure drop coefficient are varied independently and the stability [3] border traced. The most desirable method for stabilizing the system is to make the elastic constant K_E large enough. However, there is no reliable way of controlling K_E. Tests have shown that a very small amount of air trapped in one of the components such as cylinder, fittings, valve, etc., or air dissolved or entrained in the oil makes K_E very low. The airplane would be poor from service considerations if the successful flying of it depended on near perfect bleeding of the hydraulic system. It would also be dangerous since instability of the control system in flight might be disastrous. It is felt, therefore, that a safely low value of K_E should be used and the system stabilized by other means.

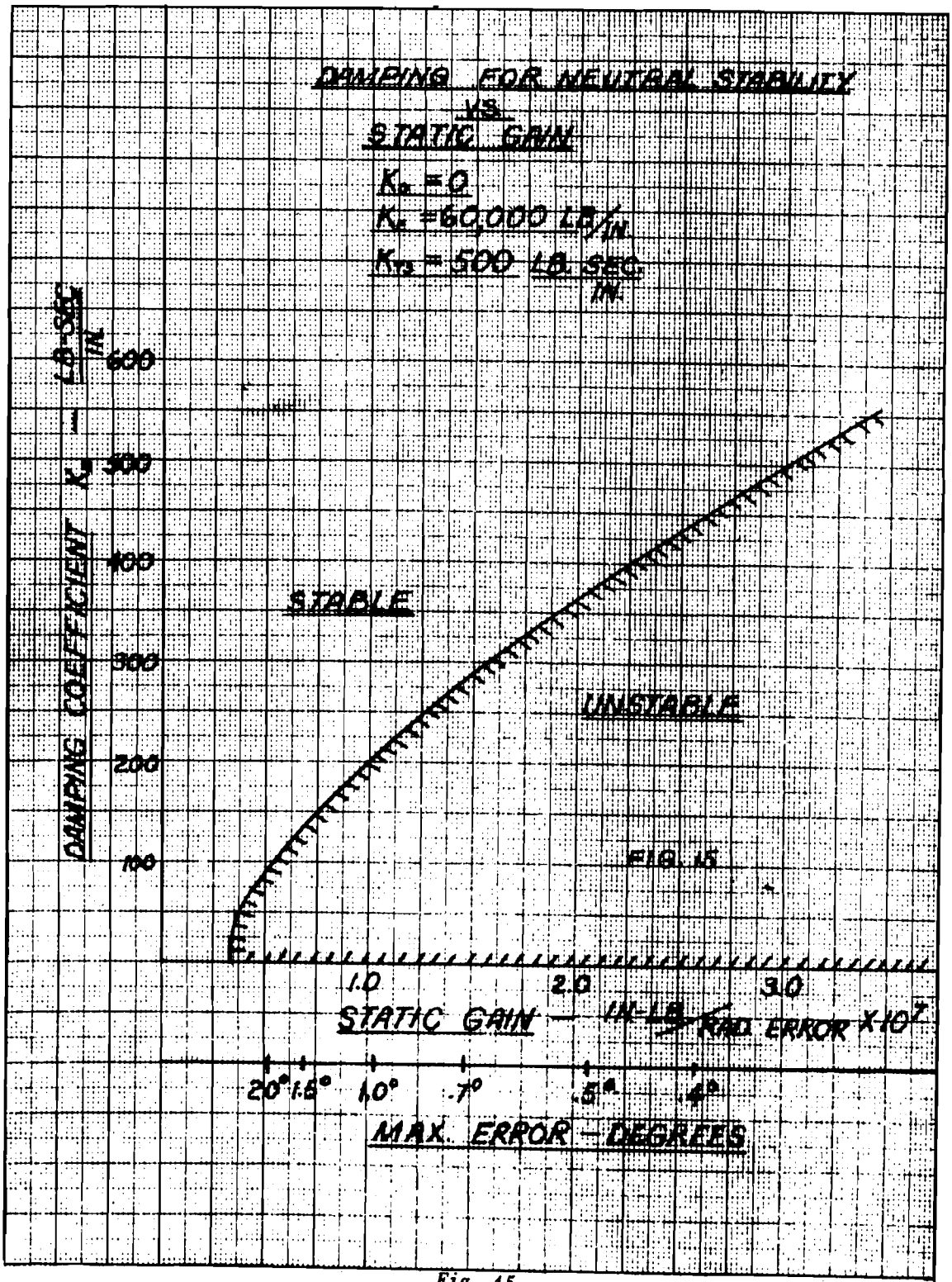
DAMPING FOR NEUTRAL STABILITY
VS.
STATIC GAIN
$K_a = 0$
$K_t = 60{,}000$ LB/IN.
$K_{T2} = 500$ LB. SEC. IN.
DAMPING COEFFICIENT K_2 = LB-SEC/IN.
600
500
400
300
200
100
STABLE
UNSTABLE
FIG. 15
1.0
2.0
3.0
STATIC GAIN — IN-LB/RAD ERROR X 10^7
20° 1.5° 1.0° .7° .5° .4°
MAX. ERROR — DEGREES

Fig. 15

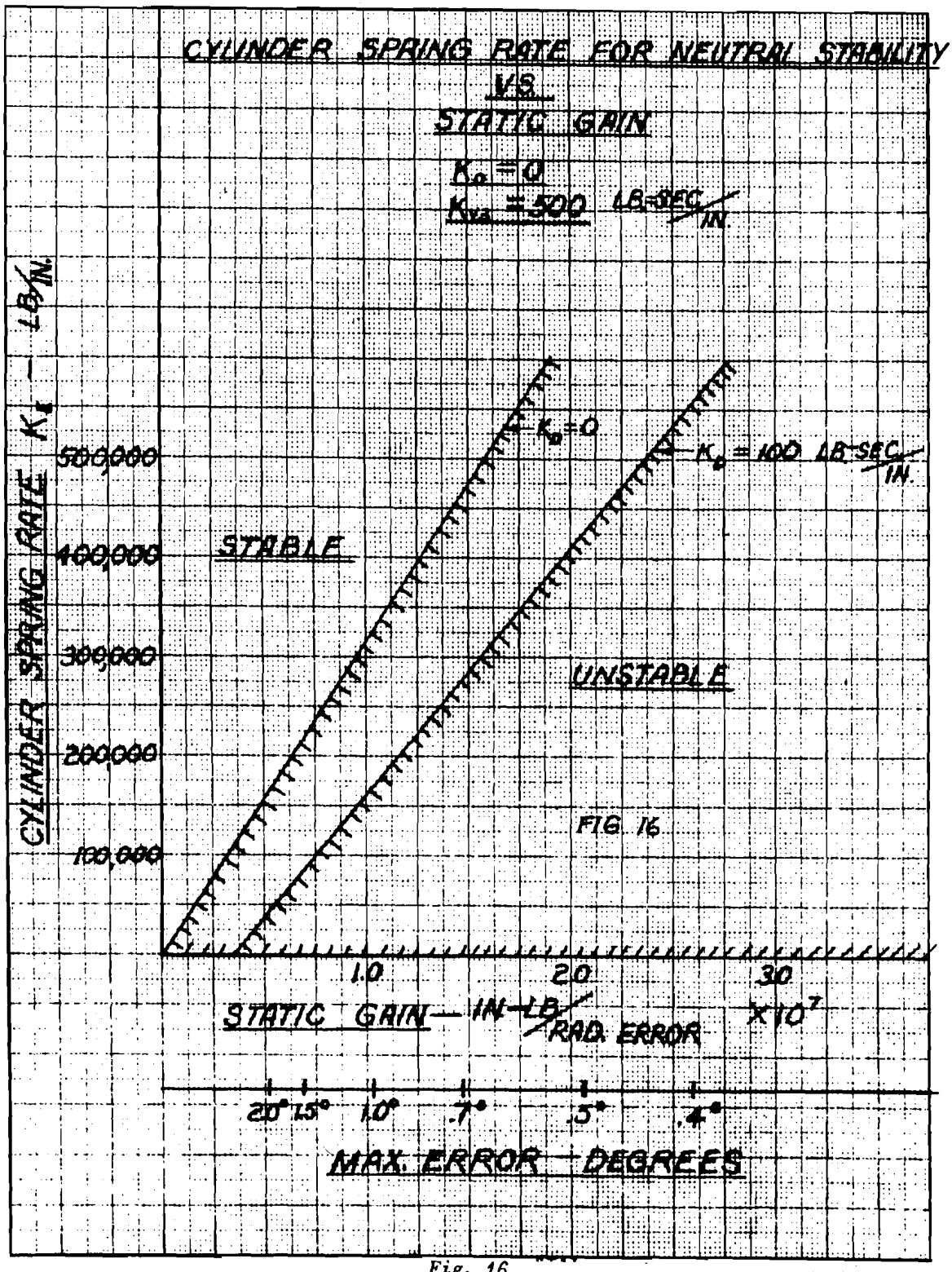
CYLINDER SPRING RATE FOR NEUTRAL STABILITY
VS.
STATIC GAIN
$K_D = 0$
$K_{VA} = 500$ LB-SEC/IN.
CYLINDER SPRING RATE K_t — LB/IN.
500,000
400,000
300,000
200,000
100,000
$K_D = 0$
$K_D = 100$ LB-SEC/IN.
STABLE
UNSTABLE
1.0
2.0
3.0
STATIC GAIN — IN-LB/RAD. ERROR
$\times 10^7$
20° 15° 10° 7° 5° 4°
MAX. ERROR — DEGREES

FIG. 16

Fig. 16

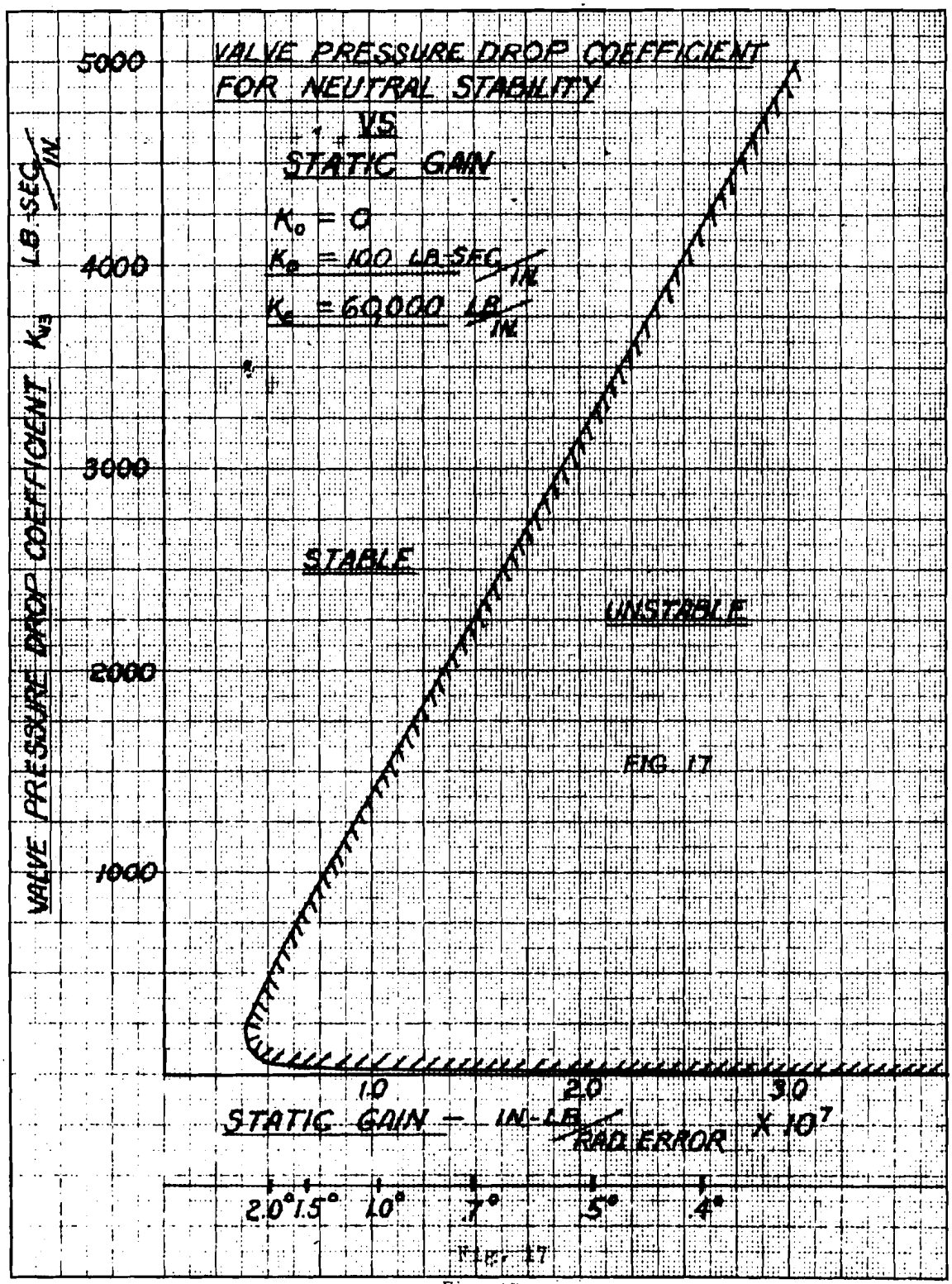
VALVE PRESSURE DROP COEFFICIENT
FOR NEUTRAL STABILITY
VS
STATIC GAIN
$K_0 = 0$
$K_e = 100$ LB-SEC/IN
$K_v = 60000$ LB/IN
VALVE PRESSURE DROP COEFFICIENT K_{V3} LB-SEC/IN
5000
4000
3000
2000
1000
STABLE
UNSTABLE
FIG 17
1.0
2.0
3.0
STATIC GAIN — IN-LB/RAD ERROR X 10^7
2.0° 1.5° 1.0° .7° .5° .4°
FIG. 17

Fig. 17

Fig. 18 shows a polar locus plot of the transfer function $K_v G_v = \frac{\delta_0}{\epsilon}$ for the basic, uncompensated system. The locus encircles the point $(-1+i0)$ and therefore by the Nyquist stability criterion indicates instability. Fig. 19 shows log modulus $|G_v|$ and phase angle plotted against frequency. The log plot in decibels is more adaptable for synthesizing and studying compensating systems for the basic system. Instability is indicated by Fig. 19 since log modulus $|G_v|$ is greater than 0 decibels when the phase angle is $180°$. A change in gain on the log plot is shown merely by moving the zero decibel line up or down. Multiplication of functions is accomplished merely by adding the values of the functions in decibels and adding the phase angles.

Stabilizing Networks

Of the several means considered for stabilizing the basic system, the two methods shown by Fig. 20 seemed to be the simplest and most promising. Both methods consist essentially of adding a damper to the control valve to cut down the valve amplitude at high frequencies. In method (a), the valve amplitude approaches 0 as $\omega \to \infty$. In method (b), the valve amplitude approaches $\frac{K_1}{K_1 + K_2}$ as $\omega \to \infty$.

Such devices are similar to those referred to by Hall[2] as undercompensated integral networks.

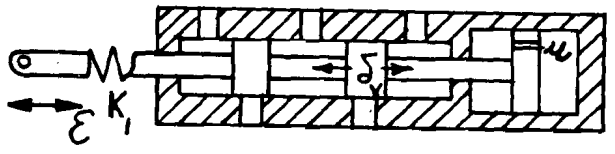

(a)

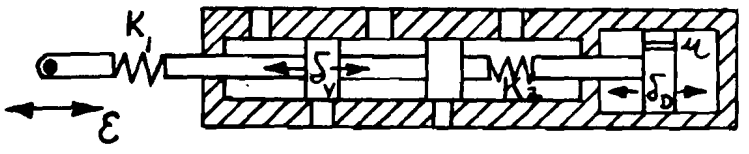

(b)

Fig. 20

[redacted]

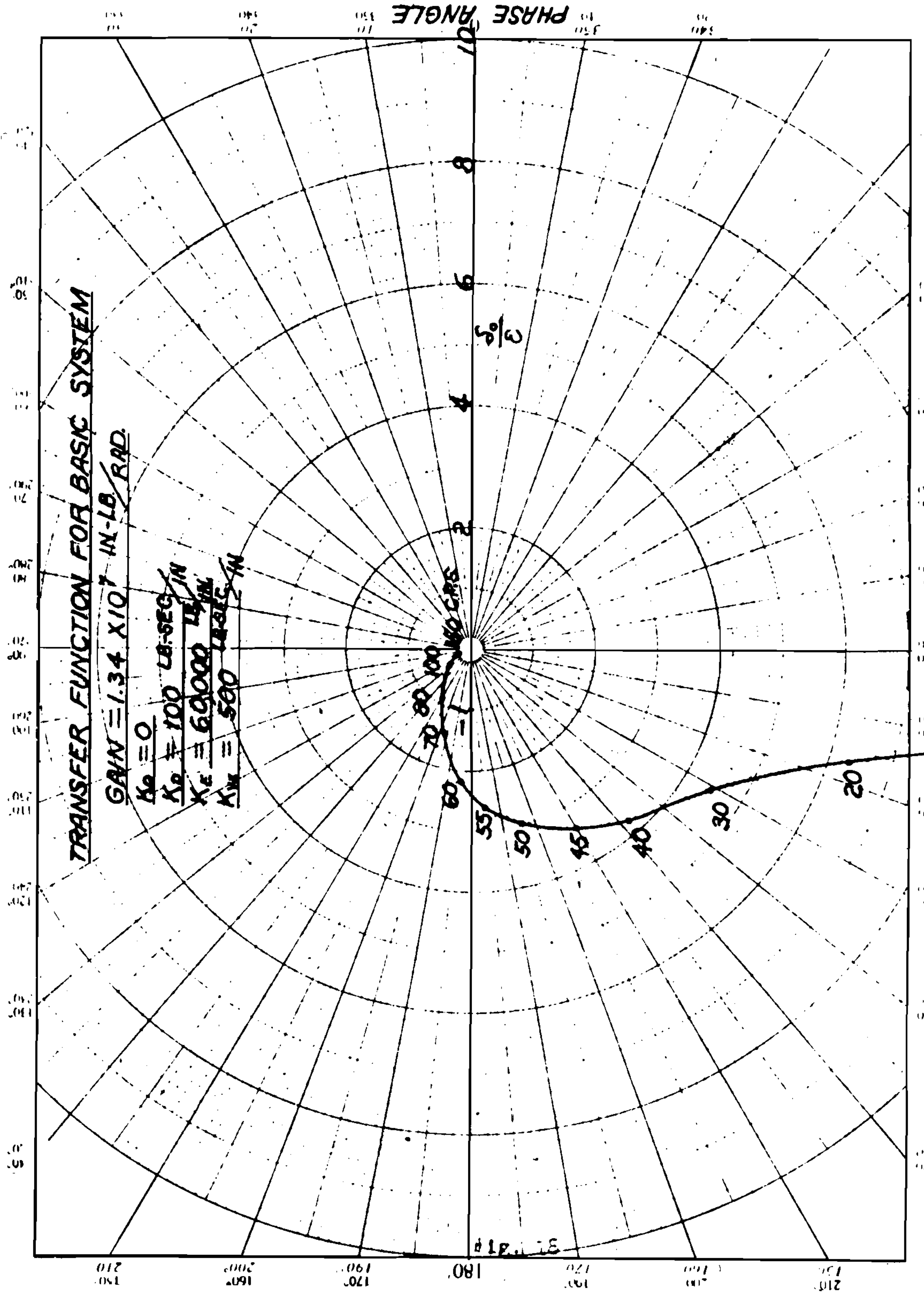

Fig. 18

[redacted]

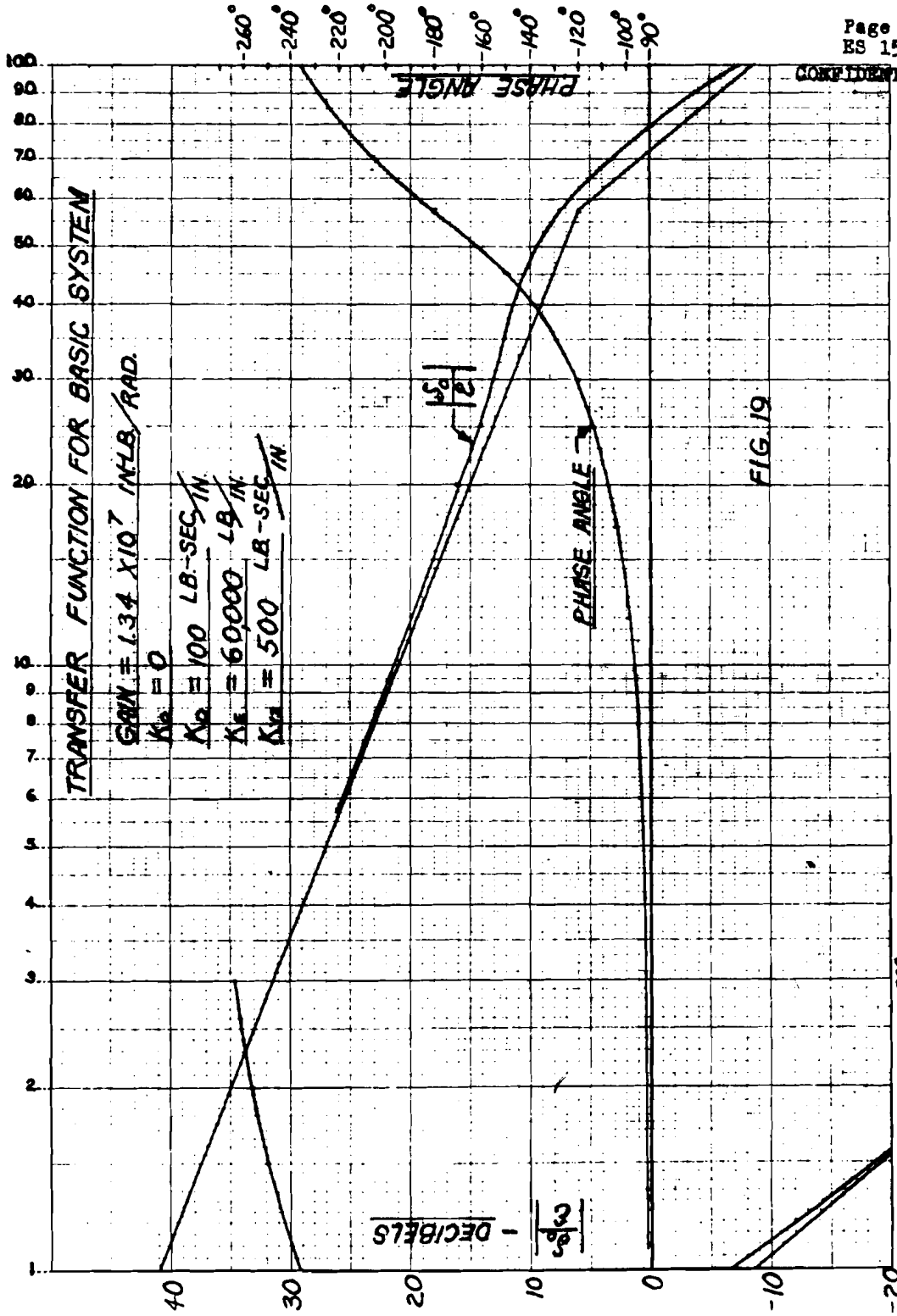
TRANSFER FUNCTION FOR BASIC SYSTEM
GAIN = 1.34 X10^7 IN-LB/RAD.
Ka = 0
Ka = 100 LB-SEC/IN
Ka = 60000 LB/IN.
Ka = 500 LB-SEC/IN
PHASE ANGLE
DECIBELS
FREQUENCY - C.P.S.
FIG. 19

Fig. 19

In Fig. 20 (b), consider the forces acting on the valve slide.

$$K_1 (\epsilon - \delta_v) = K_2 (\delta_v - \delta_D) = \mu \dot{\delta}_D \qquad (7)$$

where μ is the damping coefficient of the damper and δ_D is the damper motion

The inertia forces are neglected which means that the natural frequency of the valve must be well out of the range of frequencies to be considered.

$$\dot{\delta}_D = \frac{(K_2 + K_1) \dot{\delta}_v - K_1 \dot{\epsilon}}{K_2}$$

$$\left[\mu \frac{(K_1 + K_2) i\omega + K_1}{K_2} \right] \delta_v (i\omega) = \left[K_1 + \frac{\mu K_1}{K_2} i\omega \right] \epsilon (i\omega)$$

$$\frac{\delta_v (i\omega)}{\epsilon} = \frac{1 + \left(\frac{\mu}{K_2}\right) i\omega}{\frac{\mu}{K_2}\left(\frac{K_1 + K_2}{K_1}\right) i\omega + 1}$$

Let $$\frac{K_1}{K_1 + K_2} = \alpha$$

Then $$\frac{\delta_v (i\omega)}{\epsilon} = \frac{\alpha \frac{\mu}{K_1} i\omega - (1 - \alpha)}{\frac{\mu}{K_1} i\omega - (1 - \alpha)}$$

Or $$\frac{\delta (i\omega)}{\epsilon} = \frac{\frac{\alpha}{1 - \alpha} (\tau_L) i\omega + 1}{\frac{1}{1 - \alpha} (\tau_L) i\omega + 1} \quad \text{where} \quad \tau_L = \frac{\mu}{K_1} \qquad (8)$$

Fig. 20 (a) is a special case of Fig. 20 (b).

For Fig. 20 (a), $K_2 = \infty$ or $\alpha = 0$ and

$$\frac{\delta_v (i\omega)}{\epsilon} = \frac{1}{\tau_L (i\omega) + 1}$$

Fig. 21 shows a typical log plot of Equation 8 and shows how the transfer function may be easily constructed by standard forms. Equation 8 is formed by two functions:

$$1 - \alpha(\tau_L)\, i\omega + 1 \qquad \text{and} \qquad \frac{1}{\frac{1}{1-\alpha}(\tau_L)\, i\omega + 1}$$

The log plot of each of these functions can be approximated by two straight line asymptotes by the method described by Brown and Campbell[1].

The denominator $\frac{1}{1-\alpha}(\tau_L)\, i\omega + 1$ approaches the constant value 1 for very small values of ω.

For very large values of ω, the function approaches $\frac{1}{\frac{\tau_L}{1-\alpha} i\omega}$. Therefore, the asymptotes are OA and AB of Fig. 21. The frequency at which point A is located is equal to

$$f_B = \frac{1}{\frac{\tau_L}{1-\alpha}(6.28)} = \frac{1-\alpha}{6.28\,\tau_L} \quad C.P.S. \tag{9}$$

The asymptote AB has a slope of -6 decibels per octave since the frequency term ω appears in the first power.

The true locus is OEB and can be quickly constructed from the asymptotes by a curve of corrections which is standard for all equations of the form $iu + 1$ or $\frac{1}{iu + 1}$. This correction curve is given by Brown and Campbell.

The numerator $\frac{\alpha}{1-\alpha}(\tau_L)\, i\omega + 1$ has the asymptotes OC and CD on Fig. 21. The break point C is located at a frequency equal to

$$f_B = \frac{1}{\frac{\alpha\tau_L}{1-\alpha}(6.28)} = \frac{1-\alpha}{\alpha\,(6.28\,\tau_L)}$$

This frequency is seen to be $\frac{1}{\alpha}$ times the frequency of the break point A. The asymptote CD has a slope of 6 decibels per octave. The two curves when combined by direct addition give the log modulus plot for Equation 8. In Fig. 21 the curve OEF is the combined curve. The phase angle can be handled in a similar manner. In Fig. 21, KM is the phase angle curve for the denominator of Equation 8 and GHJ is the phase angle curve for the numerator. Curve NP is the combined phase curve. It can be seen from Equation 9 that if α is held constant, the effect of varying τ_L is to shift the locus along the frequency axis without changing its shape.

Fig. 22 shows a polar plot of a typical lag network transfer function. The shape of the plot is always a semi-circle whose radius and center is determined by the

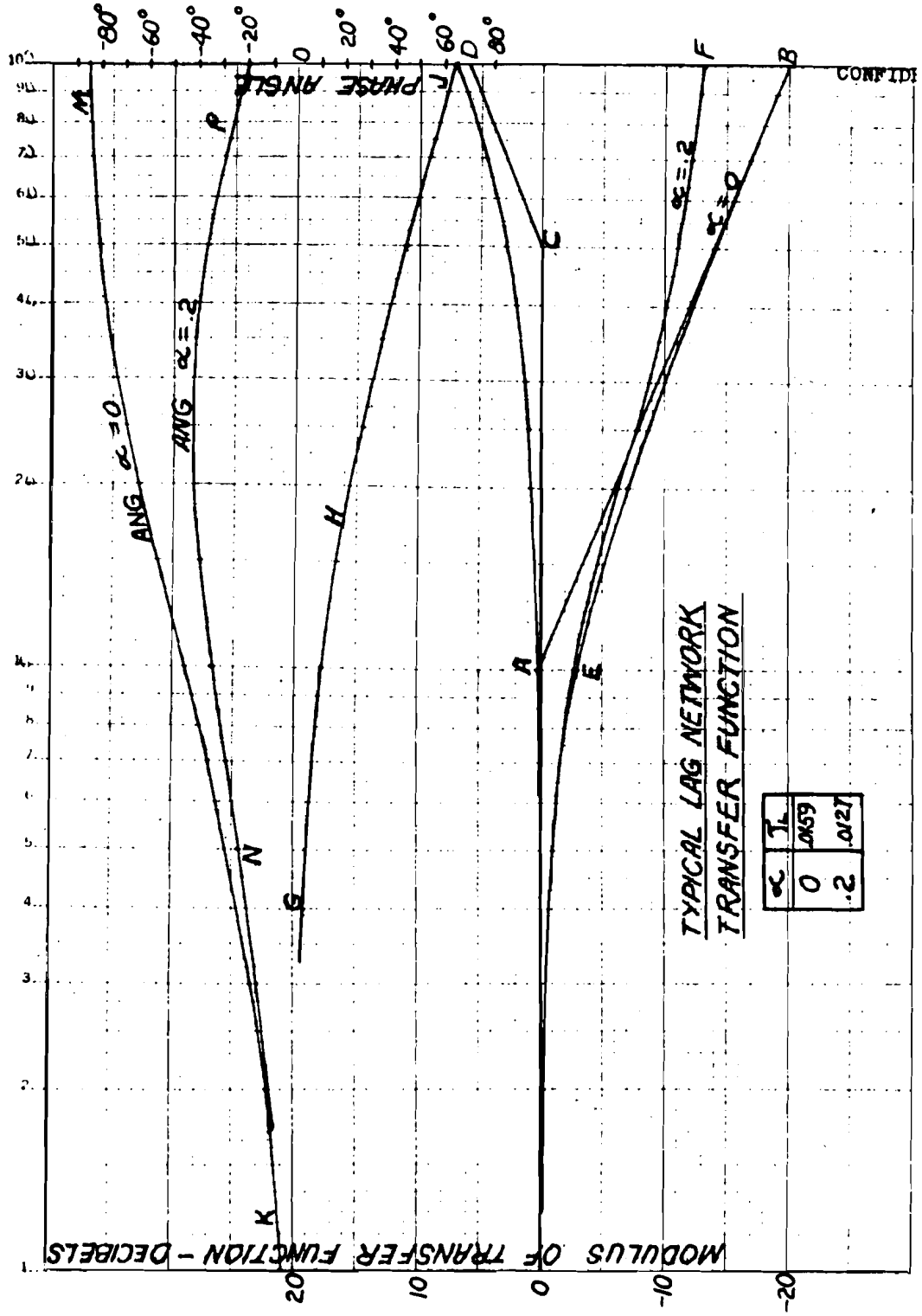
PHASE ANGLE
-80°
-60°
-40°
-20°
0
20°
40°
60°
80°
ANG α=0
ANG α=.2
α=.2
α=0
A
B
C
D
E
F
G
H
K
M
N
P
TYPICAL LAG NETWORK
TRANSFER FUNCTION
α T
0 .059
.2 .027
MODULUS OF TRANSFER FUNCTION - DECIBELS
20
10
0
-10
-20
FREQUENCY - C.P.S.

Fig. 21

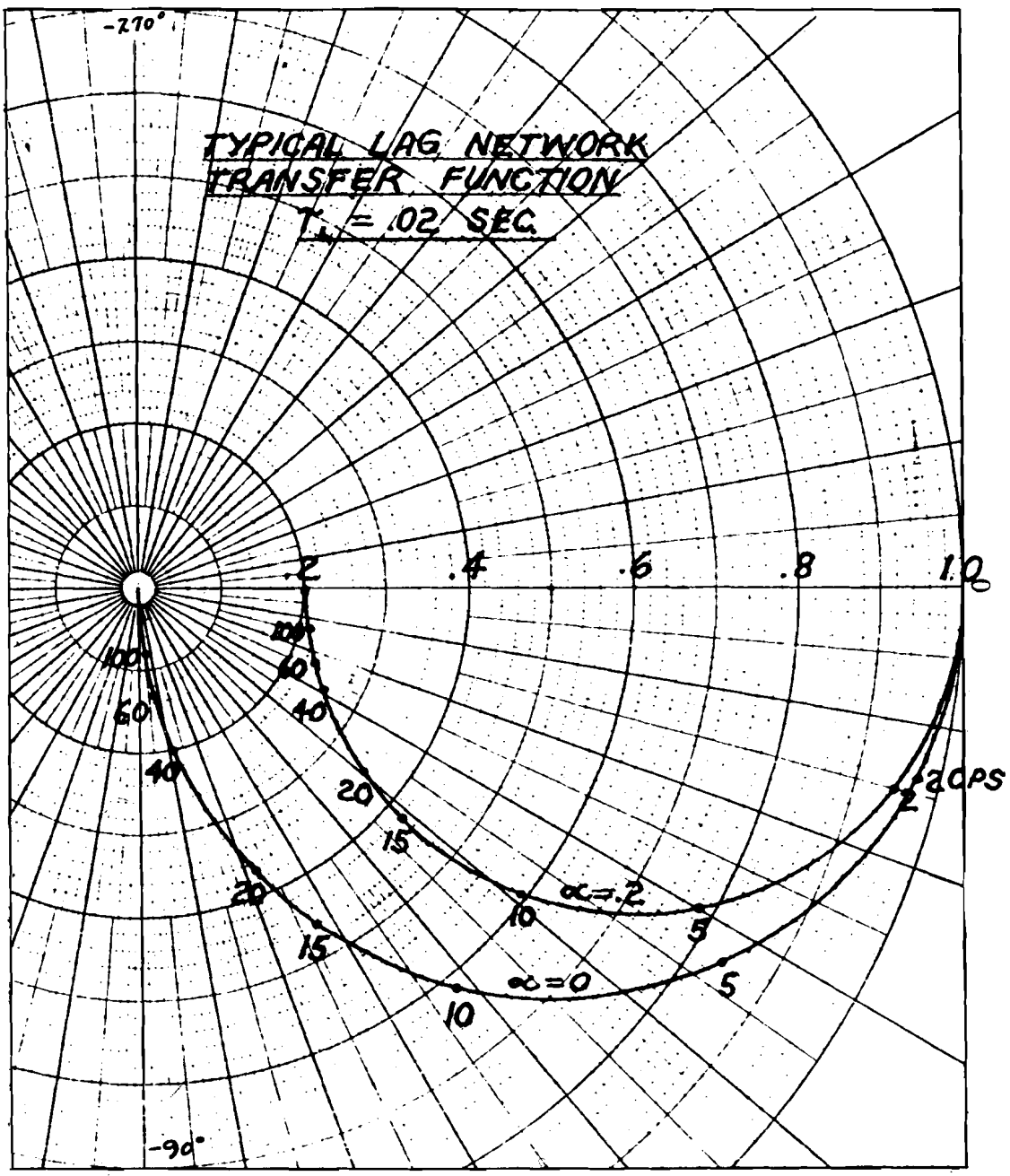
TYPICAL LAG NETWORK
TRANSFER FUNCTION
T_1 = .02 SEC.
-270°
-90°
.2
.4
.6
.8
1.0
100
60
40
20
15
10
5
2
20PS
∝=.2
∝=0

Fig. 22

value of α. α is the high frequency intercept. Changing τ_L for constant α merely shifts the frequency points.

By plotting the lag network transfer function for several values of α, the stability of the basic system with the lag network added can be determined. Fig. 23 shows the method for determining the neutrally stable gain for a given value of α and τ_L. The basic system modulus and phase angle curves G_v and Ang (G_v) are plotted. The lag network transfer function G_L and Ang G_L is then superimposed and positioned by setting the break point A at the frequency determined by τ_L. The values for the lag network are plotted to a reverse scale from those of the basic system so that distance between the curves at any frequency is a direction addition. In Fig. 23 the zero angle line for the lag network is plotted from the -180° line for the basic system; therefore, the frequency at which the angle curves intersect is the frequency at which the overall transfer function $\frac{\delta_0}{\epsilon}$ is 180° out of phase. For the particular example shown by Fig. 23, this frequency is 46 C.P.S. for $\alpha = .2$ and 19.5 C.P.S. for $\alpha = 0$. For $\alpha = .2$ the sum of the two functions is -1.9 decibels. For $\alpha = 0$ the sum is 5.8 decibels. Since the gain for the basic system is 1.34×10^7 in.lb./rad., the gain for neutral stability is

$$\frac{1.34 \times 10^7}{.81} = 1.65 \times 10^7 \text{ in. lb./rad. for } \alpha = .2$$

and

$$\frac{1.34 \times 10^7}{1.95} = .69 \times 10^7 \text{ in. lb./rad. for } \alpha = 0.$$

Thus by shifting the lag network transfer function along the frequency axis and correcting the gain for neutral stability, the stability border for a plot of τ_L vs. gain can be traced for values of constant α. This stability study can also be made by multiplying out the combined transfer function and applying Rough's discriminant to the resulting quartic equation. It is felt, however, that the method illustrated by Fig. 23 is easier and is more conducive to synthesis. Fig. 24 shows the stability boundaries for the basic system with the lag network added.

Fig. 24 shows only the stability boundaries for values of α. It is of interest also to know the lag network characteristics (α and τ_L) necessary to produce a given degree of stability for a given system. The maximum closed loop response $\left|\frac{\delta_o}{\delta_i}\right|_{max}$ is a measure of the degree of stability of the system. Fig. 25 shows a method for making a plot of τ_L vs. gain for a given value of α and $\left|\frac{\delta_o}{\delta_i}\right|_{max}$. Since

$$\frac{\delta_o}{\delta_i}(i\omega) = \frac{\frac{\delta_o}{\epsilon}(i\omega)}{1 - \frac{\delta_o}{\epsilon}(i\omega)}$$

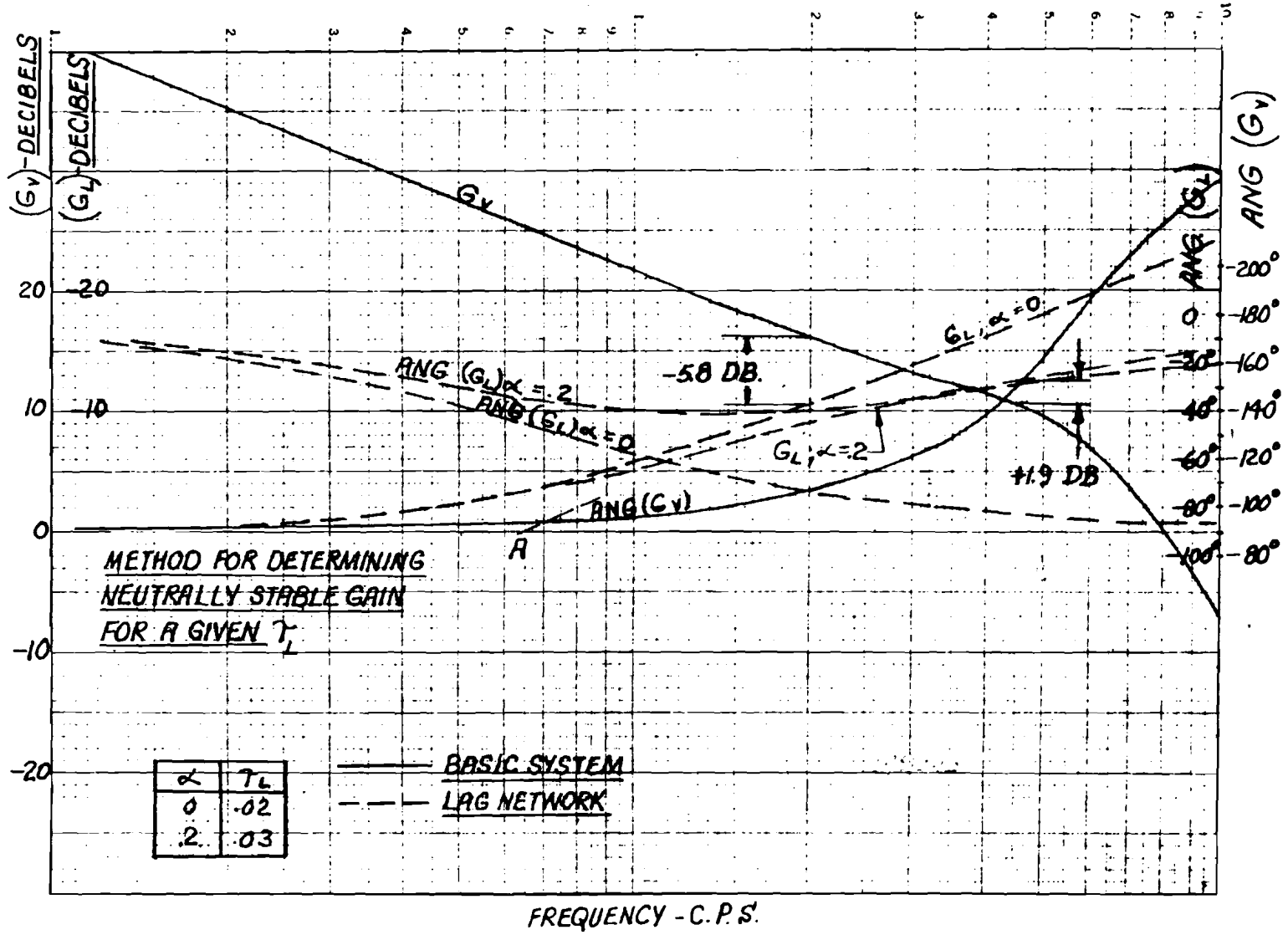
(Gv)-DECIBELS
(GL)-DECIBELS
ANG (GL)
Gv
GL; α=0
ANG (GL) α=.2
ANG (GL) α=0
-5.8 DB.
GL; α=.2
+1.9 DB
ANG (Gv)
A
METHOD FOR DETERMINING
NEUTRALLY STABLE GAIN
FOR A GIVEN τL
α
τL
0
.02
.2
.03
BASIC SYSTEM
LAG NETWORK
FREQUENCY - C.P.S.

Fig. 23

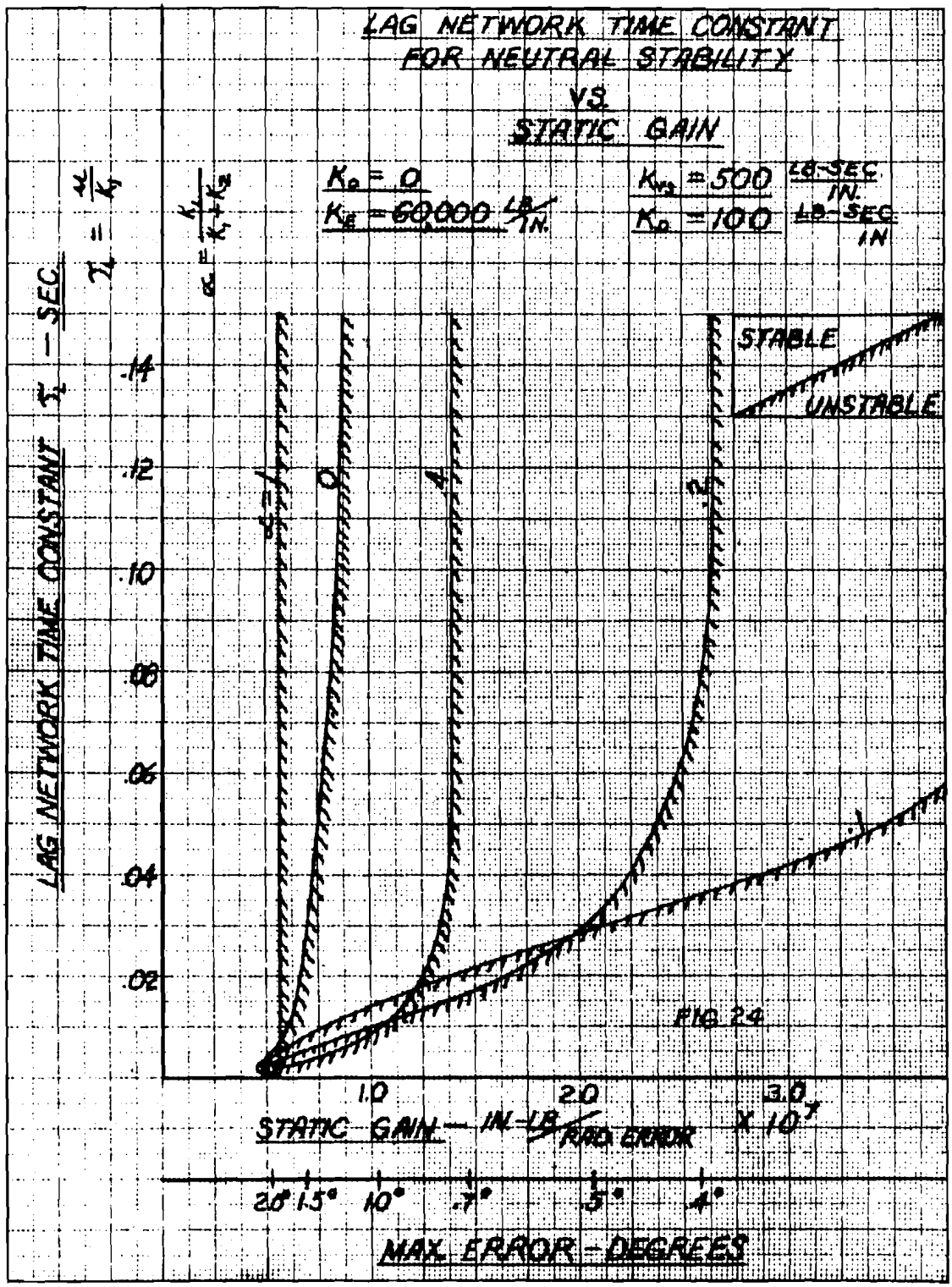
LAG NETWORK TIME CONSTANT
FOR NEUTRAL STABILITY
VS.
STATIC GAIN
$K_a = 0$
$K_{ff} = 60000$ LB/IN.
$K_{vs} = 500$ LB-SEC/IN.
$K_a = 100$ LB-SEC/IN
$\alpha = \frac{K_1}{K_1 + K_2}$
$\tau_L = \frac{\alpha}{K_1}$
LAG NETWORK TIME CONSTANT τ_L — SEC.
.14
.12
.10
.08
.06
.04
.02
$\alpha = 1$
0
.4
.2
STABLE
UNSTABLE
FIG 24
1.0
2.0
3.0
X 10^7
STATIC GAIN — IN-LB/RAD ERROR
2.0°
1.5°
1.0°
.7°
.5°
.4°
MAX. ERROR - DEGREES

Fig. 24

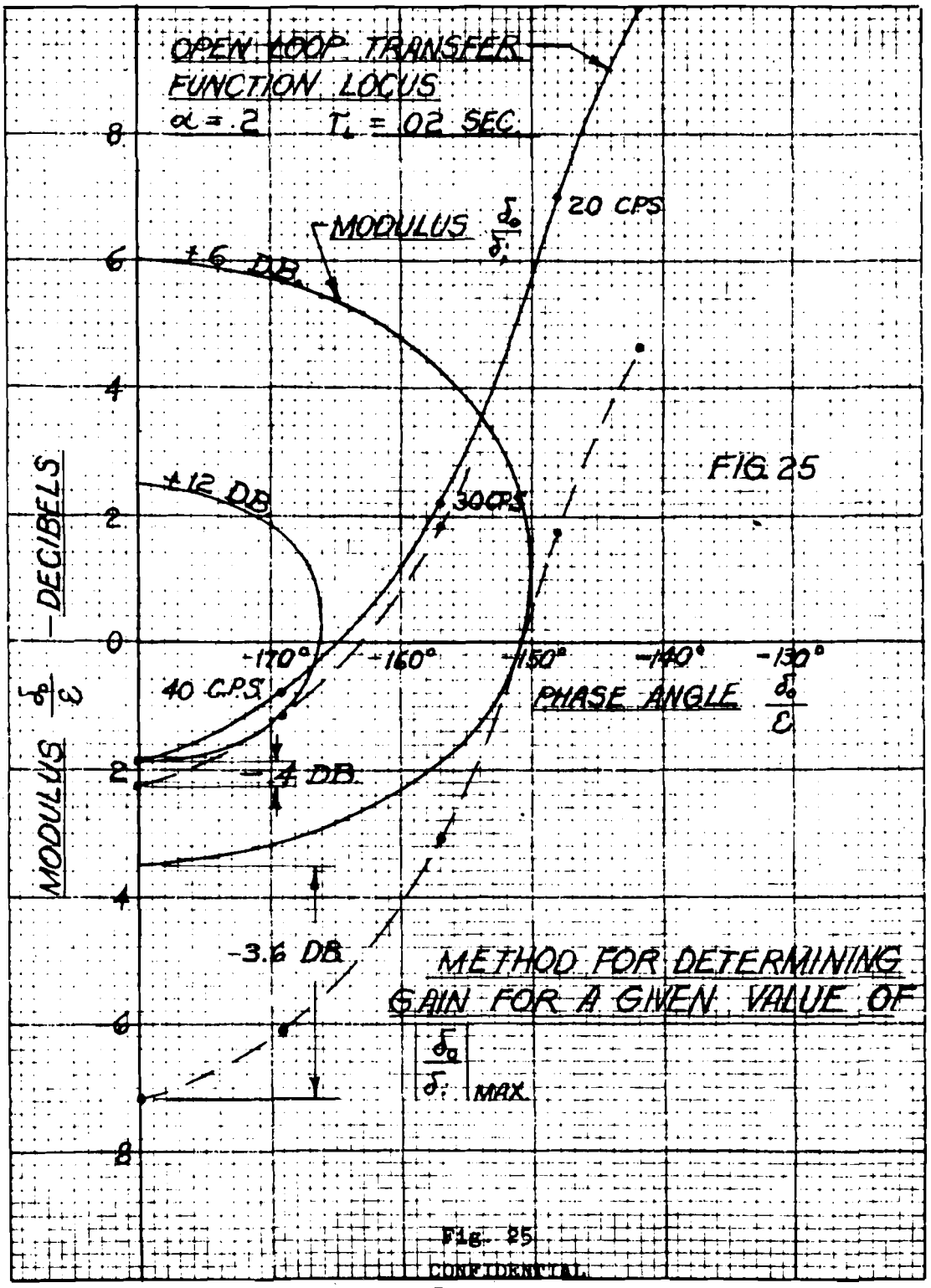

Fig. 25

CONFIDENTIAL

Fig. 25

is a complex function which is uniquely determined by the open loop function $\frac{\delta_o}{\epsilon}(i\omega)$, it is possible to draw curves of constant $\frac{\delta_o}{\delta_i}$ in the $\frac{\delta_o}{\epsilon}$, phase angle $\frac{\delta_o}{\epsilon}$ plane. In Fig. 25 curves of $\frac{\delta_o}{\delta_i} = 2.0$ and 4.0 ($\log \frac{\delta_o}{\delta_i} = 6$ db and 12 db) are shown. The open loop transfer function is plotted, then moved vertically until the locus is tangent to a curve of constant $\frac{\delta_o}{\delta_i}$. The amount of vertical movement of the locus gives a factor by which the gain of the system must be changed to produce the value of $\left|\frac{\delta_o}{\delta_i}\right|_{\max}$

In the example shown, the gain of the system must be reduced by 3.6 decibels to keep the closed loop response $\left|\frac{\delta_o}{\delta_i}\right|_{\max}$ to 2.0. For $\left|\frac{\delta_o}{\delta_i}\right|_{\max} = 4.0$ the gain has to be reduced by $.4$ decibels.

Fig. 26 shows τ_L vs. gain for different values of $\left|\frac{\delta_o}{\delta_i}\right|_{\max}$ for the case of $\alpha = .2$.

Fig. 27 shows the polar plot for the transfer function including the lag network with $\tau_L = .03$ and $\alpha = .2$.

5. *Dynamic Model and Non-Linearities*

To gain background data on the type of servomechanism to be used for the airplane, a functionally similar but non-scaled system was constructed from existing parts and tested. One of the objects was to study the effects of the non-linearities. The analytic methods above are based on the assumption that the equations of motion are linear differential equations. However, some of the components of hydraulic servomechanisms are distinctly non-linear. The damping force from the surface dampers varies as the square of the velocity. The damper on the lag network is also of the velocity squared type. The spring rate of the cylinder varies with the pressure because of the trapped air. The type of valve-cylinder characteristic assumed for the linear analysis is shown by Fig. 28 (a). The valve-cylinder characteristic for a balanced type slide with no force feedback is shown by Fig. 28 (b). Since the system is non-linear, the transfer function $\frac{\delta_o}{\epsilon}(i\omega)$ should vary with amplitude as well as with frequency. The amplitude effect was found on the model tests as shown by Figs. 29, 30 and 31. Transfer functions were measured at constant valve amplitude for three different system pressures. For each system pressure the servo loop was closed with the gain ratio equal to 1 and the amplitude and frequency of the self-excited oscillations observed. Despite the marked non-linearities of the components, the system acts much like a linear one.

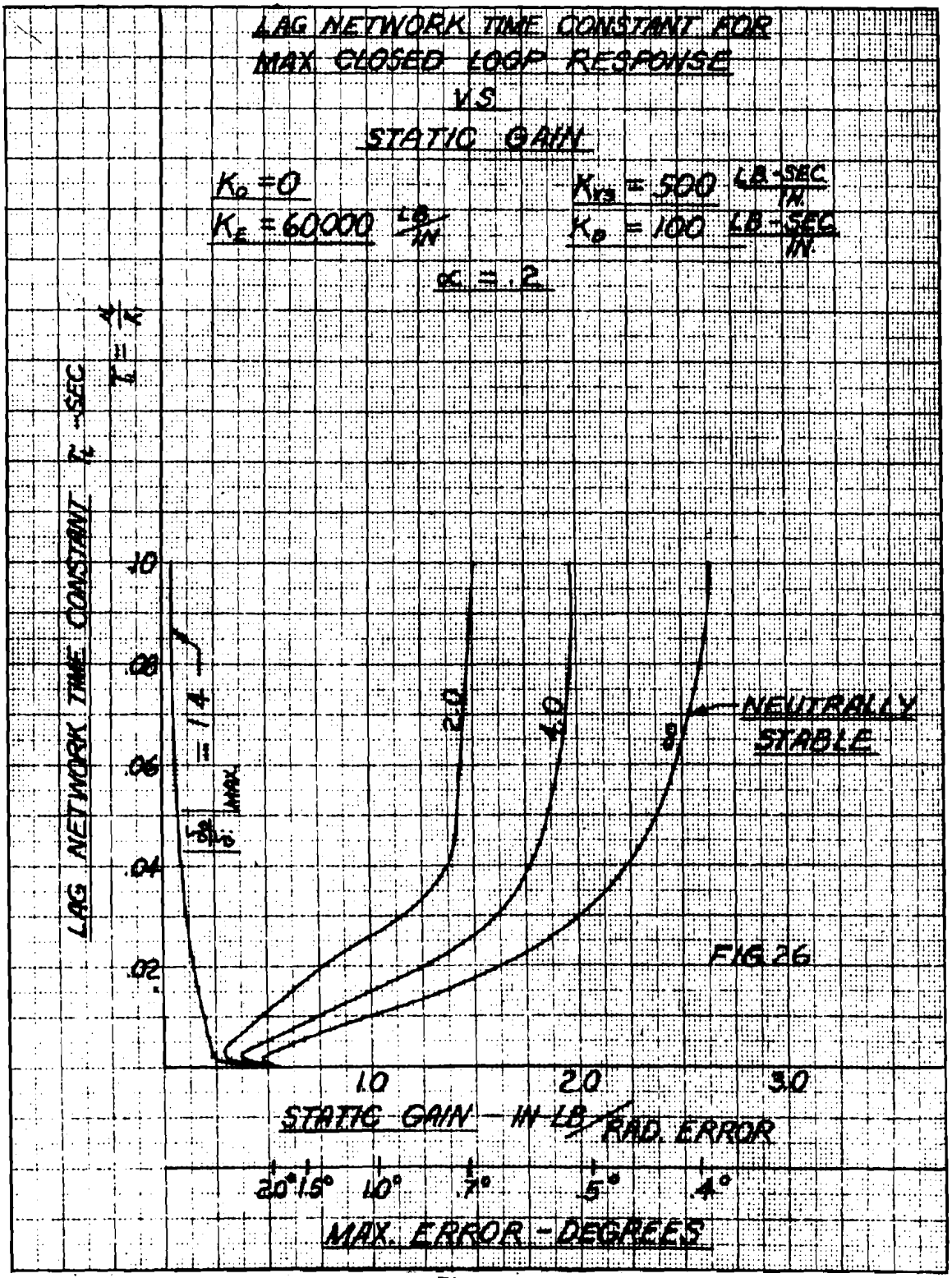
LAG NETWORK TIME CONSTANT FOR
MAX CLOSED LOOP RESPONSE
VS
STATIC GAIN
$K_D = 0$
$K_E = 60000$ LB/IN
$K_{VB} = 500$ LB-SEC/IN
$K_P = 100$ LB-SEC/IN
$\alpha = .2$
LAG NETWORK TIME CONSTANT T_L -SEC
$T_L = \frac{1}{K}$
$\left|\frac{\Delta\theta}{\theta}\right|_{MAX} = 1.4$
.10
.08
.06
.04
.02
2.0
4.0
∞
NEUTRALLY STABLE
1.0
2.0
3.0
STATIC GAIN — IN LB/RAD. ERROR
20°
15°
10°
7°
5°
4°
MAX. ERROR - DEGREES

Fig. 26

FIG 26

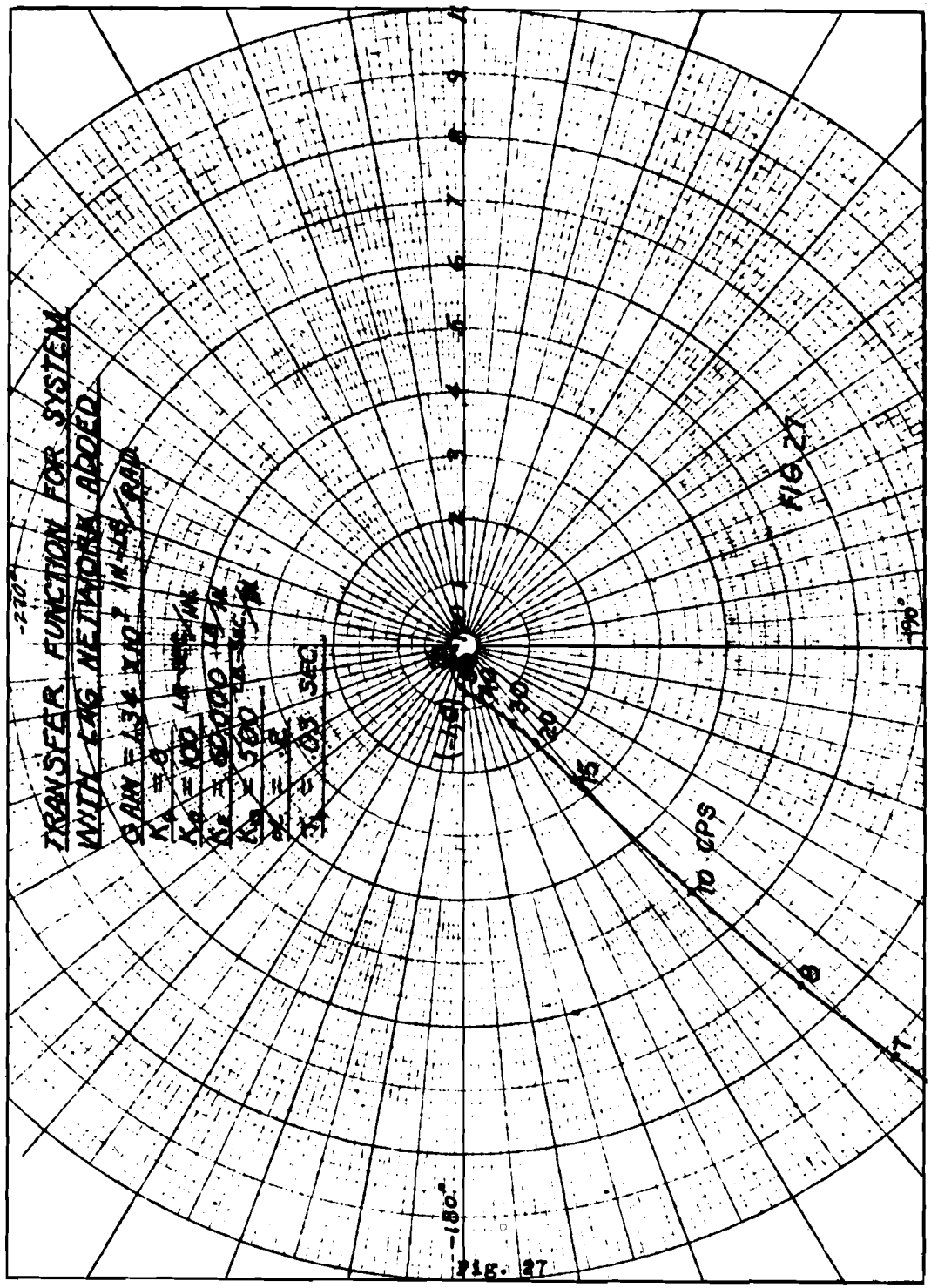
TRANSFER FUNCTION FOR SYSTEM
WITH LAG NETWORK ADDED
-270°
-180°
190°
FIG. 27
10 CPS
Fig. 27

Fig. 27

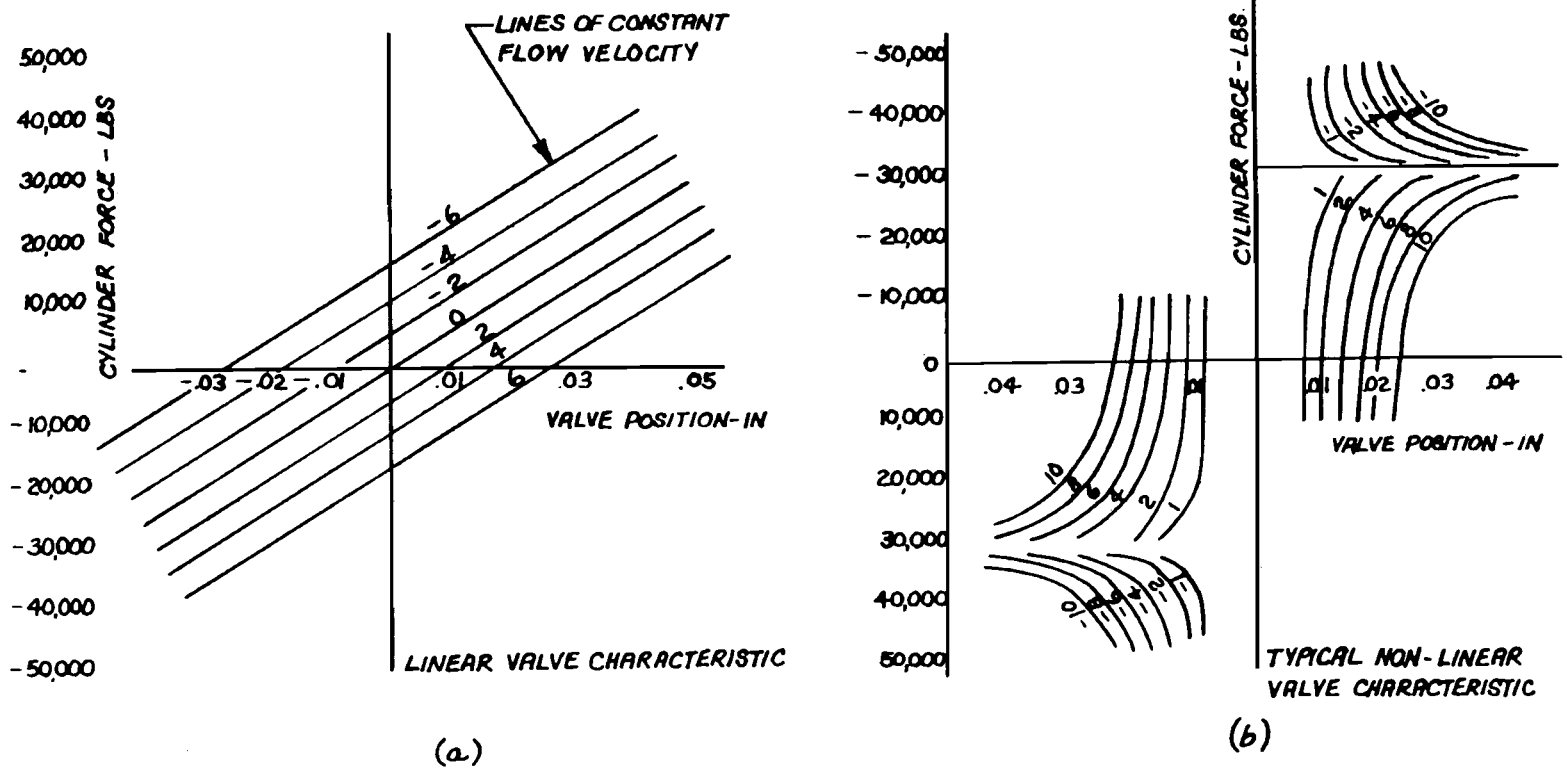
LINES OF CONSTANT FLOW VELOCITY
CYLINDER FORCE - LBS
50,000
40,000
30,000
20,000
10,000
-10,000
-20,000
-30,000
-40,000
-50,000
-.03 -.02 -.01 .01 .03 .05
VALVE POSITION-IN
LINEAR VALVE CHARACTERISTIC
(a)
CYLINDER FORCE - LBS
50,000
40,000
30,000
20,000
10,000
.04 .03 .01 .02 .03 .04
VALVE POSITION - IN
TYPICAL NON-LINEAR VALVE CHARACTERISTIC
(b)

Fig. 28

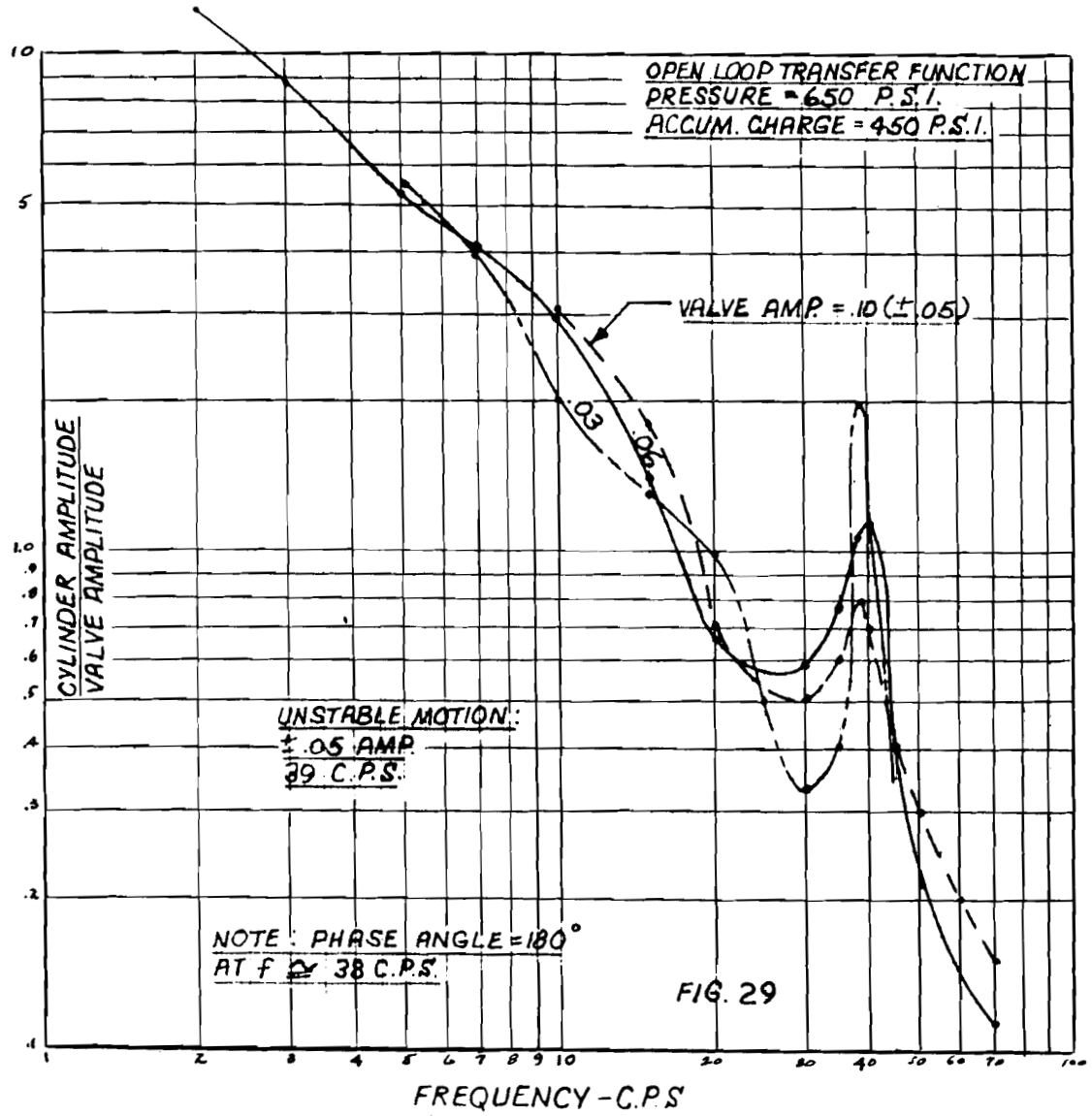
OPEN LOOP TRANSFER FUNCTION
PRESSURE = 650 P.S.I.
ACCUM. CHARGE = 450 P.S.I.
VALVE AMP. = .10 (± .05)
.03
.06
CYLINDER AMPLITUDE / VALVE AMPLITUDE
UNSTABLE MOTION:
± .05 AMP.
39 C.P.S.
NOTE: PHASE ANGLE = 180°
AT f ≈ 38 C.P.S.
FIG. 29
FREQUENCY - C.P.S

Fig. 29

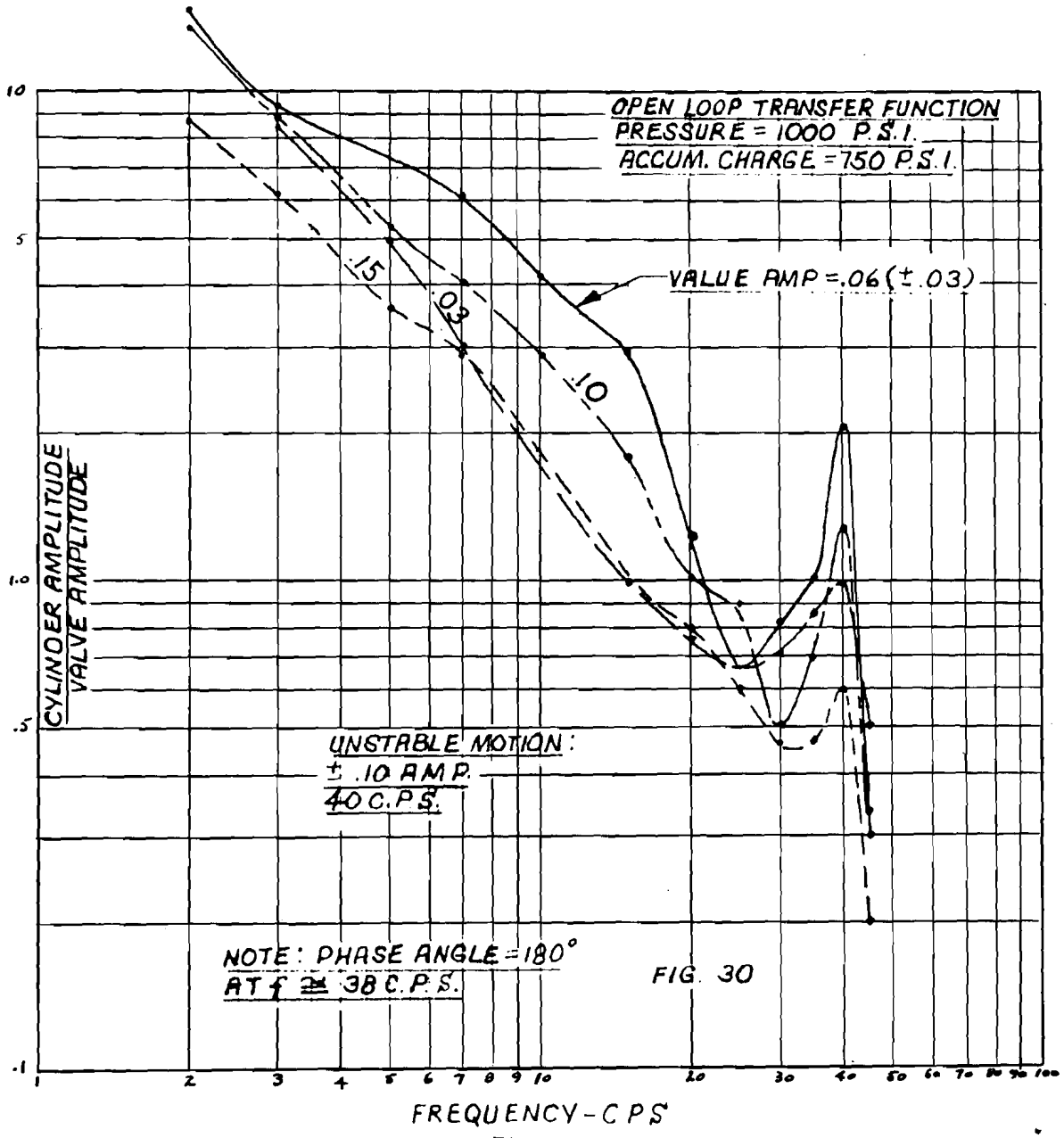
OPEN LOOP TRANSFER FUNCTION
PRESSURE = 1000 P.S.I.
ACCUM. CHARGE = 750 P.S.I.
VALUE AMP = .06 (± .03)
.15
.03
.10
CYLINDER AMPLITUDE / VALVE AMPLITUDE
UNSTABLE MOTION:
± .10 AMP.
40 C.P.S.
NOTE: PHASE ANGLE = 180°
AT f ≅ 38 C.P.S.
FIG. 30
10
5
1.0
.5
.1
1
2
3
4
5
6
7
8
9
10
20
30
40
50
60
70
80
90
100
FREQUENCY - CPS

Fig. 30

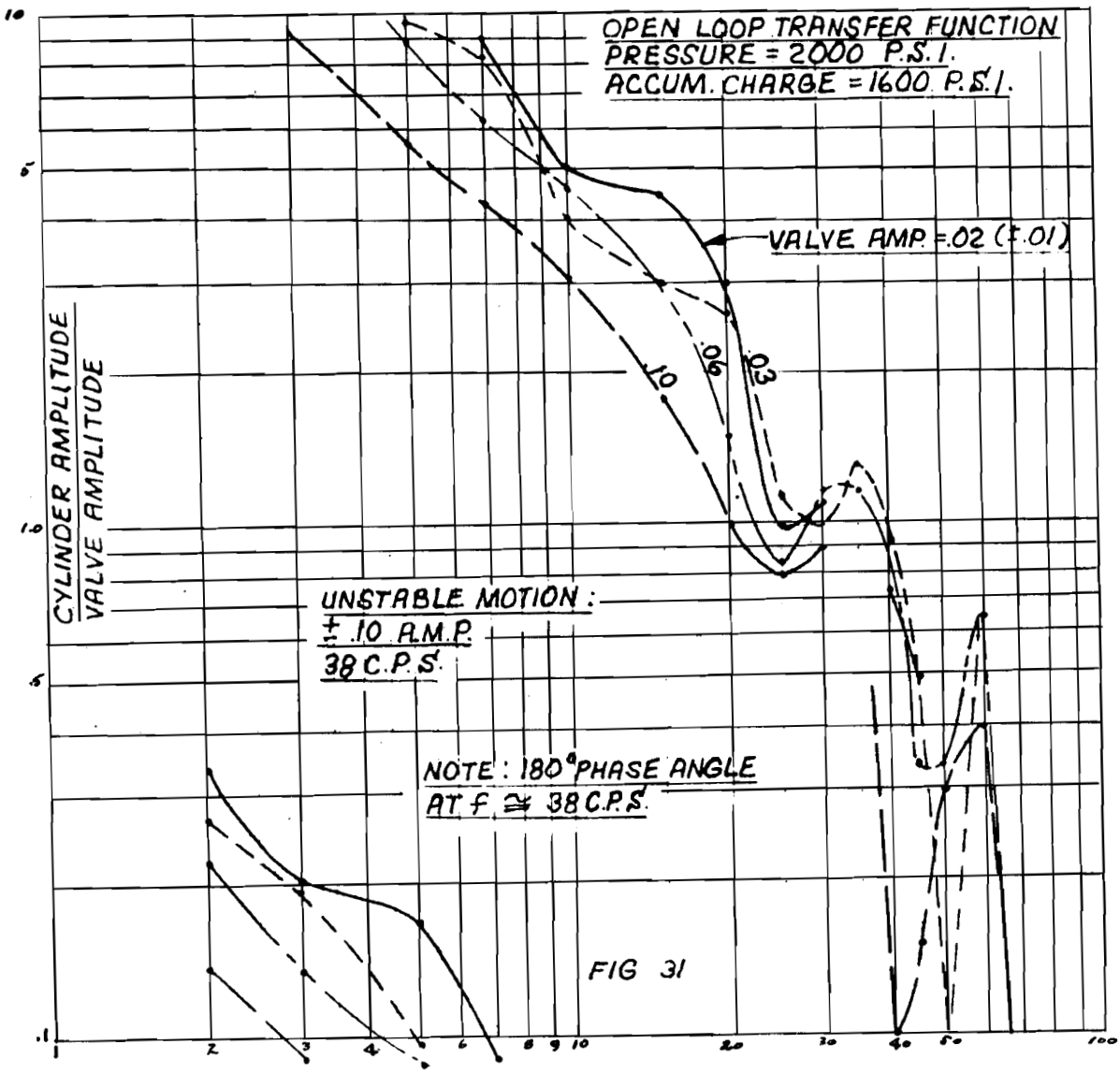
OPEN LOOP TRANSFER FUNCTION
PRESSURE = 2000 P.S.I.
ACCUM. CHARGE = 1600 P.S.I.
VALVE AMP. = .02 (± .01)
.10
.06
.03
UNSTABLE MOTION :
± .10 A.M.P.
38 C.P.S.
NOTE : 180° PHASE ANGLE
AT f ≅ 38 C.P.S.
FIG 31
CYLINDER AMPLITUDE / VALVE AMPLITUDE
FREQUENCY C.P.S.

Fig. 31

Fig. 32 shows two of the curves of Fig. 29 compared with the calculated linear solutions. As can be predicted, there is an amplitude effect. The chief discrepancy of the measured with the calculated system is that there appears to be an attenuating factor which the calculated motion does not take into account. This observed attenuation begins to be effective at about 25 C.P.S. In Fig. 31 the minor peak at 60 C.P.S. was found to be due to the natural frequency in bending of the push rod that actuated the valve.

Fig. 33 shows the transfer function of a lag network that was built up of a spring and a velocity-squared damper. The bulge in the locus at frequencies of 20 to 60 was caused by the resonance of the lag network itself. The resonant frequency of the lag network itself with no oil in the damper was measured to be 63 C.P.S. The logarithim plot of the transfer function is shown by Fig. 34. Since the resonant frequency of the lag network was above the instability frequency of the basic system and also since the addition of a lag network decreases the frequency of 180° phase lag, the lag network was very effective in stabilizing the system. Fig. 35 shows a transfer function of the basic system with a lag network added.

One effect of the non-linear valve characteristic is that the effective gain can be changed without changing the maximum force or the maximum valve travel. This effect is illustrated by Fig. 36. A valve land uncovering circular ports gives a valve characteristic similar to the solid curves of Fig. 36 (c) . A land uncovering an inverted circle will give a characteristic similar to the dotted curves. The effective gain given by the dotted curves is less than that of the solid curves yet the maximum force and the maximum valve travel are the same in both cases.

6. Conclusions

From the experience of studying and designing a power-controlled elevon system, the following conclusions are offered:

1. The type and details of the control system will be determined by the aerodynamic performance required and by the structural limitations of the airplane.

2. A system that requires high velocities of the surface for a short time can be powered most effectively by an hydraulic system with accumulators for energy storage.

3. The control system can be stabilized by sufficiently reducing the gain. Reducing the gain implies increasing the maximum error. It is felt that the system will be more flexible for future development if a stabilizing network is added. Also, the stabilizing network will help to minimize the effects of extraneous motions that will be present in the airplane.

4. The linear type of system analysis is useful for a qualitative survey of the problem and for synthesis techniques. It helps to show immediately the important factors in stability, i.e., which parameters can most effectively be

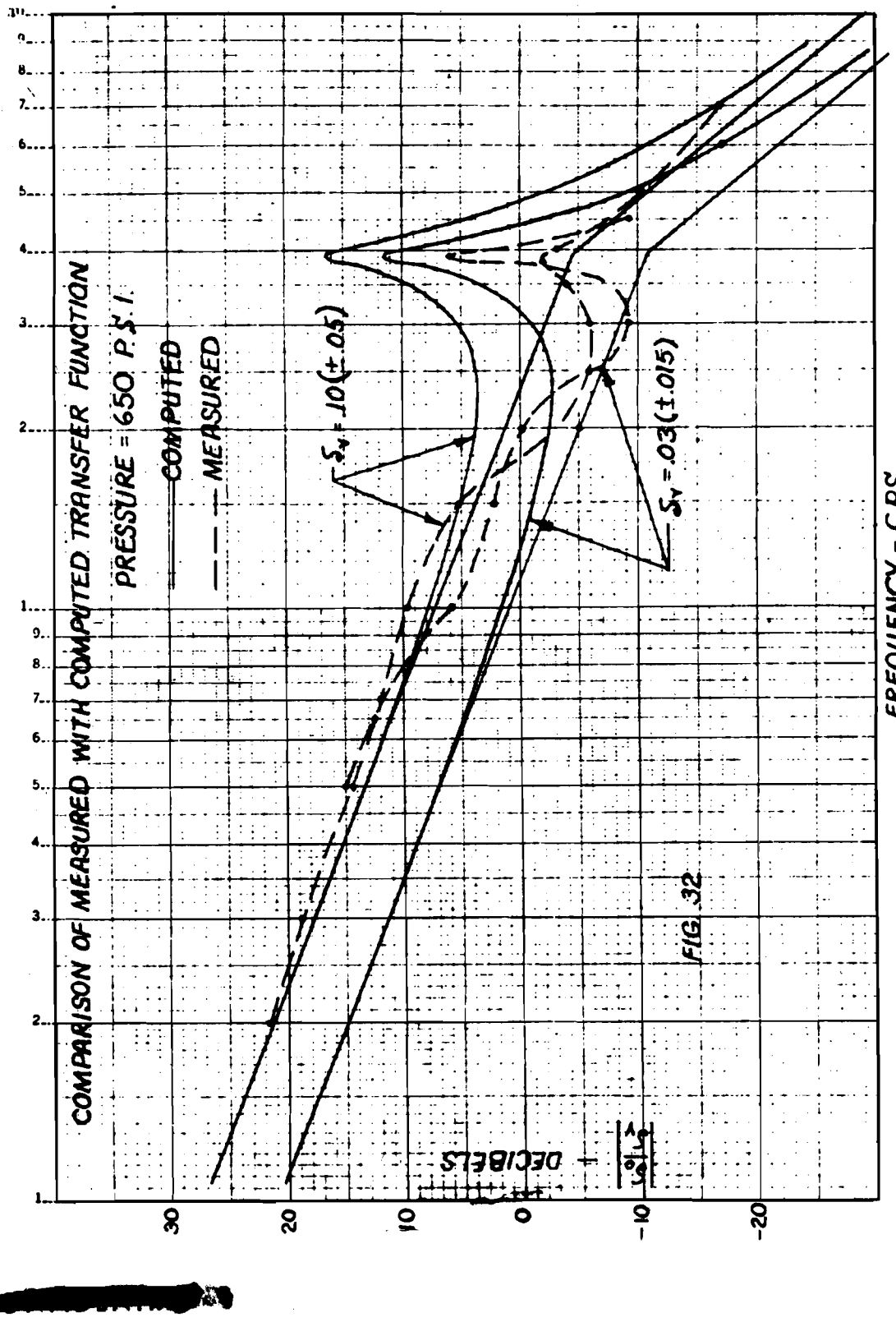
COMPARISON OF MEASURED WITH COMPUTED TRANSFER FUNCTION
PRESSURE = 650 P.S.I.
COMPUTED
MEASURED
$S_v = .10(\pm .05)$
$S_v = .03(\pm .015)$
FIG. 32
DECIBELS
$\frac{e_o}{e_i}$
FREQUENCY - C.P.S.
30
20
10
0
-10
-20

Fig. 32

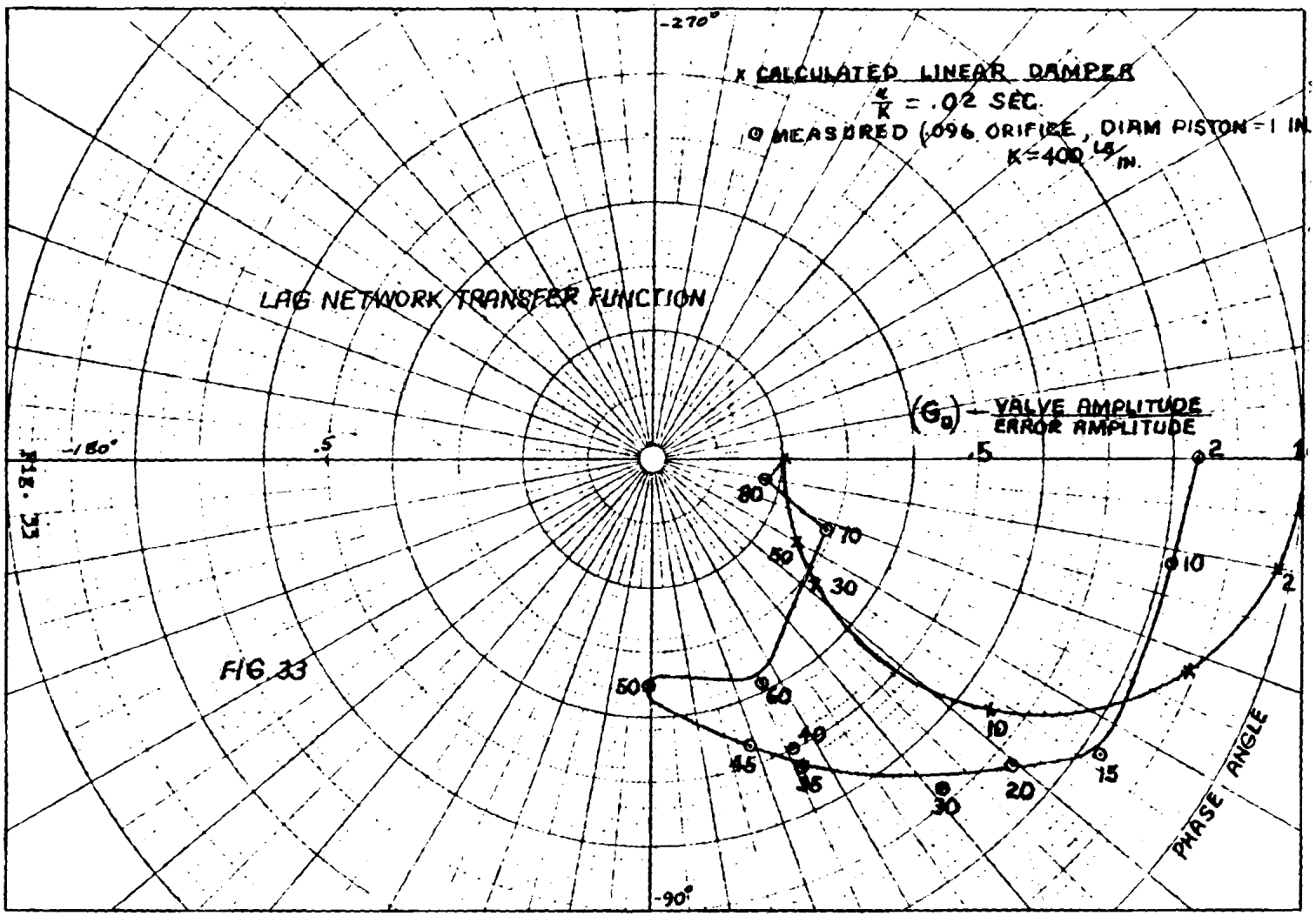
-270°
X CALCULATED LINEAR DAMPER
$\frac{a}{K}$ = .02 SEC.
O MEASURED (.096 ORIFICE, DIAM PISTON = 1 IN.
K = 400 LB/IN.
LAG NETWORK TRANSFER FUNCTION
(G_0) = VALVE AMPLITUDE / ERROR AMPLITUDE
-180°
.5
.5
2
1
80
70
60
30
10
2
50
60
40
45
35
30
20
15
PHASE ANGLE
-90°
FIG 33

Fig. 33

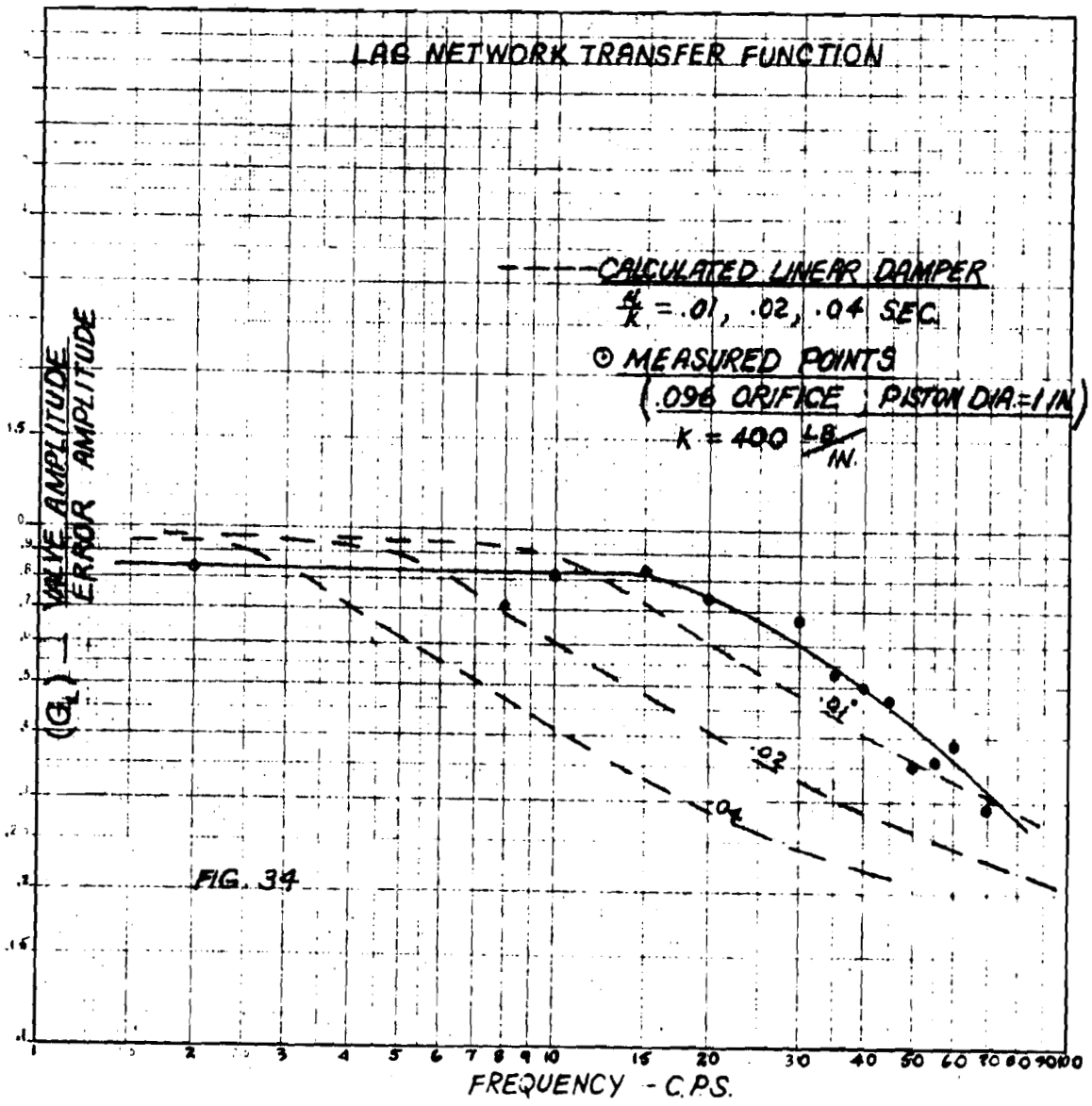
LAG NETWORK TRANSFER FUNCTION
CALCULATED LINEAR DAMPER
$\frac{d}{k}$ = .01, .02, .04 SEC.
⊙ MEASURED POINTS
(.096 ORIFICE ; PISTON DIA.=1 IN.)
K = 400 LB/IN.
VALVE AMPLITUDE / ERROR AMPLITUDE
(G_L)
.01
.02
.04
1.5
1
.9
.8
.7
.6
.5
.4
.3
.2
.15
.1
1
2
3
4
5
6
7
8
9
10
15
20
30
40
50
60
70
80
90
100
FREQUENCY - C.P.S.

FIG. 34

Fig. 34

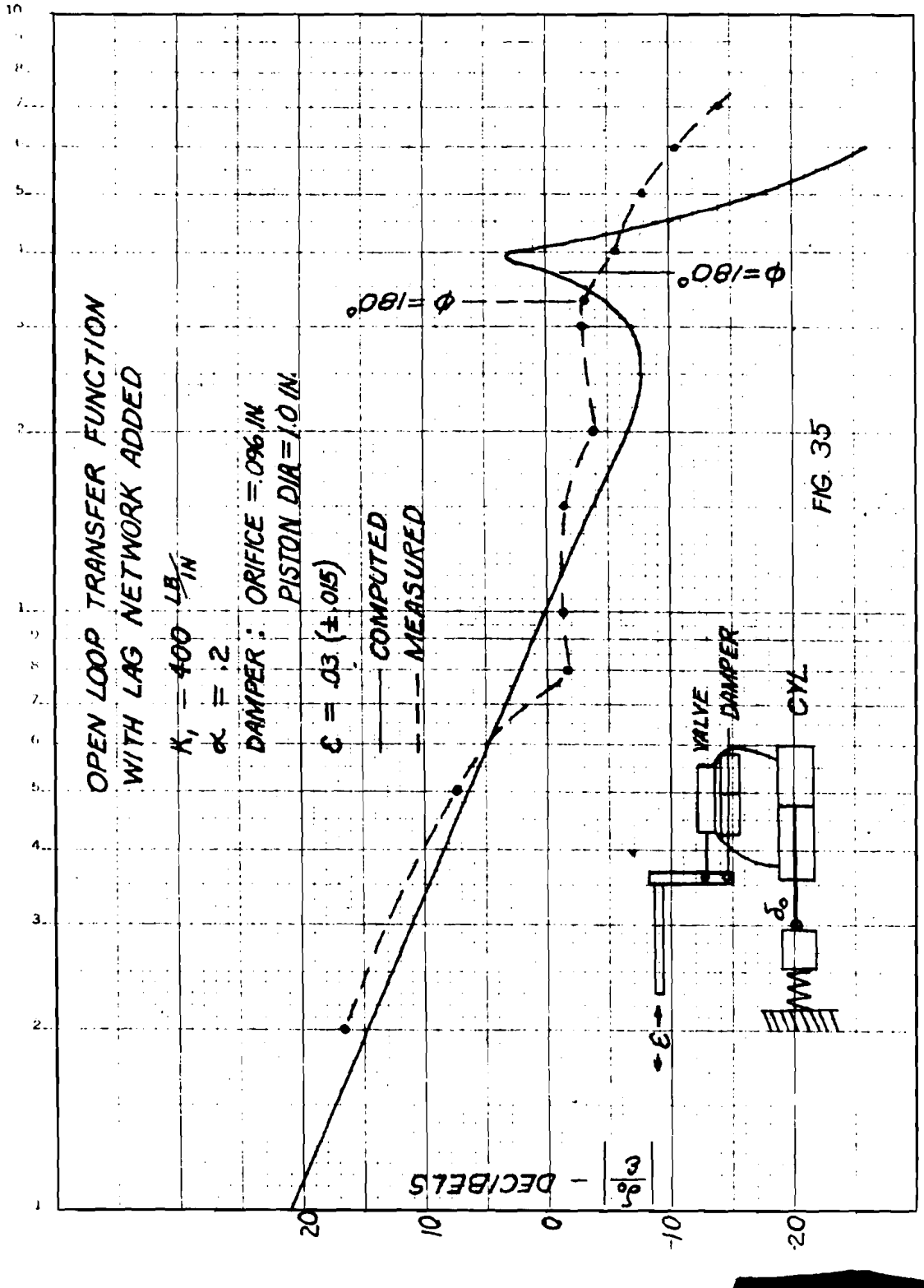
OPEN LOOP TRANSFER FUNCTION
WITH LAG NETWORK ADDED
$K_1 = 400$ LB/IN
$\alpha = .2$
DAMPER : ORIFICE = .096 IN
PISTON DIA = 1.0 IN.
$\zeta = .03$ (±.015)
— COMPUTED
- - - MEASURED
-180° = φ
-180° = φ
DECIBELS - $\frac{\delta_3}{\delta_0}$
FREQUENCY - C.P.S
20
10
0
-10
-20
VALVE
DAMPER
CYL
δ_3
δ_0

FIG. 35

Fig. 35

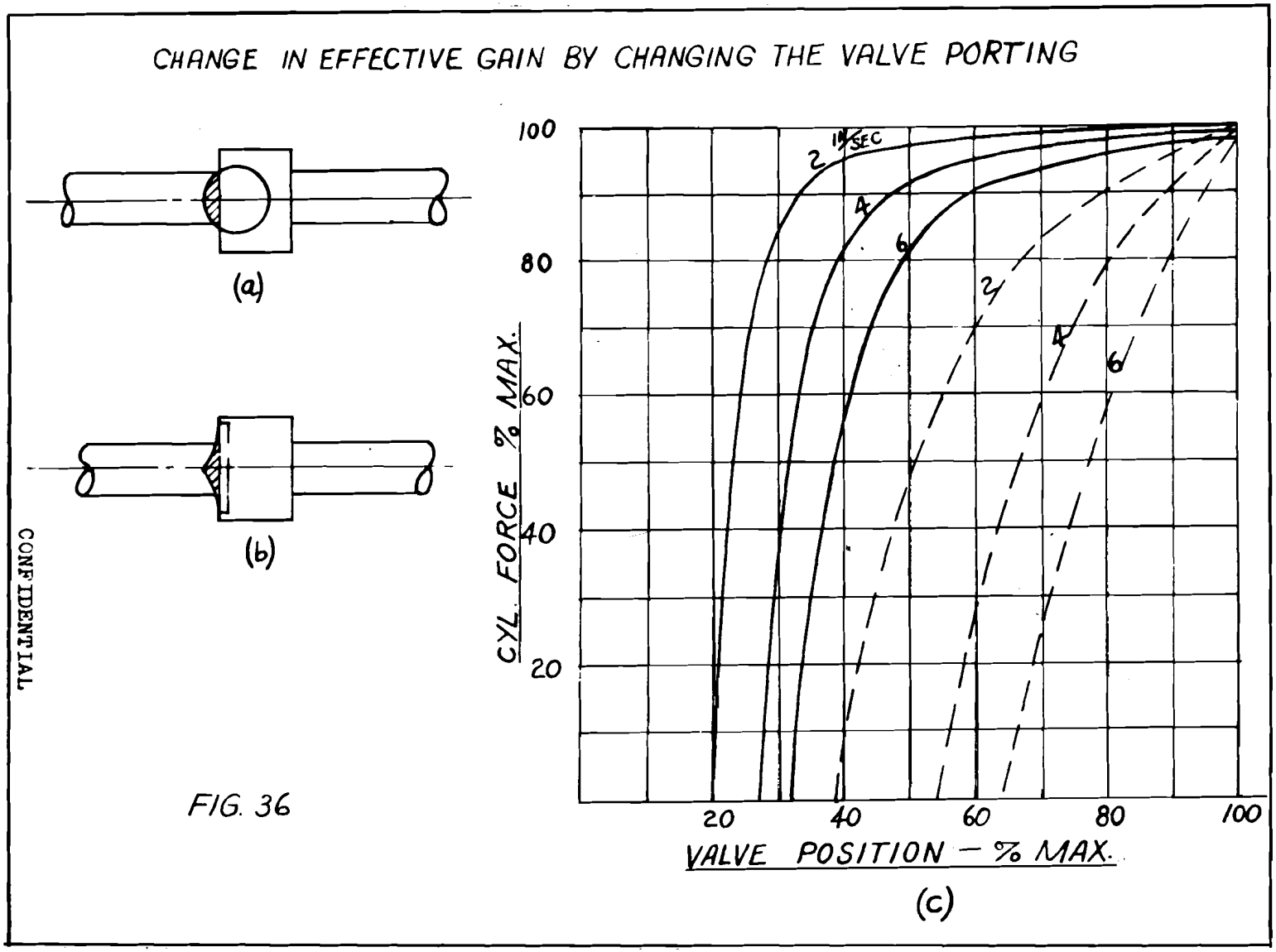

Fig. 36

manipulated. However, a detailed knowledge of the system and final adjustments will have to be found by testing the final system. Secondary factors which may present serious problems in any airplane installation are

a. Structural feedback - force feedback due to deflection of cylinder relative to control linkage.

b. Resonance of control linkages.

c. Signals to the cylinder from wing deflection due to airload.

7. *Recommendations for Future Development of Hydraulic Servomechanisms*

It is evident that increasing use of powered-control systems will be made for aircraft in the future. The requirements of high peak powers and short time responsees point toward hydraulic or pneumatic power systems. The trend toward more completely automatic controls for such applications as flying by radar and stabilization by gyro control suggests the development of electrical control of the power. It is felt that research and development effort for power-control systems can most effectively be spent on the following:

1. Gyro pickups. There is a need for the development of gyros with fast time responses.

2. Hydraulic valves. First there is a need for reliable electrically operated valves that can control high powers with small time lags. There is also a need for force proportional valves. In general, valve development should be toward the controlling of large powers with small forces, i.e., large power amplification.

3. Non-Linear Analysis. Dynamic stability of the control system is perhaps the most important design problem. Hydraulic and pneumatic systems are decidedly non-linear and are not always amenable to linear analysis. One way to attack the non-linear stability problem would be to compile a series of particular solutions of typical circuits by use of a differential analyzer. Another might be to develop reliable methods of linearizing the equations of motion. Such methods would have to be confirmed by testing many different systems.

8. *References*

1. Brown, G. S., and Campbell, D. P., Principles of Servomechanisms, John Wiley and Sons, New York, 1948.

2. Hall, A. C., The Analysis and Synthesis of Linear Servomechanisms, The Technology Press, Massachusetts Institute of Technology, 1943.

DISCUSSION

MR. FOLSE, BuAer: *In order to keep the parameters of the lag network from shifting with change of viscocity, you will have to have a compensatory device in the piston in the form, for instance, of an orifice which will close as the temperature of the oil increased to keep the dashpot traveling constant.*

DR. CLAUSER: *I think there are two things that influence that and I was glad to read in somebody's paper that they had been down to minus 70 and the system was still warm. True when you cool the system, it is liable to become sluggish. Another thing that is very important here now is if you use the flow across an orifice, the pressure drop through the orifice to the first approximation is dependent upon the density and not the viscosity. That means it is desirable to design a sharp-edge orifice across this piston. It has to be sharp-edged because there can't be any surface for the flow to flow over because that becomes viscous flow, you see, and then that is dependent upon the viscosity and not the density. Are you familiar with the way rotameters work? They are independent of temperature. They didn't get that effect until they went to the so-called sharp-edged orifice. Specifically, the rotameter has very little area for the flow to flow by to develop viscous friction. The pressure drop across the orifice is dependent almost entirely on one-half V squared and not on viscosity at all.*

DR. WILSON, Goodyear: *All oleo struts work this way and they are independent of temperature to a large extent.*

MR. AHRENDT, Ahrendt Instrument Company: *In your paper you discussed at considerable length the problem of stability of this system and what you should do to make the system stable, but surely you must have had other performance requirements that affected the choice of parameters in this system. You must have had dynamic performance requirements that suggested what those spring constants should be and what frequency the corners would be, and so on. I wondered where those originated and what they were. The problem certainly can't be one of just getting stability.*

CLAUSER: *No. For example, I mentioned the gain was determined by one of the specification requirements, meaning that .05 of a second lag. That means we wanted to keep the lag up at very low frequency, because with frequencies we are talking about, response to three or four cycles per second, you have to throw the surface at the rate of 50 degrees per second. We showed that there may be conditiins to make it want to go faster than that but you are working with fairly low frequencies.*

AHRENDT: *Are all your performance requirements at very low frequencies?*

CLAUSER: *The thing that suggested this lag network in the first place was that we wanted to cut out all the high frequencies that might interfere with the flutter frequencies. It was suggested a little bit later. Some of the people who were doing the analysis were also familiar with flutter theory, you see, and they were worried about this, so even before we suspected we weren't going to have a stable system we talked about using lag networks.*

[redacted]

MR. HARRIS, Chance-Vought: *I thought that comment you made about that apparent zero in the curve suggested that perhaps somebody would have an answer to why your curve dipped. It is very interesting, because we had almost the same frequency.*

CLAUSER: *Does anyone have any ideas?*

MR. MONROE, North American: *I had a thought that it might be the change from viscous to turbulent flow at that particular frequency, since it is somewhat correlated with velocity. A problem is what to do when you are in a transition region, whether you use turbulent flow characteristics or viscous, so it might be well to look into it from that viewpoint.*

CLAUSER: *I might mention a little bit about some of the things we have thought about that. First, every time you change, you have a slope change by 6 db. If I say any of this wrong, somebody correct me. You'll change by 6 db and if you have the type of thing we had, the asumptotes would look something like that. (indicating) We were up here and as far as we can we could go, we were right down here. This means there was a dip. That means there must have been an asymptotes. There must have been something that kicked it back so that it went through this dip here and came on back again so to bring it back. This means a factor in the numerator to do that, and since this A factor is in the denominator, it may mean that there may have to be two factors.*

HARRIS: *I am not sure whether this is the same thing or not but I would like to show one of the plots that might throw some light on it. This is the same plot you had without any damping in it. If you change that polar plot to either this one or this one to start with, it will come down to zero, and would come out again, which is the same characteristic you have here. The only thing that brings that in is this term which is the natural frequency, made by the mass or the structural stiffness, and if that goes to infinity, this disappears and this curve comes down like that. I would like to suggest that there is quite an analogy between your hydraulic damping device and the tool which electrical engineers use in notching effect and I believe the similarity in those two points to the notching effect of your damper where your damper actually becomes ineffective and then your system takes over after that. An electrical filter network will act exactly the same way.*

CLAUSER: *Yes, that is right and that is one thing I want to emphasize. It is very similar. You are trying to filter out the high frequency effects, and they get a notching effect exactly like that. If you have a system which is a very high response system and you get into structural disturbances, you want to cut your system off so you would put an electrical filter in there to cut off, and you can't have a true cut-off. All you hope to get is a notching effect and that bears a resemblance to that.*

MR. RAHN, Boeing: *I would like to ask a question on the double spring. Why did you use two springs? Why not just one--one between the valve and the damper?*

[redacted]

[redacted]

CLAUSER: *I think the reason we used it was to give a reasonable frequency response characteristic. You can't say you don't care about any of the high frequencies. Essentially, we'll plot attenuation, we 'll say, as a function of frequency. You would like to have some left, you see, some attenuation in here and then as you go out in frequency, you would like to cut it down and this becomes asymptotic, depending upon that second spring and it is just a matter of being able to shape this curve so you will get the response in this region.*

MR. MONROE: *I might add one remark to this, and that is that we put this device on the valves. On one occasion we had an opportunity to go to an airplane without much theoretical calculations to try something. We had an idea of the transfer function, the type it was, so we decided the most logical solution would be a lag network. We added that in the form of a dashpot through a control linkage to the valve. It did stabilize the airplane immediately. We didn't have an opportunity to make any calculatiins, so we had three different size orifices and two springs to try, and it had other bad effects so we didn't continue with it.*

[redacted]

APPLICATIONS OF THE ANALOG COMPUTER TO CONTROL SYSTEM DESIGN

By

R. R. Wilson

Goodyear Aircraft Company, Akron, Ohio

I am primarily a guided missile man. I have never had anything to do with inhabited aircraft, and I am not really an aeronautical engineer or anything remotely resembling that. I have a lot of aeronautical engineers doing that sort of work while I sit by. I have been sitting here for the last few days learning a great deal about the way you people operate and I want to say that I admire what you have done. It is a bit of an eye opener to me.

In talking about the computers I thought we might try first to see the way in which they fit into the overall scheme of things; second, to take a look at the computers themselves, to see how they work; and, third, to talk about the specific applications to the power boost problem. As has been brought out here in this meeting, power boost design, as is the case with most engineering design, has gone through a good many stages and is still in most of those stages.

Some of you, doing the work still based entirely on your engineering intuition, good common sense and cut-and-try methods, are apparently turning out perfectly satisfactory devices and since the proof of the pudding is in the eating, I don't see that anyone can really complain about that. Others of you, either because you have developed an interest in it or because you have hired some men who got started in that field, are going into the frequency response analysis method, which really amounts to just applying the general field of mathematics to your engineering design; and you will find as you do in other engineering fields that as long as you can stick to linear differential equations, everything is rosy. As soon as you get into non-linear differential equations, you begin to have trouble, and you use the usual methods that mathematicians use when they solve non-linear differential equations. You are using small perturbation theory and so tacitly assuming that everything is linear, or you are using series solutions and again in a way operating on small perturbation theory, using probably step-by-step calculations in which you again assume that your system is linear and change the initial conditions and boundary conditions at each step. Probably some of you are even using graphical methods. All those methods apply to the solution, by hand, of non-linear differential equations. Occasionally, it is true that you find an equation that you can solve directly without the use of these various approximate methods, but that is uncommon.

Now, the first thing that an engineer who wants to analyze his device--instead of just building it and then fixing it until it works--when he runs up against a non-linear mathematics and finds he can't get a nice clean analytical solution, is to begin to think about models.

In the aerodynamics field, of course, they went into the wind tunnels and built models and they ran up against the principle of similitude. They found out that the wind tunnel tests didn't quite check the actual airplane performance and so we have pressurized wind tunnels and we have full-scale wind tunnels and so forth. As we get

up to higher and higher speeds we still have plenty of trouble, because you can't do all the things you want to do in the wind tunnel.

In other engineering fields one of the modern methods has been the use of electric analogs or mechanical analogs or hydraulic analogs, depending on what system you are working on, and what system you want to change to. Sometimes I find it is more convenient if you are working in electricity to try to work with the mechanical analog and vice versa.

But what are you to start with? And what is the final result of such developments? We have electrical analog computers which are really just network analyzers. In operation, one decides what the electric analogs of a mechanical system are and sets them into the network analyzer, puts in as an input function what ever form he wants to put in, and get the answer as a voltage.

There are some difficulties involved. Time scales give trouble; leakages give trouble; drifts give trouble, and there are some other troubles in that all that you can substitute for a mechanical mass is an inductance. You can't have a pure inductance. You have to have some resistance connected with it. Those troubles are inherent in electric analog computers. They are, however, reasonably satisfactory. There are several of them operating now.

The next type of analog computer is the true differential analyzer and there are two varieties--possibly more than that, but two varieties of differential analyzers--that are well known. One is the mechanical analyzer of which the Bush analyzer at MIT is perhaps the most famous example, but not by any means the first. There have been differential analyzers for a great many years.

Mechanical differential analyzers basically use a variable speed drive for the integrator. One has a disc which rotates, and a wheel resting on the disc--this is not true in all cases, but we'll call it a wheel which slides on a splined shaft in and out along the radius. The function that one gets out then is the rotation of the splined shaft on which the wheel slides as it turns. It is a function of the speed of the disc and of the radial position of the wheel, and so one comes out with the integral of the radius times--well, let's make it ωdt--if this is run with a constant speed.

If, let us say, the disc is turned through an angle θ, then the wheel turns through $KR\theta$. So this is an integrator which is very flexible and very useful. You can turn it around and use it as a differentiator. You can use it without any auxiliary equipment to generate a great many functions such as squares, sines, cosines, tangents, and so forth and so on.

You can couple it with various kinds of mechanical devices such as differentials and ordinary gear trains and so forth. You can set up differential equations with derivatives with respect to time or with respect to any other variable so it is a very useful device. It is capable of high accuracy and the only drawback to it is that it is also very expensive, as any accurate piece of mechanical equipment is, and it takes up a considerable amount of space, but it has some advantages that other computers do not have, such as rate of drift, for example. It stays where it is put. Its speed of response is low. This may be overcome by changing the time base of the problem.

The other type of differential analyzer which is more common and less expensive, as well as somewhat more convenient to operate, is the electronic analog computer, which uses as the basis of its operation a feedback amplifier. In Figure 1 we have

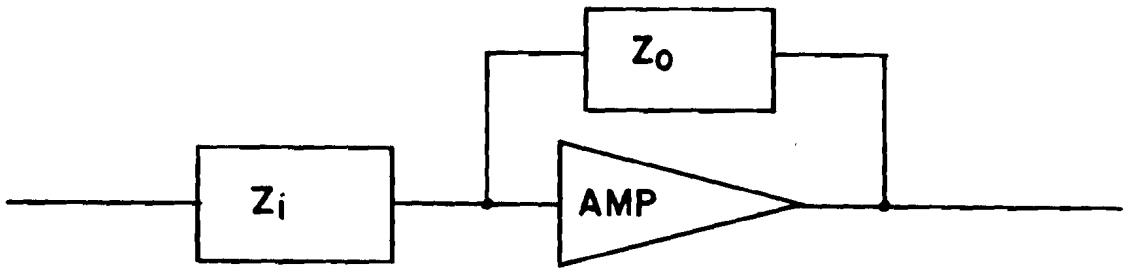

Fig. 1 - Generalized computer circuit.

a signal feeding into an amplifier through an impedance, Z_i, and from the output of that amplifier we bring a feedback, Z_o, back to the input. Our amplifier has a high gain, and also reverses the sign at the output; then, the voltage between the input and ground is going to be essentially zero, because the gain of the amplifier as in any servo network reduces the error to as nearly zero as possible. We have an input voltage across Z_i and an output voltage across Z_o, and because the voltage at the amplifier input is essentially zero, the currents passing through, though the two impedances are equal and so we can set up an equation:

$$\frac{E_i}{Z_i} = \frac{E_o}{Z_o}$$

and we can set up our equation then:

$$\frac{E_o}{E_i} = \frac{Z_o}{Z_i}$$

This the basis of the operation of the electronic differential analyzer. What happens if we put a resistor at the input and a condensee in the feedback is that

$$\frac{E_o}{Z_i} = \frac{1}{sRC}$$

where s is the differential operator, derivative with respect to time. This is an electronic integrator. If we reverse these two impedances, put the condenser in the input and the resistor in the output, then we come out with sRC and this is then a differentiator. And if we use only resistors in these points, this is then a simple scale changer. If these have different values or if these are both equal, let us say equal to unity, then it simply changes the sign from positive to negative. Several inputs can be fed into one amplifier which then acts as a summer.

So we have basically in a linear electronic analyzer integrators, differentiators, sign changers and scale changers and any combination of resistors that we want. We could, for example, feed out of our amplifier into a potentiometer and so again change the scale at that point. That is found to be very convenient at times for changing parameters in a problem.

A typical differential analyzer--I am not advertising Goodyear Aircraft computers here although my boss thinks that I should--a typical differential analyzer has a jackboard of some sort on which are generally mounted condensers of whatever size is chosen as unit, which in the Goodyear computer is one microfarad, and arrangements to couple these condensers and plug-in resistors into the amplifiers in whatever way one wants. On the front of this particular computer are a row of dials which represent the potentiometers I was talking about, so that parameters can be varied or the equations can be varied fairly simply by either plugging something different in or changing a jack cord or by turning the dials.

Initial conditions are set in by charging the condensers to voltages representing the desired conditions. The function to drive the whole network can be put in either as a step function or as a rate or as a sine function or anything else one chooses. Usually any of the values that you are interested in can be taken out at appropriate points and I will show you some typical examples shortly, so we can see how that works.

These are the devices used by a linear computer. The linear computer is capable of taking account of a great deal of non-linearity without being actually a non-linear computer. For example, it is very easy if you have a servo which has a definite limiting top speed, which is always the case, to represent the servo by the proper equations and exactly limiting the rate of the simulated servo in the machine itself. It is fairly simple to simulate a servo on a linear computer; for example, a relay servo is about as non-linear as anything one can think of, yet it is quite simple to put into a simulated relay servo, the dead space which all relay servos have. A good many of the characteristics of your devices which are essentially non-linear can be simulated with a typical linear computer.

When we come to non-linearities which are more fundamental, such as parameters which vary with, let us say, velocity, or vary with time or vary with deflection, it is necessary to go to the true non-linear computer. The difference there is largely that one then has a servo system, which takes the variable with which one is dealing, such as the velocity, and let us say, perhaps we want the drag as a function of velocity squared. The servo amplifier takes the velocity and drives a potentiometer with the servo motor to change the parameter representing the drag, as a function of the velocity squared. One could have a square law potentiometer or two potentiometers in cascade, buffering in between, so that one didn't load up the first potentiometer. We do the same thing with our own computer, having put together a few standard parts to come out with a perfectly satisfactory parameter changer, which is actually a servo multiplier.

The true servo multiplier is a little more convenient than that, although not very different in operation. Suppose we have: $\ddot{x} + x\dot{x} = F$. Now, the $x\dot{x}$ term is the non-linear factor and we can take care of that by feeding x and $\dot{x}$ to our servo multiplier and coming out with a product. If we have enough amplifiers and enough multipliers, we can solve practically all of the non-linear differential equations that one can set up. Having enough amplifiers and servo multipliers sometimes is a troublesome feature, but we find that as out analysts work with the equipment, they become more and more ingenious at finding tricks to use fewer and fewer amplifiers so that we can get more and more done with one piece of equipment. There is a limit however.

In addition to the servo multipliers, one other piece of equipment which is standard on the non-linear computers is the function generator and that can be of two

forms: the function generator, which generates a specific function such as sine, exponential, cosine and so forth, or one that generates a perfectly arbitrary function; that is, you choose your function, and set it in, and the function generator then reproduces it. Most computers are equipped with both types of function generators.

Having all this equipment, one is in a position to start analyzing a system with a computer. Unfortunately, the computer is just like a slide rule. If the wrong person picks it up, it won't do any problem solving for him because he doesn't know how to run the slides, and the same thing is true with the computer. In spite of all the advertising that analog computers have gotten recently, a high school girl can't tackle an analog problem alone because it takes somebody first to set up a differential equation. Once one has the differential equations, a high school girl can set up the computer problem and get the answers. It takes us about three months to train a girl to the point where she is quite adept with the computer and I am sure that other computing companies are finding exactly the same thing to be true.

Now, to indicate something about how one might set a problem up on the computer. I have prepared a few figures here and I would like to go through those showing about what the setup procedure is.

A mass-spring-damper setup, with the differential equation of which you are all familiar, is represented in Figure 2a.

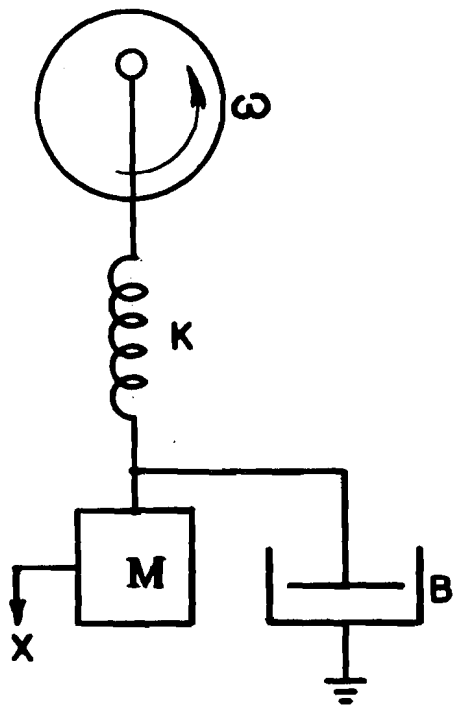

Fig. 2a - Simplified dynamic system.

Now, for purposes of accuracy and the convenience of the computer, we try never to use a differentiator because, as you probably know, when noise is differentiated, it becomes much worse. When noise is integrated, it is reduced. So whenever we possibly can, we solve the equation for the highest order derivative and then integrate it until we come out with the final variable.

In Figure 2b we have two integrators which give us $-\dot{x}$ and x, respectively. Since $\ddot{x} = \frac{-B\dot{x}}{M} - \frac{Kx}{M} + A\sin\omega t$ we sum all these values as shown here to give $\ddot{x}$. This is the summing amplifier which adds them all together. We take x, which we want, and we multiply it by K over M, the feedback impedance being $1/M$ and the input impedance $1/K$. We take $\dot{x}$ and instead of adding it directly, we have to change the sign, which is minus, and so we bring it through a sign changer, and at the same time we multiply it by B/M. We are adding in here also $A\ Sin\ \omega t$ and coming out with the sum of all three, to get $\ddot{x}$. In order to find out what x is going to do, then, we drive the system with a sine generator, giving the amplitude desired, and we can read off the values without any difficulty: x, $\dot{x}$, and $\ddot{x}$, which are in this case, all of the quantities that we might want.

Now, if we happened to have limits on the system, so that it would only go so far before it banged against stops, we could at the proper point put in an electronic limiter, which just consists of a biased diode, so that to limit x, the voltage cannot increase further, and so we would then get the results desired of the problem, showing what happens when one has an oscillating system which can bang against stops if it is driven too hard.

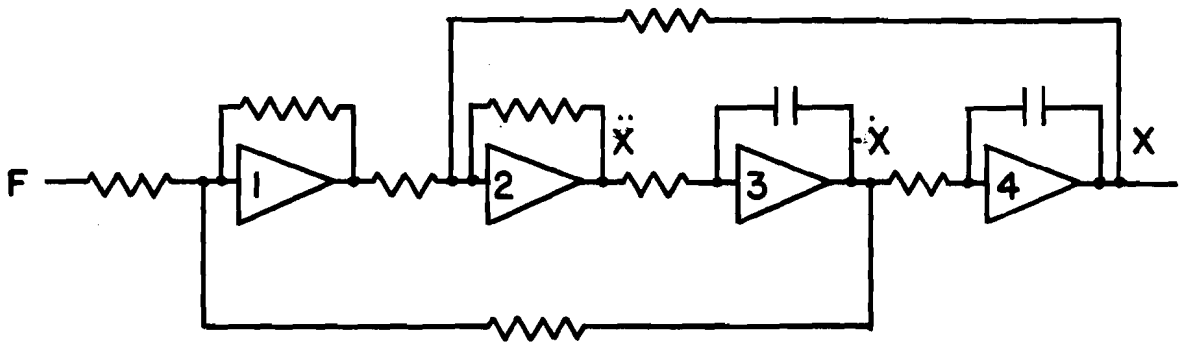

Fig. 2b - Computer analog of dynamic system.

In Figure 3 is a boost system, which I have simplified somewhat, so it is a little hard to see. This is the pivot here, so that this is a true boost system without feel--this is not a power system--this is a power boost system. And over here (indicating) we have a rudder pedal and a spring and the various coupling systems. The valve is up here and the cylinder is at this point.

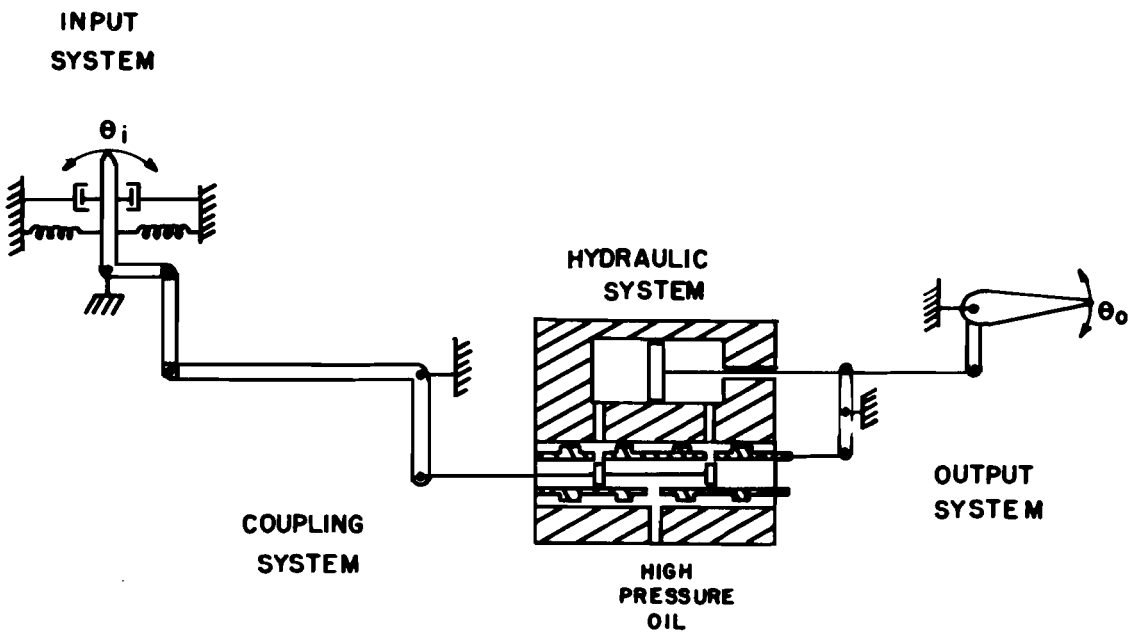

Fig. 3 - Rudder boost system.

These are the four equations which specify the complete kinetic performance of the system and, as I did in the previous problem, I have solved each one of these for the highest derivative.

(1) $$\ddot{\theta}_i = \frac{T_i}{I_i} - \frac{A_i}{I_i}\dot{\theta}_i - \frac{K_i}{I_i}\theta_i - \frac{A_2}{I_i}\dot{\theta}_2 + \frac{A_3}{I_i}\dot{x}_s$$

(2) $$\ddot{\theta}_o = \frac{C_2}{I_o}\dot{\theta}_2 + \frac{K_2}{I_o}\theta_2 - \frac{C_2}{I_o}\theta_o - \frac{A_4}{I_o}\theta_o$$

(3) $$\dot{X}_s = \frac{A_5}{C_s G_{p_2}}\dot{\theta}_i + \frac{A_6}{C_s G_{p_2}}\dot{\theta}_2 + \frac{K_2}{C_s G_{p_2}}\theta_2 - \frac{C_2}{C_s G_{p_2}}\dot{\theta}_o - \frac{K_2}{C_s G_{p_2}}\theta_o$$

(4) $$\ddot{\theta} = \frac{\ddot{X}_s + A_8 \dot{X}_s}{G_{p_2}} - \frac{G_{p_i}}{G_{p_2}}\ddot{\theta}_i - \frac{A_9}{G_{p_2}}\theta_i - \frac{A_{10}}{G_{p_2}}\theta_2$$

Now, this is a case in which you can't do everything just as you want to, and in equation (4) we have an $\ddot{x}$, which is not quite what we would like to have, because we can only solve for $\dot{x}$ in equation (3).

Figure 4 represents the system as it is set up. I am sorry that we can't refer back and forth to the equations conveniently, but we start out here with one equation. We start out with $\ddot{\theta}_o$. We start out the second equation with $\ddot{\theta}_i$ and we start out the third equation with $\ddot{\theta}_i$, and the last equation with $\ddot{\theta}_Z$, and at the proper points we take off θ_o and we bring that down to add it into a summing amplifier here to get $\dot{x}$ and we pick off $\dot{\theta}_i$ at this point and add it in here, and so forth through the whole problem. It is really just a simple proposition of taking your equation and adding terms through amplifiers integrating where you have to, to get what you want, and coupling the whole thing to solve simultaneously. In this case, we were interested in seeing how you could get the stick feel. This is a proposition of having a forced feel back through the system, as you saw, because the pivot and the cylinder are off-center and so we take out the various required functions, θ_i and $\dot{x}_g$, and $\dot{\theta}_2$ here, and sum them up, and at this point we get an electric signal which is proportional to the stick feels. We can then drive a servo mechanism with that. This is not very clear because we don't know what $\dot{\theta}$ and θ_i and $\dot{x}$ and so forth are. I think Mr. Harris does since this is his device.

Figure 5 shows an airplane in aerodynamic flight. This is the lateral part of the problem. Here we have the aileron deflection and here we have the rudder deflection going into this amplifier and I don't know what the rest of these gadgets represent. This represents the GA-2 Goodyear Aircraft amphibian which we set up with a mock-up cockpit, so the pilot could actually fly it. We put in the aileron and rudder deflections as voltages, which came from an actual rudder bar, and stick deflections. Then we brought out flight information to cross-pointer meters so one could see what was happening to the airplane. It was a crude affair, but actually the pilot thought it was quite realistic. He flew the airplane and we changed parameters by changing these potentiometers that are shown here. We could change the control power and we could change the damping, and so when we got through, between the pilot and the designer of the aircraft and us with the computer, we had decided pretty well how we wanted the controls set up, so it would be easy for a pilot to fly.

Well, these are some applications of analog computers. As you can see, I have made it sound very easy to operate them and it actually is pretty easy. You have some trouble; sometimes the answers don't come out right, and then you have to find out what is wrong, and that takes our people some time. Occasionally the computer is right and they think it is wrong and then they have more trouble than ever because they can't find any mistake. So sometimes they have to calculate the answer out in longhand to convince themselves that the computer is right.

Well, now the next question is how the computer fits into your particular scheme of things. No. 1: If you are using the frequency response system and you get your differential equations set up, you don't need to calculate the frequency response. Set it up on the computer, drive the system at various frequencies and out comes your frequency response. If the system isn't right and you want to change it and get it to be what you want it to be, turn some dials and run it through again and keep turning dials until it comes out right. Some of the dials you might have to label "do not touch" at the start because you know that you can't physically change the

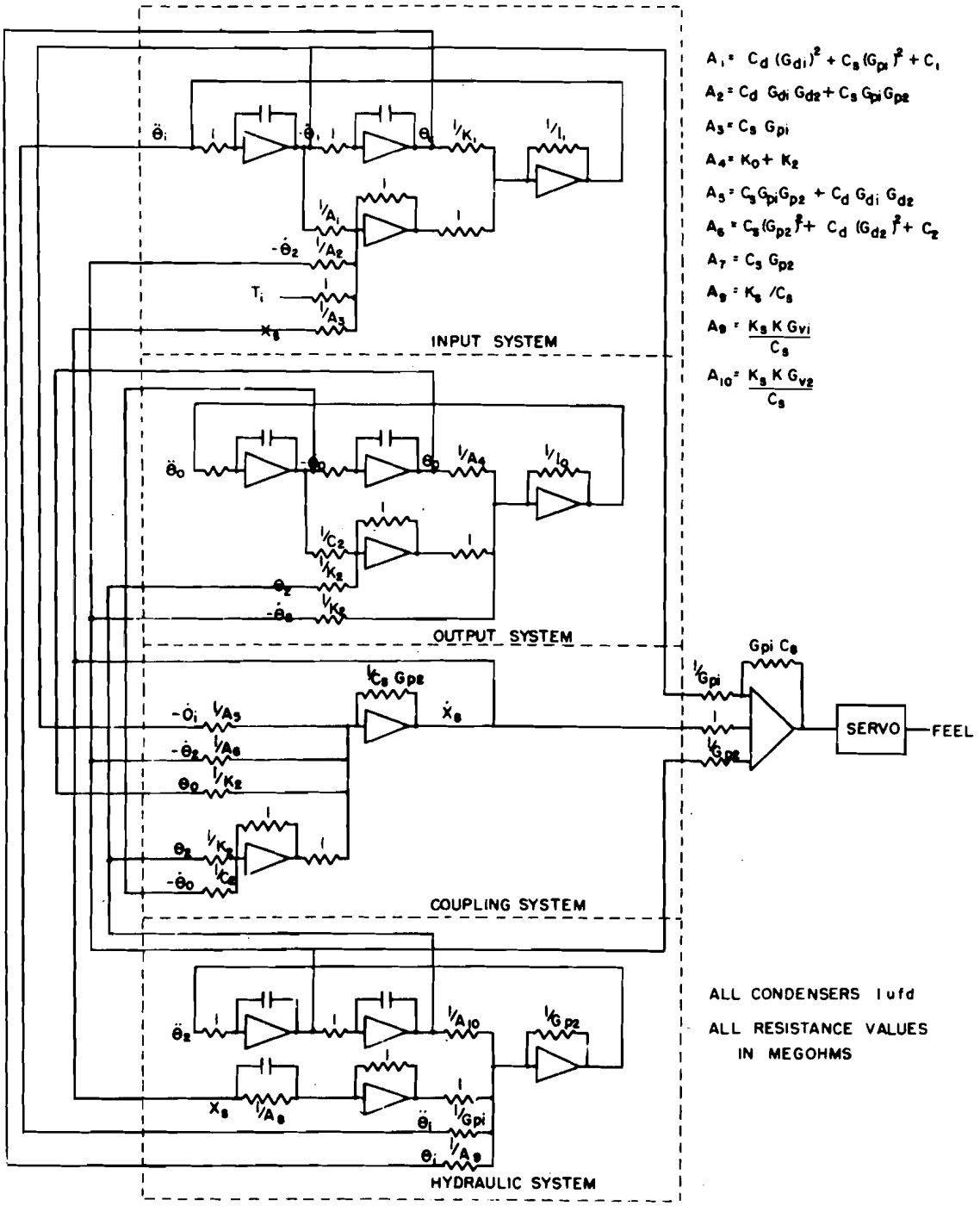

$A_1 = C_d (G_{di})^2 + C_s (G_{pi})^2 + C_1$

$A_2 = C_d G_{di} G_{dz} + C_s G_{pi} G_{pz}$

$A_3 = C_s G_{pi}$

$A_4 = K_o + K_z$

$A_5 = C_s G_{pi} G_{pz} + C_d G_{di} G_{dz}$

$A_6 = C_s (G_{pz})^2 + C_d (G_{dz})^2 + C_z$

$A_7 = C_s G_{pz}$

$A_8 = K_s / C_s$

$A_9 = \frac{K_s K G_{vi}}{C_s}$

$A_{10} = \frac{K_s K G_{vz}}{C_s}$

Fig. 4 - Rudder boost system simulation.

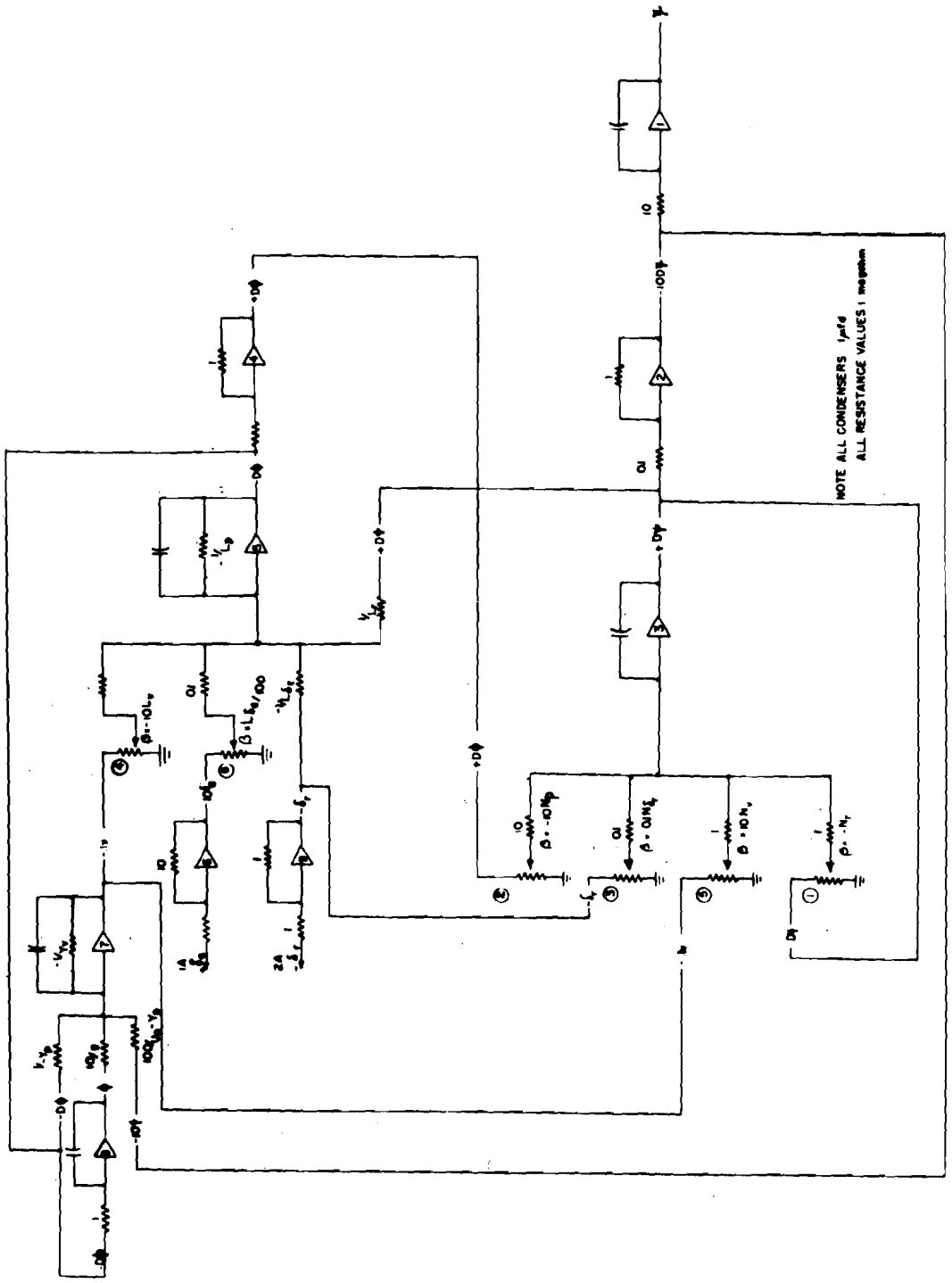

Fig. 5 - Schematic wiring diagram for lateral dynamic equations of motion.

corresponding parameters. Others you will be able to change and so you change those and when you get through, you read off the values and see whether you can physically change them that much and so make your compromises just as you do now, but the point is that when you get through, without ever having built your system, you will know what you are going to have to require of your system in order to get the response that you want.

If you have non-linear elements in your system, as all of you do now, you have a choice. You can take the linear computer and you can use limiters in some cases to change the slopes of some of your functions. Or you can build some parameter changers, or you can operate by step-by-step calculations, if you want to. The latter on the differential analyzer is fairly simple, because you can stop your problem whenever you want to, so if you want to run your problem over a small range and change your parameters and run it over another small range and change your parameters, you run it until your deflection gets to the value which you have decided will be the first increment, stop your problem set in the new conditions and so forth. A step-by-step calculation then is very simple and rapid.

If you can afford a non-linear computer, which is usually not much more expensive than the linear computer, then you can set your non-linearities in directly, either in the multipliers as squared functions or cubed functions, or, if they are purely arbitrary functions, you can set them up on function generators and get your answers out in that way. So that is point number one.

You can design your device entirely on the electronic computer. Now, this assumes that you know what you can get in your hydraulic devices. Presumably you will know how to produce it or a close approximation of it.

No. 2: The analog computer cannot only simulate your device but it can also simulate the airplane, as you fly it, either on the ground or in flight--anyway you want. For example, in the GA-2--now I realize that some of you are going to take issue with me, because I said just a little while ago that we always assumed that all airplanes are alike and I find that all airplanes aren't alike, even when they are of the same model, and make, and stand side by side on the assembly line--so let us say that we can put a typical airplane on the computer, which is really all you do anyway when you fly this system in an airplane, and you can couple your gadget into the simulated airplane either as the actual device or as a simulated model, and so you can wring it out through a long series of tests without ever taking a valuable airplane or test pilot off the ground.

To turn the situation around, if you have an airplane and you want to know how fast, for example, the controls are going to have to travel in order to do what is required, you can set the airplane up and you can find out how fast the controls have to travel in order to do what you want them to do because you can put the simulated airplane through maneuvers just as if you were flying. You can measure control rate and control position directly, so that you can answer directly with the analog computer some of the questions that you have been asking here.

The great advantage, I think, of using the analog computer in that particular respect is that you can put the whole thing into a closed loop and the closed loop response is always different from what you expect it to be when you test it on the open loop.

Now, one of the points that I breezed over here rapidly when I was talking about putting the airplane on the simulator so you could fly your power control system, was the pilot. We have done a little along that line and some other people have done a little in simulating a cockpit with controls and letting the pilot fly the plane. Some of you are going to object, I suspect, that the pilot doesn't have the proper acceleration and, of course, he doesn't. You can put in all of the accelerations that he feels except the linear accelerations which are probably somewhat important. Pilots no longer fly by the seat of their pant, I'm told, but I am sure they take into account the linear accelerations. The rotational accelerations present no great difficulty. The pilots who flew the GA-2 for us had no complaints because the accelerations were not provided, but the GA-2 is a relatively slow plane. When you get up into high-speed linear accelerations are probably considerably more important.

Well, to summarize, then, the electronic or mechanical differential analyzer is not the solution to all your problems by any means, but it is a very important tool, a tool which, if you want to, you can adapt and use to save yourselves a lot of time and avoid a lot of mistakes. You can save your computing personnel--if you already have computing personnel--a lot of pencil pushing and get your answers quickly, which is generally economically of importance, to test out new ideas very quickly, which is again economical, and you can rely on the computer for accuracies of about the order of the magnitude that aircraft people generally need.

Accuracy--just to conclude--the accuracy of the ordinary electronic analog computer is of the order of one per cent and our own aeronautical people are generally satisfied with three or four per cent, so that we feel that we have little difficulty in producing what is wanted.

One small danger in getting an analog computer--that is, you'll find that once you have an electronic analog computer and use it, you will do with a computer several times more work on the same problem than you used to, because it is so easy to do. That is, rather than calculating out one curve, you will find yourself running families of curves and selecting the optimum or something of that sort. So an analog computer saves time, but if you are not careful, it won't save as much time as theoretically it might if you just figure the time actually saved on the hand calculations.

***

DISCUSSION

MR. CHATTLER, Bureau of Aeronautics: *Would you like to cover one other point of using non-linear elements, the actual physical elements?*

DR. WILSON: *Using actual physical elements with the computer is generally not very difficult. It only involves one thing and that is devising or buying a transducer which can take the quantity from the element to feed back into the analog*

[redacted]

computer the deflection or velocity or whatever you are ordinarily feeding into the airplane. And, second, a servo mechanism which puts in the proper input from the computer into the non-linear element. Generally, that doesn't pose any problem. We have had no difficulty yet. We have run a system of auto-pilots and servo mechanisms with our system. At present with the servo mechanisms we use which are about as non-linear as an electromagnetic servo mechanism can be, we get exactly the same results with the simulated mechanism and so we don't very often use the actual device. There are two reasons for that: One is that when we use our actuators, we wear them out and we don't wear the simulated servo, and the second one is that it is more convenient to tie a simulated servo into the system. On all checks that we have carried out so far when we have simulated a device on the computer, we have gotten identical results with those that we have gotten by putting the actual device in the system.

CHATTLER: *You mean, even in non-linear devices in your linear computer?*

WILSON: *No, as I see it we have various tricks, such as limiters, of making the linear computer produce non-linear results, and anyone learns those fairly rapidly.*

QUESTION: *Do I understand that to mean you include the simulator in that, too?*

WILSON: *Yes, for example, when we are testing, let us say, an airframe, with an electromagnetic actuator in it, we simulate the electromagnetic actuator.*

QUESTION: Can you make the computer perform the function of both the computer and the simulator as often as you like?

WILSON: *That's right. We can put the actuator behind a screen and from the results that would come out of the computer, you wouldn't be able to tell which is producing the results, the real actuator, or the simulated actuator.*

QUESTION: *Why don't you build them? Others do.*

WILSON: *We don't. We use the computer. Perhaps other people like them better built. It is a simulator, yet it is a simulator in a little different respect than the usual sense of the simulator in that you are simulating through the differential equations and not through the actual electromechanical analogy. I think we might quibble and say that is the difference. It is a simulator, though.*

MR. BURSTEIN, Consolidated-Vultee: *I might add a little bit to Dr. Wilson's talk. We have taken actual records in flight of this XF-92 and put it in a simulator and made sure that it is exactly the same response that we got in flight. Then we started varying various parameters and we got a whole family of curves.*

[redacted]

WILSON: *AMC has a pair of our computers which they use and Mr. Altman would like to run frequency response characteristics from them. We don't have an output device just now that would record it directly, but it would be very simple to do that, as you could measure phase and amplitude.*

CHATTLER: *Instead of building an expensive mock-up, could we take our hydraulic or control system and tie it into a computer that will simulate all of our loads and eliminate that expense which has to be duplicated?*

WILSON: *You couldn't eliminate all of the expense, because you have to use some servo mechanisms to get your response back into the computer and you have to use some transducers but you could eliminate most of the weight and complexity. As a matter of fact, we do that.*